

**Copyright**  
**by**  
**Andrew Scott Wahr**  
**2010**

**The Thesis committee for Andrew Scott Wahr**

**Certifies that this is the approved version of the following thesis:**

**The Fatigue Performance of Cross Frame Connections**

**APPROVED BY**

**SUPERVISING COMMITTEE:**

---

**Michael D. Engelhardt, Supervisor**

---

**Todd A. Helwig**

# **The Fatigue Performance of Cross Frame Connections**

by

**Andrew Scott Wahr, B.S.C.E.**

**Thesis**

Presented to the Faculty of the Graduate School of

The University of Texas at Austin

in Partial Fulfillment

of the Requirements

for the Degree of

**Master of Science in Engineering**

**The University of Texas at Austin**

**August 2010**

## **Dedication**

To John Wahr, who made this both possible and desirable.

# **The Fatigue Performance of Cross Frame Connections**

Andrew Scott Wahr, M.S.E.

The University of Texas at Austin, 2010

SUPERVISOR: Michael Engelhardt

A new method of connecting cross-frames to bridge girders had been proposed to alleviate concerns with current design practices. This new, half-pipe detail needs to be examined for fatigue issues that may exist which would make it infeasible as a replacement candidate for the current bent-plate design. A program of laboratory testing was carried out to determine the comparative performance between the half-pipe and the bent-plate designs. These tests were then translated into a finite element model which was examined to determine behavior over a wide range of design scenarios. Finite element results, along with the laboratory testing data, were used to determine the appropriate use of the half-pipe stiffener.

## Table of Contents

CHAPTER 1 Introduction.....	1
1.1 Purpose of Research.....	1
1.2 Typical Current Connection Details .....	3
1.3 Proposed New Detail .....	5
1.4 Fatigue Concerns for Half-Pipe .....	7
1.5 Previous Research on Fatigue.....	9
1.6 Overview of Research Program .....	13
CHAPTER 2 Experimental Setup.....	15
2.1 Testing Goals .....	15
2.2 Test Specimens .....	15
2.3 Test Setup.....	24
2.3.1 Hydraulics .....	26
2.4 Measurements .....	28
CHAPTER 3 Results of Physical Testing.....	30
3.1 Overview.....	30
3.2 Inspection for Cracks .....	30
3.3 Beam One: 30 degree specimen (30A).....	36
3.4 Beam Two: 60 degree specimen (60A) .....	41
3.5 Beam Three: 30 degree specimen (30B).....	43
3.6 Beam Four: 60 degree specimen (60B) .....	43
3.7 Compilation of Results .....	45
3.7.1 Skewed Plate Stiffeners .....	45
3.7.2 Perpendicular Stiffeners.....	47
3.7.3 Half-Pipe Stiffeners .....	51
3.8 Summary of Results .....	51
3.8.1 Evaluation of the Half Pipe.....	52
3.8.2 Test Observations for Comparison with Finite Element Model .....	54

CHAPTER 4 .....	56
Development of Finite Element Model.....	56
4.1 Purpose of the Finite Element Model .....	56
4.2 Use of ANSYS .....	56
4.3 Geometry of Model.....	57
4.3.1 Selecting Sizes and Symmetry.....	60
4.3.2 Determining Parameters and Modeling Guidelines .....	60
4.4 Model Detail Selection .....	63
4.4.1 Element Types .....	64
4.4.2 Meshing.....	65
4.4.3 Connection of Elements .....	71
4.4.4 Modeling Arcs and Welds .....	72
4.4.5 Linear Solution.....	74
4.5 Interpreting Results.....	74
4.5.1 Visual Inspection .....	75
4.5.2 Hot Spot Stresses .....	76
4.5.3 Path Generation.....	85
4.6 Validating the Model .....	87
4.6.1 Development of a Plate Stiffener Model .....	88
4.6.2 Comparison to Test Results .....	91
CHAPTER 5 .....	94
Results of Finite Element Modeling .....	94
5.1 Description of Results.....	94
5.2 Selecting Critical Path.....	94
5.2.1 Critical Hot Spot .....	94
5.2.2 Meaning of Path Selection .....	95
5.3 Parameters of Interest .....	95
5.3.1 Parametric Description of Problem.....	95

5.3.2	Determining Relative Influence of Parameters.....	97
5.4	Collection of Data.....	100
5.5	Analysis Of Data.....	101
5.5.1	Goals of Analysis.....	101
5.5.2	Problems for Analysis.....	101
5.5.3	Creation of Predictive Function.....	103
5.5.4	Genetic Algorithm Solution.....	104
5.6	Results.....	108
5.6.1	Plate-Stiffener Results.....	108
5.6.2	Half-Pipe Range of Results.....	113
5.6.3	Half-Pipe Overall Range of Parameters and Stress Concentrations.....	114
5.6.4	Final Equation.....	116
5.6.5	Comparison of Half-Pipe with Plate-Stiffener.....	120
5.7	Conclusions and Recommendations.....	122
5.7.1	Overall Results.....	122
5.7.2	Use of the Half-Pipe Stiffener and Restrictions.....	124
CHAPTER 6	.....	125
Distortional Fatigue Analysis	.....	125
6.1	Fatigue Concerns for Half-Pipe Stiffener.....	125
6.2	Finite Element Model.....	126
6.2.1	Basic Model.....	127
6.2.2	Plate-Stiffener.....	128
6.2.3	Half-Pipe Models.....	129
6.2.4	Hot Spot Stress.....	132
6.3	Finite Element Results.....	132
6.3.1	Plate Stiffener Analysis and Results.....	133
6.3.2	Half-Pipe Stiffener Analysis and Results.....	136
6.3.3	Comparison of Results.....	139



6.4	Summary .....	139
CHAPTER 7 .....		140
Summary and Conclusions .....		140
7.1	Summary of Problem .....	140
7.2	Physical Testing and Results .....	140
7.3	Finite Element Modeling .....	142
7.4	Recommendation for Use .....	143
7.5	Areas for Further Study .....	144
Appendix.....		145
A	Physical Testing .....	145
A.1	Records for Physical Testing .....	145
A.2	Strain-Gauge Reading.....	154
B	Finite Element Testing for Flexural Fatigue.....	157
B.1	Plate-Stiffener .....	157
B.2	Half-Pipe Stiffener .....	158
C	Finite Element Testing for Distortional Fatigue .....	179
C.1	Plate-Stiffener Finite Element Analysis.....	179
C.2	Half-Pipe Stiffener with Intermediate Connection Plate .....	207
C.3	Half-Pipe Stiffener without Intermediate Connection Plate .....	212
References.....		226
VITA.....		228

## Table of Figures

Figure 1-1: Cross-Frames during Construction of the Lubbock 19 <sup>th</sup> St. Bridge.....	2
Figure 1-2: A Bent Plate Connection.....	4
Figure 1-3: Half-Pipe Connection in Laboratory Tests at The University of Texas, Austin (Quadrato 2010).....	6
Figure 1-4: AASHTO Fatigue Categories .....	8
Figure 1-5: An Example of a Girder with a Corrugated Web.....	10
Figure 1-6: Testing of a Corrugated Web Girder.....	11
Figure 1-7: Computationally Generated Stress Field in a Corrugated Web .....	12
Figure 2-1: Design of Specimens.....	17
Figure 2-2: A Steel Pipe is Split in Half before Installation on the Girder.....	18
Figure 2-3: A Specimen Being Measured During Fabrication .....	19
Figure 2-4: A Half-Pipe is Spot Welded into Place in Preparation for Welding .....	20
Figure 2-5: Welding Half-Pipe Stiffener to the Girder .....	21
Figure 2-6: Completed Test Specimen .....	22
Figure 2-7: Welded Details for Half-Pipe.....	23
Figure 2-8: Welded Details for Plate-Stiffener.....	23
Figure 2-9: Test Frame Set-Up .....	24
Figure 2-10: Overall Arrangement of Testing Mechanism.....	25
Figure 2-11: Hydraulic Ram, Load Cell, and Servo Valve.....	26
Figure 2-12: Application of Load to Specimen .....	27
Figure 3-1: Using an abrasive saw to cut out sections of interest for destructive testing.	32
Figure 3-2: A piece of the beam that is to be tested for fatigue cracks is cut into five, narrow sections using a band-saw (this is the perpendicular stiffener from beam 30A) .....	33
Figure 3-3: Plastic Yielding in Destructive Testing .....	34
Figure 3-4: A Specimen before Destructive testing.....	35

Figure 3-5: Destructive Testing Revealing a Crack.....	35
Figure 3-6: Beam 30A with two 30 degree stiffeners, two pipe stiffeners and two perpendicular stiffeners (only one side shown here, the reverse side is mirrored)...	36
Figure 3-7: Location of Fatigue Crack on a Skewed Plate-Stiffener.....	37
Figure 3-8: A plate is put over the crack surface to prevent the crack from spreading ....	38
Figure 3-9: Crack on the compression flange of Beam 30A .....	39
Figure 3-10: A S-N plot of the fatigue life of Beam 30A.....	40
Figure 3-11: Crack on 60A at the edge of the repair plate.....	41
Figure 3-12: A S-N plot of the fatigue life of Beam 60A.....	42
Figure 3-13: A S-N plot of the fatigue life of Beam 30B .....	43
Figure 3-14: A S-N plot of the fatigue life of Beam 60B .....	45
Figure 3-15: A S-N plot of the fatigue life of skewed stiffeners .....	47
Figure 3-16: Fatigue crack at a perpendicular stiffener on beam 60B.....	48
Figure 3-17: Location of Fatigue Crack on a Perpendicular Plate-Stiffener .....	49
Figure 3-18: A S-N plot of the fatigue life of perpendicular stiffeners .....	51
Figure 3-19: A S-N plot of each of the beams tested.....	53
Figure 4-1: An Image of the ‘Alpha’ ANSYS Model Which Simulated the Full Beam with All Six Connections Found in the Laboratory Testing.....	58
Figure 4-2: Deformed Shape of Epsilon Model, Elevation View.....	59
Figure 4-3: Deformed Shape of Epsilon Model, Rotated View.....	59
Figure 4-4: The Impact of the Model Length on the Stress Concentration Factor .....	61
Figure 4-5: Model of Half-Pipe Using Symmetry .....	62
Figure 4-6: The Impact of Imposing Symmetry on the Stress Concentration Factor .....	63
Figure 4-7: ANSYS SOLID95 Geometry.....	65
Figure 4-8: Mesh Properties of the Model.....	66
Figure 4-9: Stress Concentration Factor around Half-Pipe at Different Mesh Densities .	68
Figure 4-10: Effect of Coarse Mesh Size on the Stress Concentration Factor .....	69
Figure 4-11: Effect of Extra Fine Mesh Size on the Stress Concentration Factor.....	70

Figure 4-12: Meshing Along an Arc .....	73
Figure 4-13: Stresses in Basic Model .....	75
Figure 4-14: Stress in the Flange at the Boundary of the Weld at Increasing Mesh Densities.....	78
Figure 4-15: Stresses at Varying Distances from Weld.....	79
Figure 4-16: Taking Stresses along Paths Approaching Two Hot Spots (DNV 2010) ....	81
Figure 4-17: Calculating DNV Stress at a Hot Spot (DNV 2010).....	81
Figure 4-18: Different Methods for Determining Hot Spot Stress .....	84
Figure 4-19: Paths Used to Find Hot Spot Stresses .....	86
Figure 4-20: Plate Stiffener Model Mesh .....	89
Figure 4-21: Plate Stiffener Model, Deformed Shape and Stress Contours .....	90
Figure 4-22: Direction of the Principle Stress in Tensions Flange Adjoining a Skewed Plate-Stiffener .....	92
Figure 5-1: Impact of Scaling the Model on the Stress Concentration Factor.....	96
Figure 5-2: Study of Pipe Thickness (tS).....	97
Figure 5-3: Study of Weld Size (aS).....	98
Figure 5-4: Study of Web Thickness (tW).....	99
Figure 5-5: Computing Fitness of a Given Equation .....	107
Figure 5-6: The stress along the weld of a plate stiffener that has no skew (values taken $\frac{1}{2}$ flange thickness from weld).....	110
Figure 5-7: The stress along the weld of a plate stiffener that has been skewed 10 degrees (values taken $\frac{1}{2}$ flange thickness from weld).....	111
Figure 5-8: The stress along the weld of a plate stiffener that has been skewed 25 degrees (values taken $\frac{1}{2}$ flange thickness from weld).....	111
Figure 5-9: Stress Concentration Factor for Plate Stiffeners at Varying Skew Angles..	113
Figure 5-10: Summary of Results from Initial Parametric Testing .....	115
Figure 5-11: The FEM SCF versus the Predicted SCF from Equation 5-3 .....	117
Figure 5-12: The FEM SCF versus the (Simplified) Predicted SCF from Equation 5-4	119

Figure 5-13: Stress Concentration Factor Comparison between Plate-Stiffeners and Half-Pipe Stiffeners .....	121
Figure 6-1: Connection of Cross-Frame to Half-Pipe Stiffener.....	126
Figure 6-2: Basic Plate-Stiffener Model (Mesh Elements Shown) .....	128
Figure 6-3: Plate-Stiffener Model (Principle Stresses Shown).....	129
Figure 6-4: Half-Pipe Stiffener with Intermediate Connection Plate .....	130
Figure 6-5: Half-Pipe Stiffener with Direct Connection.....	131
Figure 6-6: Histogram of Plate-Stiffener Stresses .....	134
Figure 6-7: Stresses in Plate-Stiffener vs. Skew Angle .....	135
Figure 6-8: Histogram of Half-Pipe Stiffener Stresses .....	137
Figure 7-1: Results from Physical Testing.....	141
Figure 7-2: Results of Computational Comparison between the Plate-Stiffener and Half-Pipe Stiffener .....	142

# CHAPTER 1

## Introduction

### 1.1 PURPOSE OF RESEARCH

Cross-frames are an essential component of many steel girder bridges: they ensure stability during the construction phase and help the bridge resist lateral loads over the bridge's lifetime. In a skewed bridge system, these cross-frames present several challenges to design and construction. Figure 1-1 shows a skewed steel bridge under construction. The end cross-frames and intermediate cross-frames are visible in this photo (Quadrato 2010).



***Figure 1-1: Cross-Frames during Construction of the Lubbock 19<sup>th</sup> St. Bridge***

For skewed bridges such as that shown in Figure 1-1, the intermediate cross-frames are typically placed perpendicular to the girders. However, the end cross-frames are normally oriented parallel to the skew, as shown in Figure 1-1. The end cross-frames are therefore not perpendicular to the girder. Consequently, the cross-frame must connect to the girder at an angle. Fabricators often use a bent-plate to make the connection to the skewed cross frame. The bent plate detail is discussed in the following section. Concerns have been raised that flexibility of the bent plate connection detail can adversely affect the effectiveness of the cross-frame in bracing the girder. Concerns over the effects of the bent plate led to the Texas Department of Transportation (TxDOT) investigation of which

the research presented in this thesis was a part. Additional results from the study are presented in Battistini (2009) and Quadrato (2010).

## **1.2 TYPICAL CURRENT CONNECTION DETAILS**

The detail that is frequently used for connecting cross-frames to bridge girders is to a plate stiffener. Plate stiffeners that are connected to cross frames are referred to as connection plates. Connection plates are most often oriented perpendicular to the girder webs; however for small skew angles (less than 20 degrees) intermediate (between supports) cross frames may be oriented parallel to the skew angle and therefore the connection plates may also be oriented parallel to the skew angle. For skew angles larger than 20 degrees, the AASHTO Specifications require intermediate cross frames to be oriented perpendicular to the girder lines. As a result, the connection plates of the intermediate stiffeners are perpendicular to the girder webs. Although the intermediate cross frames are often perpendicular to the girder webs, in skewed bridges the support cross frames are typically oriented parallel to the support angle. Although the support cross frames are oriented parallel to the skew, the connection plate is most often oriented perpendicular to the girder web since skewing the connection plate results in difficulty in welding on the acute angle side of the plate. The connection that is often used between the skewed cross frame and the connection plate consists of a bent plate.





*Figure 1-2: A Bent Plate Connection*

An example of a bent plate connection is shown in Figure 1-2 (this is an intermediate cross-frame, but the detail is the same for end cross-frames). A plate-stiffener is attached to the girder with no skew; then the bent plate is bolted to the stiffener, and the cross-frame bolted to the bent plate. This is the typical solution for bridges with a skew in excess of  $20^\circ$ . When the bridge has a skew angle that is less than  $20^\circ$ , AASHTO allows the skewing of the plate-stiffener itself, as described above, instead of the use of the bent-plate (AASHTO 2007).

Although the bent plate provides a solution that makes the connection relatively easy to fabricate, the resulting connection has a significant amount of eccentricity and flexibility. The flexibility of the bent plate can lead to substantial reductions in the

stiffness of the cross frame system which is not typically considered in the design process (Quadrato 2010).

### **1.3 PROPOSED NEW DETAIL**

A solution proposed to alleviate the eccentricity and flexibility of the bent-plate connection detail is to replace the traditional connection plate at the supports with a round stiffener that is created by splitting circular pipe (Quadrato 2010). With this detail, a pipe is cut in half, and the half-pipes are then welded to the girder where the plate stiffener would have been. The cross-frame can then be attached at any angle to the pipe, allowing for simple fit-up of a skewed cross-frame at the ends of the girders. The half-pipe connection provides significantly higher stiffness than the bent-plate connection (Battistini 2009).



*Figure 1-3: Half-Pipe Connection in Laboratory Tests at The University of Texas, Austin (Quadrato 2010)*

An example of the proposed half-pipe connection is shown in Figure 1-3: the split-pipe is welded to either side of the girder. Then a plate is connected to the half-pipe on both sides at the required skew angle. The circular pipe allows for any skew angle to be easily accommodated in fit-up without having to bend a plate to a precise angle or using a skewed connection plate.

In addition to providing a stiffer cross-frame to girder connection, the half-pipe detail also provides additional torsional warping restraint at the end of the girder. This warping restraint increases the lateral torsional buckling capacity of the girder, and may permit a greater spacing between the end cross-frames and the first line of intermediate cross-frames (Quadrato 2010).

#### **1.4 FATIGUE CONCERNS FOR HALF-PIPE**

In evaluating the feasibility of the half-pipe connection detail, an issue of concern is the fatigue performance of this detail. Of particular interest is the question of whether the proposed half-pipe detail would be worse than the currently used plate-stiffener in fatigue loading. Thus an investigation is needed to ensure that replacing the plate-stiffener with the half-pipe stiffener will not lead to fatigue failures.

Bridges are subject to continual loading and unloading cycles through-out their functional life. This type of loading can cause fatigue failures that result not from yielding the material, but causing crack growth in the material itself at below-yield stress levels. A connection may be able to handle high stresses well in laboratory testing, but cause fatigue failure either in the connection itself or in the bridge element to which it's connecting, over the course of millions of repeated loads.

Fatigue results from crack-growth due to these repeated stress cycles. Fabricated steel components typically have a combination of defects in the material itself as well as the welds used to join the structural elements. Because of stress concentrations near the tips of cracks in the material and welds, the cracks can propagate due to cyclic stresses. Depending on the initial crack size, the stress concentration, and the magnitude and frequency of the stress cycles, the cracks may grow to a critical size resulting in brittle fracture of the structural element. The fatigue life of a structural element is related to the time that it takes for a defect to grow to a critical crack size.

The potential difference in fatigue life results from the dissimilar geometries of the connections. Both the half-pipe stiffener and conventional plate stiffeners are welded

to the girder flanges and web. An issue of interest is whether the half-pipe stiffener introduces stress concentrations than conventional plate stiffeners. Stress concentrations often exist at locations with changes in the structural geometry. Points of stress concentration can be sites for crack formation and growth which lead to eventual fatigue failure (Unsworth 2003).

AASHTO provides eight fatigue categories that are dependent on the geometry of the plate or structural components. The categories are classified from category A through E ratings (with the addition of B', C', and E' categories) that represent how that detail is expected to behave under repeated loading. The categories are often represented in S-N curves, which are graphs of the number of cycles (N) to failure for a particular constant amplitude stress range (S). A graph of the S-N curves for the eight AASHTO fatigue categories is provided in Figure 1-4 (AASHTO 2007).

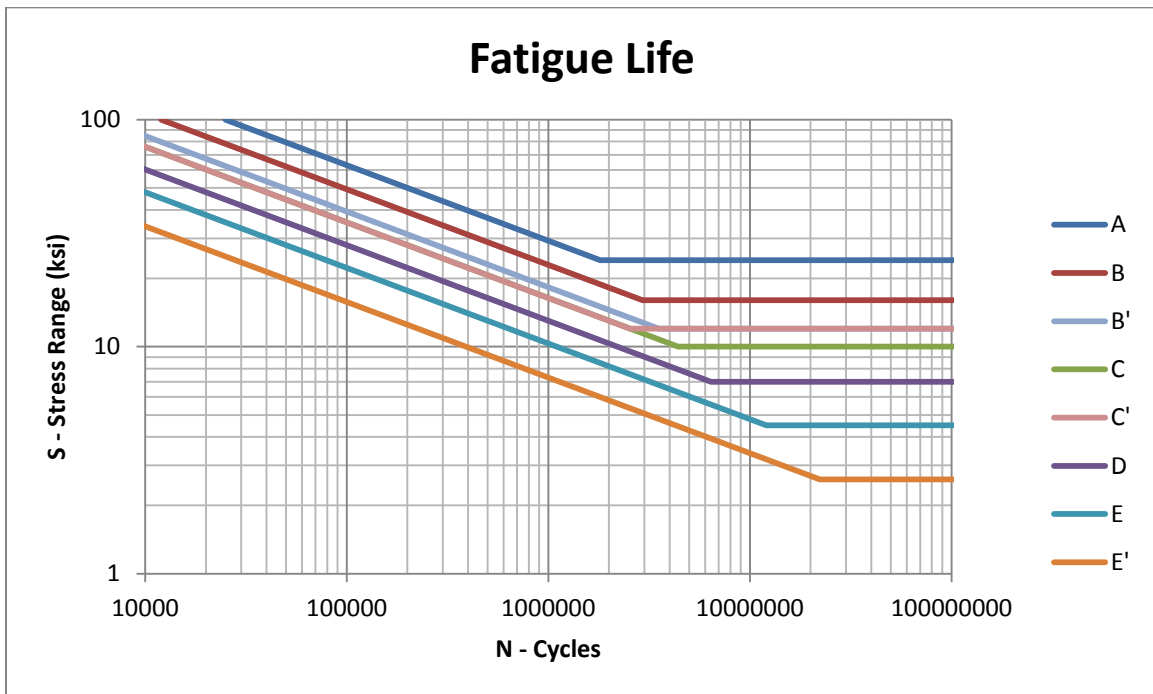


**Figure 1-4: AASHTO Fatigue Categories**

The fatigue categories and details compiled in AASHTO are based upon a wide range of laboratory tests. The plate-stiffener currently has a category C rating as designated by AASHTO. Consequently it would be desirable for the half-pipe stiffener to achieve a category C rating or better to ensure that its fatigue performance is not worse than the conventional plate stiffener.

## **1.5 PREVIOUS RESEARCH ON FATIGUE**

A review of the literature revealed no previous research on the fatigue performance of half-pipe stiffeners. Although previous research has been conducted on the warping restraint provided by half-pipe stiffeners, this work was related to building applications and thus fatigue was not a significant concern (Ojalvo and Chambers 1977). Previous research on plate-stiffeners had already resulted in a category C rating (Roy et al 2003). A goal of this project was not to investigate fatigue performance of plate-stiffeners directly, but instead to provide a comparison between plate-stiffeners and half-pipe stiffeners.

Research had been conducted on built-up girders with corrugated webs such as the one shown in Figure 1-5 (Anamia et. al 2005). The geometry and construction is somewhat similar to the welded, circular geometry in the half-pipe stiffener. An example of a girder with a corrugated web is shown in Figure 1-5. Although the two are not identical, fatigue research for corrugated webs may be able to provide insights into the fatigue behavior of the half-pipe stiffener.

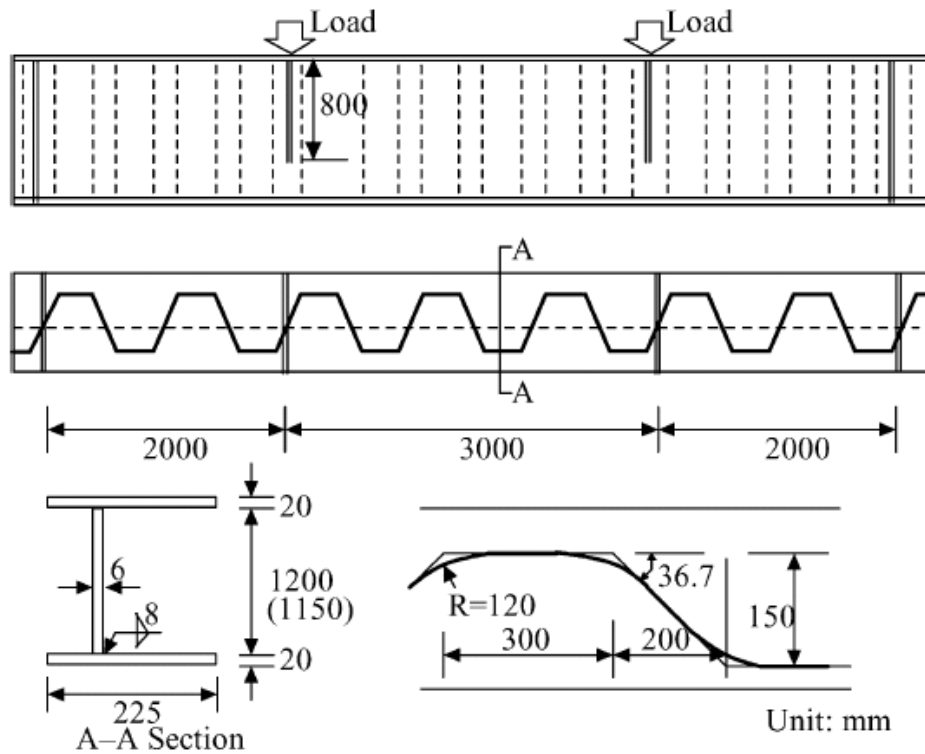


**Figure 1-5: An Example of a Girder with a Corrugated Web**

Research projects have undertaken the study of corrugated webs both through physical testing and finite element modeling. The physical testing of this detail universally involved building a girder with a corrugated web to some given specifications and then loading it repeatedly under a constant stress-range in the girder flange. Four-point loading was typically used, in which a section in the middle of the girder was under constant moment. In these experiments, the load cycling was continued until a crack developed in the girder. The location of the crack, stress range and cycle count at which it occurred were recorded. This would then serve as a data point at which to rate the connection. An example of this testing can be seen in Figure 1-6 (Anamia et. al 2005).

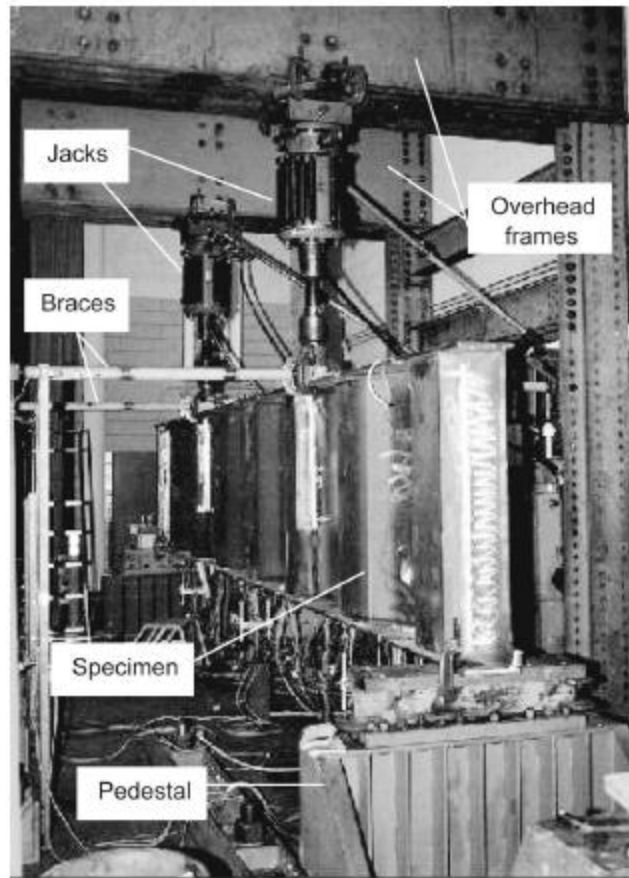


***Figure 1-6: Testing of a Corrugated Web Girder***

Other studies consisted of finite element analyses that were designed to determine how the corrugation of the web changed the flow of stresses through-out the girder. The analysis was used to locate points of maximum stress and to evaluate the magnitude of that stress in relation to what would be expected by purely flexural loading without geometric changes. An example from research on the corrugated web girder (Anamia and Sauseb 2005) is shown Figure 1-7.



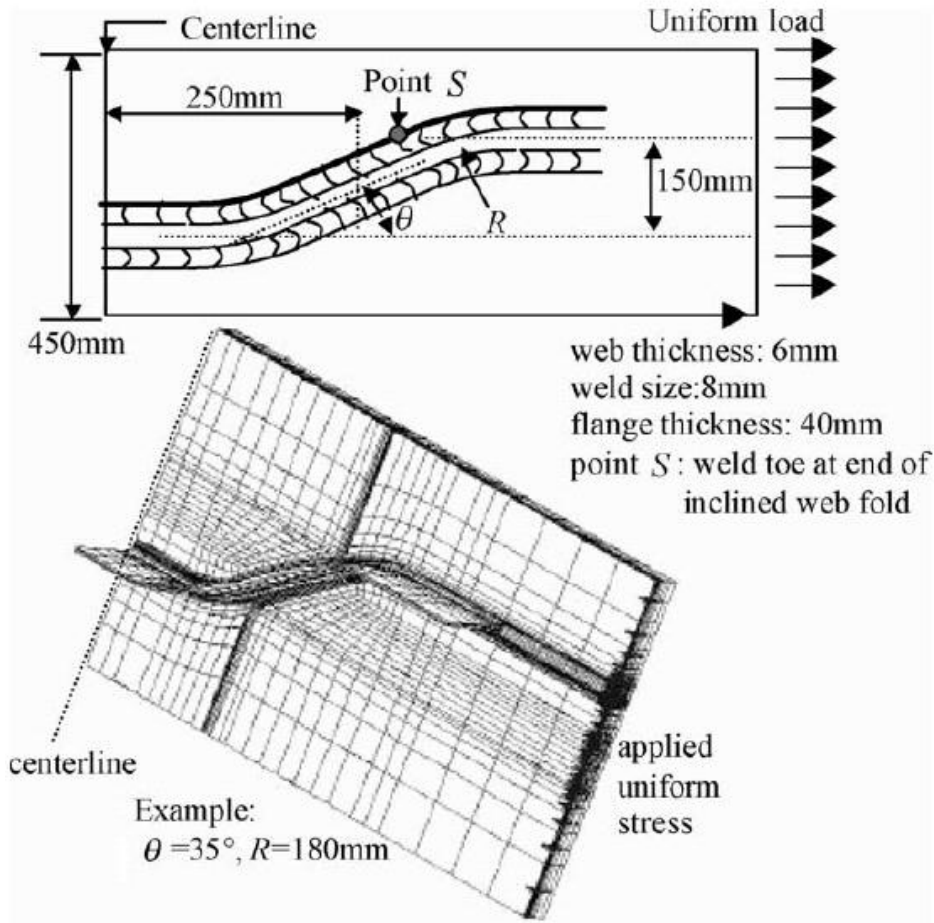


**Figure 1-7: Computationally Generated Stress Field in a Corrugated Web**

Both the physical testing and computational testing revealed the point of maximum stress to be in the center of the bend of the corrugated web along the weld toe (Sause et. al 2003). This is the equivalent of a point located at a  $45^\circ$  angle from the web, along the edge of the weld used to attach the half-pipe to the girder when comparing the corrugated web to the half-pipe. This was always the point of crack formation for the corrugated web girders, as well as the point that the various finite element analyses showed had the highest concentration of stresses for the corrugated web girders studied.

The data found in the research supported a rating of category B' for a girder with a corrugated web. Some of the physical results suggested that it was possible that it may be able to receive a higher rating with more research or better weld-quality (Sause et. al 2006). Other studies indicated that ratings higher than category B' may not be possible (Anamia and Sauseb 2005). Based on the previous work on corrugated web girders, then it may be reasonable to expect that girders with half-pipe stiffeners may also be able to achieve a category B' rating. This suggests that the half-pipe stiffener will be no worse than a plate stiffener from a fatigue performance point of view, and may in fact be better.

Additionally, the problems that resulted in fatigue failure in the corrugated web tests would be mitigated by the differences between it and the half-pipe stiffener. It was found that for the corrugated web girders, cracks formed on weld stop-start points and are influenced by the disruptions in the stress-field caused by bending the web (Anamia and Sauseb 2005). The half-pipe stiffener will not have the same impact on the stress field since a typical, planar web will still be present and serve as the primary path for flexural stresses in the web. It may also be easier to control the quality of the weld between the half-pipe stiffener and the girder flange, as this weld can likely be completed without intermediate stops and starts.

## **1.6 OVERVIEW OF RESEARCH PROGRAM**

In order to determine the fatigue properties of the half-pipe stiffener, a two-part research program was undertaken. The first was to perform physical testing on the half-pipe and the second was to do computational analyses using a finite element model to further investigate the connection.

The physical testing was designed to compare the half-pipe stiffener directly to the plate-stiffener by testing both connections simultaneously in the same girder. Due to the time and cost involved in fatigue testing, only a limited number of tests were conducted. Similar to previous tests on corrugated web girders, the girders with plate and

half-pipe stiffeners were tested using a four-point loading arrangement that provided for constant moment in the region of the girder with the stiffeners.

Once the laboratory testing was complete, finite element models were developed of the connections. These models were used to closely examine the stress-fields generated in the girder at the stiffener locations. The models were also used to examine variables that were not included in the test program, such as variations in pipe diameter and wall thickness, weld size, girder dimensions, and other parameters.

The experiments and analyses described above focused on the impact the half-pipe stiffener would have on the potential for fatigue failure of the girder. As a last stage of this research project, a brief investigation was conducted to evaluate the potential for fatigue problems within the half-pipe stiffener itself, due to localized distortions arising from the connection of the cross-frame to the half-pipe stiffener. This portion of the study was conducted exclusively with finite element analyses.

## CHAPTER 2

# Experimental Setup

### 2.1 TESTING GOALS

A program was designed and implemented to test the fatigue performance of both the proposed half-pipe stiffener connection along with the plate-stiffener connection that it would replace. This program was intended to evaluate the proportional fatigue behavior of the pipe stiffener as compared with the original solution. The data would then also be used to validate a finite element model which could be used to investigate the fatigue effects of various parameters of the half-pipe stiffener design, such as the pipe thickness and diameter.

### 2.2 TEST SPECIMENS

The specimens used in the fatigue tests consisted of four different girders. Six girders were fabricated in this process, but only four were tested and only those will be described in this report. The girders were fabricated at Hirshfeld Steel Company in San Angelo, Texas. Each girder consisted of W21x101 rolled wide flange beam of ASTM A992 steel. The specified properties of a W21x101 are listed in Table 2-1. All the girders were ordered to 25 feet lengths to provide 6 inches of overlap on either side of the 24 feet clear span of the test setup. Since the loading provided some lateral restraint, lateral-torsional buckling was not a concern in these tests. The loading on the beams was chosen to keep them within the elastic range.

**Table 2-1: Properties of a W21x101 (AISC 2005)**

Girder Depth	21.4	in
Flange Width	12.3	in
Flange Thickness	0.8	in
Web Thickness	0.5	in
Area	29.8	in <sup>2</sup>
I <sub>xx</sub>	2420	in <sup>4</sup>
I <sub>yy</sub>	248	in <sup>4</sup>

Each girder had six different stiffeners consisting of either steel plates or split steel pipes. Each piece was attached to the girder as it would be if it were to be used as a cross-frame connection plate. The pieces were welded to both flanges and to the web. The plates were placed either perpendicular to the web or at a skewed angle. The stiffeners were welded on either side of the web with each specific stiffener type positioned as it would be at the support of a typical steel interior bridge girder. The sections through the stiffeners in Detail 1 and Detail 2 in Figure 2-1 show how the stiffeners were oriented on either side of the web for the skewed stiffener and the half pipe stiffener. The normal plate stiffeners were placed at the same longitudinal location on either side of the web.

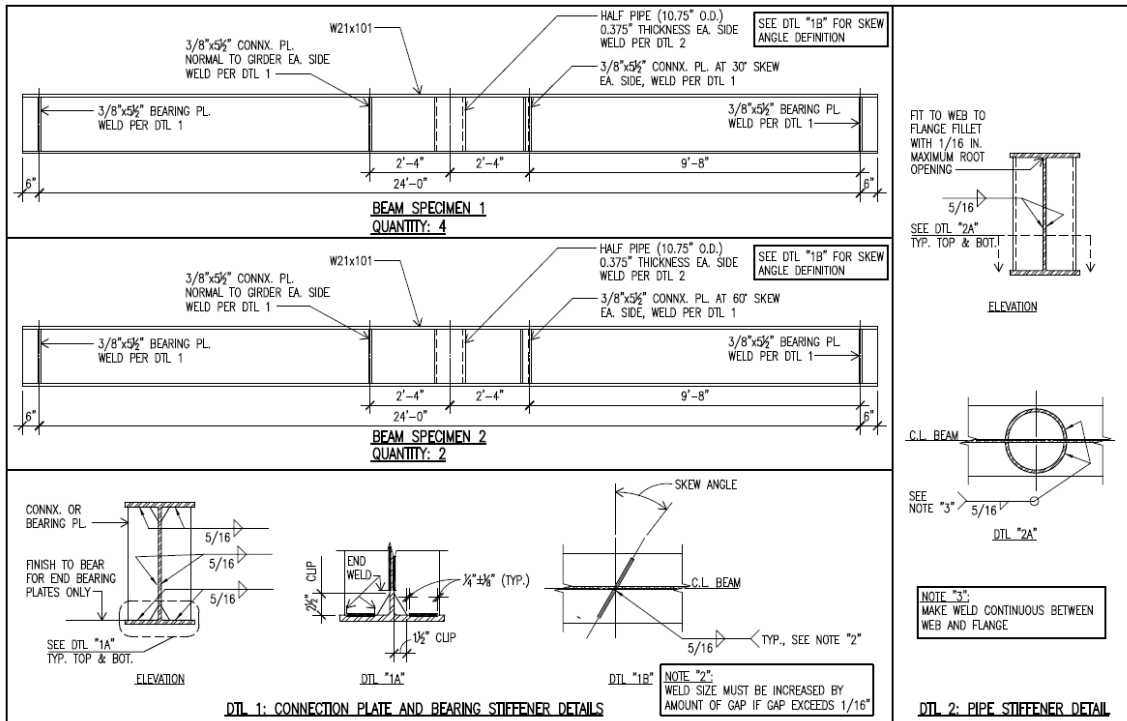


**Figure 2-1: Design of Specimens**

Figure 2-1 shows the layout of the girders that were fabricated. Figure 2-1 illustrates two different designs: each design had two girders created to those specifications. On the left of the girder, the plates were installed at a skewed angle of either 30° or 60° depending on the design. In the middle are the half-pipe stiffeners and on the right are the perpendicular plate-stiffeners, i.e. two plate-stiffeners with a 0° skew.



***Figure 2-2: A Steel Pipe is Split in Half before Installation on the Girder***

The half-pipe used on either side of the girder was created by taking a full pipe and splitting it in half with an acetylene torch as is shown in Figure 2-2.



***Figure 2-3: A Specimen Being Measured During Fabrication***

Once each individual stiffener piece had been cut and prepared and the girders cut to length, the placement of the plates and half-pipes were measured and marked on the girder. This is demonstrated in Figure 2-3. The pieces were then spot welded into place in preparation for complete welding.



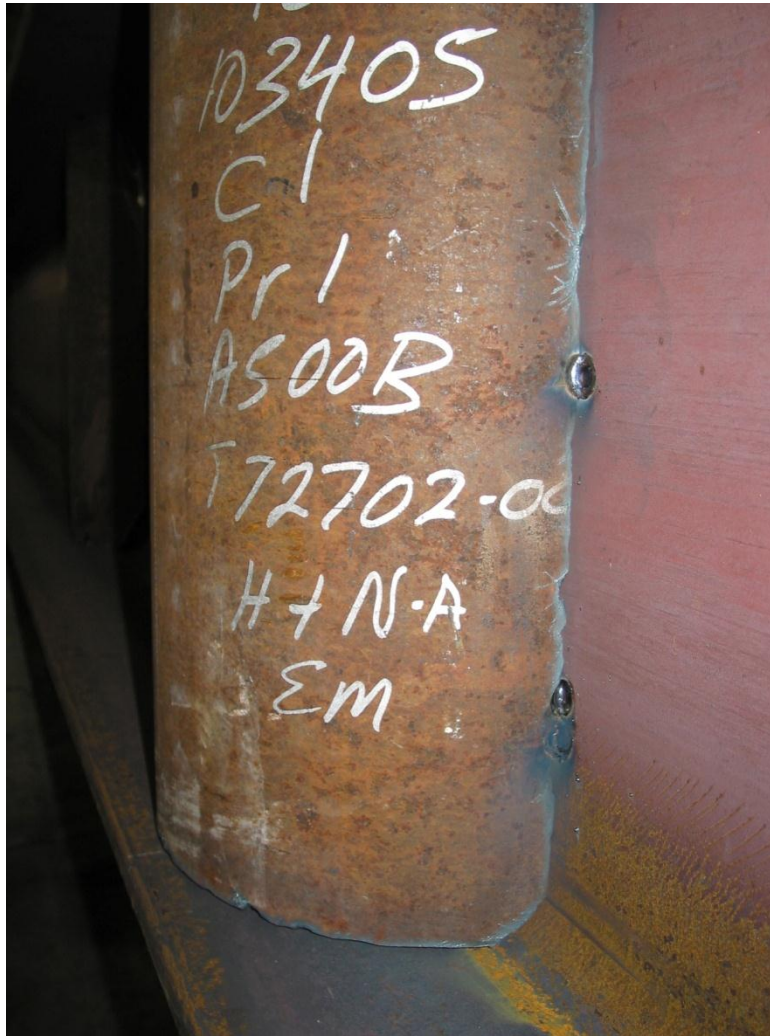


***Figure 2-4: A Half-Pipe is Spot Welded into Place in Preparation for Welding***

Figure 2-4 shows a half-pipe that has been spot welded prior to being fillet welded to the girder. As can be seen in this figure, the flame cut edges of the pipe were quite rough. Further, a small gap was left between the ends of the half-pipe segment and the inside faces of the girder flanges. That is, no attempt was made to achieve a tight fit between the half-pipe segment and the girder flanges. The specimens were prepared in this manner to assure that the quality of fabrication was not better than typically used in bridge fabrication practice, and perhaps somewhat worse. This was done so that the

fatigue tests would provide a conservative estimate of the fatigue performance of the half-pipe stiffener with respect to fabrication quality. . After spot welding, a continuous fillet weld was placed around the entire edge of the half-pipe segment, connecting it to the girder web and flanges. The weld was made continuous to completely seal the pipe to avoid collection of debris or corrosion on the inside of the pipe which could become an issue in real bridge girders. Figure 2-5 is a photo showing welding of the half-pipe stiffener.



*Figure 2-5: Welding Half-Pipe Stiffener to the Girder*

The plate stiffeners were welded on both sides to the web and to both the top and bottom flanges. The corners of the plate stiffeners were clipped to allow clearance of the

web-flange fillet. The welds connecting the stiffeners to the web and to the flange were terminated at the clip. Consequently, the welds to the web and to the flange did not meet.

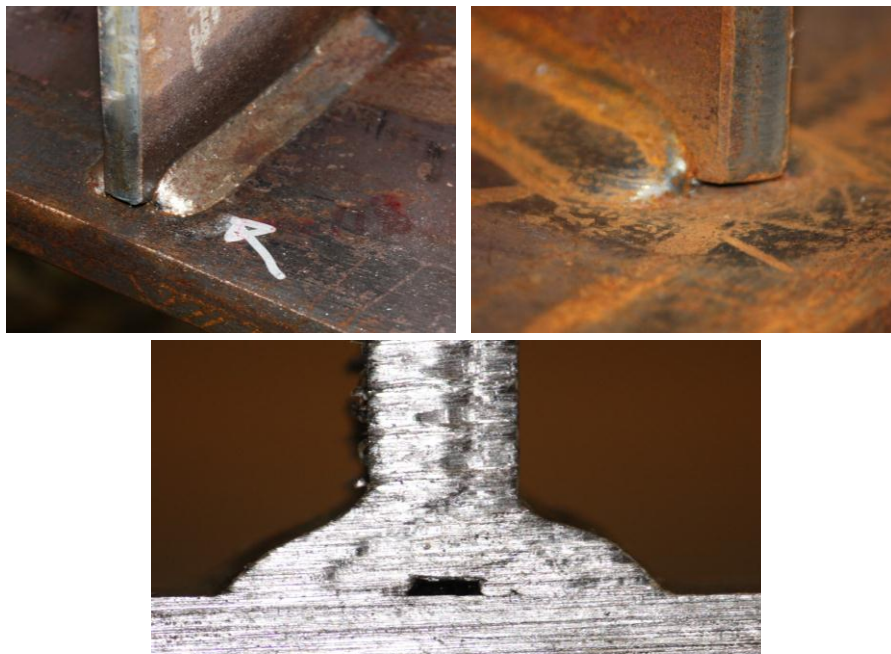
All welds were completed in building division of Hirshfeld Steel. While these welds are likely representative of welds that would be found in practice, it is likely that welds of equal or better quality would be likely in the bridge division of the fabricator since fatigue in the welds is more critical. The stiffeners would also likely have a more accurate fit by a bridge fabricator. In as such, the welds and fit up of the half-pipe and plate stiffeners are representative of the worst conditions that would likely be encountered in bridge practice



*Figure 2-6: Completed Test Specimen*



*Figure 2-7: Welded Details for Half-Pipe*



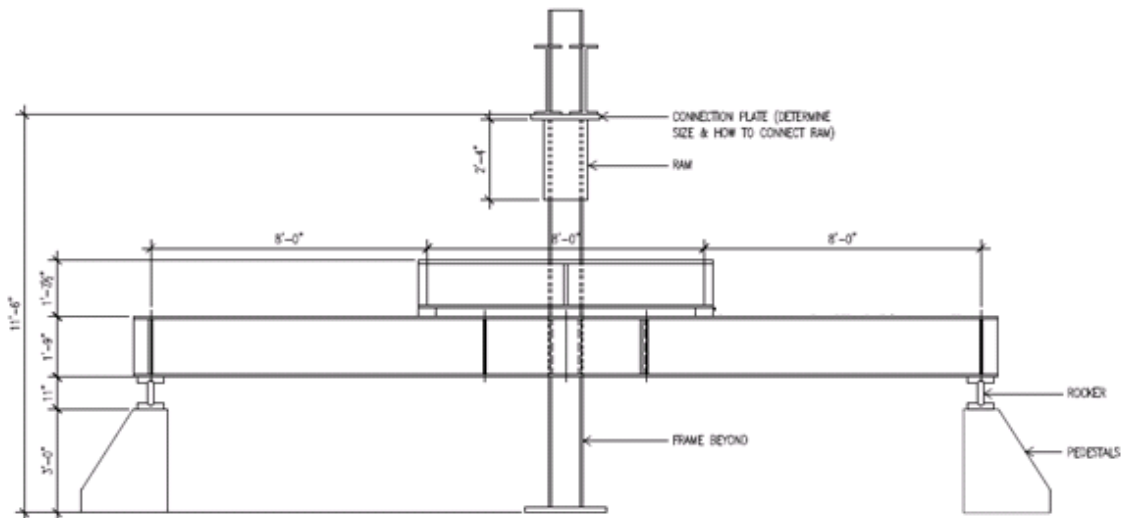
*Figure 2-8: Welded Details for Plate-Stiffener*

Figure 2-7 and Figure 2-8 show the welded connections for the half-pipe and plate-stiffener. Included in each figure is a cross-sectional image taken after the specimen was cut for autopsy following the completion of the fatigue testing. A clear gap can be seen between the stiffener itself and the girder.

Once the welding process was complete, including installation of two bearing stiffeners on each end of the girder (which were not part of the research, but were provided for safety and stability of the test specimen) the specimens were shipped from the Hirshfeld Steel Company in San Angelo to the University of Texas Ferguson Structural Engineering Laboratory for testing.

### 2.3 TEST SETUP

With the specimens fabricated, a testing system needed to be created that would allow for testing of the connections that had been installed on each girder. The overall goal of the testing was to determine the impact of repeated loading under flexural conditions. The test set-up was design to, as closely as possible; simulate this loading in a controlled scenario. This meant that a repeated and well defined flexural load needed to be applied to each connection up until failure occurred.



*Figure 2-9: Test Frame Set-Up*

A drawing of the test setup is shown in Figure 2-7. . The test specimen was a 24-ft. long simply supported beam. Loading was applied to produce a region of constant moment in the middle 8-ft. segment of the specimen around the stiffeners. The loading was applied by a hydraulic ram located at the middle of the beam. The ram applied load to a spreader beam that transferred equal reaction loads to points on the beam four feet on either side of the midspan which generated a region of uniform moment. Rubber bearings were placed between the spreader beam and the specimen. The hydraulic ram was attached to a reaction frame that was connected to the laboratory strong floor and laterally supported by struts attached to the laboratory reaction wall. An overall view of the test setup is shown in the photo in Figure 2-10.



*Figure 2-10: Overall Arrangement of Testing Mechanism*

### 2.3.1 Hydraulics

To create cyclic loading, a hydraulic ram was used. The end of the ram was attached to a load cell which was used to monitor and control the load applied to the specimen. The end of the ram was attached to a load cell which was used to monitor and control the load applied to the specimen.

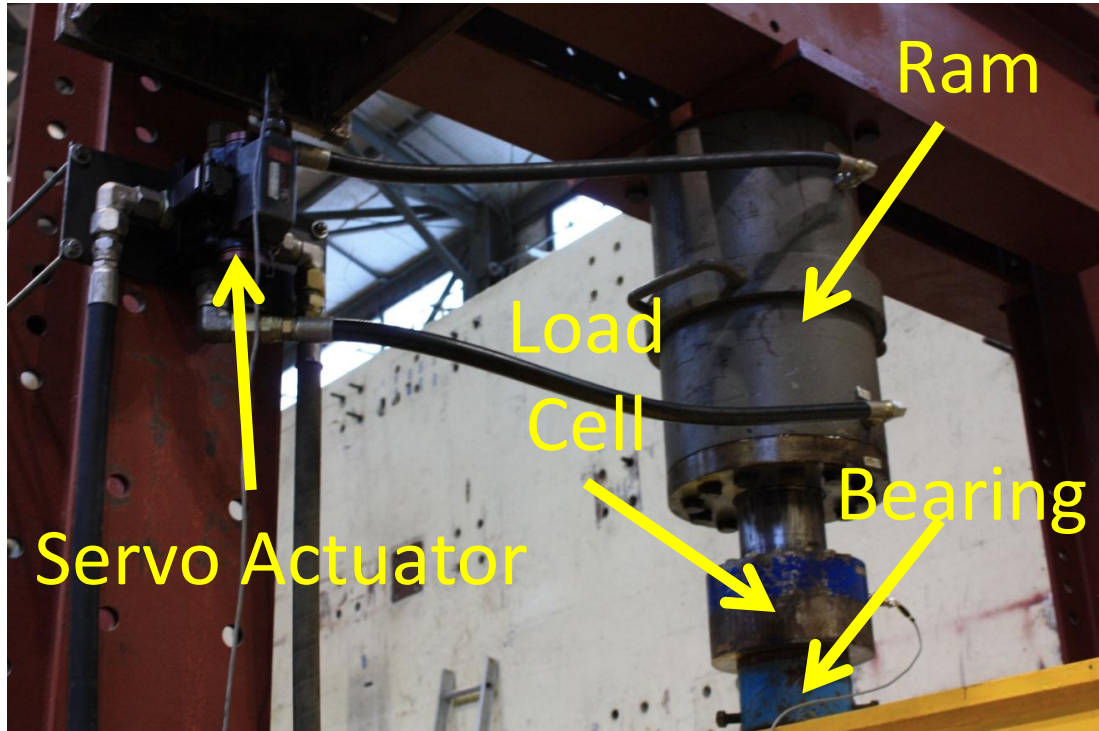


*Figure 2-11: Hydraulic Ram, Load Cell, and Servo Valve*

The components of the closed loop system are shown in Figure 2-11. An MTS hydraulic control unit was used to specify the signal to the servo valve that controlled the oil pressure to the ram based upon feedback from the load cell. Sine-loading was specified by the hydraulic control unit to achieve the desire stress range. The pump was an MTS Silent-Flo pump with a 3000 psi max pressure and a flow rate of 90-gallons per minute. All tests were run on load control, based on the signals from the load cell. Loading was chosen to produce selected stress ranges in the flanges of the test specimen.

In the closed loop system, the hydraulic control unit sends a signal to the servo-valve to direct oil to the either the pressure or return side of the ram to achieve a specific load level. The servo value continues to direct the oil until the desired load level is achieved based upon the signal from the load cell. A hemispherical bearing was used between the load cell and the loading beam to ensure the load was applied in only the vertical direction.



*Figure 2-12: Application of Load to Specimen*

The bottom of the ram, load-cell, bearing, spreader beam (painted yellow) and specimen are pictured in Figure 2-12. The load points from the spreader beam are well outside of the portion of the specimen containing the half-pipe and plate stiffeners. The hydraulic pressure is supplied from a pump located in the laboratory.



The hydraulic loading system was capable of applying cyclic loads at a frequency of approximately one hertz. The total number of cycles applied to each specimen was in the millions and this meant that several weeks were required for each test.

## **2.4 MEASUREMENTS**

The measurements that were used to evaluate the various connections tested were the stress ranges each connection was cycled at, and the total number of cycles at that stress range at failure. The cycle count was measured by the electronic controller. The stress range was determined through strain-measurements of the specimen directly.

The stress range represented the difference between the maximum and minimum stress experienced by the stiffener to girder connections through each cycle. The connections spanned the entire height of the web, but all the fatigue problems were located at the surface of the tension flange. This is where the stress was the greatest by one of the welds used to connect either the plate-stiffener or half-pipe stiffener to the girder, and fatigue is a tension-only concern (and thus the compression flange was not of interest to the test) (Fisher et. al 1998).

To determine what the stress range was at the surface (top) of the tension (bottom) flange, eight strain-gauges were placed on each specimen. These were placed on the edge of the flanges in the areas between the half-pipe stiffener and the plate stiffeners. They were located on both the tension and compression flanges: four on each, to ensure that the load was being applied to the girder appropriately.

Using the assumption that plane sections remain plane the corresponding strain at the top side of the bottom flange was calculated based on the position of the strain-gauges. This was then converted into stress by multiplying by 29,000ksi, the modulus of elasticity of steel.

When a new specimen was placed in the test frame, a static load was applied first. This load was increased from zero up until the desired, maximum stress level was reached. Each specimen was unique and so the strain-gauges were relied upon to

determine the load needed to reach a given stress level. The output from the load cell and the strain gauges were compared with the predicted analytical analysis to ensure there were no major errors, but the strain gauges were used to determine the loading.

The stress range was always set between 5ksi and some greater value, either 20 ksi or 25 ksi depending on the test. For a fatigue analysis, the stress range is primary interest rather than the absolute stress level reached (Fisher et. al 1998).

There were several problems that developed in the hydraulic loading system during the testing of the four specimens that required the loading to be stopped on multiple occasions. Each time a problem occurred the number of cycles, stress range, and all of the settings of the test were recorded. Then the faulty part or parts were identified and fixed or replaced. When the test was restarted, the count was begun from where it had left off with the settings duplicated. This allowed for an accurate continuation of the testing, with measurements taken from the strain gauges to ensure that the same stress range was being achieved.

## CHAPTER 3

# Results of Physical Testing

### 3.1 OVERVIEW

This chapter presents and discusses the results of the experimental program discussed in Chapter 2. Four individual beams were tested, each one having 6 stiffener connections. At the end of testing, each stiffener was examined for cracking that had not been observable during testing and had not caused failure in the beam. The number of cycles to reach failure in each beam, along with the stress ranges that the beams were exposed to was recorded in order to determine the fatigue behavior of the various connections.

### 3.2 INSPECTION FOR CRACKS

During the loading of the specimens and after completion of testing, each beam was examined for the presence of cracks using non-destructive and destructive testing. Non-destructive testing consisted of both visual inspection as well as magnetic particle inspection. Inspection for cracks was done both during testing and after failure. In general, most cracks were discovered while loading was taking place as the crack would open and close as a result of the load cycles and these changes made the cracks more apparent.

Magnetic particle inspection was used to find cracks developing during the loading cycles, or afterwards to find cracks that weren't visible while loading. The magnetic particle method of crack investigation works by creating a magnetic field within the beam and adding fine, magnetic particles to the surface. The particles then align themselves according to the magnetic fields that are generated in the beam. A crack in the

beam causes a change in the magnetic field that changes the pattern of the magnetic particles.

Both unaided visual inspection and magnetic particle inspection were successful in discovering cracks of around a quarter to a half inch long on the surface of the beam. The magnetic particle investigation revealed slightly smaller cracks and made it much easier to identify cracks when the beam was unloaded. It was uncertain; however, what the minimum crack length was that could be observed by either method. Visual inspection and magnetic particle inspection were both limited to crack discovery on the surface of the beam, they could not detect cracks that did not originate on, or propagate to the beam's surface.

Following fatigue testing the stiffener to flange welds were autopsied to locate cracks that had initiated below the surface of the beam, or had not become large enough to be able to see either through general visual inspection or magnetic particle inspection. This was done by first removing the part of the beam that was of interest for testing. Cuts were made with an abrasive saw to remove the part of the beam of interest (see Figure 3-1). Making cuts using a torch was also considered but not used to ensure that heat from the torch would not cause a crack surface near the cutting plane to close-up as a result of the high temperatures generated.



***Figure 3-1: Using an abrasive saw to cut out sections of interest for destructive testing***

The section of the beam which was removed was then cut into small slices, typically about three quarters to one inch wide, using a band saw (see Figure 3-2). These specimens were then bent manually. If there was a crack present, the bending of the piece would tend to open the crack, making it visible.



*Figure 3-2: A piece of the beam that is to be tested for fatigue cracks is cut into five, narrow sections using a band-saw (this is the perpendicular stiffener from beam 30A)*

Continuous plastic deflection was observed when there were no cracks in the specimen being tested, or all the crack sizes were below the threshold which could be revealed by this method. Figure 3-3 shows an example of a specimen that was bent until it was determined that there were no crack surfaces which could be exposed. The cracks observable on the bottom of the specimen were manually created with a band-saw to facilitate bending.

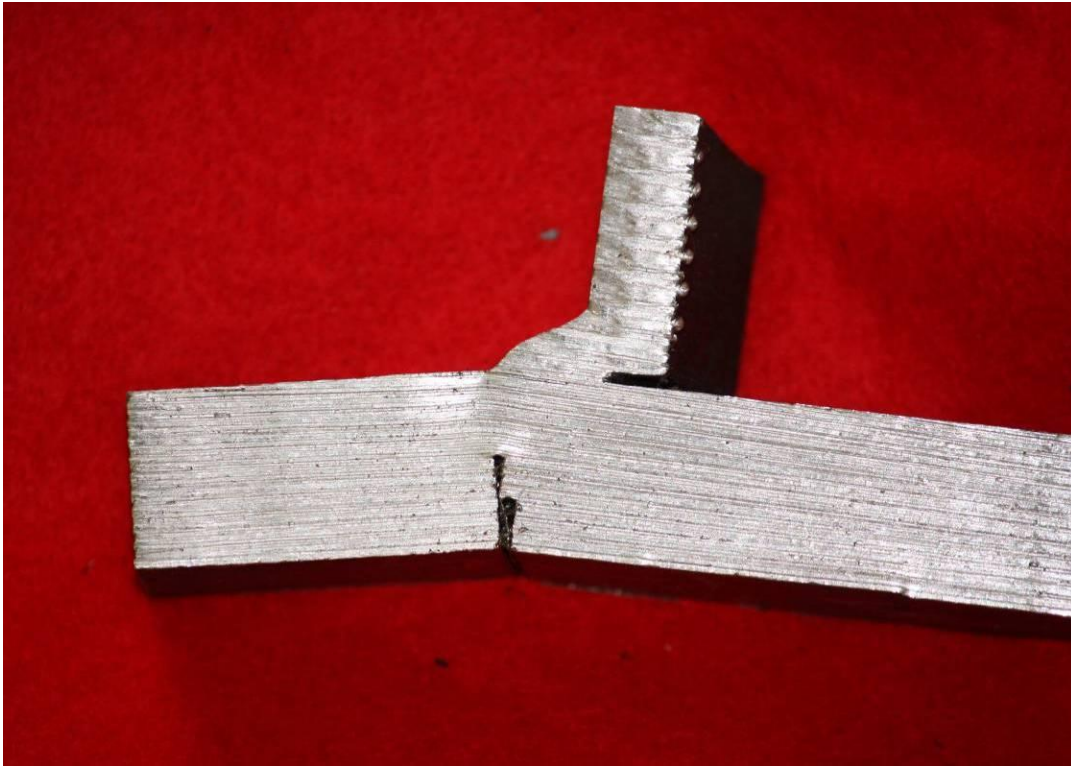


***Figure 3-3: Plastic Yielding in Destructive Testing***

When there was a crack in the specimen being tested, the crack surface would open and reveal where the crack was. Figure 3-4 shows a sliced specimen prior to bending. No cracks can be seen on the surface or looking at a cross-section of the weld. Figure 3-5 shows that same specimen after bending when a clear crack can be observed at the weld toe. This process was used to evaluate each specimen cut from the stiffener to flange weld connections.

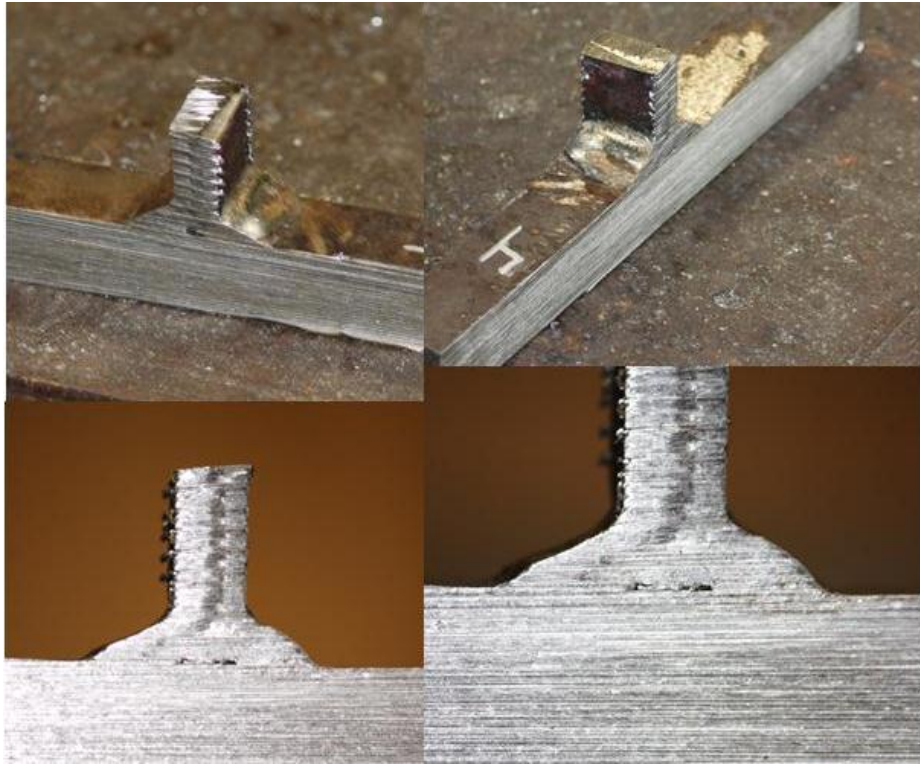


*Figure 3-4: A Specimen before Destructive testing*

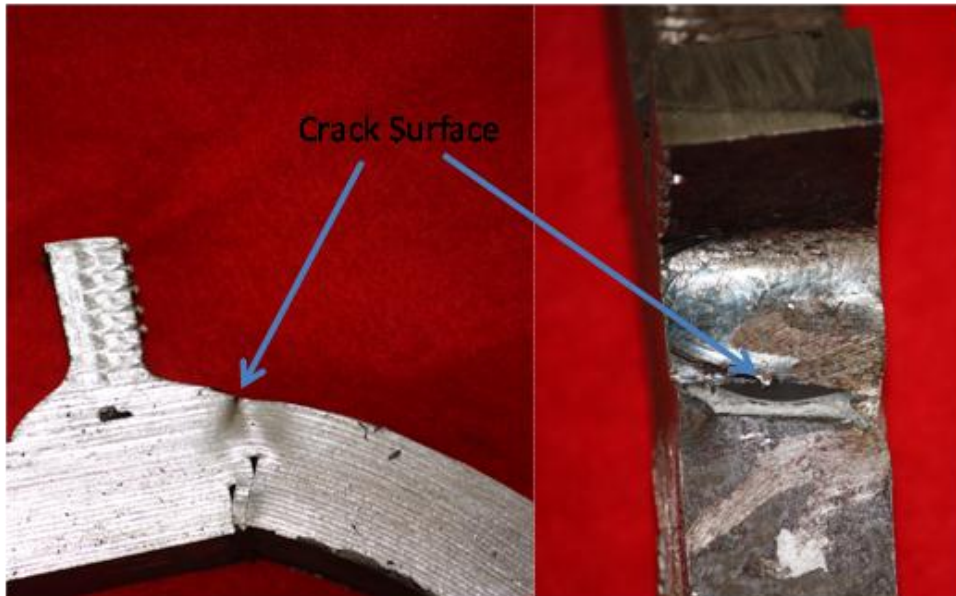


*Figure 3-5: Destructive Testing Revealing a Crack*



### 3.3 BEAM ONE: 30 DEGREE SPECIMEN (30A)

The first beam tested, given the name '30A', had two pipe stiffeners, two perpendicular stiffeners, and two stiffeners at a 30 degree angle (see Figure 3-6). It was loaded with a 15.2ksi stress range 2,059,727 times before a fatigue crack developed at the thirty degree stiffener. A plate was placed over the crack on the bottom of the tension flange and the testing was continued at the same stress range for 810,561 more cycles. At this point a fatigue crack propagated through several feet of the compression flange, initiating at the k-region, not close to any of the stiffeners but underneath one of the loading points of the spreader beam.



*Figure 3-6: Beam 30A with two 30 degree stiffeners, two pipe stiffeners and two perpendicular stiffeners (only one side shown here, the reverse side is mirrored)*

The crack at the 30 degree stiffener appeared to initiate at the weld toe, the outside of the weld, on the interior side of the stiffener (the acute angle side). This can be seen in Figure 3-7. It then propagated inwards, towards the web and out to the edge of the flange. The load cycling was stopped when the crack reached approximately four inches (stopping about one inch from the k-zone).

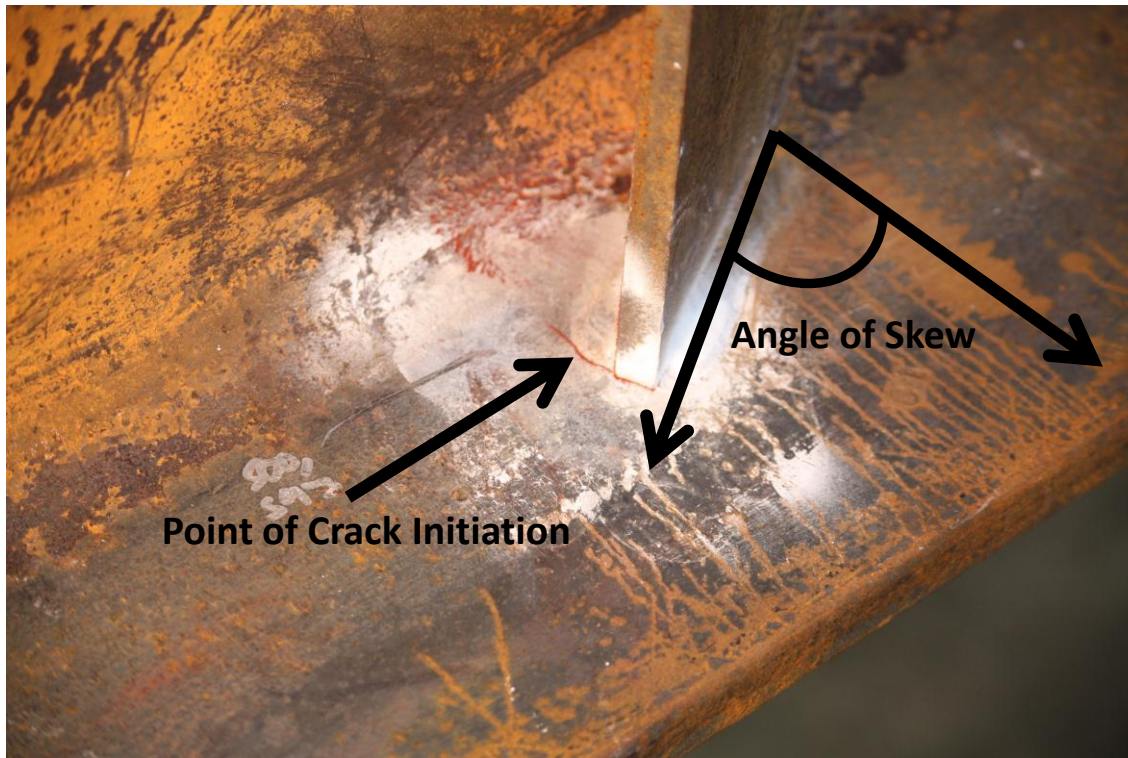


***Figure 3-7: Location of Fatigue Crack on a Skewed Plate-Stiffener***

At this point a plate with dimensions equal to that of the flange in measurements of width and thickness (see Figure 3-8), was bolted to the flange over the cracked area as well as the area that could potentially crack due to the 30 degree stiffener on the reverse side of the beam. The purpose of the plate was to significantly reduce stresses through the portion of the flange itself that was connected to the skewed stiffener, and thus keep the crack from growing and stop any other cracks that had begun to form so that the remaining four connections on the beam could continue to be tested.



***Figure 3-8: A plate is put over the crack surface to prevent the crack from spreading***

Once the overall beam had reached a total of 2,870,288 cycles (all at a stress range of 15.2ksi) a crack was observed on the top, compression flange (see Figure 3-9). This crack was twenty-four inches long, it was not noticed until it had reached this length because it was not in any of the critical areas under observation. The formation of a crack at one of the two load points on the beam at the compression flange is unaccounted for. No theories are put forward as to its cause, only the observation that it is unrelated to any of the connections that were being tested as it was too far away from them on the beam to be significantly impacted by them, and that it ended the testing of Beam 30A, as further cycling was no longer viable in its cracked state.

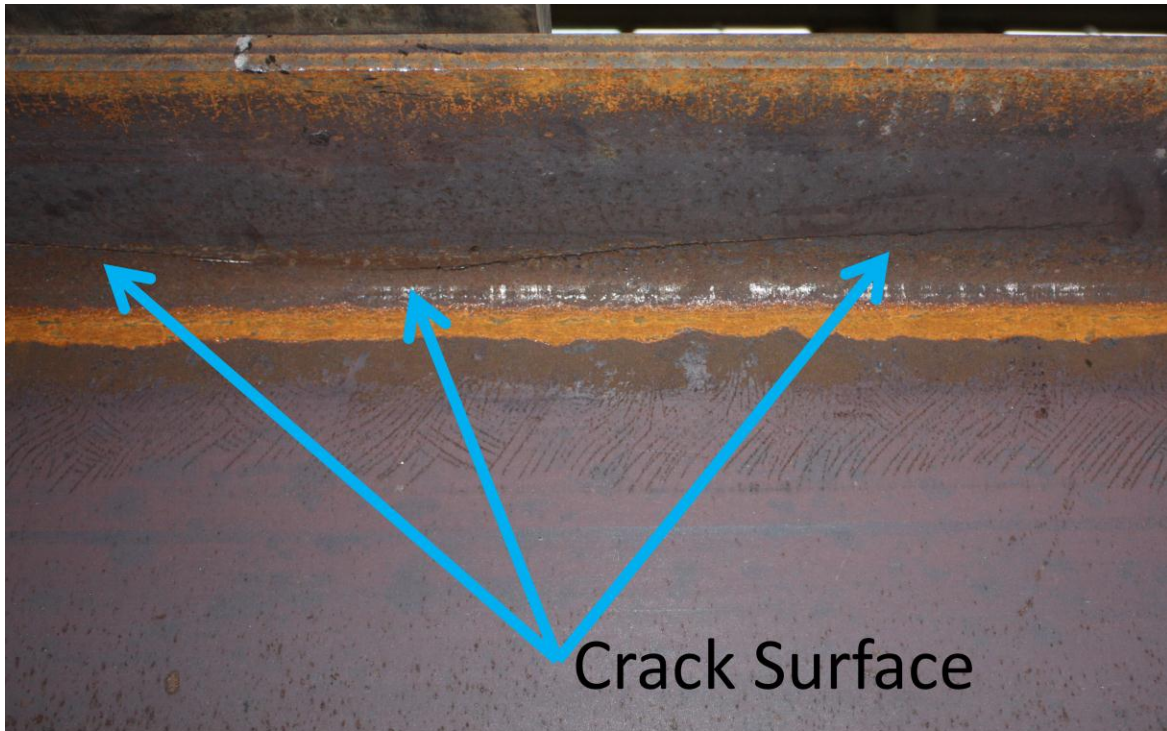


*Figure 3-9: Crack on the compression flange of Beam 30A*

For this specimen, fatigue failure occurred at the connection of the 30 degree stiffener to the girder flange. No other stiffener connections failed, thus the two half-pipe stiffeners and the two perpendicular stiffeners were termed ‘run-outs’, meaning that to the number of cycles they were taken, they did not crack. As a result, all that can be said of them is that they performed above the demands that this test imposed.

To determine if any cracks had formed that had not reached the surface of the flange, or had otherwise escaped visual inspection, both the half-pipe stiffeners and the perpendicular stiffeners were removed from the beam, cut into strips, and bent past their yield state to find any crack initiation sites. No incipient cracks were discovered around the half-pipe stiffener, but a crack was found on both of the perpendicular plate stiffeners. They had formed on the outside of the weld connecting the stiffener to the bottom flange, approximately halfway down the weld’s length.

The test results are compared to AASHTO's fatigue ratings, or categories in Figure 3-10 (AASHTO 2007). For the connections in this beam, one of the 30 degree stiffeners failed after having passed the B' line (doing better than the lower limit of that category), the performance of the second 30 degree stiffener was unclear, as the flange plate installed altered the stresses going through the flange at that area after the first, 30 degree stiffener failed.

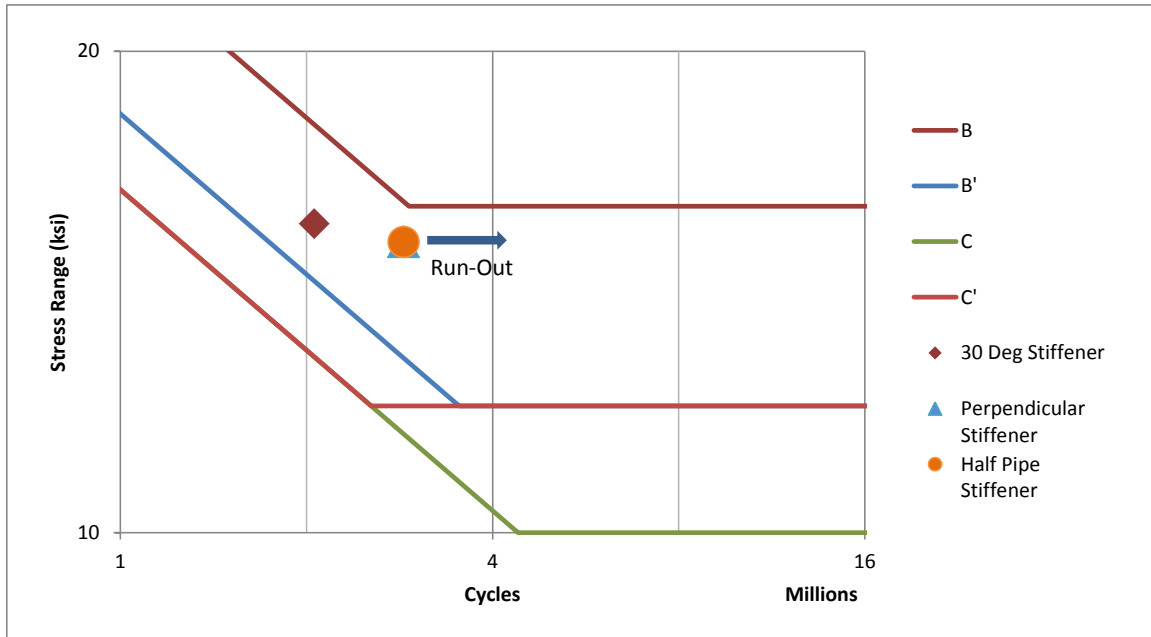


**Figure 3-10: A S-N plot of the fatigue life of Beam 30A**

The half pipe stiffeners and perpendicular stiffeners both ran-out, again beyond the B' line. At 15.2ksi, the stress range was too low to demonstrate that any connection could perform above the B category, as B category details are assumed to never fail at a stress range lower than 16ksi. The additional cycles undergone by the remaining stiffeners therefore did not change the AASHTO fatigue category.

### 3.4 BEAM TWO: 60 DEGREE SPECIMEN (60A)

The second beam tested, given the name '60A', had two half-pipe stiffeners, two perpendicular stiffeners, and two stiffeners at a 60 degree angle. It was loaded with a 15.6ksi stress range 1,451,654 times before a fatigue crack developed at the sixty degree stiffener. A plate was placed over the crack on the bottom of the tension flange and the testing was continued at the same stress range for 1,565,975 more cycles. The beam, including both half-pipe stiffeners and both perpendicular stiffeners reached a total of 3,017,629 cycles. Testing was stopped at this point because a fracture had developed at the edge of the plate used to cover the initial crack (at the edge of the fraying surface: see Figure 3-11).



*Figure 3-11: Crack on 60A at the edge of the repair plate*

Destructive testing was performed on this beam as well, for both the pipe stiffeners and the perpendicular plate stiffeners. No cracks were discovered on any of the

tested areas for this beam. The method of testing (bending small strips of the flange connected to the weld) does not yield conclusive proof that no cracks were forming, but would generally reveal any significant fractures, including those too small to observe without testing. Each strip can only be bent in one direction, which limits the testing to either just one side of the weld, or half of each side of the weld.. The latter approach was used in this project. Thus, that no cracks were discovered in these tests is not proof that they did not exist. However, when cracks are observed by this method, as was the case with Beam 30A, it gives information as to the location of future crack growth as well as showing that the limit of that particular connection’s fatigue life is being approached.

Test results for Beam 60A are compared to the AASHTO fatigue categories in Figure 3-12. Here one of the sixty degree stiffeners passed the category C rating, but not the category B’ line. The two half-pipe stiffeners and two perpendicular stiffeners both ran out after having passed the category B’ line. The stress range used here, 15.6 ksi, was again too low to pass the minimum 16 ksi limit for the B category.

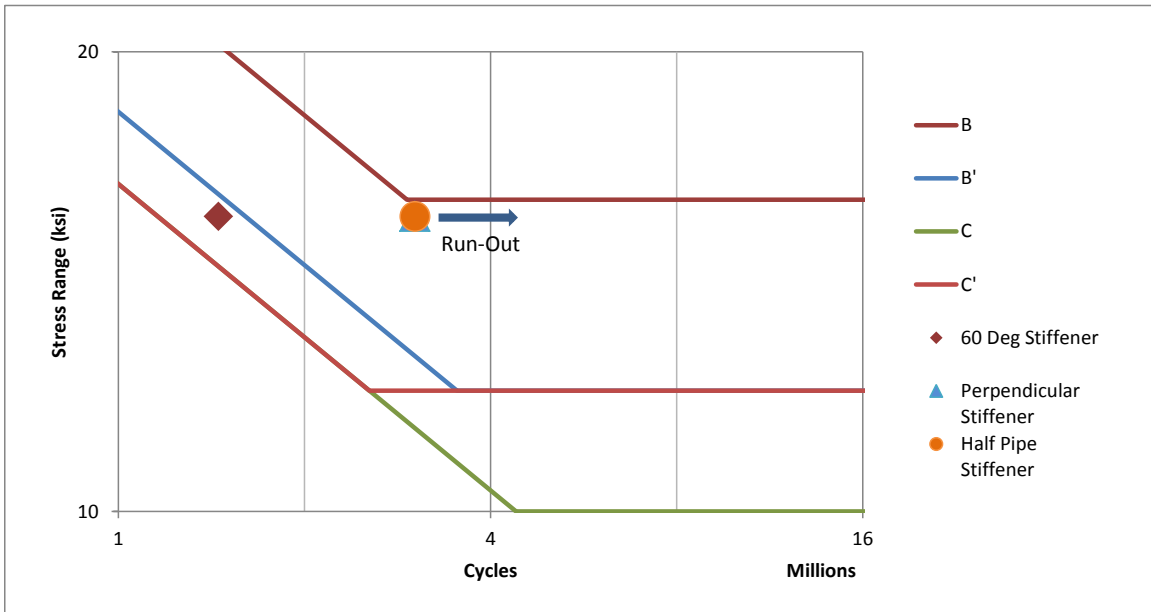


**Figure 3-12: A S-N plot of the fatigue life of Beam 60A**

### 3.5 BEAM THREE: 30 DEGREE SPECIMEN (30B)

The third beam tested, given the name '30B', had two half-pipe stiffeners, two perpendicular stiffeners, and two stiffeners at a 30 degree angle. It was loaded with a 15.4 ksi stress range for 3,250,000 cycles before the testing was stopped. No fatigue crack was observed at any point along the beam at the time the decision was made to end the test and switch to the next beam.

The stress range used, 15.4 ksi, was again too low to pass into a category B range, and the category B' range was passed at about 1.5 million cycles less than half the total cycles undergone by this beam. It was determined that no further information could be provided by continuing to cycle the beam. Figure 3-13 shows the test results in comparison to the AASHTO fatigue categories.

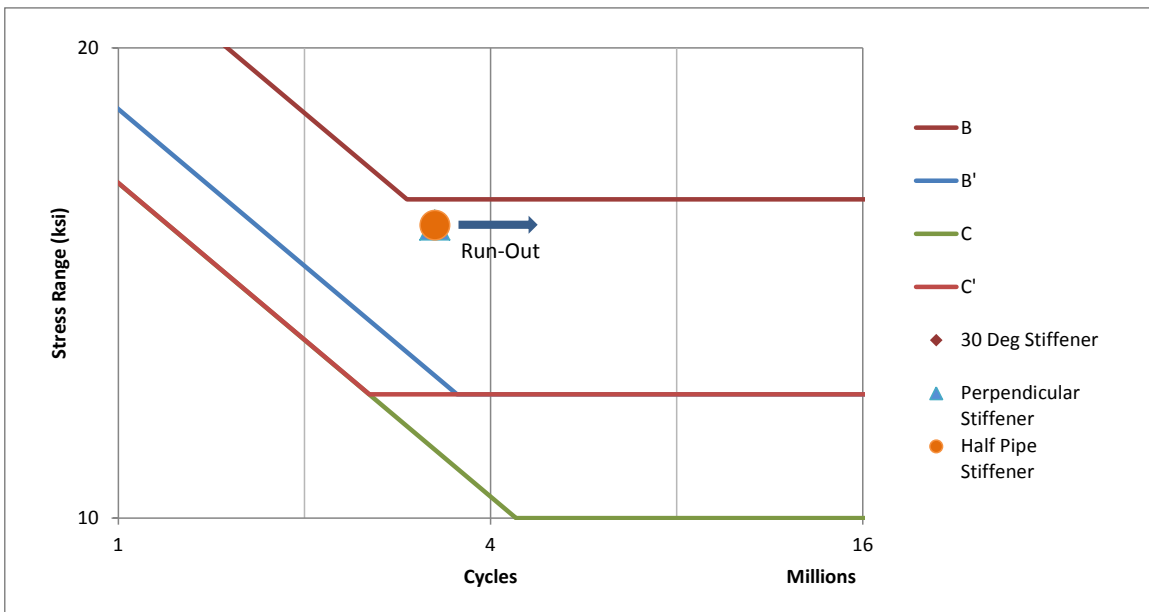


*Figure 3-13: A S-N plot of the fatigue life of Beam 30B*

### 3.6 BEAM FOUR: 60 DEGREE SPECIMEN (60B)

The fourth beam tested, given the name '60B', had two half-pipe stiffeners, two perpendicular stiffeners, and two stiffeners at a 60 degree angle. It was loaded with a



21.7 ksi stress range for 501,593 cycles before a fatigue crack was observed in the girder tension flange at the sixty degree stiffener. A plate was placed over the crack on the bottom of the tension flange and the testing was continued at the same stress range for 599,445 more cycles. The beam, including both half-pipe stiffeners and both perpendicular stiffeners reached a total of 1,101,038 cycles. Testing was stopped at this point because a crack was observed in the girder tension flange at one of the perpendicular stiffeners.

Though the total number of cycles is significantly lower than previous tests, the high stress range makes the results consistent with them when comparing against the AASHTO fatigue categories. This was also the only case where a crack was observed at a perpendicular stiffener during the test besides the small cracks detected during the autopsy. The crack observed at the 60 degree stiffener was similar to that seen with the previous 60 degree stiffener and with the 30 degree stiffener that failed. A crack started at the acute, exterior weld toe and propagated through the flange perpendicular to the longitudinal axis of the beam.

For Beam 60B, the crack in the girder flange at the perpendicular plate stiffener occurred along the length of the weld. The location of the crack initiation could not be determined more precisely than being on the toe of the weld. The crack spread along the entire length of the weld through the flange, and testing was stopped before it progressed through the entire flange width.

Overall testing on Beam 60B had to be stopped at the formation of this second crack, causing both the half-pipe stiffener and the perpendicular stiffener to be placed at the same location on the S-N plot. However, for the half-pipe stiffener, this point denotes run-out whereas for the perpendicular stiffener this point denotes failure. Figure 3-14 shows the results for Beam 60B on an S-N plot with the ASSHTO fatigue categories. The higher stress range for this specimen would have allowed for the half- pipe stiffener to have potentially passed into the range of category B. However, the test was terminated before reaching a category B rating and so it remains undetermined if the pipe stiffener

could reach that rating. The 60 degree stiffener passed the C category, but did not reach B', as the other two stiffener types did.

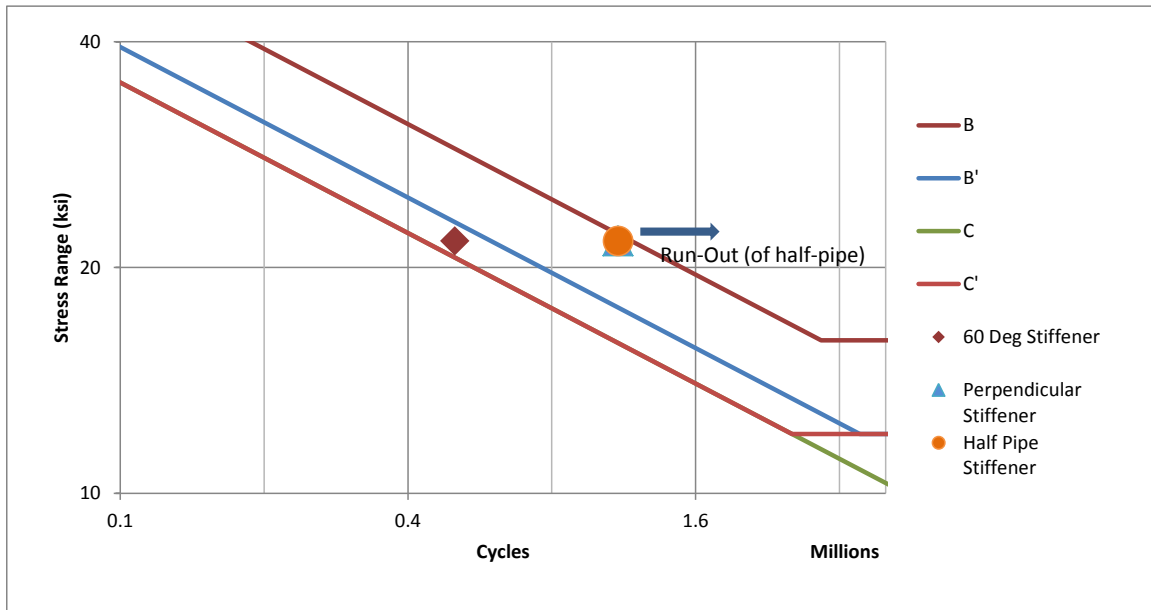


*Figure 3-14: A S-N plot of the fatigue life of Beam 60B*

### 3.7 COMPILATION OF RESULTS

Each beam tested represented six individual connections between stiffeners and the girder tension flange. These six connections included two perpendicular stiffeners, two skewed stiffeners which were placed at either a 30 degree or 60 degree angle, and two half-pipe stiffeners. In the following sections, the results of the tests are summarized.

#### 3.7.1 Skewed Plate Stiffeners

There were eight different plate stiffeners tested at an angle to the web, or skew, four at 30 degrees and four at 60 degrees. Of those eight, three failed during testing. Because of the method employed to stop crack propagation: the addition of a plate over the crack, the equivalent skewed plate stiffener that was on the reverse side of the beam

was not tested after the cracking of its partner and so can only be said to be better than the fatigue life achieved by the first one to fail.

**Table 3-1: Performance of Skewed Stiffeners**

Beam	Stiffener on Specimen (deg)	Stress Range (ksi)	Total Cycles (cycles)	Failure / Run-Out
30A	30	15.2	2,059,727	Failure
30B	30	15.4	3,250,000	Run-Out
60A	60	15.6	1,451,654	Failure
60B	60	21.7	501,593	Failure

Table 3-1 shows a summary of each of the skewed or angled stiffeners. In none of the four beams tested did the skewed stiffeners outperform either of the other two connection types (the half-pipe stiffener and perpendicular plate stiffener). Both failures of a 60 degree skewed plate stiffener occurred after they had passed the category C threshold but before they reached the B' category. The failure of the 30 degree skewed stiffener occurred past the B' category, and two 30 degree stiffeners (those on Beam 30B) ran-out past the B' category (but at a stress range that did not allow passing the B category line). This can be seen in Figure 3-15, which shows the skewed stiffener results plotted against the relevant AASHTO fatigue category lines.

The failure of the skewed stiffeners initiated, in every case, on the exterior weld toe on the interior side of the stiffener. That is, at the edge of the weld, on the end nearest

the outside of the flange, on the acute side of the skew angle. These cracks developed at the weld toe, and then grow perpendicular to the longitudinal axis of the beam. The orientation of the cracks was therefore perpendicular to the direction of the flexural stress in the flange.

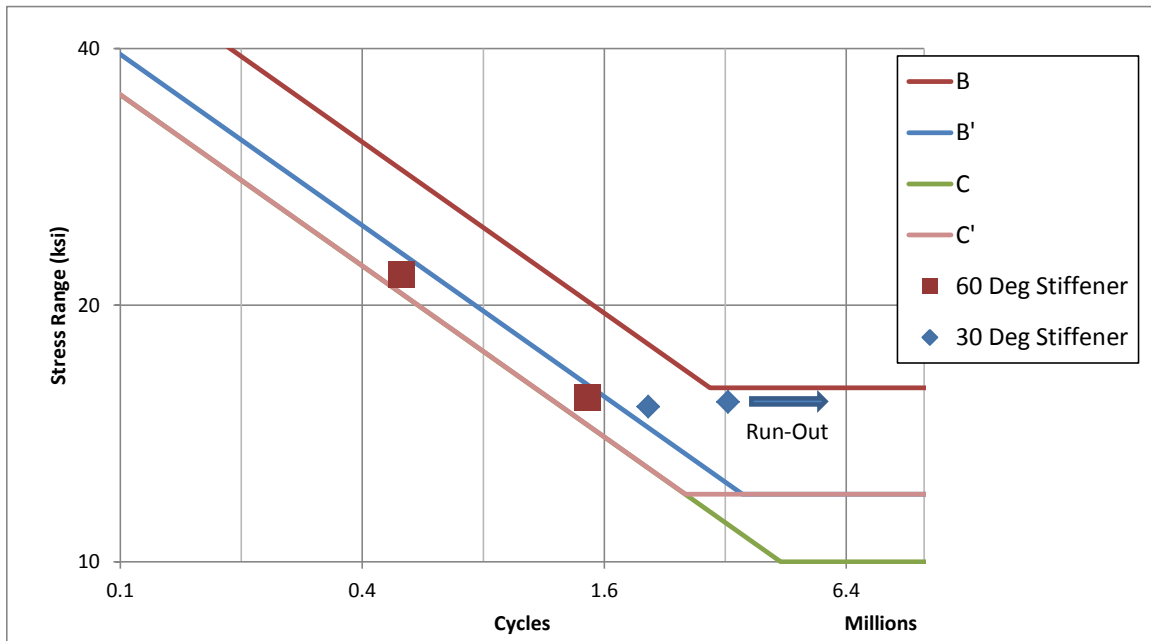


*Figure 3-15: A S-N plot of the fatigue life of skewed stiffeners*

### 3.7.2 Perpendicular Stiffeners

Every one of the four beams tested had two perpendicular stiffeners welded to them. Thus a total of eight perpendicular stiffeners were tested, out of which one failed due to fatigue cracking. Two of them, when taken apart following testing, showed evidence that fatigue cracks had developed, but had not been detectable before dissection. The remaining five did not crack and showed no incipient cracks upon dissection.

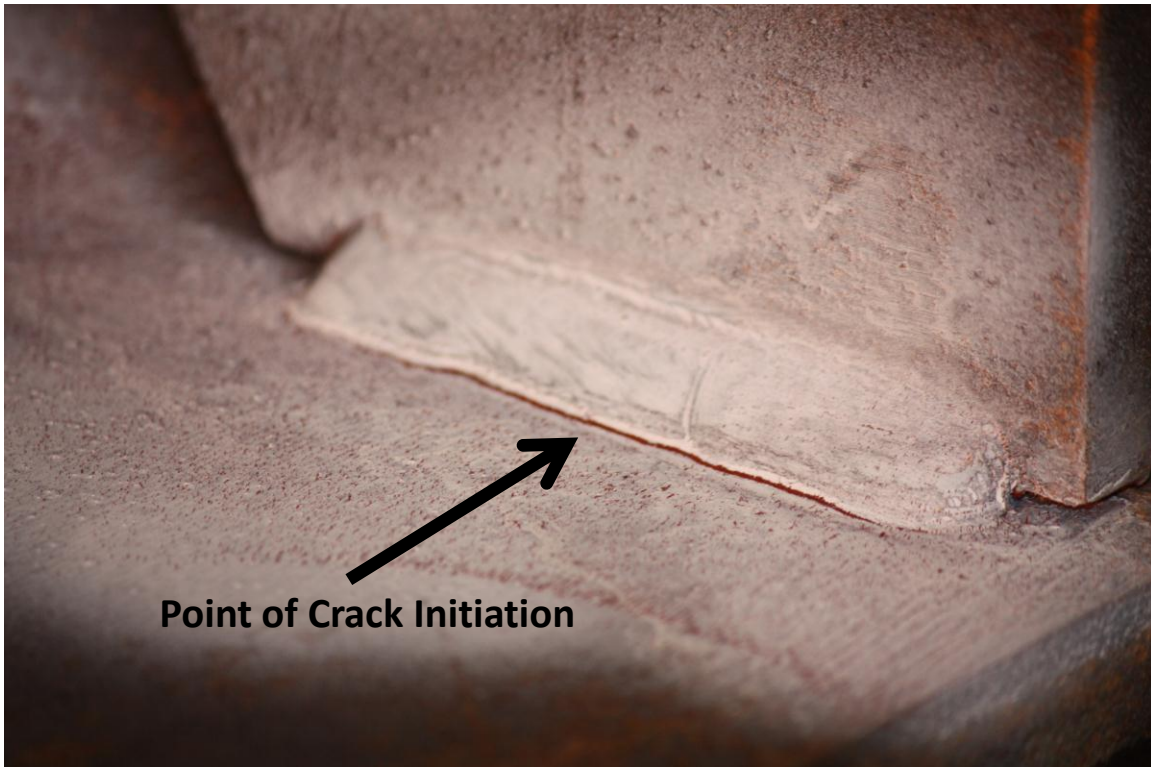
The failed perpendicular stiffener developed a crack on the weld toe, at the outside of the weld: closest to the edge of the flange. Figure 3-16 shows a picture of this crack, taken after magnetic particle inspection. The red metal particles lay along lines of material discontinuity: in this case a fatigue crack. The metal particles were also

attracted to the edge of the weld, and the plate stiffener itself, but these lines both represent geometric discontinuities even without a fatigue crack. This made it impossible to determine if the crack observed here was a continuation of a crack along the length of the weld, or if the entire crack was located at the end of the stiffener near the free end of the flange.



***Figure 3-16: Fatigue crack at a perpendicular stiffener on beam 60B***

The two cracks discovered through dissecting a beam after cycling were both found on Beam 30A. Each showed a semi-circular area beginning at the top of the flange and moving down approximately one third of the thickness. Each crack was found about half-way along the length of the weld, at the weld toe as seen in Figure 3-17.



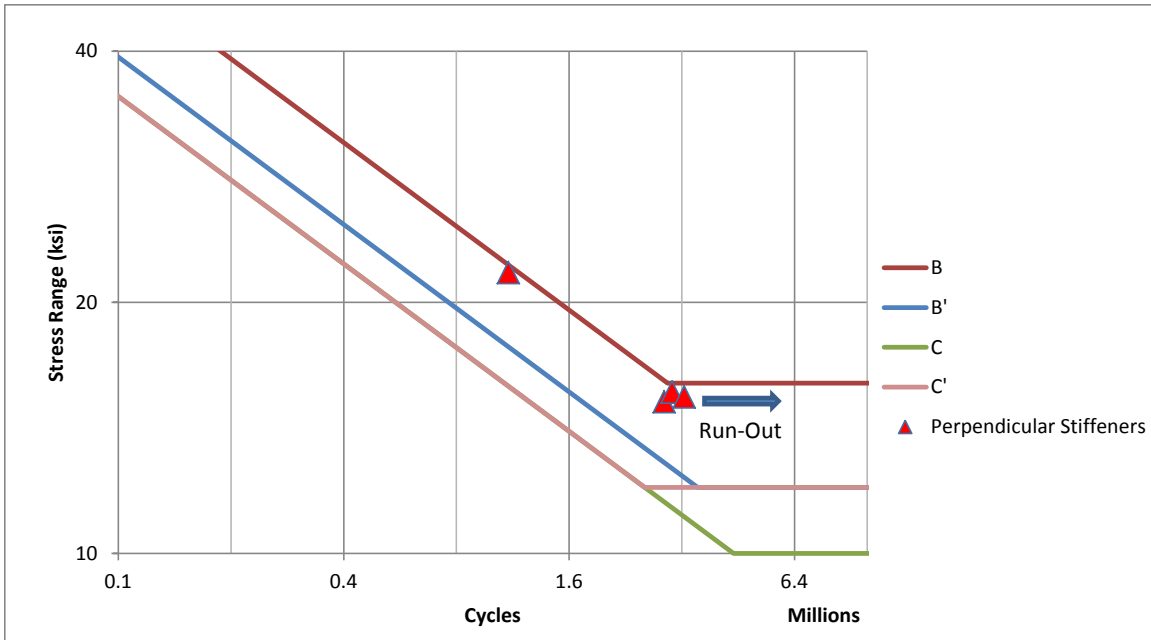
***Figure 3-17: Location of Fatigue Crack on a Perpendicular Plate-Stiffener***

Table 3-2 shows a summary of the performance of the perpendicular stiffeners. The discovery of incipient cracks in two of the perpendicular stiffeners would indicate that they were near failure, but do not provide a specific number of cycles to failure; thus all that can be said of the three beams which had both perpendicular stiffeners run-out without a test-ending fatigue crack is that those stiffeners performed better than the stress-range and cycle count that the beam underwent. The beam that did experience a failure of its perpendicular stiffener also had a second one that did not fail.

**Table 3-2: Performance of Perpendicular Stiffeners**

Beam	Stress Range (ksi)	Total Cycles (cycles)	Failure / Run-Out
30A	15.2	2,870,288	Run-Out
30B	15.4	3,250,000	Run-Out
60A	15.6	3,017,629	Run-Out
60B	21.7	1,101,038	Failure

Figure 3-18 shows a S-N plot of the perpendicular stiffeners with the relevant AASHTO fatigue categories. All of the perpendicular stiffeners performed above the B' category, but the stress range of three of the beams was below the theoretical limit for a category B failure. The fourth beam, which was cycled at an increased stress range, had a failure on the perpendicular stiffener before crossing into category B range.



*Figure 3-18: A S-N plot of the fatigue life of perpendicular stiffeners*

### 3.7.3 Half-Pipe Stiffeners

There were two half-pipe stiffeners on each of the four beams tested, none of which failed or showed developing cracks after dissection. In every testing case some other method of failure forced termination of testing before any cracks could be detected at the half-pipe stiffeners. Table 3-2 and Figure 3-18, who that the results for the perpendicular stiffeners also represent the results for the half-pipe, except that in every case there was run-out of the half-pipes. Each data point exceeded the AASHTO category B' limit, but did not reach category B. The half-pipe stiffener connections in this test can be said to be better than the category B' as specified in AASHTO.

### 3.8 SUMMARY OF RESULTS

The primary purpose of the laboratory testing was to evaluate the half-pipe stiffener's fatigue performance in relationship to that of conventional plate-stiffeners.



The tests were also intended to provide data for validation of finite element models that can be used for further in depth studies.

### 3.8.1 Evaluation of the Half Pipe

*Table 3-3: Summary of Results*

Beam	Stiffener on Specimen (deg)	Stress Range (ksi)	Failure of Skewed Stiffener (cycles)	Second Failure (cycles)	Type of Failure
30A	30	15.2	2,059,727	2,870,288	Flange Crack
60A	60	15.6	1,451,654	3,017,629	Friction Crack
30B	30	15.4	N/A	3,250,000	Run-Out
60B	60	21.7	501,593	1,101,038	Crack at Perpendicular Stiffener

Table 3-3 shows the full results for each beam tested. The first three tests, (30A, 60A, and 30B) all had a stress range of approximately 15ksi, and reached about three million cycles. In none of these cases did anything but the skewed stiffener fail. The fourth beam was tested at a stress range of approximately 22ksi for about one million cycles. Here both the skewed stiffener and the perpendicular stiffener failed.

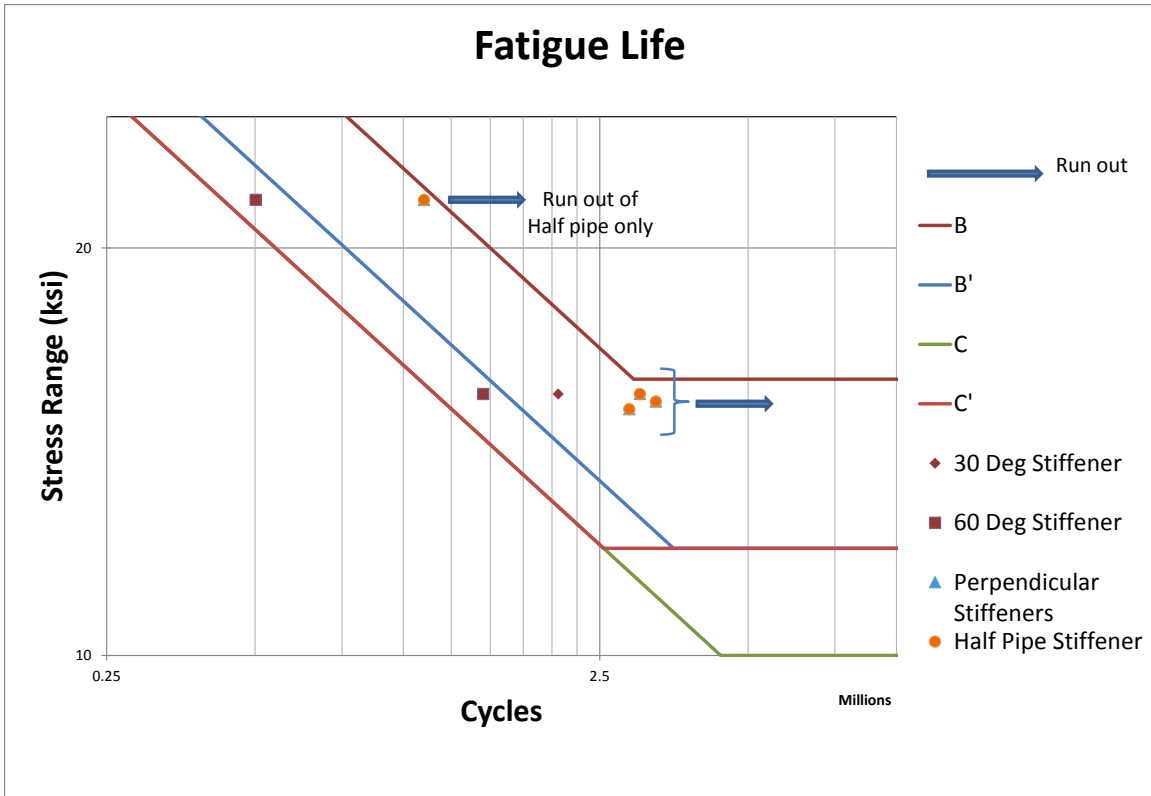


**Figure 3-19: A S-N plot of each of the beams tested**

Figure 3-19 shows the final results of the laboratory testing. Each of the 24 connections tested performed above the AASHTO category C line, and all but the sixty degree skewed stiffeners out-performed the category B' line. However, it should be noted that the reference AASHTO lines are drawn for design, and are two standard deviations below the mean. The testing concluded for this project had an insufficient number of data points to obtain a reliable standard deviation; however, passing the design C category line by such a small margin, it is unclear that the 60 degree stiffeners would actually achieve a C category rating after more exhaustive testing.

With no failures occurring in the half pipe stiffeners, there can be no metric for determining a standard deviation of performance. There were a total of eight, half-pipe stiffeners tested, each one having performed as well as or better than any of the other

connections tested. The run-out of the half pipes occurred at a cycle count 30 to 70 percent greater than what was required to reach a category C rating. If failure actually occurred at every test instead of a run-out, the standard deviation (using Student's T distribution because of the small sample size) would be 16% of the necessary cycles to reach category C, with an average of 154% of a category C rating cycle-count, or more than two deviations above the category C line. This suggests that the half-pipe stiffener detail can provide fatigue performance corresponding to a category C rating or better.

The central question as to the half pipe stiffener's performance as compared to the other stiffeners' performances was answered as conclusively as is possible by the four beam tests. In every case testing revealed that the half-pipe stiffener performed as well as or better than all the other stiffener types.

### **3.8.2 Test Observations for Comparison with Finite Element Model**

The next chapter describes a finite element model that was developed to permit more in-depth study of the fatigue characteristics of the half-pipe stiffener and the conventional plate stiffeners. The model is intended to permit investigation of the effect of a number of variables on fatigue performance, such as pipe or plate thickness, girder flange thickness, weld size, and others. To help validate the finite element model, key behaviors were noted from the laboratory testing. All the observations used to correlate the model with the tests were of a qualitative nature, as no quantitative data collected in the tests could be used to correlate directly to quantitative values produced computationally.

The first general observation was the comparative failure life of each stiffener. The skewed stiffeners failed first in each specimen with the 60 degree skewed stiffener failing before the 30 degree skewed stiffener. The perpendicular stiffener failed once and the half-pipe stiffeners did not fail at all. That relationship may not indicate that the perpendicular stiffener detail is worse than the half-pipe detail, as there was insufficient data to make such a conclusion, but it does suggest that the two are either close, or the

half pipe is better. With no failure of the half-pipe stiffener there is no lower bound given from the physical testing.

Secondly, the skewed stiffener failed along a line that was perpendicular to the direction of the flexural stress in the flange. The fatigue crack propagated 90 degrees to the longitudinal axis of the beam, or in the direction that suggests that the bending stress was in the same direction as the principle stress at the crack. The skewed stiffeners also always had crack initiation on the exterior edge of the weld toe, on the interior side of the skew.

Finally, the perpendicular stiffeners showed the development of cracks on the weld toe, in the middle of the length of the weld after destructive testing. The only crack that became visible during testing was located on the exterior edge of the weld toe. These are non-definitive results, but suggest that the stress may be more evenly distributed along the length of the weld, rather than concentrated in one location.

## CHAPTER 4

### Development of Finite Element Model

#### 4.1 PURPOSE OF THE FINITE ELEMENT MODEL

The laboratory testing that was completed examined only one design for a half-pipe stiffener. No modifications of the size of any component of the total design (for the half-pipe itself or the girder dimensions) were examined in the physical testing. Therefore it is unknown if the results from these tests apply to other possible designs. A computational model was therefore needed to examine different geometries of the design to determine the impact of changing various parameters.

The model that was produced was used to examine the impact of geometric factors on the stress concentrations produced by the half-pipe detail. Other factors impacting the fatigue life, such as weld quality, were not included in the model. The only indicator of fatigue performance taken from the finite element models was the maximum stress concentration generated.

The results of the computational analyses are intended to provide insight into the range of applicability for the findings of the laboratory testing. If a wide range of stress concentrations are found in the analysis based on small changes in the geometry, then further physical testing may be needed to evaluate the fatigue performance of the half-pipe stiffener. On the other hand, if the stress concentrations predicted by the analysis vary over only a limited range for typical design variations, then the half-pipe stiffener can be used with reasonable confidence based on the limited testing.

#### 4.2 USE OF ANSYS

A finite element model divides the overall structure into many, smaller pieces for the purpose of analysis. Based upon the applied forces or displacements, the model can be used to determine the stress flow through the elements. By breaking down the overall

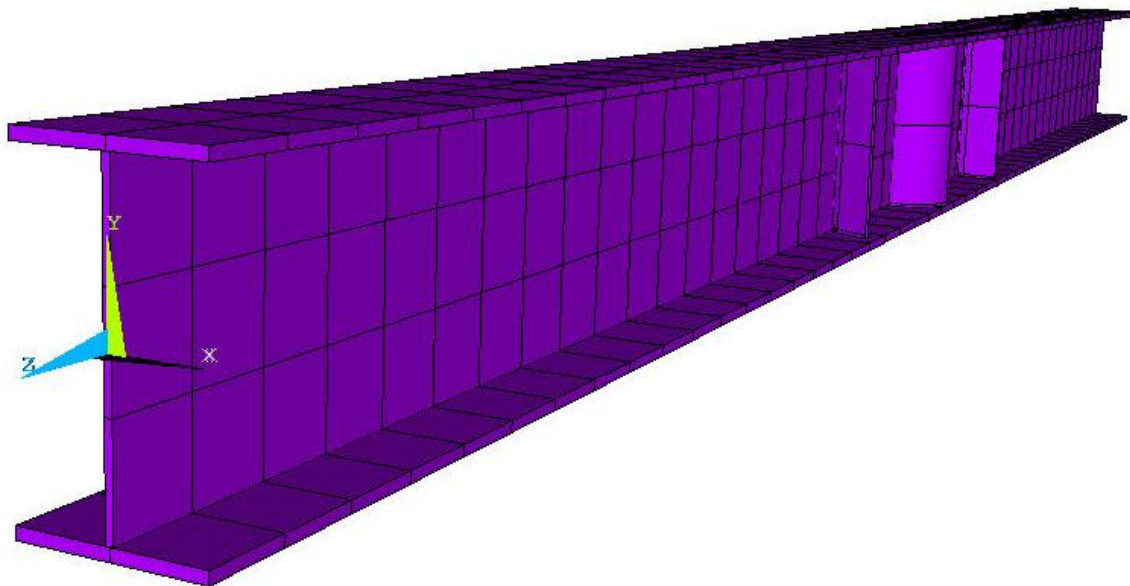
structure into many smaller parts, the impact of discontinuities or small geometrical changes can be found in terms of the stress or strain at any point of interest on the structure.

To create a finite element model a program had to be selected which could carry out an analysis of sufficient detail so as to produce physically meaningful results. This meant that the elements used in the analysis had to be small enough so as to accurately capture the geometry of the welded connection as well as the stress field that was to be produced by the analysis. The actual values selected for the modeling and the motivating factors for those selections are discussed in 4.4.2, but the general selection of a computational product was based on the knowledge that a 3D mesh of a high density would be needed in order to accurately model the behavior of the problem.

ANSYS version 11.0 (ANSYS 2007), a multi-purpose analysis software, was chosen to perform the modeling for this project. ANSYS has the ability to handle a very high mesh density (limited only by the power of the computer used to run the program) as well as perform all the analysis that was needed for the project. It can vary mesh densities through-out the model to allow for run-optimization, create high-precision results based on the stress fields that developed, and the model could handle arbitrary geometries which removed any restrictions on choosing how to model the overall half-pipe detail.

### **4.3 GEOMETRY OF MODEL**

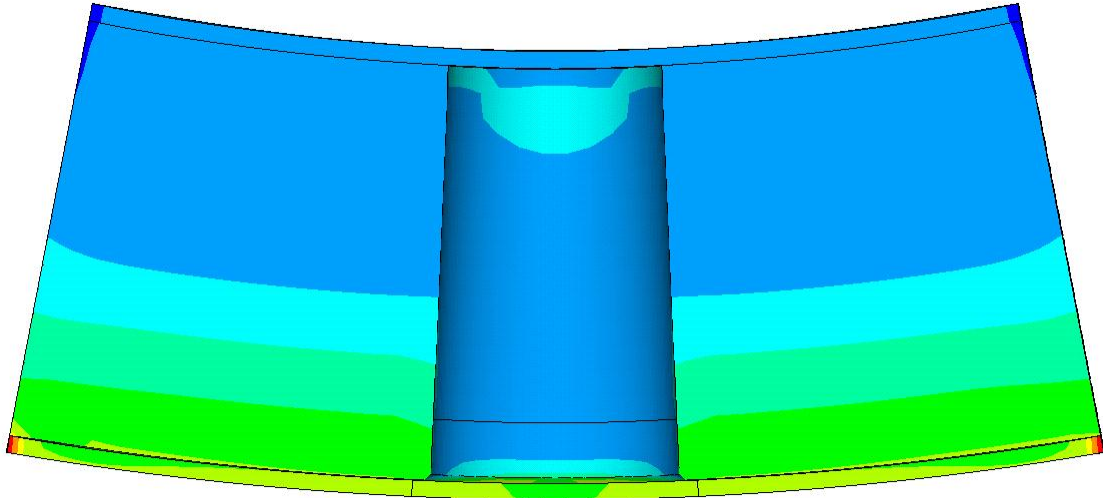
The first model created was a simulation of the specimen that was tested in the laboratory. Various versions of the model were created to recreate the physical test results. A full length beam with all six connections found in the laboratory model was looked at, but found to be too large for efficient testing when using a sufficient mesh density that would be able to capture the true behavior of the different connections. It was also found to be unnecessary, as a much smaller model served to give accurate results and do so with significantly reduced computational time.



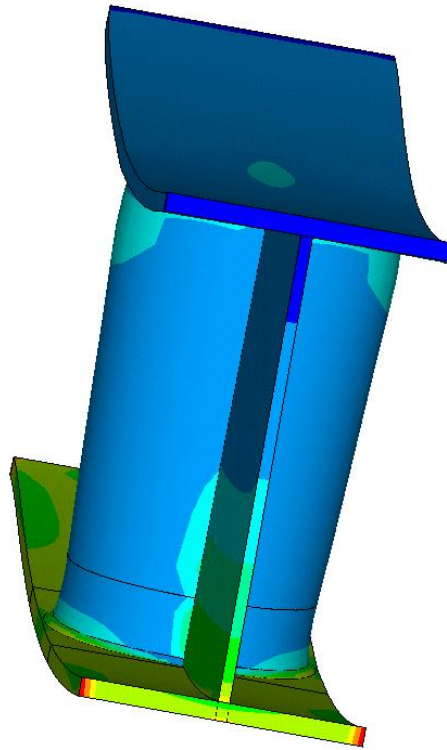
***Figure 4-1: An Image of the ‘Alpha’ ANSYS Model Which Simulated the Full Beam with All Six Connections Found in the Laboratory Testing***

Figure 4-1 shows an image of the first model created in ANSYS, labeled the ‘alpha’ model. This model was continually varied and improved upon until the final model was created. This final model (the ‘Epsilon’ or fifth model version only included a small portion of the beam and one connection, either a half-pipe or plate stiffener. In order to eliminate the majority of the beam while retaining accuracy, deflections were imposed on the ends of the beam that induced pure flexure.

Figure 4-2 and Figure 4-3 shows the deformed shape of the model version which includes two half-pipe stiffeners. Figure 4-2, an elevation view, shows the displacement control of the ends of the beam. This simulates a constant moment section as was created in the laboratory using a spreader beam. The colors in the model represent stress concentrations.



*Figure 4-2: Deformed Shape of Epsilon Model, Elevation View*



*Figure 4-3: Deformed Shape of Epsilon Model, Rotated View*



### **4.3.1 Selecting Sizes and Symmetry**

When a satisfactory model had been built, various parameters were defined to ensure accuracy and reduce computational time. The addition of symmetry, determining of model geometry necessary to minimize the impact of shear lag on the stresses at the stiffener, and sensitivity to mesh density were all considered. A sensitivity analysis of some of the pertinent parameters was conducted by monitoring fluctuations in the stress concentration at the half pipe stiffener was altered as a result of changes in model/mesh geometries. This ensured that the solution was not sensitive to parameters which were only meaningful in the model (such as the length of the beam modeled) and that the final values selected allowed for sufficient accuracy.

### **4.3.2 Determining Parameters and Modeling Guidelines**

Figure 4-4 shows the change that varying the length of the section modeled has on the stress concentration factor. The stress concentration factor is discussed in detail in Section 4.5.2; it represents the result of interest for the overall study. If the changes are too large it would indicate that the model being used is not reliable, or not enough of the beam is being modeled to ensure precision. This method of examining the stress concentration, or stress concentration factor to identify the appropriate values to use for the model was employed through-out the process of model creation.

The length of the modeled section is a computational variable only, and should not have an impact on the final results if the modeling is done properly. Figure 4-4 shows very slight changes in the stress concentration factor as the model length changes, and a total length equal to 1.75 times the depth of the girder was selected to ensure that there was sufficient precision.

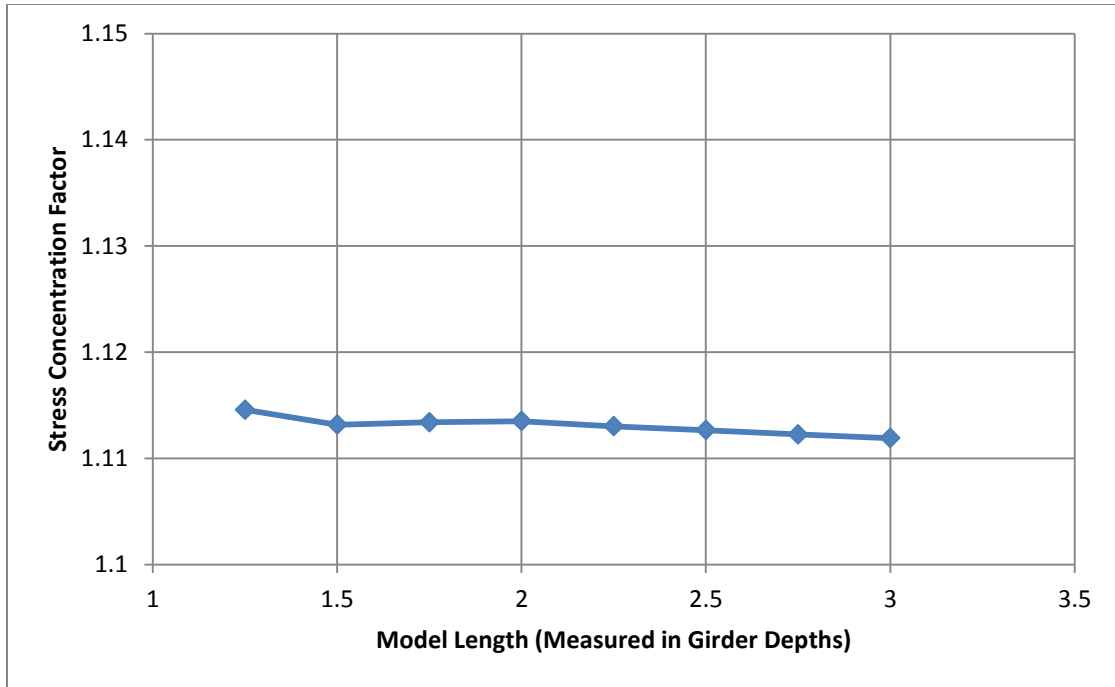


***Figure 4-4: The Impact of the Model Length on the Stress Concentration Factor***

Whenever a value of this type of variable, i.e., one important only for the computer model to function accurately, but not descriptive of a real world variable was needed, it was always chosen in terms of another variable, not as an absolute. In the case of the model length, it was measured as a factor of the depth of the girder. This relationship was chosen as the girder depth controlled the effect of shear lag, a possible source of error against which a larger model length was protecting.

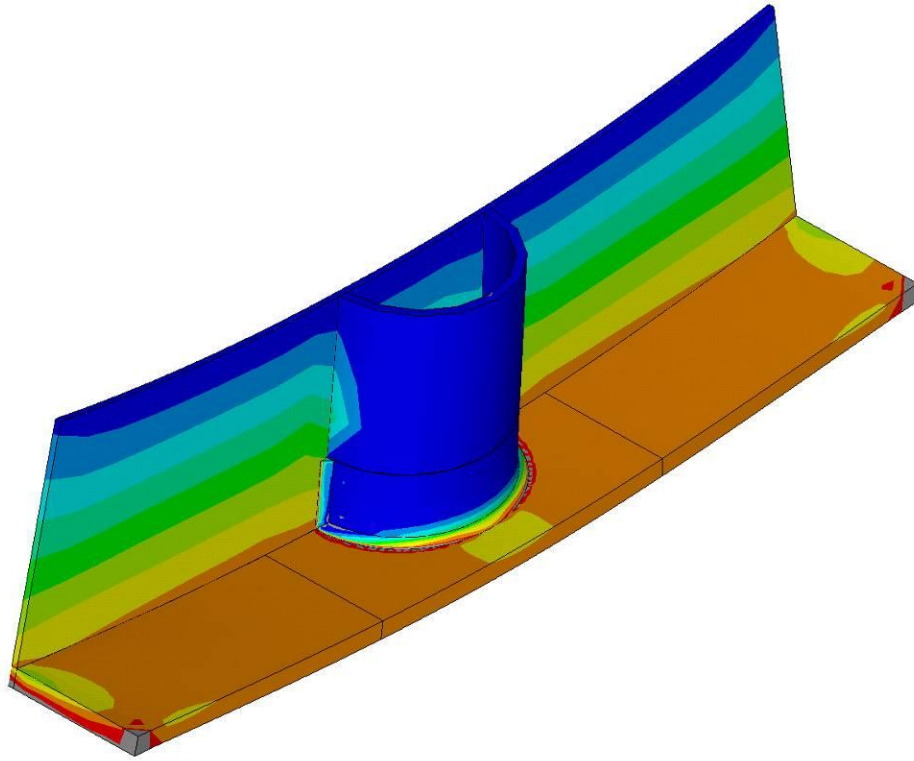


***Figure 4-5: Model of Half-Pipe Using Symmetry***

To allow for significantly increased speed of analysis, and thus a greater number of total data points collected, symmetry was employed to reduce the number of mesh elements and connections needed. Figure 4-5 shows an image of the model reduced with the use of symmetry conditions. Here symmetry is applied in the middle of the web, along the plane of the web, and anti-symmetry half-way through the cross-section. It is anti-symmetric as the imposed moment on the doubly-symmetric section causes the reverse stresses on the top half of the section.

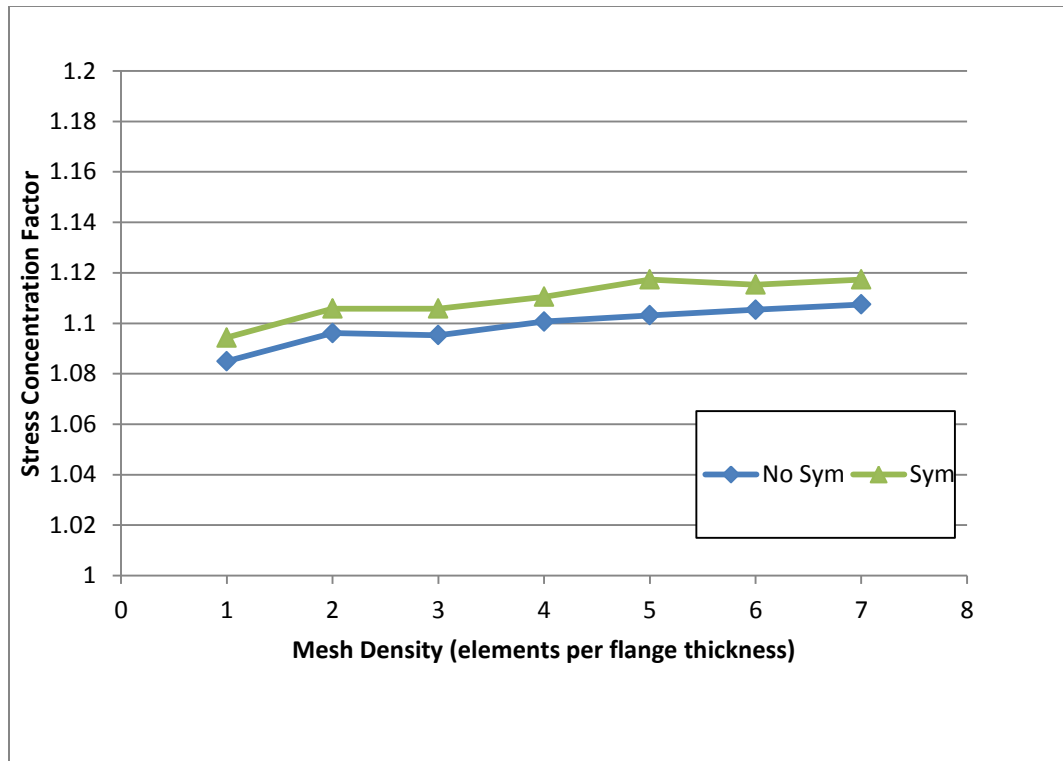


**Figure 4-6: The Impact of Imposing Symmetry on the Stress Concentration Factor**

Figure 4-6 shows the change in the stress concentration factor that results from including symmetry in the model. In all cases, there is a slight reduction of the stress concentration factor in the overall results by using symmetry. The mesh density selected for the overall analysis was four elements per flange thickness; this is discussed in detail in Section 4.4.2. The difference in stress concentration between the full model and the model using symmetry at this mesh density is 0.0098, or 1%. This difference was deemed acceptable.

#### 4.4 MODEL DETAIL SELECTION

There are many details that define the overall model, all of which needed to be selected so as to maximize accuracy and minimize run-time in that order of importance. Some of these details are a result of the use of ANSYS such as the selection of which

elements were used to build the model; others include how to define the geometric properties of the overall section, such as the welds. The choices on what values to select for these different details were made to ensure sufficient accuracy and secondarily to reduce computational time. This required a large amount of trial and error using different variables before the final values were selected.

#### **4.4.1 Element Types**

It was decided to use all solid elements in this model, though ANSYS does offer the ability to mix 1D, 2D, and 3D elements in one model. In all cases, a SOLID95 element (named so by ANSYS) was employed to simulate the section. The SOLID95 element is a 20 node element that allows for three degrees of freedom at each of its nodes as is pictured in Figure 4-7 (ANSYS 2007). Non-linear analysis options are also possible with the element, but were not used in this project. SOLID95 elements allow for stress or displacement output at each node, or anywhere in between the nodes using a quadratic equation to estimate the intermediate values. This element automatically collapses into a prism if that shape is specified rather than a full box. This was the case for modeling the welds in the connection (see section 4.4.4).

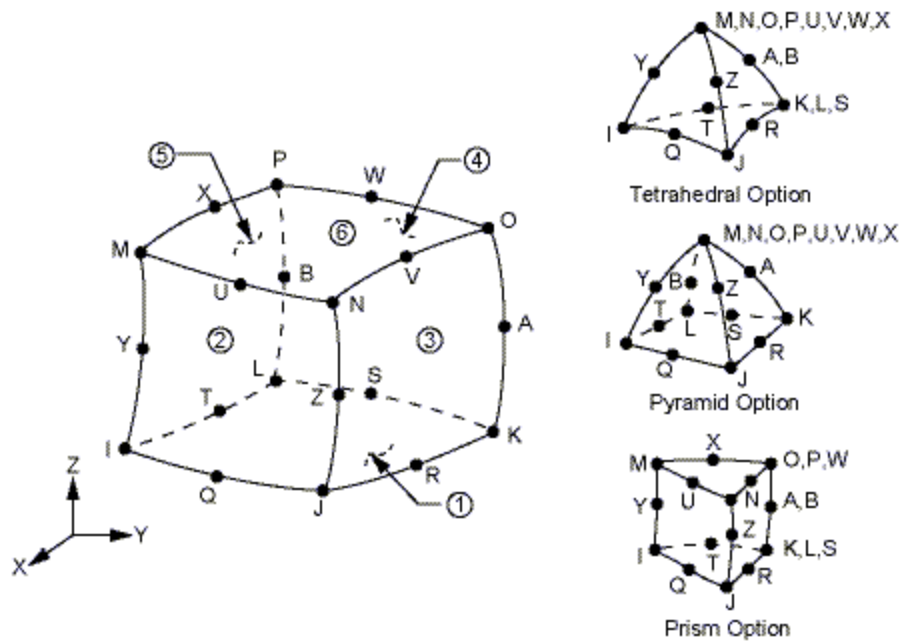


**Figure 4-7: ANSYS SOLID95 Geometry**

#### 4.4.2 Meshing

Any finite element program, including ANSYS, works by taking a large object and dividing into many, smaller components. This process is called ‘meshing’, and the density of the mesh is the number of elements, or smaller objects, created by meshing. The mesh properties impacts both the accuracy and computation time of the model. The mesh density can vary through-out the model, and it is good practice to have a high density mesh in locations where the stresses are changing rapidly over small areas, and a low density mesh where stresses are changing more gradually.

The model was divided into different areas and each area was meshed with an element size appropriate to the importance of that area. These different areas and different components of the model were then connected, and the resulting model analyzed.

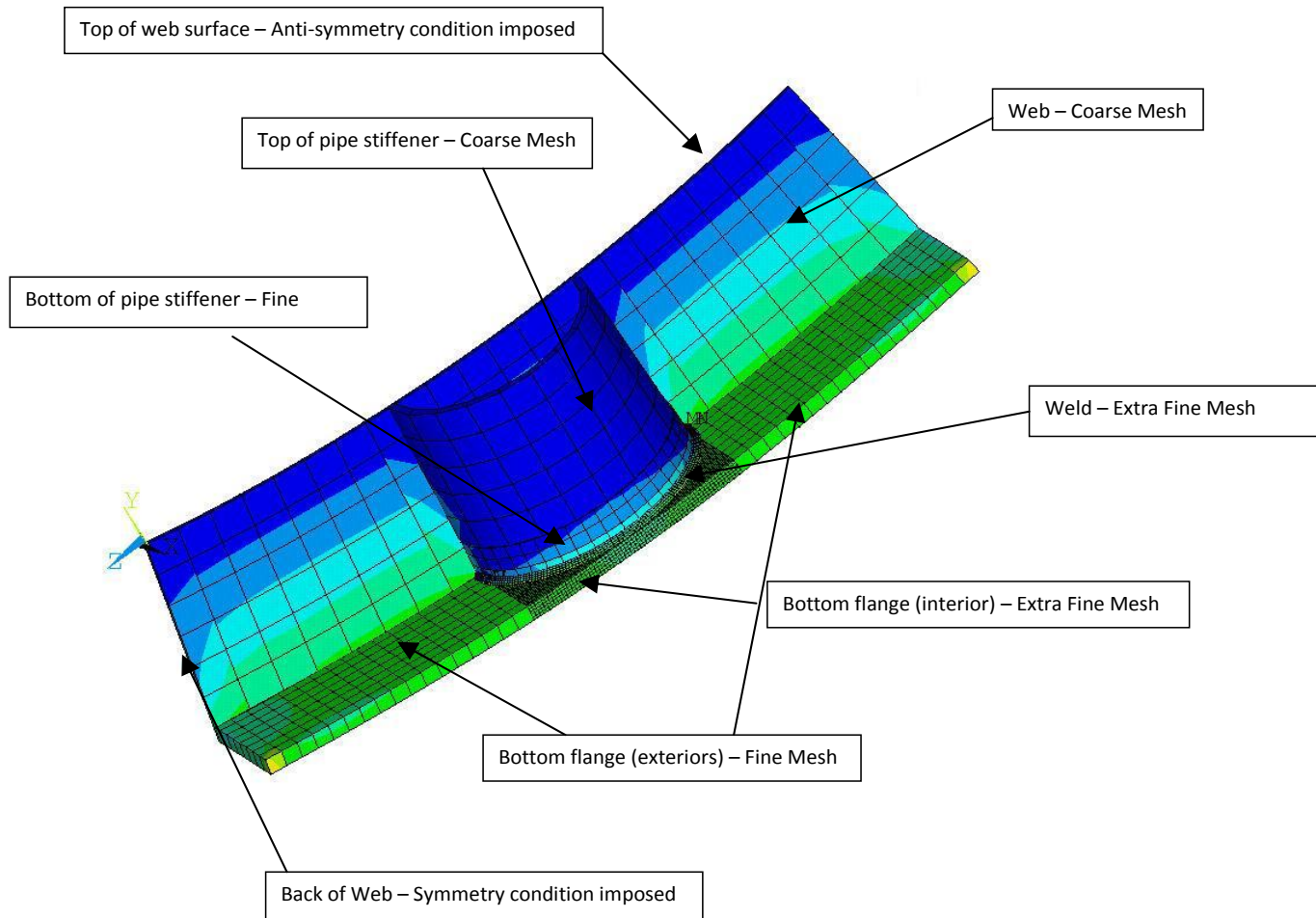


***Figure 4-8: Mesh Properties of the Model***

#### ***4.4.2.1 Selecting Mesh Categories***

The model was divided into three different mesh categories: a coarse mesh, a fine mesh, and an extra fine mesh. Figure 4-8 shows the different areas of the model and what mesh category they were placed in. The width that the extra fine mesh extended into the center of the bottom flange as well as the height of the fine mesh at the bottom of the pipe stiffener were both parameters that were selected based on the process described in Section 4.3.2. The final value chosen for the extra fine mesh is a distance three flange thicknesses away from the edge of the weld on either side of the pipe stiffener, and the fine mesh in the half pipe was chosen to extend up to 30% of the modeled half-pipe volume or 15% of the actual web depth.

#### ***4.4.2.2 Impact of Mesh Size***

As discussed above, changing the mesh or element size alters the accuracy and computational time of the model. Different values of element sizes were tried for all three mesh categories in order to find values that would not reduce the accuracy, but still allow for efficient testing.

Very low levels of the mesh density were shown to degrade the precision of the analysis beyond the point of usefulness. Figure 4-9 shows the stresses, taken half a flange thickness away from the weld, in the flange along the outside of the half-pipe stiffener's weld. At low mesh densities, there is significant variation of the stress concentration. Even if the low density analysis is accurate, it becomes impractical to determine the stress value at specific locations. High densities are needed to remove this level of variance.



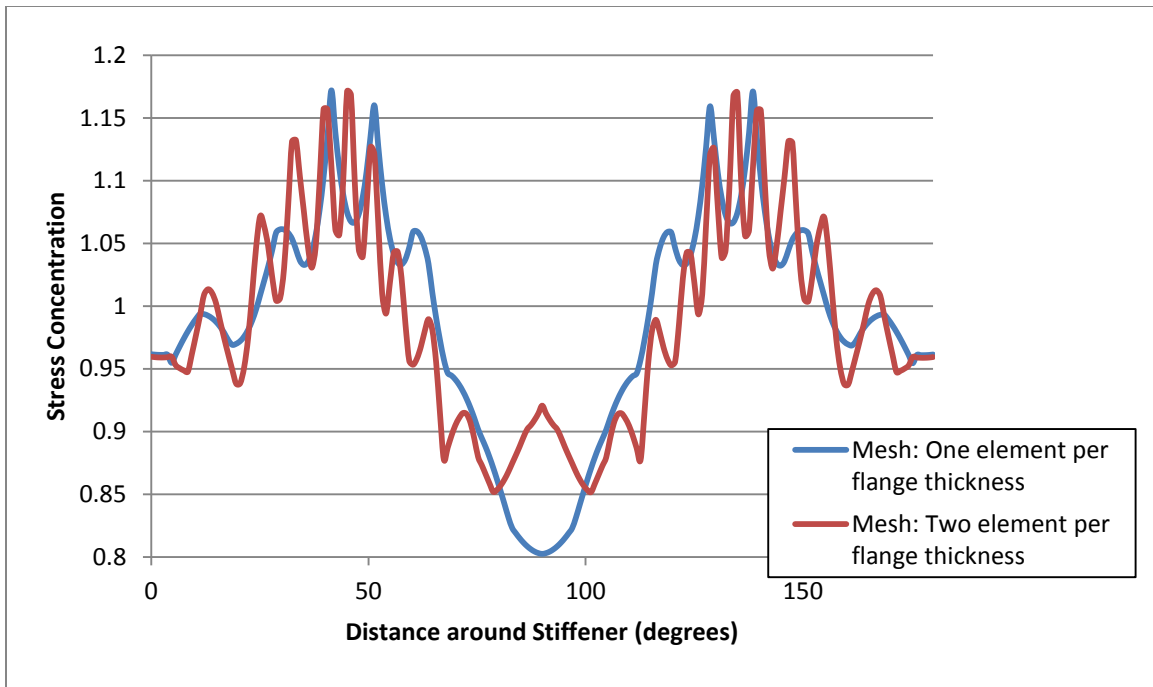


**Figure 4-9: Stress Concentration Factor around Half-Pipe at Different Mesh Densities**

At high mesh densities, the analysis takes much longer, making it infeasible to examine as many variables as were desired for the study. At ten elements per flange thickness (see Section 4.4.2.3) the analysis takes over 24 hours to complete. The final values selected for the model resulted in an analysis time between 15 and 30 minutes (depending on the parameters being tested which could contract or enlarge the model).

#### **4.4.2.3 Selecting Mesh Density**

Once the different mesh categories had been chosen, determinations were made for the appropriate element sizes for each category. Consistency of the stress concentration at the weld of the half-pipe stiffener was the measure used to judge the impact of different mesh densities.

Figure 4-10 shows the impact that changing the coarse mesh size had on the stress concentration factor. The coarse mesh size was correlated to the width of the flange taken as the whole flange width, not the simulated half-width which had been reduced by the application of symmetry conditions. It is clear that the coarse mesh density has very

little influence on the stress concentration factor. It also has very little impact on the computational time as well. The final selection for the coarse mesh size was one seventh the flange width, or about 14% of the flange width.

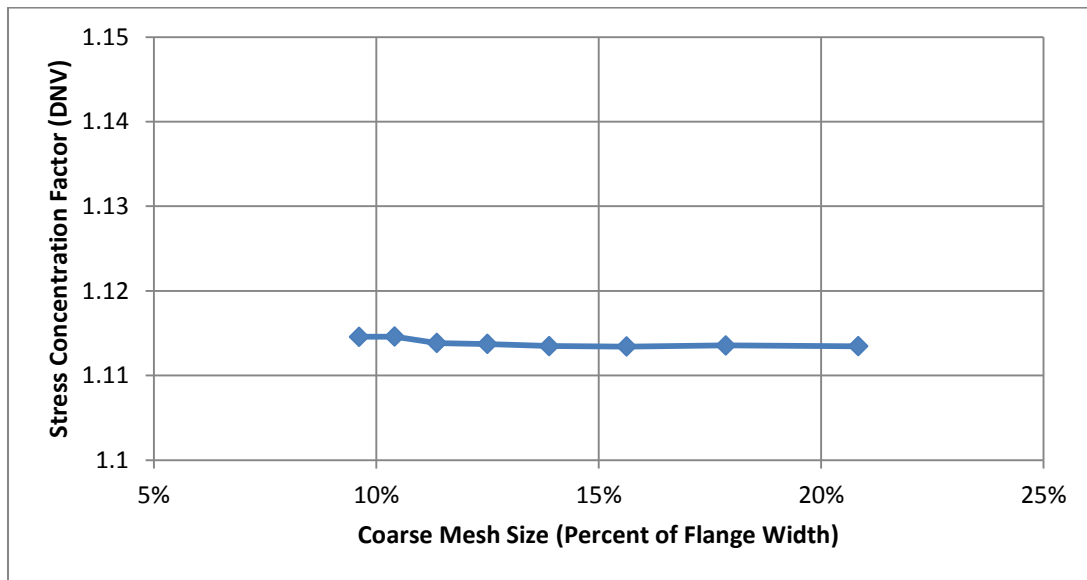


***Figure 4-10: Effect of Coarse Mesh Size on the Stress Concentration Factor***

The fine mesh was selected in a similar manner; it was found that leaving the element size equal to the flange thickness produced a sufficiently accurate result. This was ideal because it allowed for near perfectly cubical elements which ANSYS recommends for better performance (ANSYS 2007).

Finding the appropriate size for the extra fine mesh, which was to be used in the area of the model in which stresses would be measured, was the most important part of the mesh creation. The element size was based on the flange thickness, and values were tested ranging from one flange thickness to one tenth of a flange thickness. The values were always in integral divisions of the flange thickness, as the result would generate a certain number of elements across the thickness, and partial elements cannot be created.

Limitations on the computers used for running the analysis restricted the mesh density to ten elements across the flange thickness, which defined the maximum mesh density that could be utilized. It proved unnecessary to have such a high level of mesh

density, and thus the limits of the computers available did not negatively influence the results.

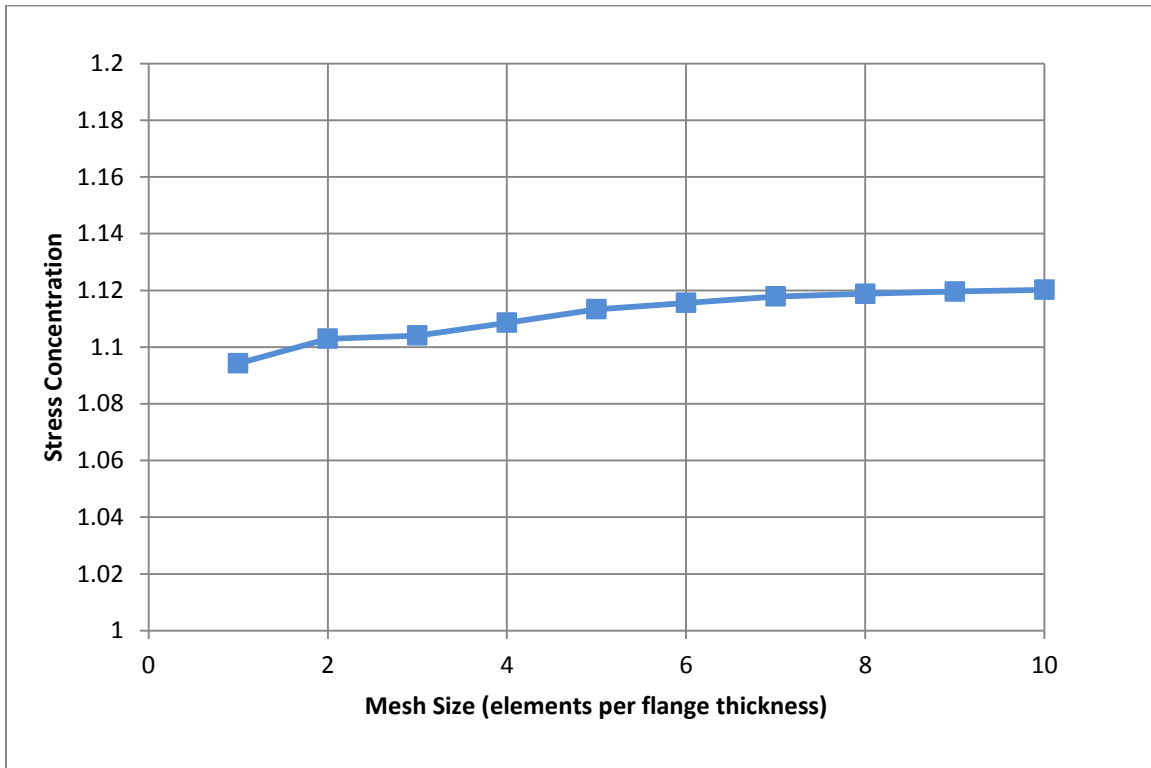


**Figure 4-11: Effect of Extra Fine Mesh Size on the Stress Concentration Factor**

Figure 4-11 shows a graph of the sensitivity analysis on the mesh sensitivity. As the mesh density increases, represented here by a greater number of elements per flange thickness, the stress concentration also increases, but at a *decreasing rate*. Table 4-1 shows the actual value of the variations as the mesh density changes. The changes themselves are relatively small, and represent what was deemed a reasonable level of precision.

**Table 4-1: Impact of Mesh Density for Extra Fine Mesh Volume on Stress Concentration**

Elements per Flange	Increase in Stress from Previous	% Increase From Previous
2	0.00867	0.79%
3	0.00116	0.11%
4	0.00453	0.41%
5	0.00469	0.42%
6	0.00226	0.20%
7	0.00229	0.21%
8	0.00092	0.08%
9	0.00079	0.07%
10	0.00062	0.06%

The final selection of the extra fine mesh element size was one fourth of a flange thickness, or four elements per flange. This created a model that was sufficiently accurate for analysis, and took no more than 30 minutes of computation time. An increase of mesh density to five elements per flange thickness increased computational time by a factor of three. The significant increase in computational time was deemed excessive compared to the accuracy, which therefore did not justify the increase in mesh density since this would have likely reduced the total number of analyses performed.

#### **4.4.3 Connection of Elements**

Wherever the model had a break in either the geometry or the mesh density, or both, it was necessary to add a connection. If neither of these boundaries existed the elements generated could simply have their nodes tied to each other: causing them to distort together, as they shared the same location. When a break in the geometry or mesh density occurred, the nodes no longer lined up with each other, and could not be automatically paired. Even when the locations were identical, if the nodes represented elements from different mesh sizes or objects (such as the half-pipe and the weld

connecting it to the flange) an additional connection was still needed to link the nodes together structurally.

Several solutions were considered to connect these elements, but the final method selected was the use of constraint equations. Constraint equations allowed for specific nodes to be tied to entire elements. One node is selected along with the element closest to it that it is to connect to; if tying together two different mesh densities, the nodes from the denser mesh and elements from the coarser mesh are used. ANSYS then generates equations to tie the node to the element so that the node deforms in the same way as the point on the element closest to the node.

Every single node to be connected was selected, and then the available elements were searched for the one closest to the node. When the adjoining sections were planar, such as at the break in mesh densities at the bottom flange (see Figure 4-8) the node always lay on an exterior plane of the adjoining element. When connecting different geometries that were not planar, such as the circular geometries of the weld to the half-pipe the node was not always co-planar with the element. When a node and an element were chosen, the built-in routines in ANSYS were used to create constraint equations to link the two together. Equations were created to link the chosen node with every node in the selected element.

#### **4.4.4 Modeling Arcs and Welds**

Circular geometry was created in ANSYS by using cylindrical coordinates to describe the volume representing the half-pipe and the weld connecting it with the bottom flange. A cylindrical volume is created within the cylindrical coordinates, there defined by a flat plane which becomes a cylinder when transposed into rectangular coordinates.

When meshing the model, ANSYS approximates the curved lines by generating rectilinear elements long the length of the arc. The smaller the elements and thus more elements used, the closer the approximation is to the actual arc being represented.

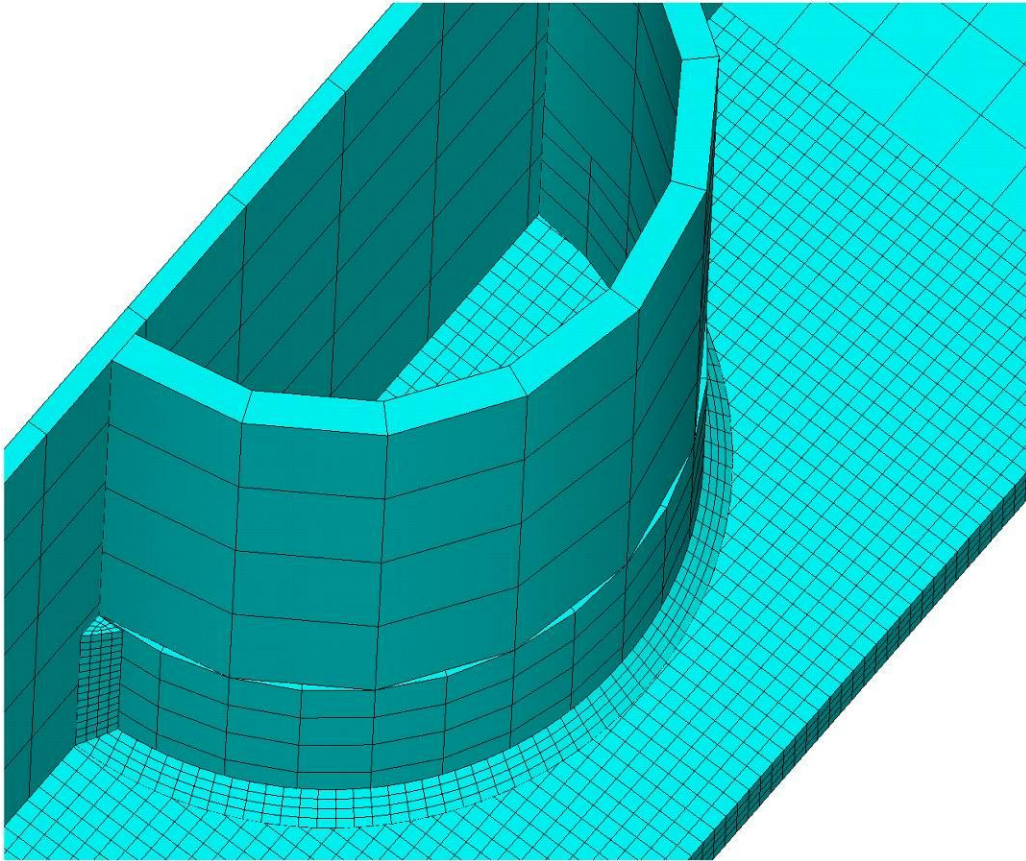


***Figure 4-12: Meshing Along an Arc***

Figure 4-12 shows the impact of different mesh densities on simulating the cylindrical half-pipe stiffener. The top, coarse mesh clearly shows the approximation of the arc of the pipe. The fine mesh at the bottom portion of the half-pipe more closely resembles a circular shape, and the weld as defined by the extra fine mesh very closely represents a circular arc.

The welds, which can also be seen in Figure 4-12, are described by a geometry which has a triangular shape, extended along the length of the weld. More complex geometries, such as circular ones, were considered but deemed to not have a significant impact, nor could the mesh density define a shape of significant complexity.

The welds were a constant size, described by the length of the triangle's legs which adjoined the objects being connected by the weld. The length on both sides was

also always constant. Though no true weld has perfect geometry as defined in the model, any deviance from it would be arbitrary and unless it greatly deviated from the standard: have little impact on the results.

The weld's connections were designed to function just as they do in actual welding. The half-pipe was not connected directly to the girder anywhere except above where the weld was modeled.. Instead, the half-pipe was connected to the adjoining weld face, and the girder to its adjoining weld face.

#### **4.4.5 Linear Solution**

There are several different methods allowed by ANSYS in finding a solution once boundary conditions are defined. The simplest and fastest solution method was chosen, as the results which were of interest did not require a more detailed analysis. Since the issue being studied is fatigue, non-linear material behavior was not a concern. It was assumed that the stresses of interest never exceed the yield stress of the steel. Additionally, no large geometric changes are anticipated that would result in buckling, or non-linear geometric effects of any kind. A linear, static solution was therefore used to find the solution.

#### **4.5 INTERPRETING RESULTS**

The final solution given after the model had been analyzed contained the deformed position and stresses of every node in the model. Most of this data is not of interest to the determination of the fatigue performance of the given model. One or more specific points of interest must be selected within the model, and then the relevant results taken at those points.

The desired results were the stress concentration factors (described in Section 4.5.2.1) at the points in the model which had the highest stresses in the bottom flange. These would show which points on the half-pipe stiffener connection would be most likely to fail, and their magnitude would determine how likely a failure was.

### 4.5.1 Visual Inspection

Previous experiments of a similar nature led to the examination of three specific points of interest in the model (Anamia et. al 2005). Several different models built using different parameters such as pipe-radius or flange thickness were generated and analyzed. The results, displayed as color-coded stresses on the model, were then examined visually to see if there were any other points in the connection that showed high stress concentrations.

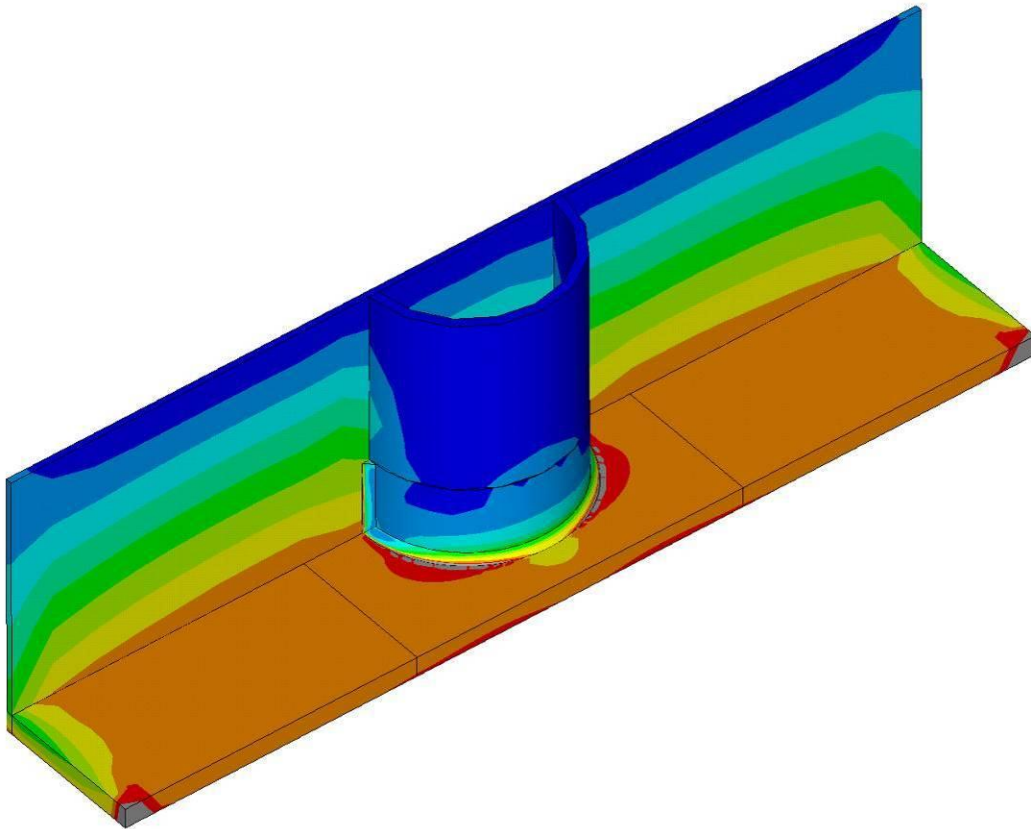


*Figure 4-13: Stresses in Basic Model*

Figure 4-13 shows an example of one of the models that was used to visually inspect for stress concentrations. The three points chosen prior to modeling which were deemed to be of interest were at the junction of the flange and the web, 45 degrees along the half-pipe stiffener, and the outside of the half-pipe, or 90 degrees along the half-pipe.



The visual inspection showed no other point of concern. There were stress concentrations at the edges of the model where the boundary conditions were applied, but these were artifacts of the modeling process.

In this project the absolute magnitude of the stresses generated were not important, rather the concern was for high *relative* stress. In every case it appeared that the maximum stress generated by the half-pipe connection occurred 45 degrees along the half-pipe stiffener. The stresses at the three points of concern, but on the inside of the pipe stiffener were significantly lower than on the outside, and thus were not of concern either. Only those three points, located on the outside of the half-pipe stiffener were deemed to provide meaningful results.

#### **4.5.2 Hot Spot Stresses**

The points on the model that showed high stress concentrations are referred to as ‘hot spots’. These represent the points that have the greatest potential for the initiation of fatigue cracks. Picking the specific point that is of interest is the first step followed by the determination of the true stress at that point. The true stress is the stress value that actually exists in the physical specimen, which is not necessarily the same as the stress in the finite element model at that point. Though there is no way to ensure that the value from the finite element model is actually representative of the value of a real specimen, there are steps that can be taken based on previous testing to generate as close to the true value as possible.

##### ***4.5.2.1 Stress Concentration Factors***

The stress values of interest are not the absolute magnitudes of the stresses at any point, but rather the way in which the stresses concentrate at the given hot spots. The stress concentration factor represents the amount the stress is increased by the inclusion of the half-pipe connection as compared to what it would be if the girder were left plain. For example, if the value of the applied flexural stress was 10ksi, a stress concentration factor of 2.0 would have a hot spot stress would be 20ksi.

The boundary conditions, as described in Section 4.3 are deformation controlled. The magnitude of the deformation imposed on the beam was chosen so that the top side of the bottom flange would be under a stress of exactly 1ksi. This was checked in all the models away from both the ends of the model, and the connection to the half-pipe, and found to consistently be within a range 0.1% of the desired 1 ksi. Forcing a 1 ksi stress at the top of the flange no matter the size of the specimen being modeled allows direct comparison the stress concentration factors between all models.

The stresses determined from the ANSYS models also represented the stress concentration factors. This is because the base-level stress in the flange remained constant at 1 ksi, so the resulting stress (measured in ksi) represents the stress concentration factor, a unit-less value.

#### ***4.5.2.2 The Notch Effect***

At sharp geometric changes, it is common to find that as the density of the mesh increases, the stress also increases. This effect does not dissipate as the mesh density continues to increase. Rather the stress continues to increase with the mesh density away from the true value of the stress. This is called the notch effect, and must be accounted for in the results or the values obtained will not be accurate. (Fricke 2002)

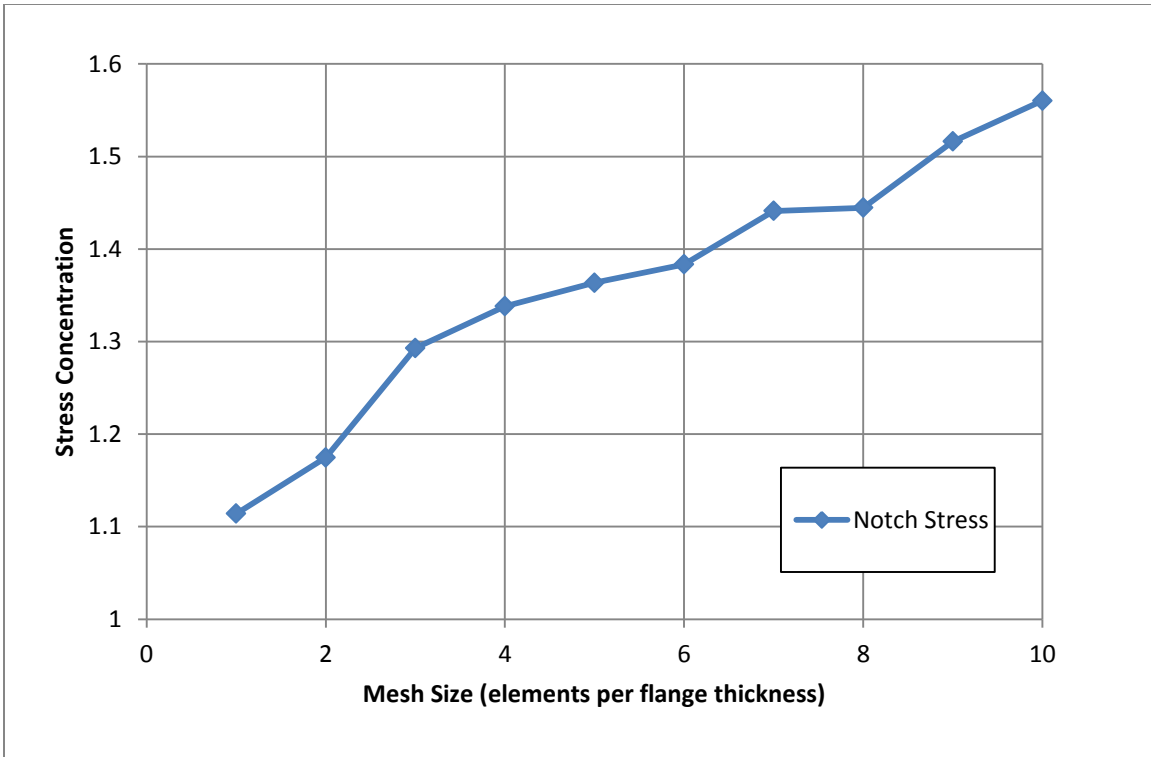


***Figure 4-14: Stress in the Flange at the Boundary of the Weld at Increasing Mesh Densities***

Figure 4-14 demonstrates the notch effect. It shows the stress measured directly at the boundary of the weld on the bottom flange at varying mesh densities. As the density of the mesh increases the stress concentration factor increases. The stress concentration factor does not appear to approach convergence with increasing mesh density.

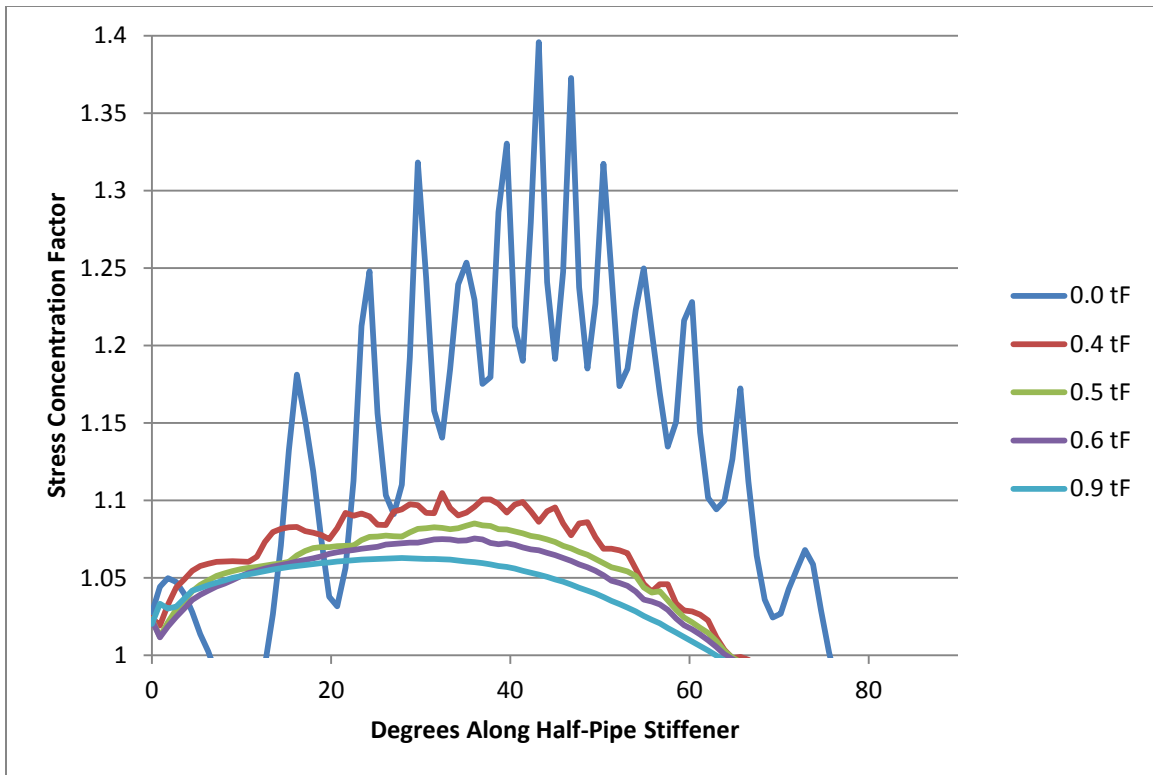


*Figure 4-15: Stresses at Varying Distances from Weld*

In addition to the different mesh densities generating unrealistic stress concentrations, they also can create high variance in the stresses along the edge of the weld. Figure 4-15 shows this variability. The stresses recorded at different distances from the edge of the weld are shown. The stresses read directly at the weld (the data labeled 0.0 tF, or zero flange thicknesses away) show a great deal of variation that results purely from the mesh distribution. Moving away from the edge of the weld, these factors dissipate until at about half a flange thickness from the weld, where the variation is no longer significant as compared to the precision of the model output.

#### **4.5.2.2.1 Maximum Stress**

One of the stresses always measured for every model was the maximum stress, which was found to be equivalent to the notch stress, or the stress measured at the edge of the weld. For the reasons listed above, this was not taken as the true stress that would be

measured in an actual specimen, and so another approach had to be taken to determine the stress concentration factor.

In order to eliminate this notch effect, two different approaches were tried. There are many more approaches that have been used in other studies. The two chosen here both made the same basic assumption about the nature of the stress in the flange. Both assumed that as the edge of the weld was approached, the stress in the flange increased in a linear fashion.

#### ***4.5.2.2 DNV Stress Factor***

DNV, which stands for Det Norske Veritas (DNV 2010), is a Norwegian organization which provides codes and guidelines for fatigue analysis and design. DNV has provided a method to eliminate the notch stress effect, and instead produce a result which gives consistent results across different mesh densities and more closely approximates the true stress found in a real structure.

The DNV method assumes that as the hot spot stress point is approached along the surface of the element under consideration, the true stress increases linearly up to the hot spot itself. Two points are chosen, always in the same plane of the structure, and a line is extended through those points up the plane where the hot spot stress is to be approximated. The intersection of the created line, and plane of interest is the DNV stress. The two points selected are always 50% of the plate thickness (being the plate along which the stresses are being taken) away from the hot spot and 150% of the plate thickness away. Figure 4-16 shows a generic set-up in which this process can be used as well as possible paths along which the stresses could be measured. Figure 4-17 demonstrates this approach in an elevation view of Figure 4-16.

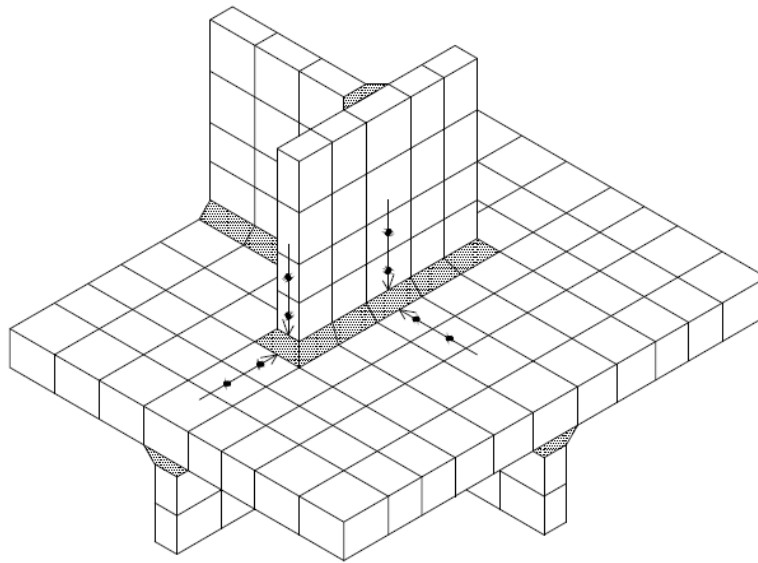


**Figure 4-16: Taking Stresses along Paths Approaching Two Hot Spots (DNV 2010)**

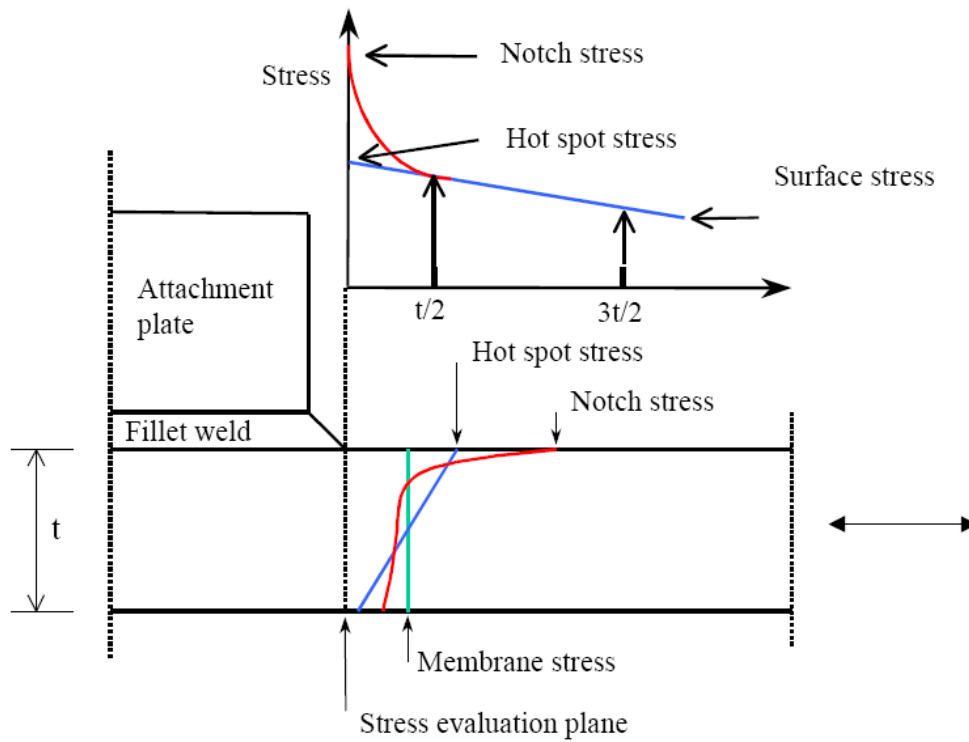


**Figure 4-17: Calculating DNV Stress at a Hot Spot (DNV 2010)**

In the case of the half-pipe stiffener and plate stiffeners studied in this project, the stresses were taken along the top of the tension flange as they approached the weld toe. Selecting the position of the paths for each connection is discussed in 5.1, but the general approach used to determine the hot spot stress and thus eliminating the notch effect is the same for any DNV analysis.

$$\sigma_{Hot\ Spot} = 1.5 * \sigma_{0.5\ Plate\ Thickness} - 0.5 * \sigma_{1.5\ Plate\ Thickness} \quad (4-1)$$

Equation 4-1 gives the basic formulation for determining the DNV stress based on two points approaching the hot spot (DNV 2010). This was the equation used to generate all of the stress concentration factors (and all of the hot spot stresses) used in this project. It is the equation for the intersection of the line defined by these two points with the hot-spot stress. Both these points lay outside the critical region for variant stresses resulting from mesh density, as described in Section 4.5.2.2.

#### ***4.5.2.2.3 Ordinary Linear Regression***

The ordinary linear regression method of eliminating the mesh effect from calculating the hot spot stress relies on the same assumption as the DNV method. However, instead of picking two specific points from the path of stresses approaching the point in question, a series of points are chosen and an ordinary linear regression is performed on them. In a sense, the DNV method is a specialized version of the ordinary linear regression method in which the series of points consists only of the two specific points used for the DNV method.

Ordinary linear regression is a statistical method of approximating a line of best fit through a series of data points. It functions by minimizing the sum of the square of the distances between the generated line and each data point. The distances are calculated as the vertical distance between the data point and the line, instead of the smallest distance between the two. This is what makes the method ‘ordinary’ linear regression, and typically yields results that are similar or identical to a more rigorous linear regression method. Equation 4-2 shows the calculation of the hot spot stress using ordinary linear

regression (Weisstein 2010). Here, ‘y’ represents the measured stress, ‘x’ the distance from the weld, and ‘n’ the number of points sampled.

$$\sigma_{Hot\ Spot} = \frac{y_{avg} * \sum x^2 - x_{avg} \sum (x*y)}{\sum x^2 - n * x_{avg}^2} \quad (4-2)$$

The advantage of this method is that is more flexible in being able to capture the behavior of stresses approaching the hot spot, and examines a far greater number of points. This is also its major draw-back, in that there is no definitive standard which can be used to select what series of points to use in order perform the ordinary linear regression. This makes comparison across different models difficult. This also, is not a method which is used in practice, so no data in previous practice can be used as comparison with the data found utilizing this method.

Ordinary linear regression was used here as an alternative method to evaluate the data, in an attempt to verify the DNV method. However, because there was no standard approach, all the results are analyzed and reported in terms of DNV stresses. Figure 4-18 shows the three different methods used for determining the stress. The actual stresses measured, the DNV stress (here, a line between the two points used in this method is extrapolated out on either side to allow for visualization of the predicted stress) and the OLR method. In this case, the OLR was performed on the points between 50% and 150% of the flange thickness from the hot spot, as a comparison to the DNV method.



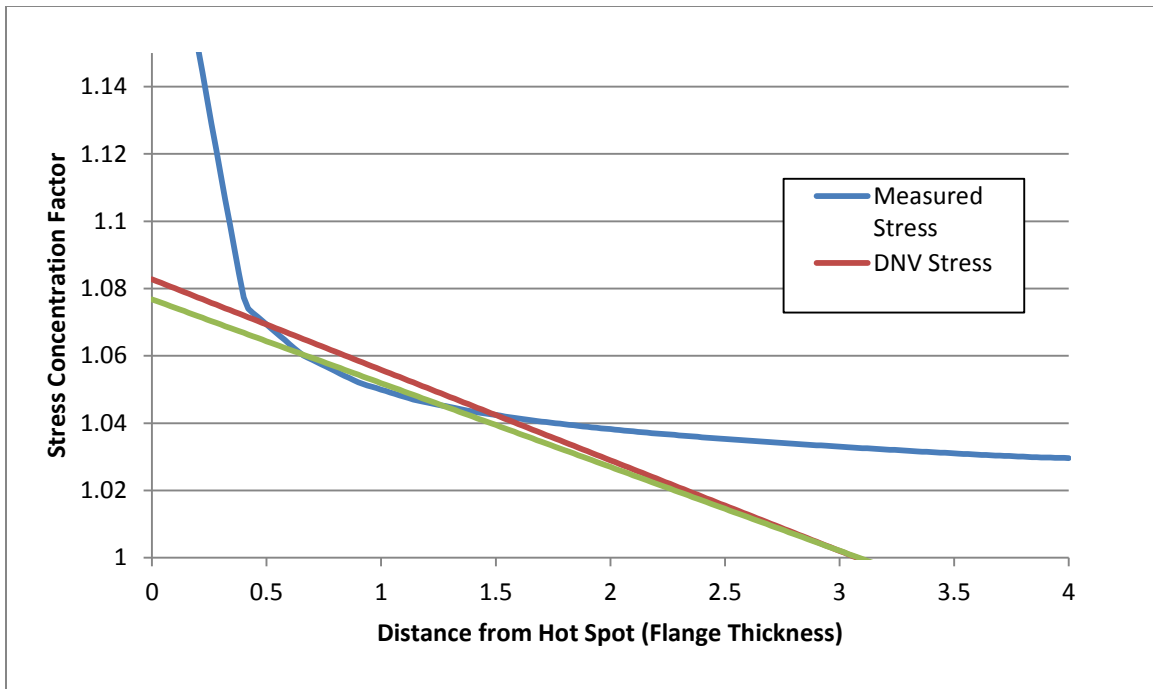


**Figure 4-18: Different Methods for Determining Hot Spot Stress**

The DNV stress line and the OLR stress line both deviate from the measured stress. These two lines are close, but result in slightly different predictions for the hot spot stress. Both eliminate the impact of mesh density from the final results, but show the uncertainty inherent in trying to accurately estimate stress concentration factors.

#### 4.5.2.3 Stress Type and Orientation

All references to the measured stress in the model up to this point do not specify what stress is being measured. ANSYS provides a number of different options: the principle stress, the stress in any orthogonal direction, shear stresses, and numerous generated stresses such as ‘Von Misses Stress’ and ‘Plastic Equivalent Stress’. For stresses in the orthogonal x,y,z directions, the z-axis is along the longitudinal direction of the girder, the y-axis is in the direction of the web, and the x-axis is along the direction of the flange width.

Any ANSYS specific stresses, such as ‘Plastic Equivalent Stress’ were not used, as they did not represent any actual stress. The two main options remaining where using

the principle stress and using the stress that was perpendicular to the face of the weld, where the hot spot stress was being measured.

The principle stress would represent the maximum normal stress being experienced by the structure at that point. The stress perpendicular to the weld face is the stress that could generate a crack at the toe of the weld. If this stress is not the same as the principle stress, the structure may perform better than one that has the principle stress perpendicular to the weld. This means that a measure of perpendicular stress may be a better indicator of fatigue life. It was decided to use the principle stress for this project as it was more critical when comparing against the plate stiffener (it will always be the largest measured stress) but the perpendicular stresses were also measured and used as comparison to the principle stress. The findings, as a result, are conservative for evaluation of the half-pipe stiffener.

### **4.5.3 Path Generation**

In order to implement the DNV stress method, or any other method that would determine the hot spot stress, a path needed to be created along which stresses could be measured. ANSYS is designed to allow this kind of data extraction from an analyzed model. The user defines a geometric path (based on the un-deformed geometry) and ANSYS will determine the stress along the path at any given interval. Interpolation is done to find the stresses between nodes in the model, so any level of measurement precision can be specified but the true precision and accuracy is limited by the mesh density and accuracy of the model itself.

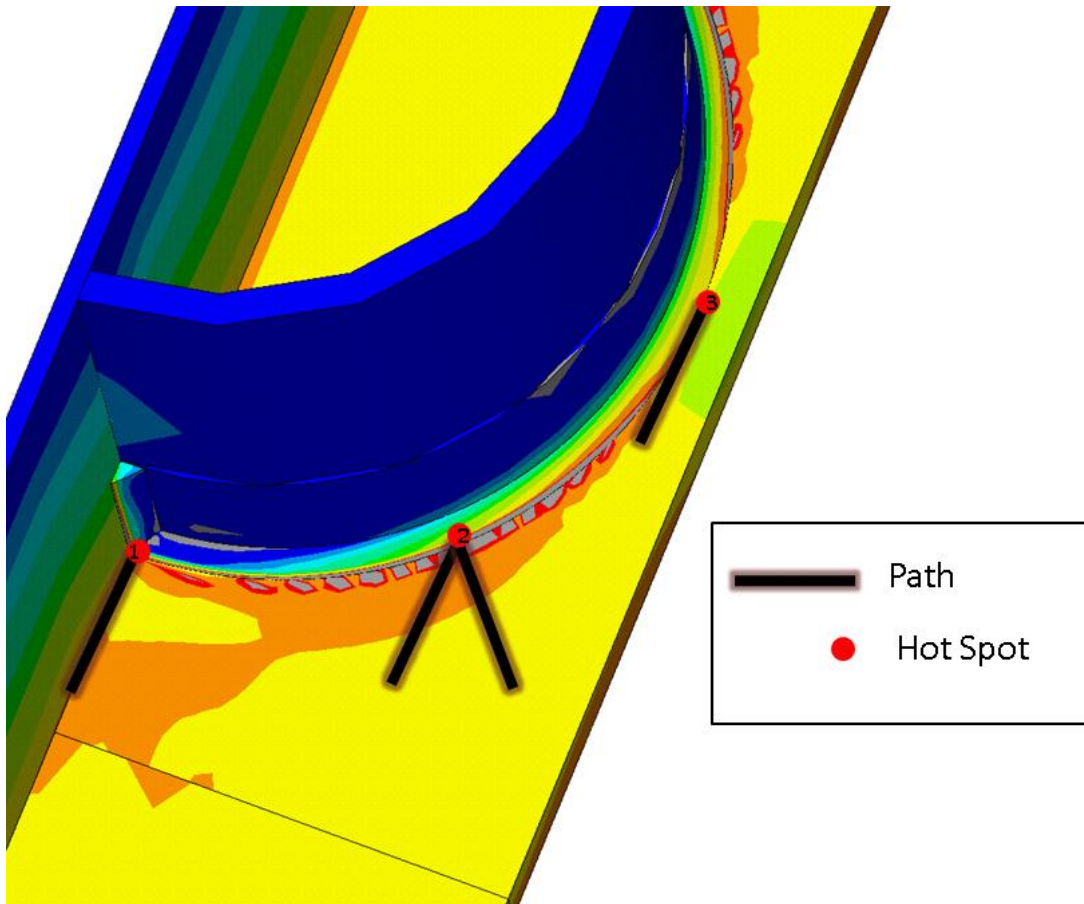


***Figure 4-19: Paths Used to Find Hot Spot Stresses***

Three critical hot-spots were found (see Section 4.5.1) and measured for every model that was analyzed. Figure 4-19 shows the location of all four paths used to find the hot spot stresses, and the locations of the three hot spots. The first hot spot, located at the intersection of the flange, the web, and the exterior of the half-pipe weld required one path to monitor the stress. Here, the principle stress was perpendicular to the face of the weld to within less than one half of one degree. Thus, a path along that axis was used to determine the stresses, and the principle stress measured on that path.

The third hot-spot of interest was on the outside of the half-pipe weld at the point closest to the outside of the flange. Here there was no stress perpendicular to the weld face. Instead, the principle stress was nearly parallel to it. A measurement of zero stress

was of no interest although this had significance as to how critical this hot spot was, and was not measured. Instead, the principle stress was measured along a path that was in line with the axis of the principle stress, which was the same as the stress that would be generated by pure flexure without any discontinuities.

The second hot spot examined had the most uncertainty as to how to measure the stress, and was of the greatest importance out of the three hot spots as it experienced the highest stresses. Two different paths and three different measurements were used to attempt to capture the behavior of the stress flow at this point. The point itself lay 45 degrees along the half-pipe weld, or half-way in between the first and third hot spots. Here, the principle stress was not perpendicular to the weld face, nor was the stress perpendicular to the weld face equal to zero as at the third hot spot.

To ensure that all relevant data would be collected, one path was used which approached the weld on a line perpendicular to its face. Along this path both the principles stress, and the stress in the direction of that line were recorded. Another path was used which was in the direction of the principle stress as it approached the hot spot. The principle stress was approximately 1.5 degrees off of the beam's axis, and this was the direction along which the path was created.

#### **4.6 VALIDATING THE MODEL**

As described above, considerable care was taken in the development of the ANSYS finite element model to assure meaningful results were obtained in regard to fatigue performance of the half-pipe stiffener. In order to further evaluate the model, the next step was to validate the model with experimental results.

Ideally, validation would be done by quantifying the difference between the behavior of the specimens tested in the laboratory and the results of the computational model. This was not possible for this project, as none of the numerical data collected in the laboratory could directly correlate to numerical data from the finite element model.

The stress concentration factors that were the primary result of the finite element model were only representative of general fatigue behavior. These results could not be

translated directly into a fatigue-life prediction which could be compared with that seen in the laboratory. None of the specimens in the laboratory were instrumented so as to record the stresses along any critical portions of the flange due to the difficulties in measuring stresses in areas of very high localized stress gradients. The only stress values collected, which were measured in terms of strain and converted to stress using the Young's Modulus for steel, simply determined the average strain at the top of the tension flange. This value was a control in the finite element model, and thus could not be used for comparison to the physical results.

Having no direct, numerical checks it was still possible to evaluate the model by comparing with physical observations. This could be done in a qualitative manner by examining what type of connection would be expected to fail first, and where the cracks were expected to initiate based on the stress concentrations predicted by the model. This type of qualitative comparison would give credence to the ability of the model to discern the relative fatigue performance of different details. However, as noted earlier, the modeling techniques used here cannot predict the actual fatigue life of any detail.

#### **4.6.1 Development of a Plate Stiffener Model**

In laboratory testing no fatigue failures occurred at a half-pipe stiffener, nor were any incipient cracks discovered. Though this was a positive result for the goals of the project, it severely limited validation of the finite element model with physical testing. All the meaningful results in the laboratory, in terms of model validation, were found either exclusively in the plate stiffeners, or in comparison between the plate stiffeners and the half-pipe.

Though studying the fatigue properties of the plate stiffener was not a main goal of this project, it became necessary to model the skewed stiffeners in ANSYS as well as the half-pipe stiffener in order to examine the modeling techniques that were being used and ensure that they were capturing the observed performance of the plate stiffener relative to the half-pipe stiffener.

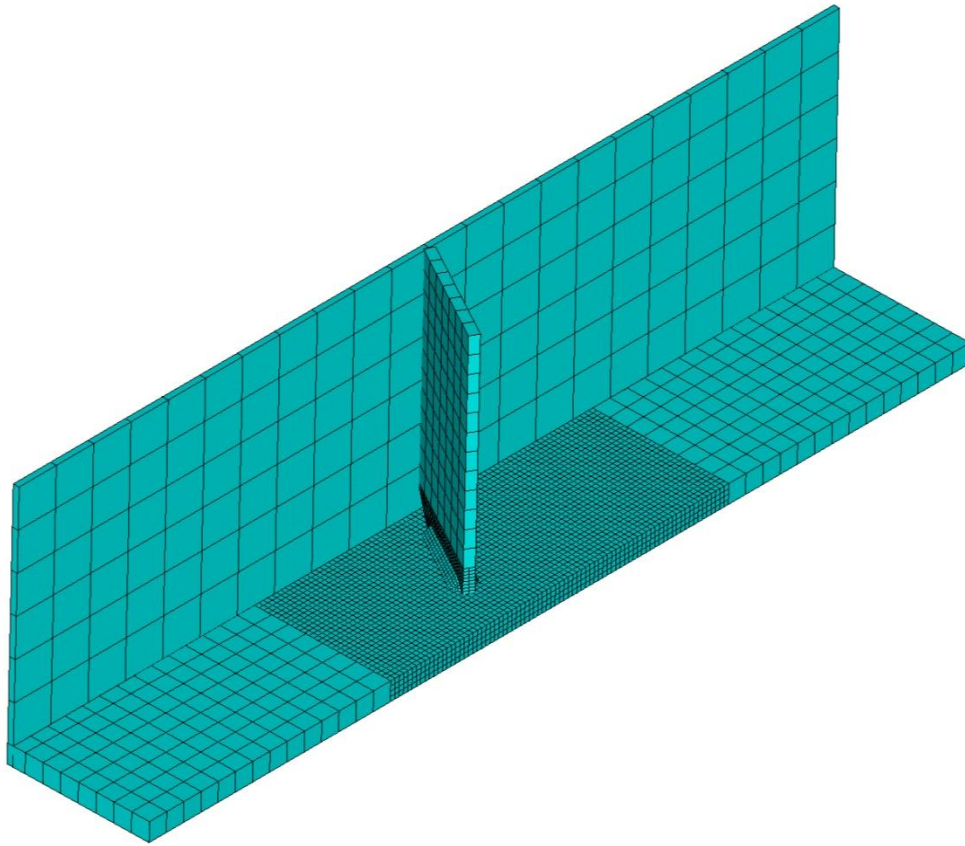


***Figure 4-20: Plate Stiffener Model Mesh***

Figure 4-20 shows an example of the plate stiffener model that was created. All the same processes used in creation of the half-pipe stiffener were employed in the creation of the skewed stiffener model. Type of elements, use of symmetry, connection types, and any other properties which directly or indirectly related to the half-pipe were used. Additionally, the same methods to determine model parameters (such as the length of the model) were used in creating the skewed-stiffener as were in the half-pipe model.

There were several parameters that needed to be chosen for the skewed stiffener in representing its geometry that were not equivalent to anything in the half-pipe model. These included the size of the cope of the plate stiffener that was present to allow fit-up around the weld joining the flange to the web (or the k-area) and the geometry of the end of the welds. Such parameters were picked to best represent what was seen in the

laboratory, and were not changed to influence the results in any manner. Figure 4-21 shows typical results of this model, as well as a closer view of the components of the plate stiffener itself.

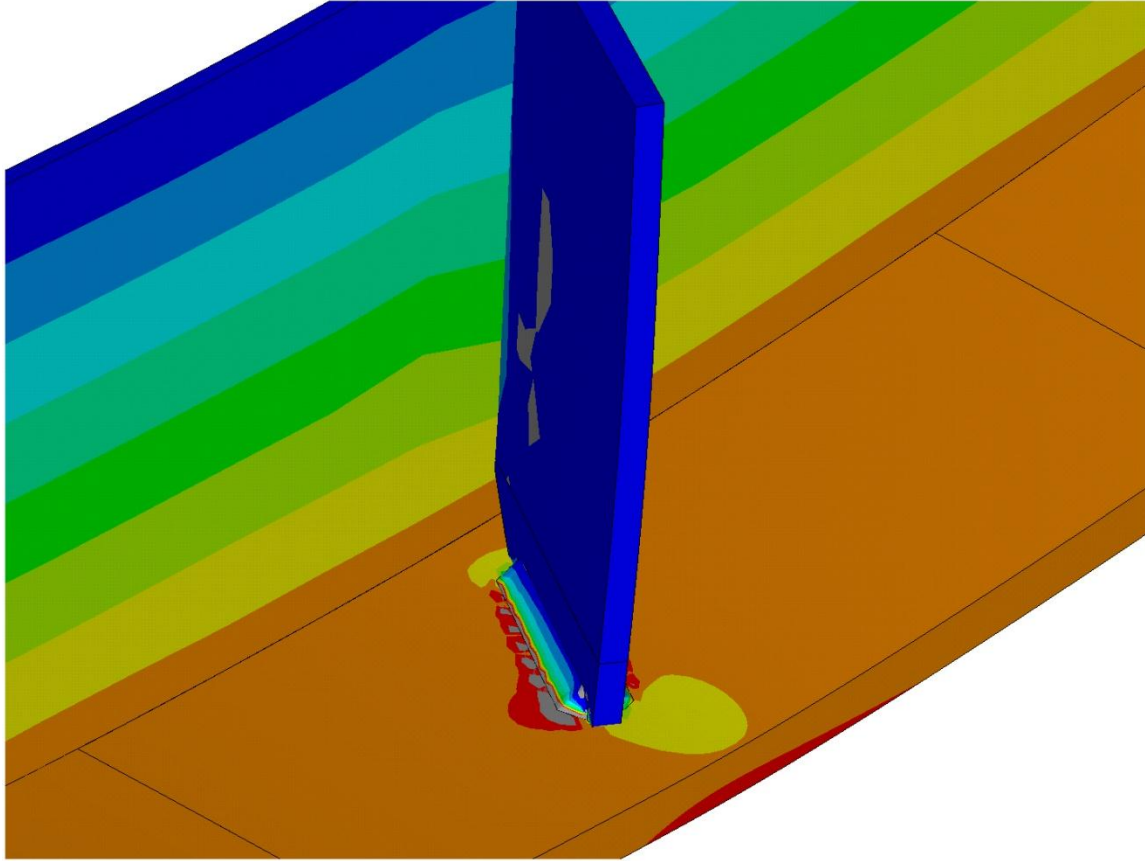


***Figure 4-21: Plate Stiffener Model, Deformed Shape and Stress Contours***

The plate stiffener and the half-pipe are very different geometric entities, but as much similarity in modeling techniques as possible was used to allow for a comparison of results between the two. Whenever it was feasible, the same ANSYS code was used to generate each model, such as the code to define the girder itself, or the code used to run the solution.

#### **4.6.2 Comparison to Test Results**

A summary of the data obtained from the physical results that can be used to validate the computational model can be found in Section 3.8.2. The full results from the finite element analysis will be presented and discussed in Chapter 5, but a description of how the model results compared with the laboratory results is provided here.

The first experimental observation was that the skewed stiffeners failed before the perpendicular stiffeners or half-pipe, and the sixty degree stiffeners failed before the 30 degree stiffeners. The model showed that the stress concentration was correlated to the degree of skew of the plate-stiffeners. The greater the skew angle, the greater the stress concentration. This is in line with the general experimental observations. Additionally, a similar stress concentration factor was found for the perpendicular plate stiffener as the maximum anywhere on the half-pipe, which is also consistent with laboratory findings.



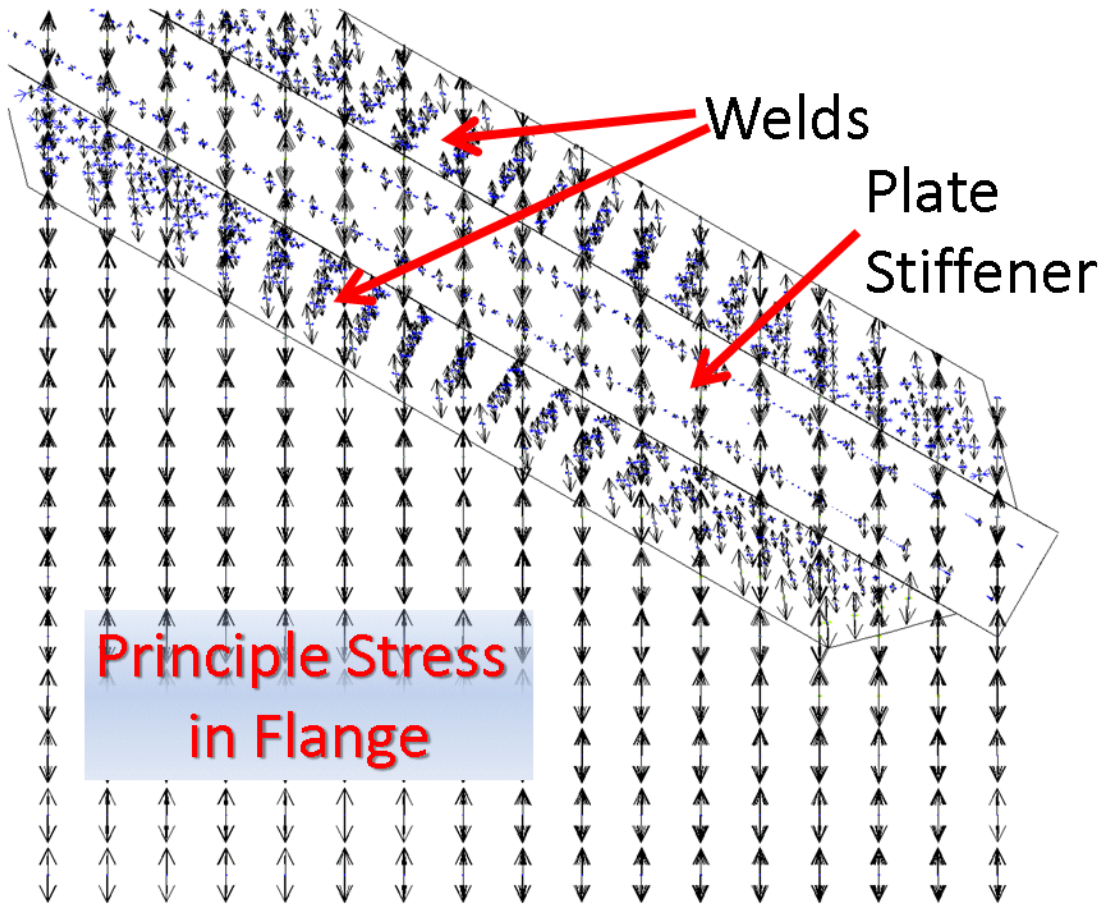


*Figure 4-22: Direction of the Principle Stress in Tensions Flange Adjoining a Skewed Plate-Stiffener*

The second experimental observation was the method in which the cracks opened on the skewed stiffeners. The cracks propagated along a line that was perpendicular to the axis of the beam, not the skew angle, indicating the principle stress was along the beam's axis. Figure 4-22 shows the principle stress in the girder flange for a 30 degree skewed plate. The direction of the principle stress is directly along the beam's axis.

The cracks observed in the laboratory specimens at the skewed stiffeners initiated on the edge of the welds closest to the outside of the flange, and on the weld that is on the side of the acute angle. This position is the bottom right of Figure 4-22. The finite model showed this to be the point with the highest stress concentration on any plate-stiffener

with a skew greater than 15 to 20 degrees. Both these observations show a qualitative match between the physical results and the computational model.

The final experimental observation related to the results of the perpendicular stiffeners. Cracks were found originating on the toe of the weld, in the middle of the weld lengthwise along the plate-stiffener. The only failure occurred on the exterior edge of the weld toe. The finite element model showed almost uniform stresses along the weld length for perpendicular, or nearly perpendicular plate stiffeners, with a slight increase in stress at the middle of the length of the weld.

Though all the comparisons that could be performed were qualitative rather than quantitative, all observations from the laboratory testing were in agreement with computational modeling. These comparisons provide some confidence that the finite element model is capable of discerning how variations in design details, such as thickness of the half-pipe stiffener, thickness of the flange, weld size, etc., will affect fatigue performance. Results of extensive analyses examining the impact of various design details on stress concentration factors, and therefore on fatigue performance, are described in the next chapter.

## CHAPTER 5

# Results of Finite Element Modeling

### 5.1 DESCRIPTION OF RESULTS

Once the finite element model had been created and validated, a series of tests were performed. The plate-stiffeners were examined to determine the general range of results for different skew angles. The half-pipe was investigated in greater detail than the plate-stiffener, examining which geometric parameters were influential in determining the stress concentration factor for the half-pipe, and then running parametric analysis on the chosen parameters. The results were used to evaluate how design variations for girders with half-pipe stiffeners may affect fatigue performance.

### 5.2 SELECTING CRITICAL PATH

In determining the most important results of the finite element analyses, several different hot spots and stress paths were considered. To ensure that the most important data was collected through-out the modeling process, all data that was of possible value were kept. It was not until the results were collected that it became possible to determine the critical hot-spot or stress path.

#### 5.2.1 Critical Hot Spot

After analysis of all completed modeling, it was found that the greatest stress concentration occurred 45 degrees along the weld of the half-pipe stiffener in every design tested. In no case did either of the other two hot spots produce stresses that exceeded the 45 degree spot for that model. All data presented, unless otherwise noted, are for the stress concentration factor at the 45 degree hot spot.

### **5.2.2 Meaning of Path Selection**

Three different path data sets were used to determine the 45 degree hot spot stress concentration factor. The stress perpendicular to the face of the weld was always significantly less than the principle stress. Consequently, the principle stress was used as the basis for computing the stress concentration factor. There were two paths used to find the principle stress concentration factor. The first was perpendicular to the face of the weld, and the second was along the line of action of the principle stress. Though the results of both paths were always similar, they were not identical. It was decided to use the path along the line of the principle stress, as it represented the most likely mechanism for crack formation. All results presented that reference the principle stress at the 45 degree hot spot use this path to calculate the stress concentration factor.

## **5.3 PARAMETERS OF INTEREST**

Once the model was created, verified, and the method of data extraction determined, the next step was to determine which design parameters to investigate using the model. To do this, the important parameters that defined the girder, the half-pipe and the weld were altered both separately and together to determine their impact on the fatigue life of the connection. The first step of this process was to determine which of the parameters had an influence on the stress concentration factor, and which were not critical.

### **5.3.1 Parametric Description of Problem**

In building the finite element model, seven different parameters were used to describe the geometry of the overall connection. Table 5-1 shows what these parameters. Each one is a measure of length, and all were recorded and reported here in units of inches.

**Table 5-1: Parameters Defining Problem**

Parameter	Symbol	Notes
Girder Depth	dG	Total depth including flanges
Flange Thickness	tF	Equivalent for top and bottom and constant across model length
Web Thickness	tW	Constant through-out the model
Flange Width	bF	Width across entire flange, not the half-flange modeled
Half-Pipe Thickness	tS	
Half-Pipe Radius	bS	Measured to the outside of the pipe, the same parameter is used to denote the plate
Weld Size	aW	Length of the legs of the weld against the connecting element

As described in Chapter 4, there were several more parameters that defined the model. Though they can be described in terms of one the parameters listed in Table 5-1 a test was run to ensure that these seven parameters were the only ones that influenced the results. There were many parameters that apply to a real-world connection that were not modeled such as the space left between the pipe and the girder and the shape of the weld, among others. The testing here was to ensure integrity within the model itself.

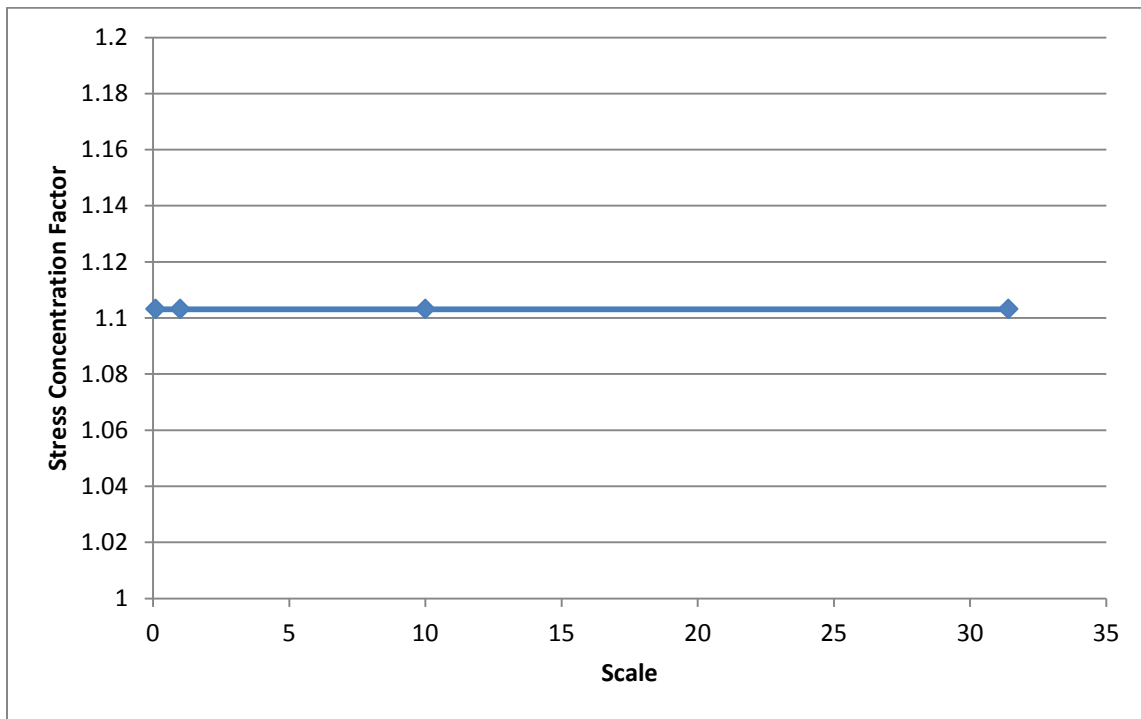


**Figure 5-1: Impact of Scaling the Model on the Stress Concentration Factor**

This goal was accomplished by analyzing the model while multiplying all of the seven geometric parameters that are listed in Table 5-1 by a scalar. Only those seven parameters were multiplied, and four different scalar values were used. Figure 5-1 shows the results of these tests: all the stress concentration factors are nearly identical no matter the scalar used. This indicates that these seven parameters define the entirety of the problem being modeled, which means that the testing can be limited to studying the impact of these seven parameters alone.

### 5.3.2 Determining Relative Influence of Parameters

Once the seven key parameters had been identified, they were each tested alone to determine their individual impact on the results. They were tested by themselves over a range of values that was considered reasonable for real design. The full range was not crucial, only that a wide enough range was examined so as to ensure that changes in the results that would come from more extreme values of the parameter were captured. All of these tests were run using the laboratory model as the base, and altering the remaining parameters from their values as taken from the laboratory specimen.

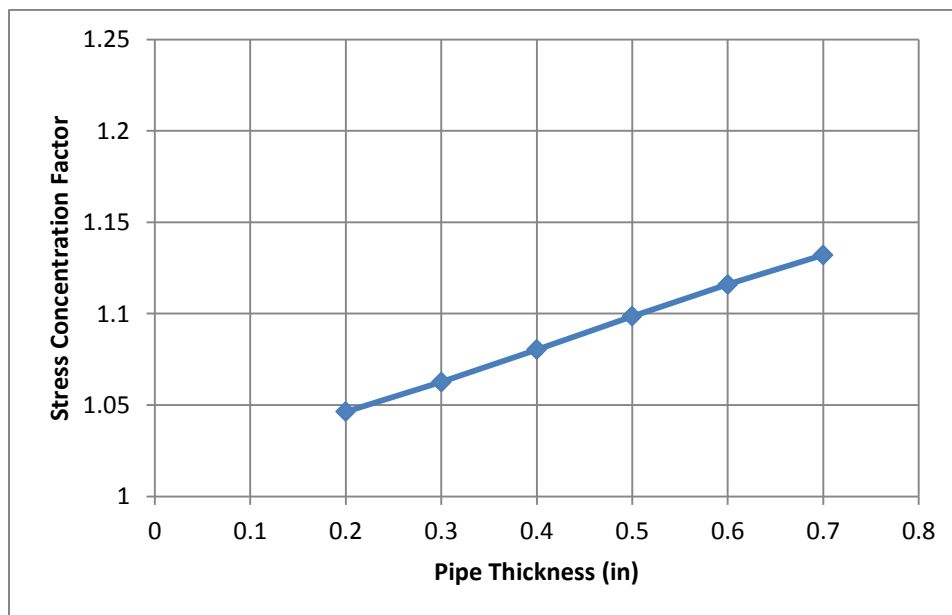


*Figure 5-2: Study of Pipe Thickness (tS)*

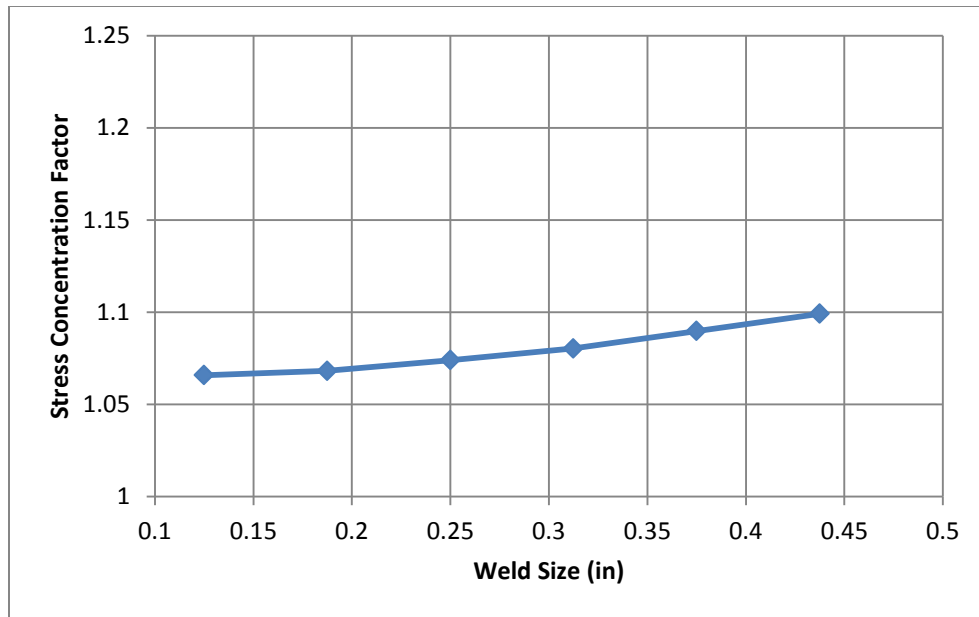


*Figure 5-3: Study of Weld Size (aS)*

Figure 5-2 and Figure 5-3 show the results for two of the seven parameters: the thickness of the pipe ( $tS$ ) and the size of the weld ( $aS$ ). Similar graphs were made for all seven parameters showing their impact on the stress concentration factor. Both of these parameters and four of the remaining five were determined to have influenced the stress concentration factor sufficiently so as to warrant further study.

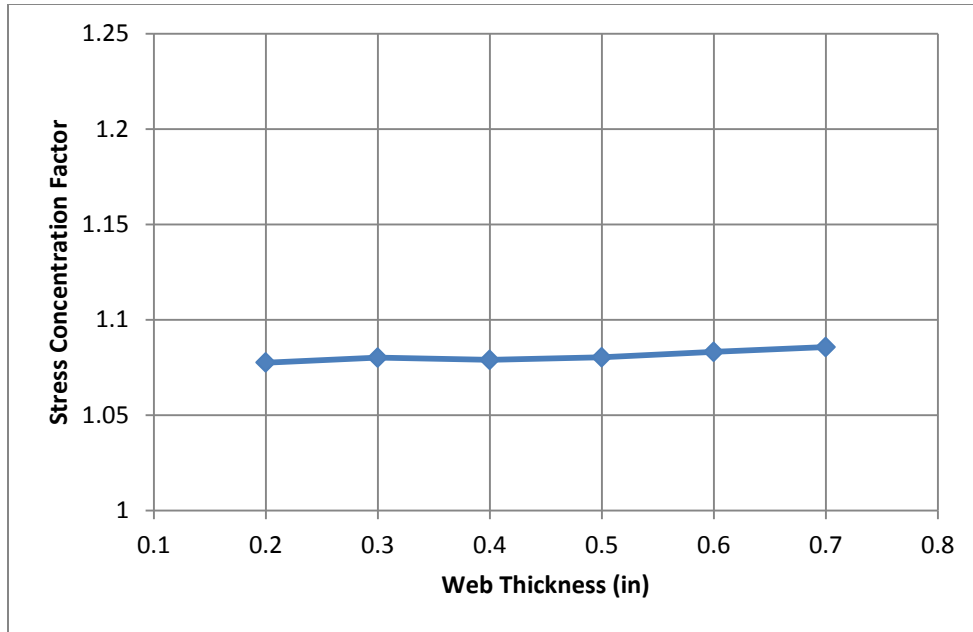


***Figure 5-4: Study of Web Thickness ( $tW$ )***

Figure 5-4 shows the results from the study of the impact of the web thickness ( $tW$ ) on the stress concentration factor. It was not anticipated that this parameter would have a significant influence on the results, and these findings support this observation. The total variation from two tenths to seven tenths of an inch for the web thickness resulted in less than a one percent change in the stress concentration factor (rising from 1.077 to 1.085). This made the web thickness the only parameter that was determined to not have an impact significant enough as to warrant investigating further, leaving the other six parameters to study.

The resulting parameters were: girder depth ( $dG$ ), flange thickness ( $tF$ ), flange width ( $bF$ ), half-pipe thickness ( $bS$ ), half-pipe radius ( $tS$ ) and weld size ( $aS$ ). It was shown that these parameters were the only ones that significantly influence the results, and so an equivalent change to all six of them would result in no net change of the stress concentration factor measured.

This meant that one of the six parameters could be removed from the study, as including all six would be redundant. If one parameter was left constant and all of the



remaining five parameters were increased, it would be equivalent to decreasing the other parameter. Likewise, any change to all five parameters could be marked as an equivalent change to the sixth, and so if all five were tested together, the results for the sixth could be extrapolated. The parameter chosen to remain constant across the test was the flange width. This parameter was selected because it had a large influence on computational time for each model, and leaving it constant made it less likely to make a mistake and use a combination of pipe radius, thickness, and weld size that would extend beyond the edge of the flange.

#### **5.4 COLLECTION OF DATA**

A program for the analysis was determined so that each parameter was given a set of values to test, and every combination of values for each parameter was modeled and analyzed. The number of values for each parameter was limited; since there were five parameters being tested directly, the total number of models needed to run all of the necessary tests was  $n^5$  where 'n' is the number of values used for each parameter.

Once the program of testing was determined, a batch analysis was run to test each variant sequentially without user input, to allow for continuous testing. This meant that not every model was individually examined, introducing the possibility of error. To mitigate this, the test was stopped periodically and both the model and the results examined to catch any possible input errors, such as faulty values inputted or program break-downs. Any data that appeared out of the ordinary would prompt a re-run of the model and a detailed examination that specific parametric combination.

The results from each model were sent as output into a text file which contained the current values of all relevant parameters, and the stresses from each of the four paths used for data collection as described in Section 4.5.3. Every path had 100 points of data collected along its length and this resulted in 700 total data points. The extra 300 points come from the need to measure multiple stresses along one of the paths to collect and generate all the necessary information for determining the principle and directional stresses (see Section 4.5.2.3).

This text file was then input into a program written in C++ which converted the stress values into DNV stress predictions, OLR stress predictions, and maximum stress readings. The program then output these values along with their accompanying parametric information into a comma separated file to be examined using Excel. This C++ program was later modified to also perform data analysis on the results generated here (see Section 5.5.4).

## **5.5 ANALYSIS OF DATA**

The first set of data collection involved altering only one parameter at a time. The main purpose of these experiments was to determine if the parameter in question had a significant impact on the results. This was accomplished purely through visual analysis by creating a graph of the results and looking for a pattern.

Once the critical parameters had been chosen and the testing completed several hundred data points had been generated. It became impractical to determine the relationship between the varying parameters and the stress concentration factor by simple, visual inspection. Some more complete method had to be developed so as to examine all possible factors and do so without requiring human judgment for every analysis as the time taken for such an approach would be prohibitive.

### **5.5.1 Goals of Analysis**

The major goal of the computational analysis was to determine if the results of laboratory testing could be applied across a wide spectrum of designs. However, it was also hoped that the modeling would lead to a determination of what factors most influenced the fatigue life, how potential problems could be avoided, and as a guide to possible further research.

### **5.5.2 Problems for Analysis**

In order to accomplish the goals of the finite element modeling, the main objective was to determine the relationship of each parameter, and parametric

combination to the stress concentration factors they generated. The selection of parametric values and numerical results are presented in Section 5.6; the original batch testing of the half-pipe model included over 400 different parametric combinations. These runs represented the testing of 150 different possible relationships between various parametric combinations and the stress concentration factor. This is why it was deemed impractical to analyze all possible combinations by hand.

Some overall ‘first-look analysis’ could be performed with some simple, min-max and graphing techniques. Determining the range of results, and looking for obvious patterns such as one parameter clearly dominating the response over others were done manually. Once this had been completed, it still remained to determine the relationship of the parametric input to the stress concentration factor output.

One possible outcome of the analysis was that there was no clear relationship between the parameters and the stress concentration factor. This would imply that computational modeling had given no additional insights into the problem in terms of predicting the application of the experimental results. That is because without a clear relationship there is no way to demonstrate that within a given range of possible designs, one or more them do not cause a significant increase in the stress concentration factor without testing every single one. Since within any given range there are an infinite number of possibilities this approach is impossible, and thus the computer modeling would give no assurance as to the application of the results. In this case generalizations such as “the stress concentration factor was never bigger than...” and “never smaller than...” could be used, but would be based on the values chosen to be tested rather than an intrinsic property of the stress connection itself.

The opposing outcome is that there exists some definite relationship between the six, tested parameters and the stress concentration factor. This result would clearly demonstrate to what extent the laboratory results could be applied to alternate designs by showing when the stress concentration factor became significantly greater, and thus possibly a concern for fatigue life. Proving this outcome would disprove the first, and the only way to prove the first was to disprove this possibility. Thus the analysis was done in

order to determine a direct relationship between the parameters and the output, but the possibility of no relationship existing was always considered.

### 5.5.3 Creation of Predictive Function

Should a relationship exist between the tested parameters and the stress concentration factor, it could be written in the form of an equation. Equation 5-1 shows the most general form of this equation: some unknown function with the six tested parameters as input produces the stress concentration factor (SCF). If the function could be found which satisfied this description then that would show a well correlated relationship between input and output, as well as giving the ability to predict the stress concentration factor of untested designs. If no function could be found then either there was no relationship, or the function did not exist amongst the range of those searched for in this project. Because there are an infinite number of possible functions, it could never be proved that there was no function that would serve to fit the data. However, the two possible results (finding no function or there actually existing no function) were functionally equivalent as they both resulted in the conclusion that no proof could be found such as to ensure that the laboratory testing was indicative of general behavior.

$$f(dG, tF, bF, tS, bS, aW) = SCF \quad (5-1)$$

The desired function represented by Equation 5-1 could be of any type, but basic intuition into the behavior of structural systems provided guidelines as to how it should look. This intuition, along with considerations as to what could be tested with computational assistance guided the search for a matching function.

$$C_1 \mathbf{dG}^{C_2} \frac{\pm}{*} C_3 \mathbf{tF}^{C_4} \frac{\pm}{*} C_5 \mathbf{bF}^{C_6} \frac{\pm}{*} C_7 \mathbf{tS}^{C_8} \frac{\pm}{*} C_9 \mathbf{bS}^{C_{10}} \frac{\pm}{*} C_{11} \mathbf{aW}^{C_{12}} + C_{13} = SCF \quad (5-2)$$

The generalized version of the function that was used to predict the stress concentration factor is given in Equation 5-2. The values  $C_1$  through  $C_{13}$  represent thirteen unknown constants, the “ $\frac{\pm}{*}$ ” symbols show that the values here are either multiplied together or added. The bolded values are the six parameters that serve as input

to the function. Though here they are given a specific order, the general version of this equation that was tested considered any possible order of these parametric values.

The constants in Equation 5-2 could be positive or negative, and any real number, meaning they can represent values between zero and one. This flexibility allows for the given equation to have many possible, final shapes as well as eliminating one or more of the parameters from consideration.

Once the general form of the equation had been decided upon, it still remained to find a method which would allow for the selection of appropriate parameters such as to accurately capturing the model's behavior. Ideally, every possible permutation of the equation would be tested against the given data. This was not possible in theory because the constants could take an infinite number of values, but infinite precision was not required, and thus the number of possible solutions tested for each constant could be written as a finite set.

A brute-force method of computational analysis was still determined to be impractical, even after the range of values for the constants was narrowed. In order to achieve even a rudimentary level of precision, it was found that approximately  $10^{18}$  different permutations of Equation 5-2 would have to be tested. Any given equation required  $10^5$  floating point operations to compare it to the finite element results which lead to  $10^{23}$  total floating point operations to perform a complete, brute-force analysis. Given that the computers available for use performed at about 10 gigaFLOPS (or perform  $10^{10}$  Floating point Operations Per Second) (Wikipedia 2010). This would result in a test time of hundreds of thousands of years. Either the desired precision would have to be reduced dramatically, or some other methods had to be found to determine the best, final equation to be used.

#### **5.5.4 Genetic Algorithm Solution**

The solution chosen to find the best-fit equation which would describe the output of the finite element analysis was the use of a genetic algorithm. This is a search

heuristic algorithm that allows the search of an arbitrarily large solution space for an optimal solution in less than  $O(n)$  time, or fewer total calculations than possible solutions (Sedgewick 1998). The algorithm formation is based on the principles of natural evolution: allowing cross-breeding and mutation of various solution-descriptions based on fitness evaluations in order to ‘breed’ better solutions (Wikipedia 2010).

#### ***5.5.4.1 Algorithm Formation***

The basic components of a genetic algorithm are: genomes, phenotypes, parents, children, population, mutations, and fitness ratings. First a population of genomes is initialized. Genomes represent the instructions for forming a phenotype, or problem solution. The population is the complete set of genomes created. The initialization process is either done randomly, creating a string of instructions which make of the genome, or based on previous findings as to what some good guesses are of optimal solutions. It is important that the initialization of the population be wide-spread enough that the algorithm is capable of branching out into all viable solutions spaces; initializing the population with all identical or near-identical solutions will force the process into one chain of possibilities and may miss the optimal class of genomes.

Once the population is initialized, the genomes are turned into phenotypes by following the instructions they provide for creating the actual solution just as genes provide the basic instructions to produce the living creature or phenotype. When the phenotype is generated, a fitness algorithm is run which determines how well that particular phenotype actually solves the problem. The entire population of phenotypes is then ranked against each-other based on their fitness evaluation.

When a list has been created of all the genomes expressed by their phenotypes, ordered based on their fitness, the next level, or population of genomes is populated. This is equivalent to reproduction in the evolutionary cycle. Some algorithm picked by the designer selects two or more parents by weighting to a higher likely-hood selection of the phenotypes with better fitness ratings, and then mates them. The mating of the parent genomes is accomplished by splicing together their instructions to form a new genome

which contains parts of both of its parents. At this point, some chance mutation can be included, not all genetic algorithms have mutation but allow the testing of a wider range of solutions and help the algorithm keep from boxing itself into a corner.

Once a full population has been created through mating the selected parents (each genome created selects two or more parents specific to that one, not all are created using the same set of parent genomes) the process begins again. This continues either a specified number of cycles or until a desired fitness level has been reached.

#### ***5.5.4.2 Algorithm Implementation***

The genomes implemented for this problem were the instructions used to generate the equation including values for the constants, when to use addition or multiplication, and what order to place each of the parameters in. The phenotypes are the equations themselves, built from the genotypes.

First a population of equation-creating genomes was created. These were then turned into the phenotypes, or equations. The fitness of those phenotypes was tested using ordinary linear regression (see Section 4.5.2.2.3). The equation generated as the phenotype was used to predict a stress concentration factor for each of the data points generated from the finite element analysis based on those points' parametric values. These were not compared directly to the finite element analysis; rather they were used as paired values in a linear regression. The fitness of each phenotype was then determined by the squared correlation coefficient, or  $R^2$ . The higher the coefficient's value is, the better the fitness rating for the given phenotype.

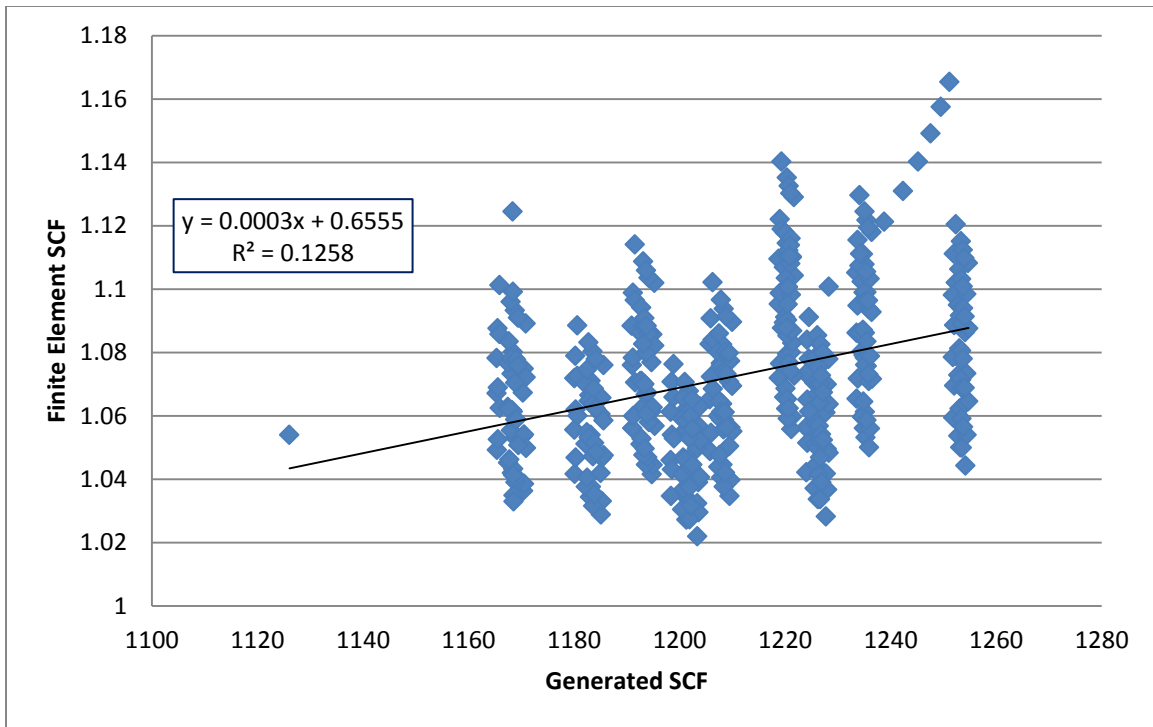


**Figure 5-5: Computing Fitness of a Given Equation**

Figure 5-5 shows an example of how the fitness is. The generated SCF is considered the independent variable against which the actual value from the finite element analysis is plotted. The line of best fit (again using ordinary linear regression) is determined and the  $R^2$  value is used as the fitness ranking of the equation. In this figure, the generated SCF is significantly larger than the actual values found in the finite element analysis, but that is not considered as it can easily be accounted for after the best-fit equation is found. What makes this particular equation a poor match is the amount of variation from the best-fit line pictured. Use this method, instead of forcing the magnitude of the predicted SCF to match as well as the pattern, allows for much more complete and quicker testing. The best value for magnitude, as well as the intercept value can be found analytically. This effectively removes two degrees of freedom computationally.

Once the fitness ratings have been determined, they are then ordered by those ratings. The program begins to select parent genomes, the algorithm used selected only



from the top quarter of the solutions, and then the remaining solutions are picked with a greater fitness rating corresponding to a higher likelihood of selection. Only two parents were used per child for this implementation, mutation was used, and the two genomes were combined randomly: with each value in the genome chosen by randomized pick from the parents. After a specified number of cycles, the program exited and recorded the final fitness value as well as the selected equation to file.

This algorithm reduced the time required to find an optimal solution sufficiently so as to allow for it to be run on a desktop computer. The drawbacks of this method is that there is no grantee that the solution arrived upon is the optimal solution; however, an optimal solution is not required for this problem. Any solution which accurately captures the behavior of the SCF will be sufficient so as to demonstrate the applicability of the laboratory results and predict the SCF for untested designs. It was found that a final solution to the equation could be converged upon in less than one minute, though typically more runs were allowed to continue for several minutes to maximize the precision of the final result.

## **5.6 RESULTS**

The final results from the analysis performed include general observations about behavior, specific relationships between the parameters studied and the stress concentration as well what conclusions can be drawn about the fatigue performance of the connections investigated. The plate stiffeners were not a focus of this study but had to be modeled to provide a validation of the modeling techniques as well as a baseline against which to evaluate the half-pipe connection. The overall results as well as some conclusions that can be drawn about the design and performance of plate stiffeners are discussed first.

### **5.6.1 Plate-Stiffener Results**

The plate-stiffener connection was not investigated as thoroughly as the half-pipe, as it was not the focus of the study. Fewer models were investigated with no in-depth

look at the impact of various parameters. Approximately fifty models were analyzed with the main variation between them being the angle at which the plate stiffener was skewed.

#### ***5.6.1.1 Location of Hot Spot***

Determining the point of maximum stress was more challenging for the plate stiffener than it was for the half-pipe connection. Visual inspection of the model showed that the hot spot for any given design would occur on the toe of the weld connecting the plate with the bottom flange. When high angles of skew were examined the point on the weld on the acute side of the skew and the exterior of the flange was always the maximum stress point (see Section 4.6.2 and Figure 4-21). However, this was not found to be the case when plate-stiffeners with lower angles of skew were examined. Instead the hot spot appeared to drift along the length of the weld toe depending on the angle.

The problem was examined by taking the stress along the length of the weld toe at varying angles of skew between zero degrees and twenty degrees, after which the edge of the weld by the flange's exterior dominated the stress field. At lower degrees of skew, the stresses were found to be highest at the middle of the weld length. As the angle of skew increased, the hot spot appeared to shift from the center to the outside of the weld length.

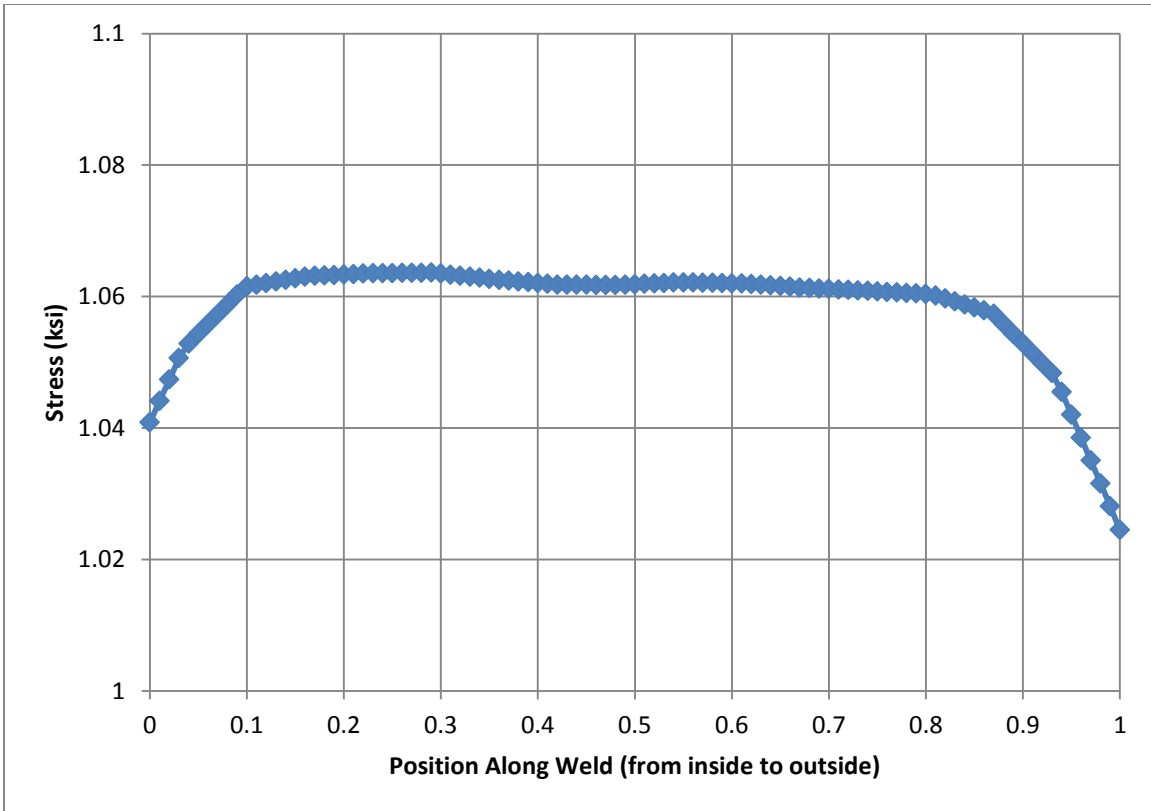


*Figure 5-6: The stress along the weld of a plate stiffener that has no skew (values taken  $\frac{1}{2}$  flange thickness from weld)*



**Figure 5-7:** *The stress along the weld of a plate stiffener that has been skewed 10 degrees (values taken  $\frac{1}{2}$  flange thickness from weld)*



**Figure 5-8:** *The stress along the weld of a plate stiffener that has been skewed 25 degrees (values taken  $\frac{1}{2}$  flange thickness from weld)*

Figure 5-6 through Figure 5-8 demonstrate how the stress concentration varies along the length of a plate stiffener as the angle changes. When there is a  $0^\circ$  skew the stress concentration factor remains fairly constant across the length of the weld with a slight increase along the middle. As the skew increases the location of the largest stress concentration factor begins to shift to the outside, or the edge away from the web. At around  $20^\circ$  of skew, the far edge of the weld becomes the dominate hot spot and remains so for all skew angles greater than  $20^\circ$ , this was tested up to  $70^\circ$ .

The final results were taken from both the middle of the weld and the far edge of the weld. For those plate stiffeners with skew angles such that neither of these measurements captured the maximum stress concentration factor, both values could be examined and the true maximum approximated. The range of angles for which this was an issue was small enough, and the numerical difference was both consistent and of minimal value such as to render this procedure sufficient for the limited purposes of this study.

#### ***5.6.1.2 Range of Results***

The plate stiffener detail was examined in ANSYS using the same dimensions as were tested in the laboratory. The weld size, plate thickness, flange thickness, etc. were all identical. The only factor changed was the skew angle of the stiffener. In the laboratory an angle of  $0^\circ$ ,  $30^\circ$ , and  $60^\circ$  were tested. Using the finite element model a range of angles between  $0^\circ$  and  $70^\circ$  were tested at an increment of  $2^\circ$  for a total of 36 different skew angles.

The results of this analysis were the stress concentration factors at either the middle of the weld or at the end closest to the edge of the flange. These were determined using the same DNV process described in Section 4.5.2.2.2. The values ranged between stress concentration factors of 1.05 and 1.35.

### 5.6.1.3 Impact of Skew Angle

The wide range of stress concentration factors found from this study showed a significant impact of the skew angle on the stress concentration for plate stiffeners. As the angle of the skew increased so did the stress concentration factor in a nearly linear relationship.

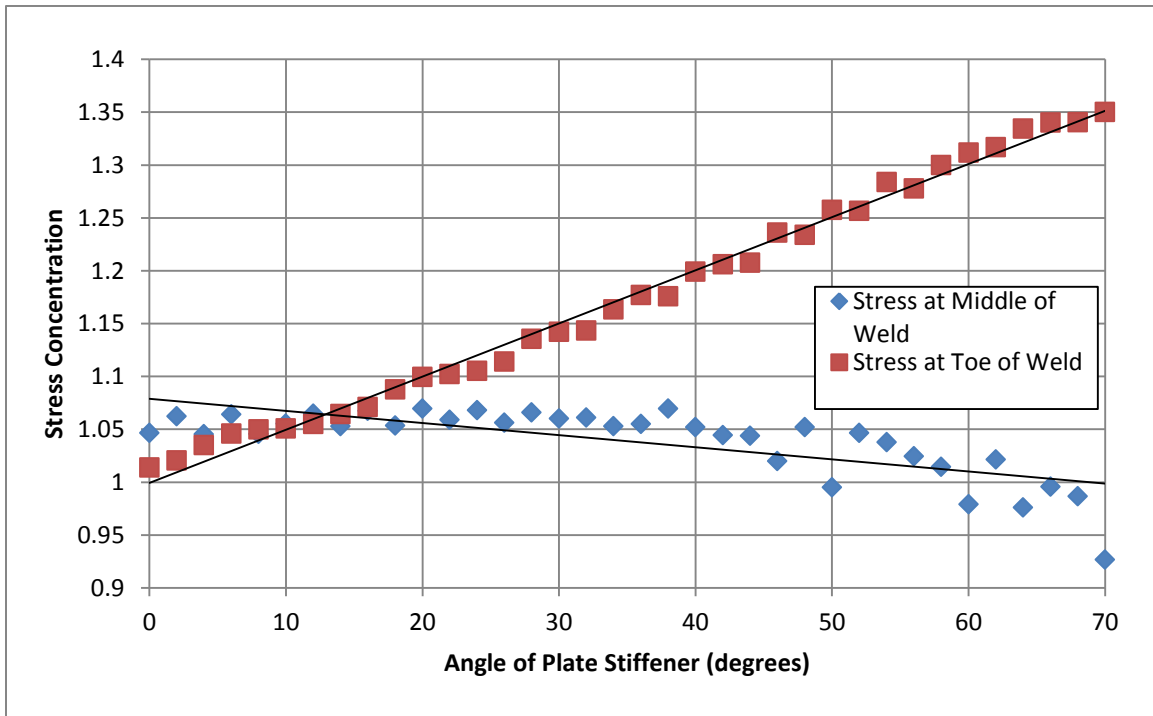


*Figure 5-9: Stress Concentration Factor for Plate Stiffeners at Varying Skew Angles*

Figure 5-9 shows the results of the 36 different models tested. The clear, linear relationship can be seen as the stress concentration factors increases up to a value of approximately 1.35 at a skew of 70°. These values clearly show the increase of the stress concentration factor with the skew angle.

### 5.6.2 Half-Pipe Range of Results

After about 450 different model runs of the half-pipe stiffener with parameters picked in an attempt to simulate the assortment of designs most likely to be seen in the

field, a small range of results was generated. The smallest values went down to a DNV stress concentration factor of 1.02 and ranged upwards to 1.14.

### 5.6.3 Half-Pipe Overall Range of Parameters and Stress Concentrations

The six different parameters and the mathematical reduction to testing all six through varying five of them were discussed in Section 5.3. The original tests done to validate the model were based on the geometry of the connection that was found in the laboratory. The main testing in which the parameters were varied in an attempt to determine their relative relationships to the stress concentration factor were done with geometry more consistent with what is seen in real bridges. The major difference between the two was being a larger overall dimension size and a flange that is thinner relative to the other parameters as the laboratory specimen has a proportionally thick flange as compared to a typical design value.

**Table 5-2: Values used in Parametric Testing**

Parameter	Symbol	Values Tested (in)
Girder Depth	dG	30, 50, 60, 70, 100
Flange Thickness	tF	3/4, 15/16, 5/4
Web Thickness	tW	3/4
Flange Width	bF	15
Half-Pipe Thickness	tS	5/16, 3/8, 1/2
Half-Pipe Radius	bS	3.5, 5, 6
Weld Size	aW	1/4, 5/16, 3/8

Table 5-2 shows the complete list of parametric values tested. The flange width and web thickness remained constant through-out the testing: the latter because it was determined to have negligible impact on the results and the former to reduce computational time (see Section 5.3.2). All possible combinations of the listed values were tested, which totaled 405 different models.

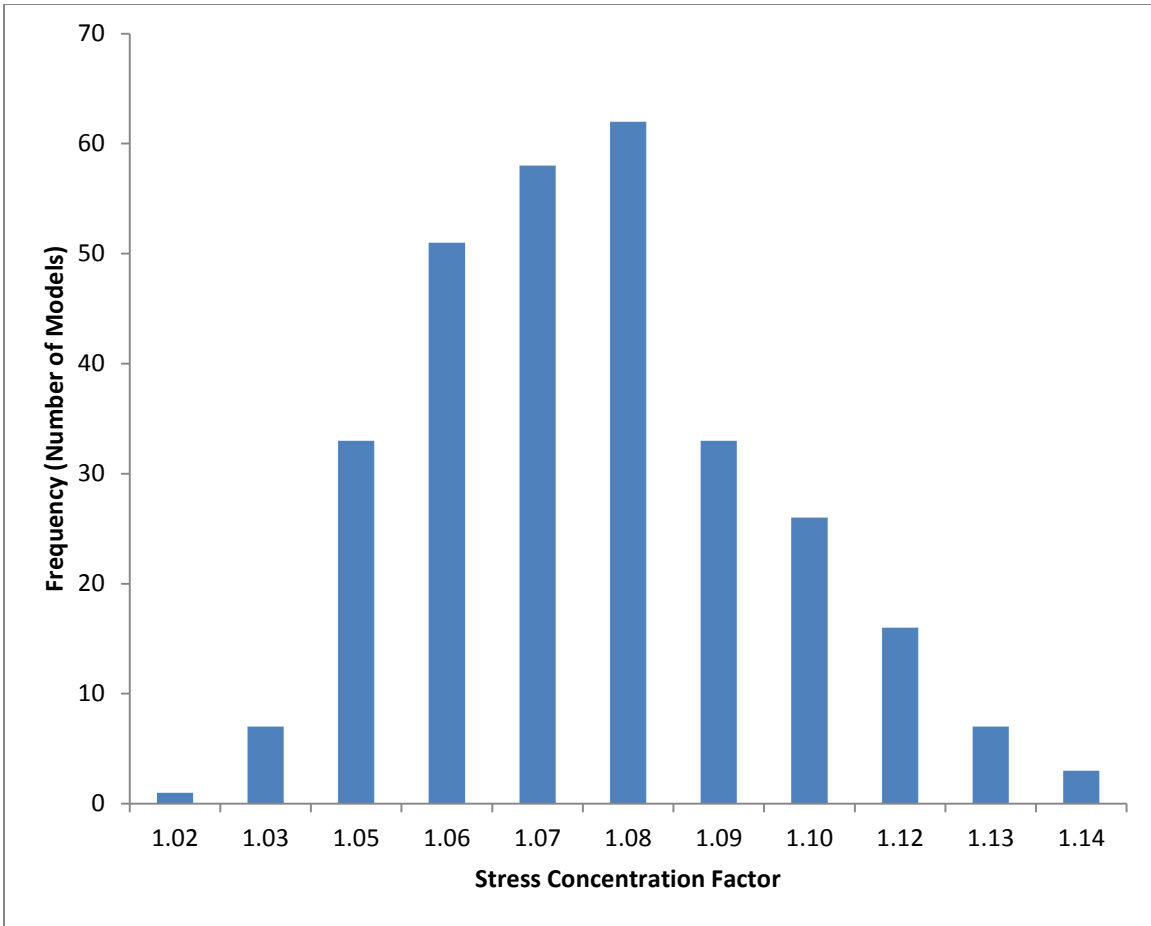


***Figure 5-10: Summary of Results from Initial Parametric Testing***

Figure 5-10 shows the stress concentration factors generated from all 405 models run. The histogram demonstrates an average stress concentration factor of 1.07 about which it appears to be normally distributed. This does not prove that the stress concentration is a normally distributed variable as the dependent inputs, the parametric descriptors, were not chosen randomly but by design. It does show that if those values picked do represent random input or an adequate sampling of typical design values then the stress concentration factors are normally distributed.

If the stress concentration can be considered normally distributed, then the standard deviation of the results is 0.023. This gives a range of 1.02 to 1.12 for two



standard deviations from the mean (representing a 95% confidence interval for normally distributed data).

#### 5.6.4 Final Equation

Once all of the data was collected, the genetic algorithm described in Section 5.5.4 was applied to determine the equation that would best describe the behavior of the stress concentration factor in relation to the given parameters.

$$SCF = 0.343117 \times (dG^{-0.1283} \times aW^{0.411435} \times tS^{0.734428} \times bS^{-0.349864} \times tF^{-0.899167} \times bF^{-.23147}) + 0.983528 \quad (5-3)$$

Equation 5-3 shows the full equation that was generated through use of the genetic algorithm. The values are unrealistically precise as this equation represents the direct output of the program. The coefficient of determination, or R-squared factor for this equation was found to be 0.98, demonstrating a very high degree of correlation.. The results show that the correlation is purely multiplicative, and all the powers are less than one. Furthermore it appears that the key parameters are the flange thickness and pipe thickness, with the weld size and pipe radius playing a smaller role.

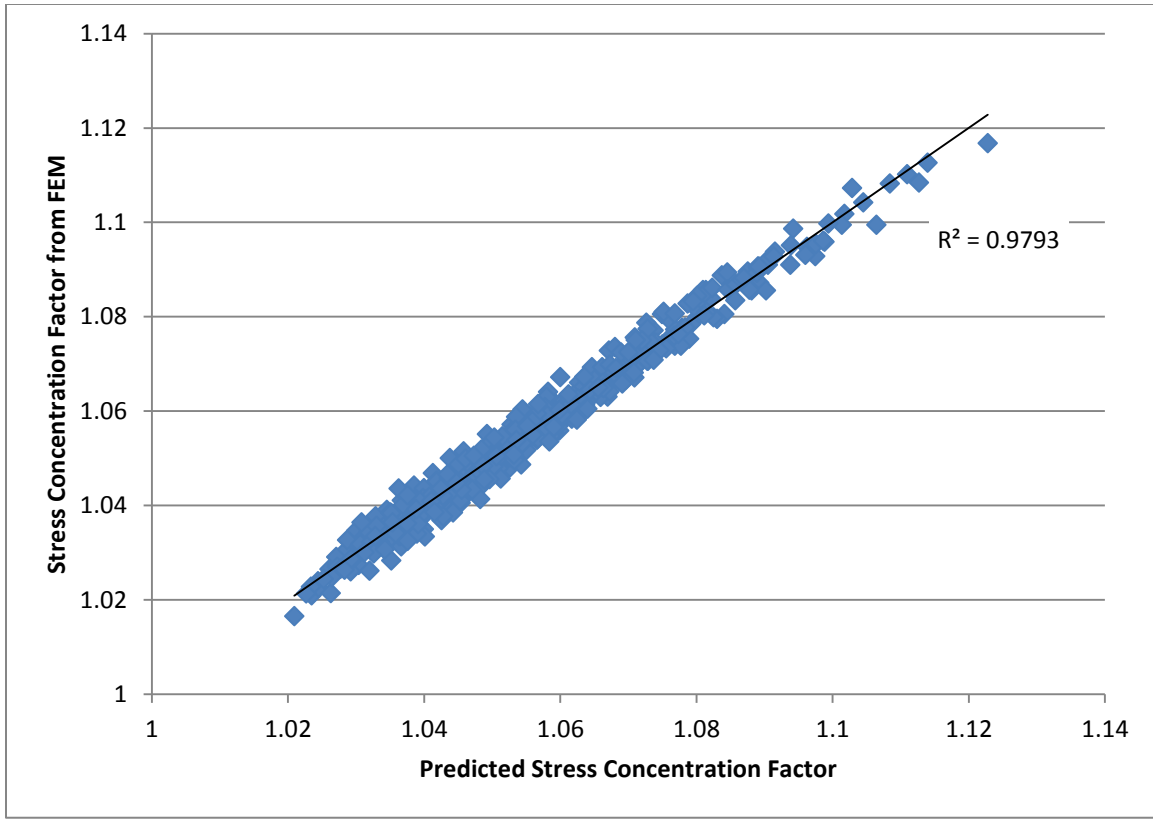


**Figure 5-11: The FEM SCF versus the Predicted SCF from Equation 5-3**

Figure 5-11 shows the high correlation of Equation 5-3 with the finite element results. The equation predicted results are shown on the x-axis and the actual results on the y-axis (a trend-line is included to show the relationship). This demonstrates a strong ability to be able to predict the stress concentration factor, and thus determine what can be done from a design perspective to reduce the chance of a fatigue failure.

$$SCF = \frac{tS}{tF} \sqrt{\frac{2 \times aW}{5 \times bS}} + 1.0 \quad (5-4)$$

In order to facilitate use as well as more clearly show the relationship between the various parameters and the stress concentration factor Equation 5-3 was simplified into Equation 5-4. The girder depth and flange width were deemed to be of minimal importance and removed from the equation, and the exponents were changed to be either

a square root or one. Equation 5-4 gives a clear indication of the importance of each parameter as it relates to the stress concentration factor.

The two main factors in determining what the stress concentration factor will be for a given design may be written as the pipe thickness divided by the flange thickness, and two fifths of the weld size divided by the pipe radius. The first factor is of greater importance than the second. Both of these factors make intuitive sense from a structural perspective. As the influence of the pipe-stiffener becomes greater through an increase in its thickness or the weld size, then the stress concentration factor increases. As the flange of the girder becomes proportionally stiffer the impact of the pipe-stiffener is reduced. The reason a larger pipe-radius makes the flange of the girder stiffer in proportion to the half-pipe itself is that it forces the point of concern farther from the web against which the half-pipe is secured, and thus it becomes less stiff.

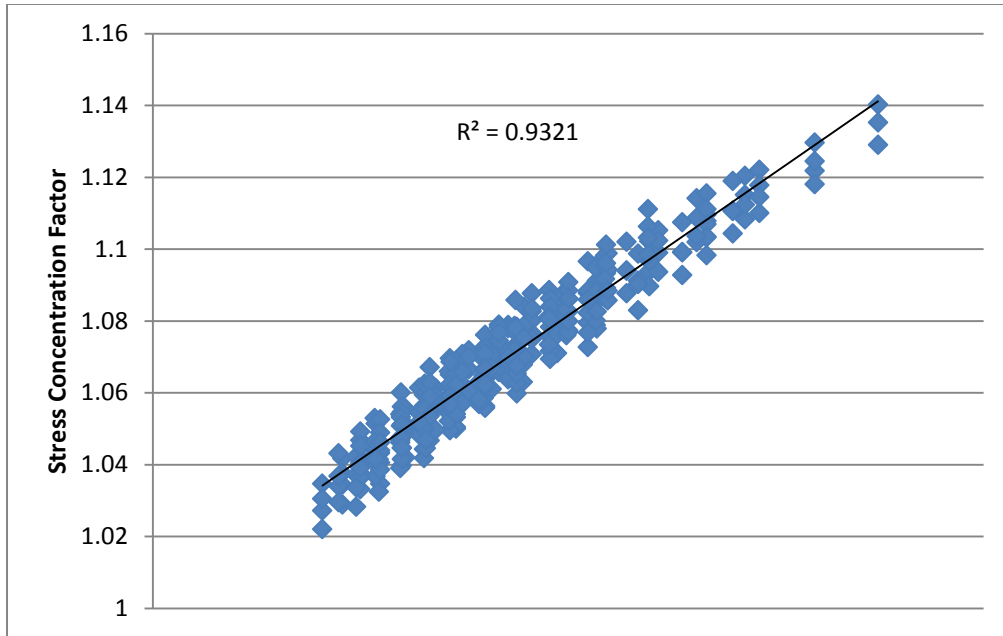


*Figure 5-12: The FEM SCF versus the (Simplified) Predicted SCF from Equation 5-4*

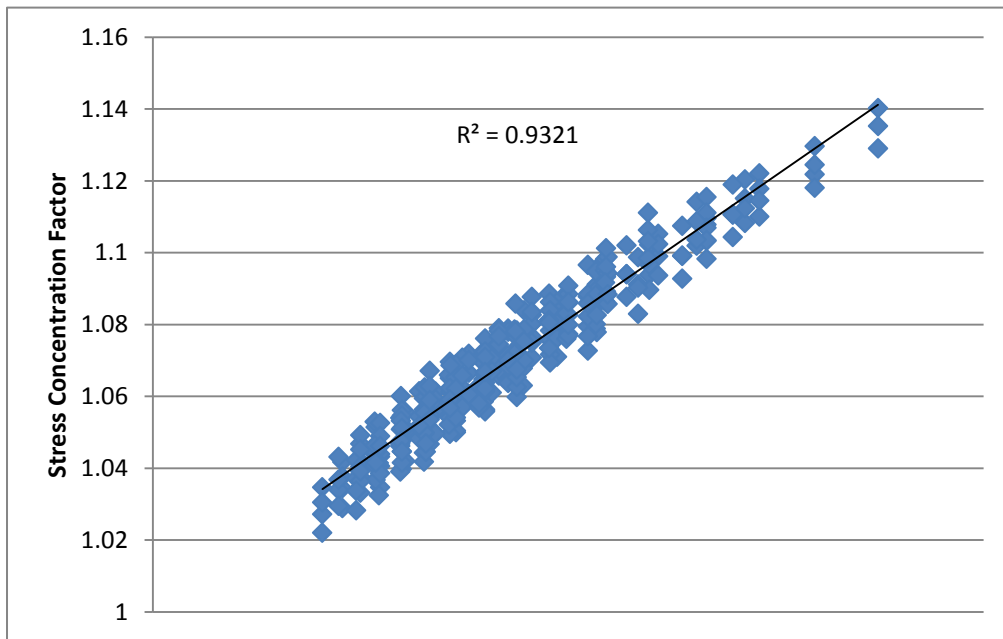
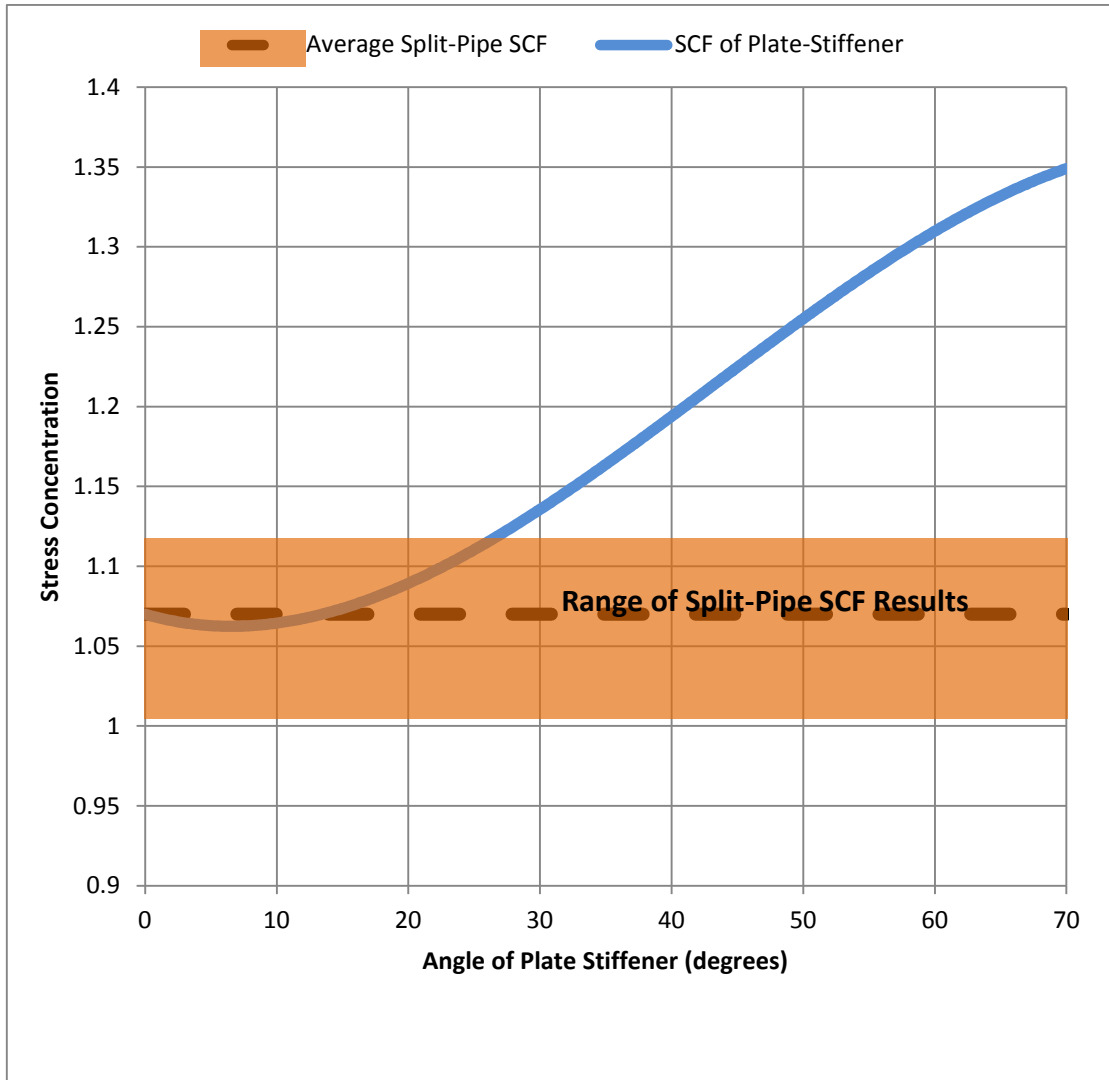


Figure 5-12 shows the results of using the simplified equation. As is to be expected the reduction in precision of the values used, in addition to the removal of two parameters from consideration has resulted in a decrease in the coefficient of

determination. The data exhibits a greater amount of scatter than would be found in the unaltered, computer-generated equation. Yet the decrease in correlation is not great, as the r-squared value drops from 0.98 to 0.94 and all the FEM data remains centered along the line of best fit. There are no errant data points suggesting neither unexplained phenomena, nor indications that as the SCF grows significantly larger or smaller than those found in these particular experiments the FEM values will diverge from the predicted. This shows that Equation 5-4 is both simple to use and understand as well as being an accurate predictor of behavior.

#### **5.6.5 Comparison of Half-Pipe with Plate-Stiffener**

Part of validating the model, as described in Section 4.6.2, was to compare the plate-stiffener results to those of the half-pipe stiffener and ensure that the former performed worse than the latter. When comparing the two specimens tested in the laboratory, the computational model showed a stress concentration factor of 1.08 for both the half-pipe stiffener and the perpendicular plate-stiffener based on a line of best fit from the data. As the skew angle increased the plate-stiffener's stress concentration factor increased with it up to a value of 1.35 for a 70° degree skew.



**Figure 5-13: Stress Concentration Factor Comparison between Plate-Stiffeners and Half-Pipe Stiffeners**

A direct comparison of the plate-stiffener to the half-pipe stiffener is provided in Figure 5-13. This figure shows the results for the plate stiffeners at various skew angles (with the same geometry as the specimen tested in the laboratory) as compared to the general results from the half-pipe stiffener. The shaded box represents the range of SCFs that were found for the half-pipe stiffener, and the dashed line is the average value. The stress concentration factor for the plate-stiffeners appear to drop slightly below the

average value for the half-pipe stiffeners for skew angles less than  $10^\circ$ , but this is a result of the method used to calculate the line of best fit, as well as the impact of the changing location of the hot spot (see Section 5.6.1.1).

These results are more telling for the plate-stiffener than the half-pipe stiffener. The plate-stiffener at low skew angles appears to perform at about the same level as the half-pipe. At  $30^\circ$  skews and less it is within two standard deviations of the half-pipe's average stress concentration factor level. As the skew angle increases, the SCF quickly jumps out of range of the half-pipe stiffener. This indicates that plates welded to a girder at greater than  $30^\circ$  may be of concern from a fatigue performance point of view.

## **5.7 CONCLUSIONS AND RECOMMENDATIONS**

The overall goal of this analysis was to determine if the laboratory results could be extended to multiple design scenarios, and not just the specific one tested. The results of the laboratory testing showed that the half-pipe could be considered as good as the plate-stiffener detail at low skew angles, and provided for the possibility that it may be better than it. It also showed that the half-pipe stiffener was better than the plate-stiffener when it came to the higher skew angles.

### **5.7.1 Overall Results**

The findings of the laboratory testing were verified by the computational study. A direct comparison of the stress concentration factors between the plate-stiffener and the half-pipe reveal them to be very similar for low skew angles. There is no reason to believe that the half-pipe stiffener would perform noticeably worse than the plate stiffener at any point, assuming similar designs for parameters such as plate thicknesses, flange width and others. The plate stiffeners with higher skew angles had demonstrably greater stress concentration factors, indicating that they would behave worse in fatigue than the half-pipe stiffener.

The possibility of the half-pipe stiffener being better than the plate-stiffener even at low degrees of skew is also substantiated by the computational model. Though the

stress concentration values themselves appeared to be nearly identical, within the limitations of this study, between the half-pipe and the plate, or even favor the plate-stiffener this does not give a complete picture.

The stress concentration factor provides an indication of how the geometry of the connection, and in particular the weld, will impact the flow of stresses through the girder. The actual fatigue life is not directly determined by this, but rather includes also the introduction of imperfections into the steel. Some imperfections exist in any steel girder even before welding. However, welding generally creates significantly greater flaws in the steel which make the structure more susceptible to fatigue-type failures (Sause et. al 2006).

The increase in stress at the location of weld related flaws can decrease fatigue life. This occurs when the stress acts perpendicular to the plane of the imperfection, which is the plane of the weld-face (Fisher et. al 1998). In the case of the plate-stiffeners there always exists a plane of the weld such that it is perpendicular to the principle stress, which is along the axis of the girder. For low or no-skew plate-stiffeners the entire weld has its face, and thus imperfections, perpendicular to the action of the principle stress.

For the plate-stiffeners with a higher skew angle, the stress concentration moves to the edge of the weld. The principle stress is no longer perpendicular to the face of the weld along the length of the stiffener, but the weld curves around the plate-stiffener at the hot spot. This creates a face of the weld to be positioned perpendicular to the principal stress at the point of highest stress concentration, allowing for a crack to form there and then propagate through the remainder of the flange. This phenomenon was the observed method of failure in for the skewed stiffeners tested in the laboratory.

This is not the case for the half-pipe stiffener. The hot-spot studied, and reported here was always representative of the greatest stress, but the stress was never perpendicular to the weld face. Instead, the stress acted at an angle of almost  $45^\circ$  from the face of the weld. Theoretically this should lead to a better fatigue life than if the stress were acting directly perpendicular to the weld. The component of the stress here



was in the range of 0.6-0.7, instead of the principle stress magnitude of 1.0-1.1, representing a significant reduction.

### **5.7.2 Use of the Half-Pipe Stiffener and Restrictions**

This research indicates that a half-pipe stiffener can be used in place of a plate stiffener without adversely affecting the fatigue life of the girder. Further, this research suggests that plate stiffeners at skew angles equal to or greater than  $30^\circ$  may adversely affect the fatigue life of a girder.

The plate-stiffener detail is given a category C rating by AASHTO, and this research showed that the half-pipe stiffener performs at least as well. It is possible that the half-pipe stiffener may be superior to the plate-stiffener detail, but that has not been shown conclusively. Until further study is done, it is recommended that the same category C rating be used for the half-pipe stiffener.

The results of computational testing show that the stress concentration factors for the half-pipe stiffener are tightly grouped and uniform within typical design scenarios. Specific limits on its use are not readily apparent from the research. However, if concern remains as to its fatigue performance, Equation 5-4 could be used to estimate the stress concentration factor.

## CHAPTER 6

# Distortional Fatigue Analysis

### 6.1 FATIGUE CONCERNS FOR HALF-PIPE STIFFENER

The main focus for this research, both experimental and computational, has been to evaluate the potential for fatigue failure in the tension flange of a bridge girder at the location of a half-pipe stiffener. An additional concern, considered in this chapter, is the potential for fatigue failure of the half-pipe stiffener itself due to forces imposed on the half-pipe by the connected cross-frame members. It is anticipated that cross-frame members will be attached to the half-pipe stiffener through the use of a connection plate. The connection plate is welded to the half-pipe, and the cross-frame members, in turn, are welded to the connection plate. An example of this arrangement is shown in Figure 6-1. The connection plate is welded to the stiffener but is not welded to the girder flanges. The connection plate is not welded to the girder flanges because the connection plate would be at a skewed angle to the girder. As described in the previous chapters, welding the connection plate to the girder at a skew leads to potentially poor fatigue performance of the girder flange (see Section 5.6.1.3).

Since the connection plate is not welded to the girder flanges, any forces imposed by the cross-frame members on the connection plate will be transmitted directly to the half-pipe stiffener. This, in turn, may cause localized bending of the wall of the half-pipe in the region between the end of the connection plate and the girder flange. This region is highlighted by the circles in Figure 6-1. These localized distortions in the wall of the half-pipe could potentially lead to a fatigue failure of the half-pipe in this region. This phenomenon is referred to as “distortional fatigue” herein. Distortional fatigue is a well-recognized phenomenon when plate stiffeners are welded to the web of a girder but not to the flanges (Berglund and Schultz 2006).

Due to schedule and financial constraints on this project, it was not possible to investigate distortional fatigue of the half-pipe stiffener through laboratory experiments.

However, a preliminary evaluation of the potential for distortional fatigue was conducted through the use of finite element analysis. That analysis is described in this chapter.



*Figure 6-1: Connection of Cross-Frame to Half-Pipe Stiffener*

## **6.2 FINITE ELEMENT MODEL**

All of the investigation of the distortional fatigue concerns occurred through the creation and testing of a finite element model. This model was designed, just as those described in previous chapter, to determine the maximum hot spot stresses. Parametrical

studies were conducted to evaluate the influence of various design variables on the hot spot stresses.

The principles used to create the model, as well as much of the code, were the same as those employed in the previous chapters. However, with no physical testing the models created for distortional fatigue investigation could not be validated.

The modeling done allowed a comparison between the stresses that would develop in the half-pipe stiffener and those that are found in the plate-stiffener as a result of cross-frame forces. The author is aware of no fatigue issues that have been observed in plate-stiffener connections from this kind of loading. If it could be shown that the stresses in the half-pipe stiffener are the same or less than those found in the plate-stiffener then it would support the use of the half-pipe stiffener as an alternative to the plate-stiffener and indicate that no fatigue problems should arise through cross-frame forces.

The plate-stiffener connection is not subject to distortional fatigue, but rather stress-concentrations that develop as a result of cross-frame forces. The phenomena of distortional fatigue as is typically seen in the webs of girder when welded to plate-stiffeners which are not in turn welded to the flange (Berglund and Schultz 2006) is functionally equivalent to the half-pipe connection, not the plate-stiffener connection. The plate-stiffener model served as the basis of comparison for a cross-frame connection that did not have any fatigue issues against the half-pipe connection, which had the potential for distortional fatigue.

### **6.2.1 Basic Model**

The models that were used in this investigation did not employ any symmetry constraints that could have reduced the computational time. The issue of distortional fatigue causes a loading that was not conducive to symmetric-model reduction. The change in the location of interest, i.e. the location where the stress concentration was highest, resulted in a change of meshing patterns. The girder itself was no longer of concern for fatigue issues. Instead the half-pipe or plate-stiffener was the location of the

stress concentrations. The basic break-up of mesh densities: coarse, fine, and extra-fine, were still used but in different places in the model. The stiffeners themselves and the welds connecting the cross-frame to them had the densest mesh.

### 6.2.2 Plate-Stiffener

The plate-stiffener had a connection-plate connected to it that was bent at a given angle of skew. The plate-stiffener itself remained perpendicular to the web through all the tests, only the bend of the connection plate changed, based on the skew. This bent plate was then connected to the cross frame itself which was represented by a given, axial loading.

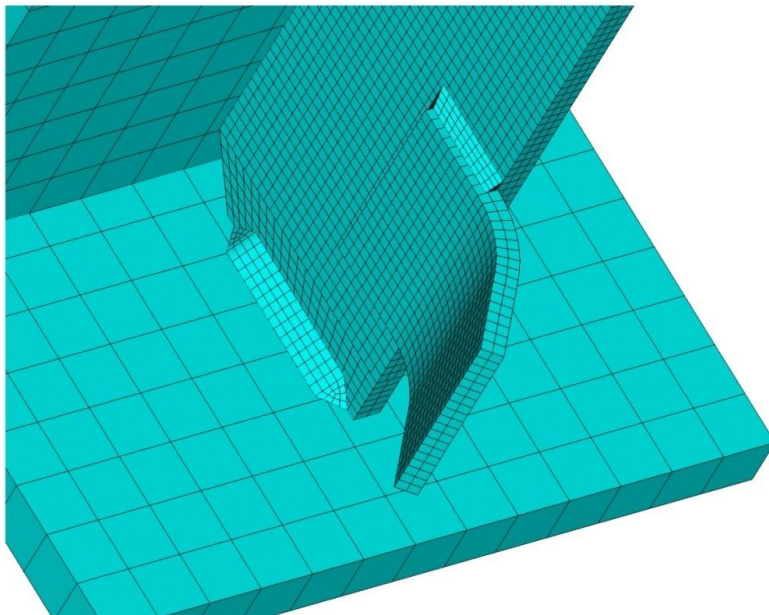


*Figure 6-2: Basic Plate-Stiffener Model (Mesh Elements Shown)*

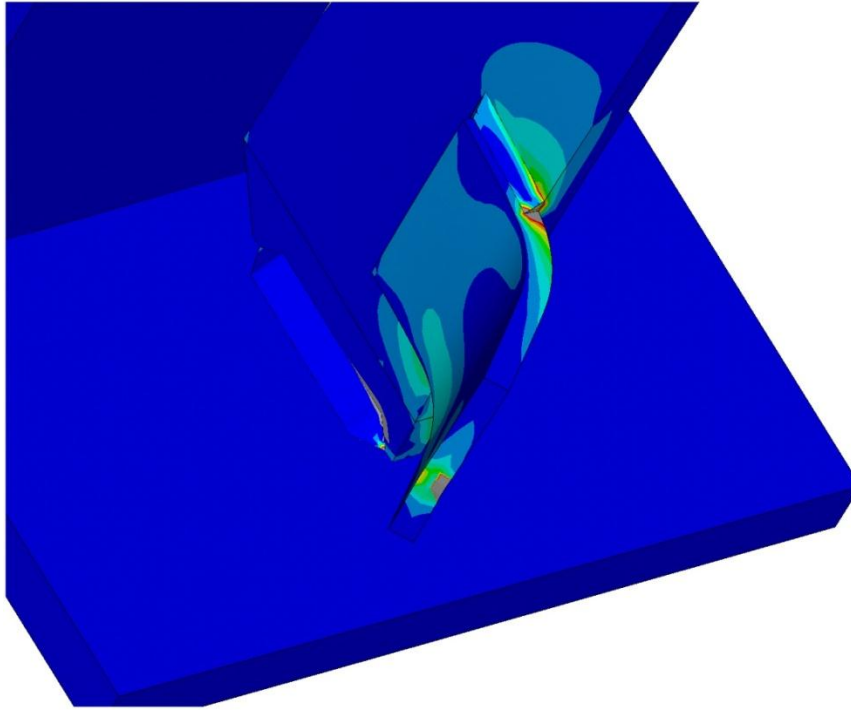


*Figure 6-3: Plate-Stiffener Model (Principle Stresses Shown)*

The basic layout of the plate stiffener model can be seen in Figure 6-2; the bent plate is welded to the plate-stiffener which is in turn welded to the girder. A load is distributed across the middle of the end of the bent plate, in plane with the bend, pulling at the skew angle in relation to the girder, and the resulting stress field is shown in Figure 6-3.

Unlike the previous flexural fatigue analysis, a parametric study was done on the plate stiffener as well as the half-pipe stiffener for distortional fatigue effects. This was primarily because of the large number of unknowns involved in this study, eliminating the impact of varying parameters by testing for them helped reduce the uncertainties.

### **6.2.3 Half-Pipe Models**

The half-pipe model was created using the same code that was used for the flexural fatigue investigation. Like the plate-stiffener, the location of the extra-fine mesh densities was shifted so as to allow for appropriate measurements. A connection to the

cross-frame was also added to the original model and a load applied in the same manner as was done for the plate-stiffener's distortional fatigue model. The load was applied along the direction of the cross-frame, which correlated to the angle of the skew. Unlike the flexural fatigue model, the angle of skew mattered for the half-pipe in this analysis and not just the plate-stiffener.

### ***6.2.3.1 Intermediate Connection Plate***

Two different models were created to study the half-pipe stiffener representing two different methods of connecting the cross-frames to it. The first included plate that extended nearly the full depth of the pipe stiffener and was in turn attached to a connection plate that was itself attached to the cross-frame.

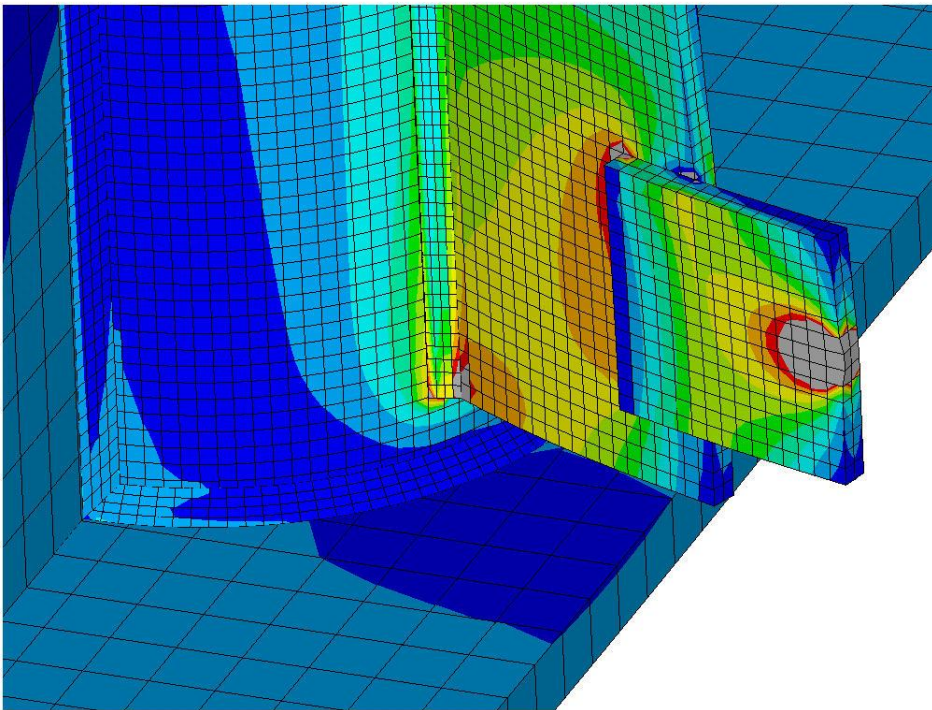


***Figure 6-4: Half-Pipe Stiffener with Intermediate Connection Plate***

An example of this model is shown in Figure 6-4 which displays the element densities along with the stress distribution. As was done with the plate-stiffener model,

the force from the cross-frame is applied as a distributed load to the center of the end of the connection plate and the girder restrained at the edges.

### ***6.2.3.2 Direct Connection***

The alternate method of joining the cross-frame to the half-pipe stiffener that was examined here was to remove the full-depth plate and attach the smaller connection plate directly to the half-pipe. This served as a means of determining the sensitivity of the method of connection. An example of this model is shown in Figure 6-5.

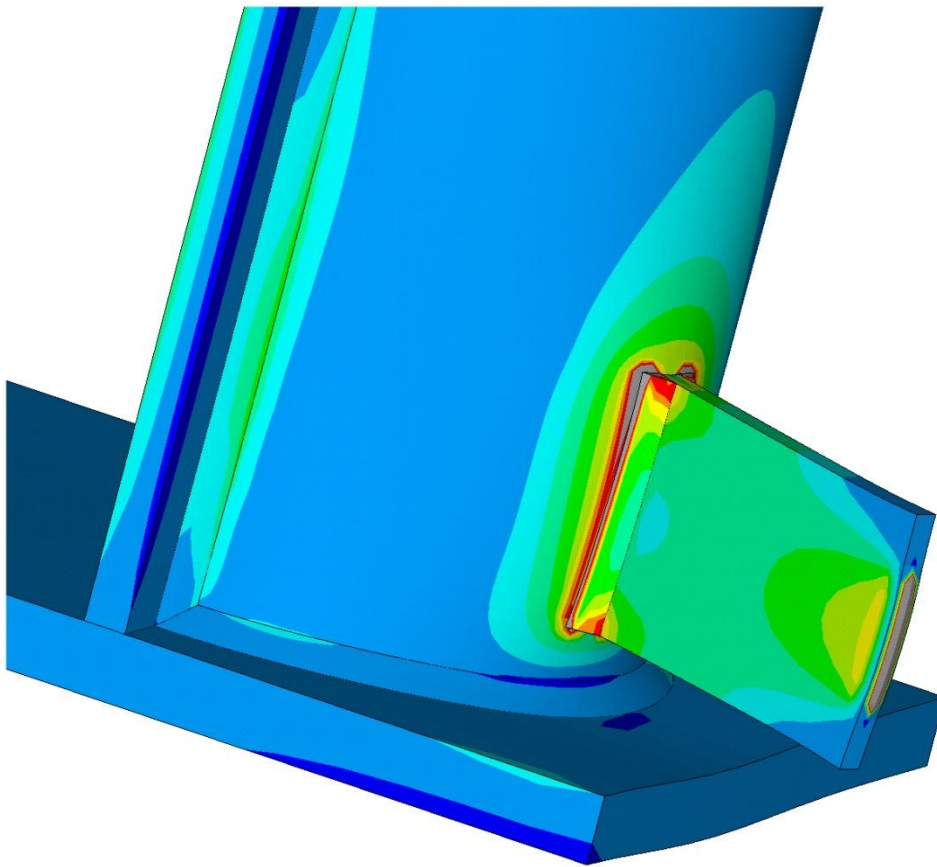


***Figure 6-5: Half-Pipe Stiffener with Direct Connection***



#### **6.2.4 Hot Spot Stress**

When completing the flexural fatigue study, a stress concentration factor was used as an indicator of how the geometric changes which the connection introduced would impact the flow of stresses through the girder. For the problem of distortional fatigue this was not a viable option, as creating a base stress level was not feasible within the constraints of the geometry. No corollary could be found for the stress concentration factor, and so a less descriptive and more qualitative approach had to be taken.

Instead of generating a number that had a definite meaning independent from the computational modeling like the stress concentration factor, a comparative means of measurement was used. A force of 10 kips was applied to each model along the angle of the skew. The highest concentration of stress was then found in the model and the absolute value of the stress at that point was taken as the result. The stress concentrations always occurred at places that were impacted by the notch effect (see Section 4.5.2.2). To address this problem, the DNV method of extracting stresses from notch-effect stresses was used. The hot spots themselves were at the bottom edge of the weld connecting the bent plate to the plate-stiffener, or at the edge of the weld connecting the plate (the full-depth plate or the connection plate itself depending on which one was connected to the half-pipe) to the half-pipe.

As noted earlier, no laboratory testing was conducted to evaluate distortional fatigue in the half-pipe stiffener, so the computational studies described herein should be viewed as a preliminary assessment only.

### **6.3 FINITE ELEMENT RESULTS**

The plate-stiffener model required less computational time to complete per analysis than the half-pipe stiffener. This time difference allowed for more plate-stiffener models to be processed. A total of 1038 different models of the plate-stiffener were completed, and 688 for the half-pipe stiffener. The parameters of interest were chosen from those that defined the problem, and varied in the same process as was used in the flexural fatigue study (see section 5.3).

### 6.3.1 Plate Stiffener Analysis and Results

The plate stiffener analyses showed a large range of results. The stress concentration was always greatest at the bottom weld which connected the bent plate to the plate-stiffener. The principle stress was perpendicular to the face of the weld, and the path chosen for DNV extraction was along this principle direction (approaching the face of the weld from the bottom of the plate-stiffener).

*Table 6-1: Parameters Used in testing Plate-Stiffener*

Parameter	Symbol	Notes	Values (in)
Heigh of Bent Plate	hC	Measured from Top of Flange to Bottom of Plate	1, 2, 3, 4
Angle of Skew	aS	Expressed in the Bent Plate	5, 10, 15, 25, 35, 40, 45, 55
Stiffener Thickness	tS		0.2, 0.3, 0.4, 0.5, 0.6, 0.7, 0.8
Bent Plate Thickness	tC		0.1, 0.2, 0.3, 3/8, 0.4, 0.5, 0.6, 0.7, 0.8
Size of Weld	aCW	Refers to Weld between Bent Plate and Stiffener	1/16, 2/16, 3/16, 4/16, 5/16

The parameters that were analyzed as well as the values considered are shown in Table 6-1. The greater number of pieces involved in the problem of distortional fatigue was paired with an increase in the number of parametric descriptors. There were a number of parameters that appeared to have little influence on distortional fatigue, such as the girder flange width, that were not included in the study. This meant that a sixth parameter could not be included by extrapolation as was the case in the flexural fatigue study. These five parameters shown here represented the entirety of what was tested.

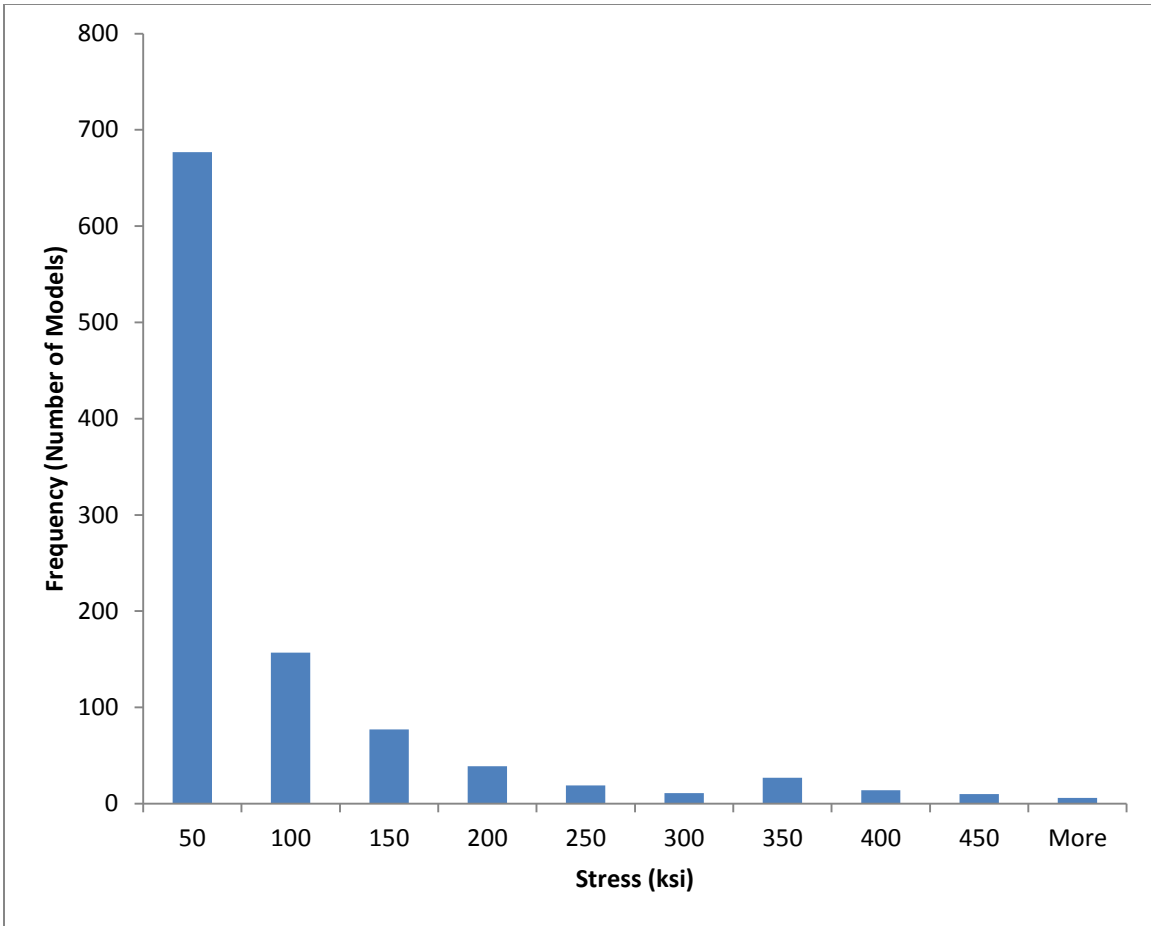


***Figure 6-6: Histogram of Plate-Stiffener Stresses***

The wide range of stresses that result from the plate-stiffener testing can be seen in Figure 6-6. The majority of parametric combinations lead to a maximum stress that was 50 ksi or less, but approximately 35% were greater than 50 ksi, and several reached close to or in excess of 1000 ksi. This large range shows that hot spot stresses in the plate-stiffener are highly sensitive to the parametric values chosen in the design. The average value of the stresses was 67 ksi and the median value was 25 ksi. These results were clearly not normally distributed, meaning the standard deviation was not a meaningful value for this data set.

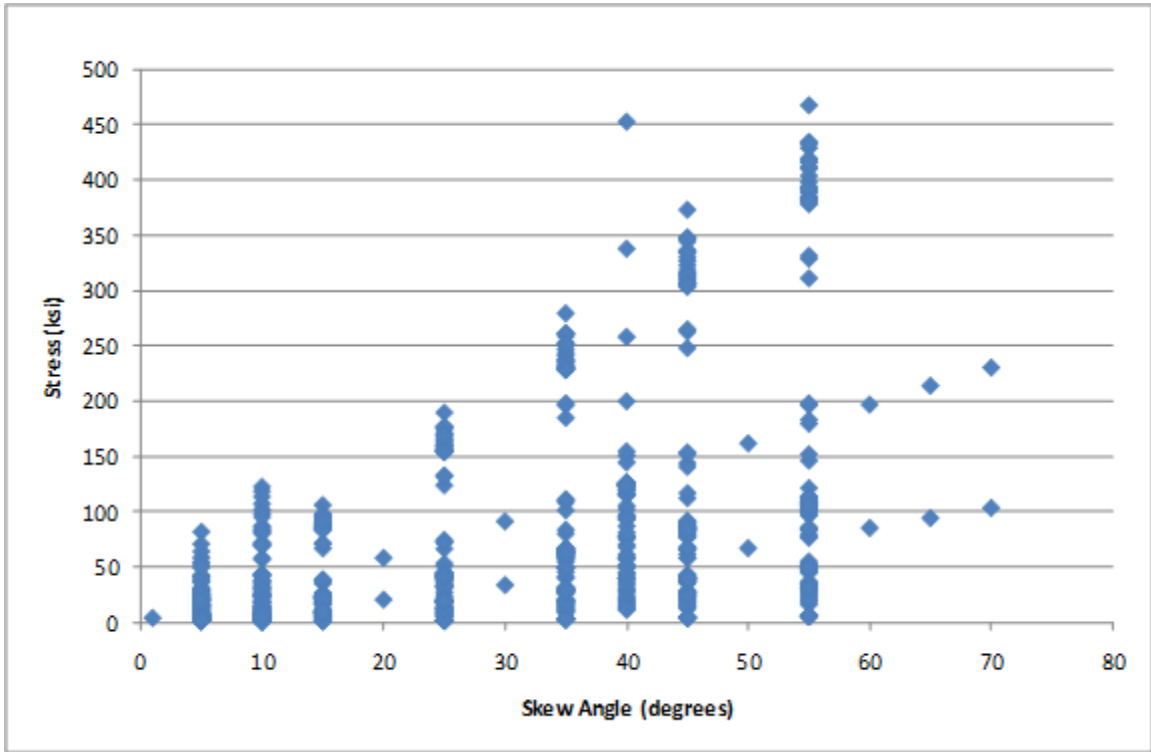


*Figure 6-7: Stresses in Plate-Stiffener vs. Skew Angle*

The histogram revealed little about the data itself other than its range and average. A more descriptive image is found in Figure 6-7 which shows the relationship between the skew angle and the maximum stress. The stress concentration appeared to be generated from the prying away of the bent plate from the plate-stiffener. This means that as the angle of skew increases, the stress will increase with it. Though the other parameters clearly played a role, it can be seen that the skew angle dominated the stress concentration.

The same equation that was used in investigating flexural fatigue (Equation 5-1) was utilized here to determine the influence of each parameter. The same genetic algorithm was also employed to solve for the best-fit equation, now using the parameters relevant to the plate-stiffener study.

$$Stress = 0.0602695 \times ((hC^{0.561861} \times aS^{1.1673} \times tS^{-2.58924} \times tC^{-0.0537889} \times aCW^{-0.197195}) + -3.04295) \quad (6-1)$$

The results of the genetic algorithm are shown in Equation 6-1. Again the numerical values are unrealistically precise as the equation represents the direct output of the computer. The most influential parameter appears to be the plate-stiffener's thickness. This is in line with expectations as the value represents the stress that would appear in the plate-stiffener given a constant, applied load. As the plate-stiffener's size decreases the stresses will go up since the load is maintained. This does demonstrate that increasing the plate stiffener's thickness can reduce fatigue concerns.

The skew angle, as mentioned above, also acts as a highly important variable showing the impact of increasing the angle at which the force acts. This increases the prying stress at the edge of the weld. The distance above the bottom flange at which the cross-frame is connected appears to have some impact as well, showing that the closer the cross-frame can be to the girder's flanges the better the plate-stiffener will perform. The thickness of the connection plate and weld size appear to have little impact.

The R-squared correlation coefficient for Equation 6-1 is 0.97, a very high value. This is the most important result, demonstrating that the stresses in the plate-stiffener are well behaved. They act in predictable ways as the various parameters are changed and thus are the results here can be extrapolated to general design.

### 6.3.2 Half-Pipe Stiffener Analysis and Results

The half-pipe stiffener results spanned a much smaller range than those of the plate stiffener. Like the plate-stiffener, the stress values were primarily on the low end of the spectrum, and tailed off for higher stresses.

**Table 6-2: Parameters Used in testing Half-Pipe Stiffener**

Parameter	Symbol	Notes	Values (in)
Heigh of Connection Plate	hC	Measured from Top of Flange to Bottom of Plate	0.5, 1, 1.5, 2, 3, 4
Angle of Skew	aS	Expressed in the Connection Plate	15, 35, 40, 55
Stiffener Thickness	tS		0.3, 0.5, 0.6, 0.7
Connection Plate Thickness	tC		0.1, 0.3, 3/8, 0.5
Size of Weld	aCW	Refers to Weld between Connection Plate and Stiffener	1/16, 2/16, 3/16, 4/16

The parameters used in testing the half-pipe stiffener were the same ones used for the plate stiffener, except that the half-pipe model used a general connection plate instead of a bent plate, and the stiffener refers to the half-pipe instead of the plate.

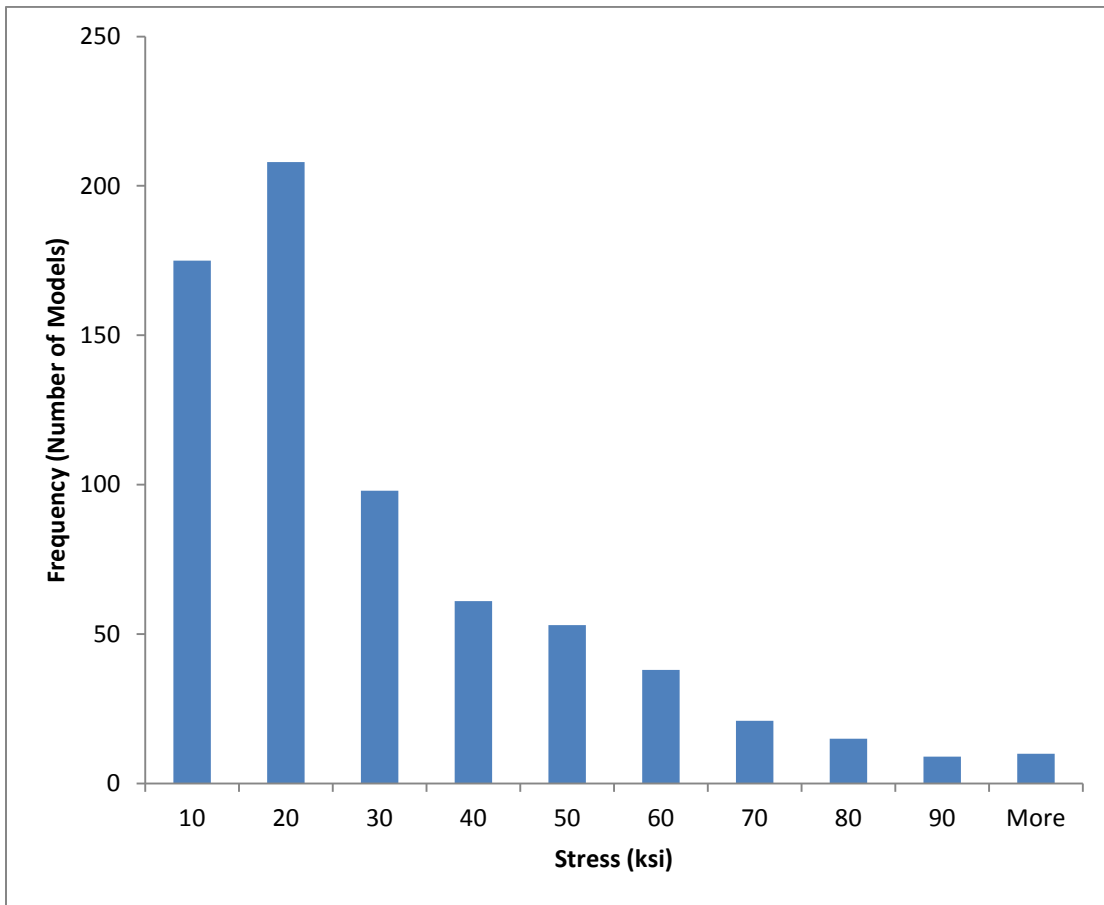


**Figure 6-8: Histogram of Half-Pipe Stiffener Stresses**

Figure 6-8 shows a histogram of the half-pipe stiffener results. A high grouping of models exhibited stresses in the lower ranges with progressively fewer model exhibiting the higher stresses. Here the total range is from a stress of 1 ksi up to 110 ksi. The average value was 25 ksi and the median was 17 ksi.

An attempt was also made to generate an equation that would predict the stresses in the half-pipe stiffener. However an R-squared correlation coefficient could not be achieved that exceeded 0.55, which demonstrates a low-level of correlation. It was discovered that this resulted from the impact of the skew angle. The angle of skew appeared to have a sinusoidal impact on the stresses. When the cross-frame was connected away from both the web and the edge of the flange at around  $45^{\circ}$ , the same location the maximum stress was found in the flexural fatigue model, the stress was at its lowest. When the skew approached either extreme of the outside of the half-pipe or coming close to the web, the stress would increase. These shifts were not dramatic, indicating that large variations were not to be expected. However, they could not be captured by the polynomial nature of the equation that was used in the attempt.

It was discovered that when the impact of the skew angle was removed, by examining each angle as a separate data set, the equation could perform very well.  $R^2$  values in the range of 0.9 to 0.95 were found, showing a well-behaved solution. An exact equation including the skew angle could not be written as a result of this behavior. It was demonstrated though, that the half-pipe stiffener did have predictable results, and thus the specific values found in this study are indicative of overall behavior and not random distribution.

The difference between using an intermediate connection plate and not using one was examined, but found to be negligible. It was assumed that using an intermediate plate would be the usual method chosen when creating a final design as it would greatly facilitate construction in the field. However, the results here demonstrated that either of these options would have similar results, and that the stress generated was not sensitive to the method of connection.

### **6.3.3 Comparison of Results**

Both the plate-stiffener and the half-pipe stiffener had results that demonstrated predictable behavior. This, along with keeping the parametric input equivalent allowed for a comparison between the plate-stiffener and the half-pipe stiffener. The values of the stresses were all from equivalent loads, each one having a 10 kip force applied where the cross-frame attached to the connection plate.

The first and most important observation was that the average value and median value, which was more descriptive of behavior for these data sets, was lower for the half-pipe stiffener than it was for the plate-stiffener. The difference was significant. The average for the plate stiffener was 67 ksi and the average for the half-pipe stiffener was 25 ksi, 40% less than for the plate-stiffener. The median values followed that same pattern, being 25 ksi and 17 ksi respectively. The range of results also favored the half-pipe stiffener. The plate stiffener produced stresses of which more than 25% exceeded 100 ksi. The half-pipe stiffener had only one result that exceeded 100 ksi. The wide variability demonstrated by the plate-stiffener indicated that designs within the scope of typical detailing could result in large stress concentrations.

## **6.4 SUMMARY**

The results of this preliminary finite element analysis suggest that peak stresses developed in the half-pipe stiffener from the cross-frame connection are generally less than peak stresses in the bent-plate connection. Since there is no history of fatigue problems with the bent plate connection, this result suggests that cross-frame connections to the half-pipe are not expected to cause distortion-induced fatigue problems. However, it should be recalled that this study was largely qualitative in nature, and there was no laboratory test data available to validate the model. Laboratory testing of the cross-frame to half-pipe connection would be desirable in the future to provide additional insights into the potential for distortional fatigue problems in the half-pipe stiffener and to provide data for validation of computational models.



## CHAPTER 7

### Summary and Conclusions

#### 7.1 SUMMARY OF PROBLEM

The overall goal of this investigation was to determine if there were any fatigue issues that might limit the use of the half-pipe stiffener in place of a plate stiffener for cross-frame connections in skewed bridges. The plate-stiffener is currently given a fatigue category rating of “C” by AASHTO. An objective of this investigation was determine if the half-pipe stiffener performed better or worse than the plate stiffener with regard to fatigue, and to suggest a fatigue design category. This portion of the study focused on fatigue of the girder tension flange at its connection to the half-pipe stiffener, and included both experimental and computational studies. An additional objective of this study was to conduct a preliminary investigation into the potential for distortion-induced fatigue in the half-pipe stiffener at its connection to the cross-frame. This portion of the investigation was addressed by computational studies only.

#### 7.2 PHYSICAL TESTING AND RESULTS

To study the fatigue performance of the girder tension flange at the connection to the half-pipe stiffener, a series of fatigue tests were conducted. The test specimens included both half-pipe stiffeners and conventional plate stiffeners for comparison. The plate stiffeners in the specimens were oriented perpendicular to the web and also at a skew angle to the web. Plate stiffeners at both a 30° and at 60° skew angle were tested.

The test specimens were all subjected to cyclic loading causing pre-determined stress ranges until fatigue cracks formed. Then the test was stopped, the total number of load-cycles it took to reach failure was recorded, and the test was continued until the beam was no longer usable. All beams were installed with both plate-stiffeners and half-pipe stiffeners that were tested together simultaneously.

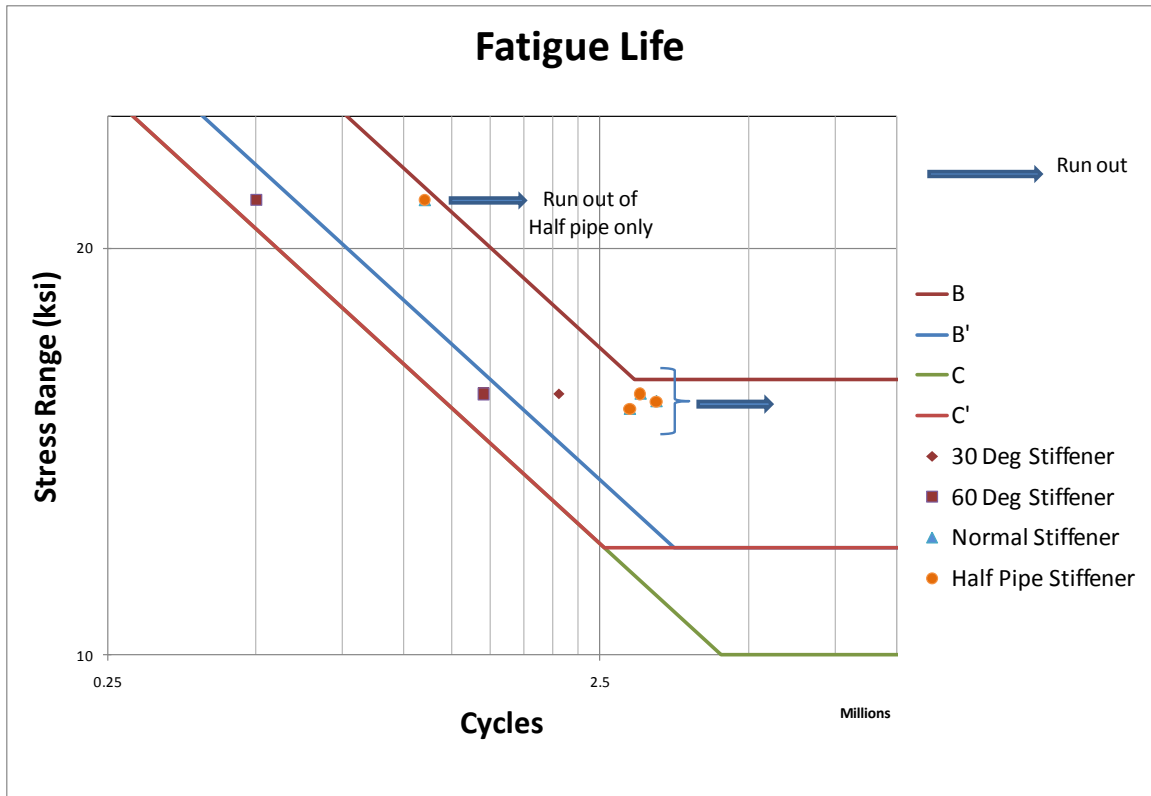


**Figure 7-1: Results from Physical Testing**

The results of the testing are shown in Figure 7-1. The AASHTO fatigue categories are also shown. All of the stiffeners to girder connections that were tested passed the category C, and most passed the B' category rating. The two connections that did exceed the C category but not the B' rating were the plate-stiffeners that were skewed at 60 degrees. These performed the worst of all of the connections, with the 30 degree stiffeners performing slightly better.

The perpendicular plate-stiffeners performed above the level of the skewed stiffeners, but they showed incipient cracking in one case, and did crack in another. The half-pipe stiffeners never exhibited any fatigue cracking. Autopsies that were conducted after the testing was complete revealed no cracks forming in the half-pipe stiffeners. These results showed that the half-pipe stiffener performed as well as or better than the currently utilized plate-stiffener.

### 7.3 FINITE ELEMENT MODELING

After the physical testing was completed, a finite element model was generated in ANSYS that simulated both the half-pipe stiffener and the plate-stiffener as computational models. A parametric analysis was performed on the half-pipe stiffener to determine how stable the results were, and what values impacted the stress concentration factors.

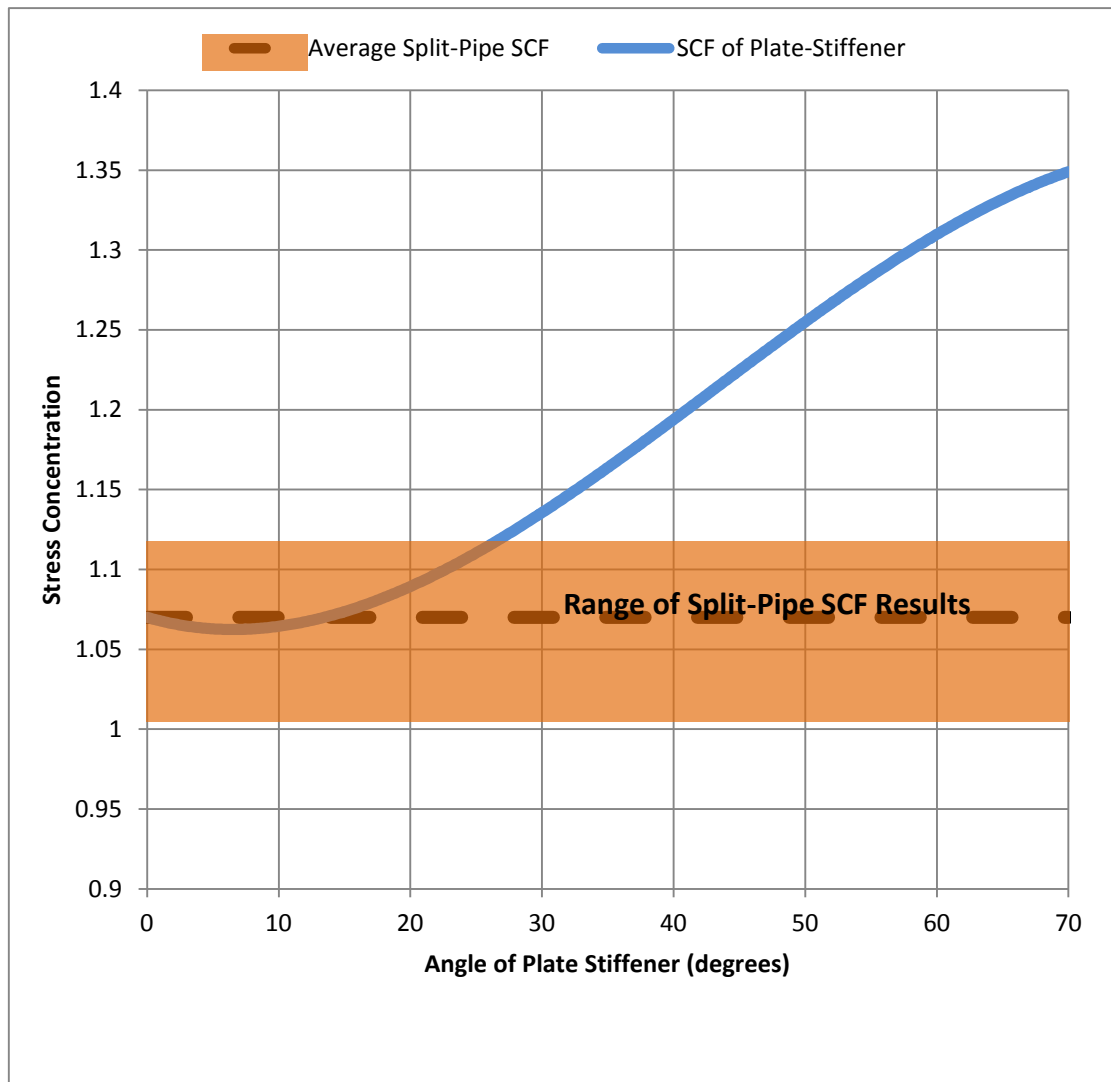


*Figure 7-2: Results of Computational Comparison between the Plate-Stiffener and Half-Pipe Stiffener*

The final results can be seen in Figure 7-2. The half-pipe stiffener performed as well as the plate-stiffener, and better than it by a significant margin at high skew angles. The range of results for the half-pipe stiffener were concentrated within a small range, showing that it did not have the tendency to rapidly reduce performance given changes in the design. This indicates that there would be no drop in fatigue life should the half-pipe stiffener be substituted for the plate-stiffener.

A finite element analysis was also completed comparing the half-pipe stiffener with the plate-stiffener for distortional fatigue concerns. This study likewise found no indication that the half-pipe would perform worse than the plate-stiffener. The average and median stresses generated in the half-pipe under identical loading were less than those found in the plate-stiffener. The results appeared to show consistent behavior that would not quickly devolve under slight changes to the basic connection design.

#### **7.4 RECOMMENDATION FOR USE**

Based on the physical and computational results, it is recommended that the half-pipe be given a category C rating and be used in place of the plate-stiffener where applicable. There was no indication by any of the results found here that the half-pipe stiffener would perform worse than the plate stiffener, and thus no reason to give it a worse rating. Though there was some justification found for improving the rating, it was not sufficient so as to recommend a higher AASHTO fatigue category rating.

If concern remains as to the performance of the half-pipe stiffener, restrictions could be placed on its use. Limits to specific values could be used to ensure that high stress concentrations don't develop. For instance, disallowing a weld size greater than  $\frac{5}{16}$  inch would reduce the possibility of fatigue failure without severely limiting the use of the half-pipe. A similar restriction could be placed on the ratio of the half-pipe's thickness to the flange thickness. Should this be done, a value of  $\frac{2}{3}$  is recommended, which would again reduce the potential for failure without being overly restrictive.

Another possibility, should there still be concern for fatigue performance, is to use the generated equation found in 5.6.4 to limit the predicted stress concentration.

$$SCF = \frac{tS}{tF} \sqrt{\frac{2 \times aW}{5 \times bS}} + 1.0 \quad (7-1)$$

Limiting the value produced by Equation 7-1 for implementation of the half-pipe would be a simple way to allow for the majority of designs while still providing a robust protection against fatigue failure. If this approach is taken a value of 1.15 is recommended as the limit for design.

## **7.5 AREAS FOR FURTHER STUDY**

The research conducted for this project was sufficient so as to confidently recommend the use of a category C rating for the half-pipe stiffener. However, it also opened up avenues for continuing study that would help gain a greater understanding of the fatigue performance of the half-pipe stiffener. Two main areas appear to be relevant for further investigation.

Both the laboratory testing and computational studies suggested a strong possibility existed for a fatigue rating above the category C, possibly significantly better. This could be studied through a larger program of laboratory testing that would look exclusively at the half-pipe stiffener. Such research might allow for a better fatigue category rating, improving the potential use of the half-pipe stiffener.

The second area that would benefit from further research is the impact of distortional fatigue. The computational study undertaken here included a large number of assumptions, and could not be validated through physical testing. Further research into how such distortional forces occur, quantification of those forces, and then laboratory testing would greatly increase understanding of the problem. Currently the half-pipe's only proposed use at the ends of girder or over supports where distortional effects are minimal. Its use could be expanded if more were known about distortional fatigue.

# Appendix

## A PHYSICAL TESTING

This portion of the appendix contains data from the physical testing portion of the research. The summary data and conclusion can be found in CHAPTER 3.

### A.1 Records for Physical Testing

A paper record was kept of the physical testing noting the settings of the electronic controller, the cycle count, stress range, etc... Any developments on the specimen itself (such as formation, or possible formation of a fatigue crack) were also noted along with any event that caused the test to be temporarily suspended (such as an equipment failure). These records are included here.

# Data Log for Fatigue Testing (Bent Plate Project)

Project # 0 - 5701

CHANGED

Specimen: 30A and 30B Date: JUNE 23, 2009

Desired Measurements: 65 Displacement (in): 10 Maximum: 10 Minimum: 10

Frequency: 40 Displacement (in): 10 Maximum: 10 Minimum: 10

Settings: P Gain: 2.2 V/V I Gain: 3.2 V/S D Gain: 0.4 MS F Gain: 0.2 MS

Date	Time	Cycles	Set Point (k)	Scan (k)	Frequency (Hz)	Displacement (in) Maximum	Displacement (in) Minimum	Load (kips) Maximum	Load (kips) Minimum	Controlling Variable Error (k) Maximum	Controlling Variable Error (k) Minimum	Notes
6/24/09		ADD	3363	CYCLES	TO	ENL	CYCLE	COUNT	FROM	TEST	0	1 V P GAIN
6/24/09	9:30 AM	0	65	415	0.4999			10.494	25.27	15.81	-19.5	RE-START TEST
6/24/09	12:45 PM	5806	65	45	0.7503	0.80	0.82	105.12	24.40	24.04	-22.52	DISPLAY WAS FROZEN
	4:00 PM?	49,455										> TEST WAS STOPPED
6/25/09	10:00 AM	49,450	65	45	0.7503			104.83	24.66	24.56	-21.83	RESTART TEST
6/25/09	12:53 PM	55,679	65	43	0.7503			105.50	25.07	19.03	-18.4	
6/25/09	1:02 PM		65	45	0.9			105.6	25.1	24	-22	
6/25/09	2:20 PM	57,701	65	47.5	1.1004			105	25	30	-27	
6/25/09	10:39 AM	137,826	65	47.5	1.1004			105.1	24.97	30.22	-28.4	
6/25/09	9:14 AM	416,094	65	47.5	1.1004			105.2	26.11	30.2	-28.2	
6/25/09	9:10 AM	511,490	65	47.5	1.1004			105.2	25.1	30.5	-28.6	
7/1/09	9:07 AM	607,110	65	47.5	1.1004			105.1	25.0	30.5	-28.7	
7/2/09	9:32 AM	703,936	65	47.5	1.1004			105.1	25.1	30.5	-28.7	
7/3/09	9:25	799,787						105.2	25.07	30.12	-28.00	
7/3/09	11:14	880,672						105.1	25.11	30.3	-28.4	
7/3/09	8:30	1083,196						105.0	25.0	30.3	-28.5	
	1:55	1,104,179										
	2:30											
7/04/09	9:00	1,177,883						105.1	25.1	30.3	-28.4	
7/05/09	8:50	1,273,150						105.2	25.0	30.3	-28.4	
7/07/09	8:30	1,368,646						105.1	25.1	30.3	-28.5	
7/08/09	2:30	1,394,029										

WUE 580 ← FARNET  
 STOPPED TO  
 LRE START  
 stopped to test load cell cable

Date	Time	Cycles	Set Point (k)	Span (k)	Frequency (Hz)	Displacement (in)		Load (kips)		Controlling Variable Error (k)		Notes
						Maximum	Minimum	Maximum	Minimum	Maximum	Minimum	
7/10/09	3:00	1,391,145	65	45	1.1004			105.1	25.1	30.4	-28.4	Restart, same
7/10/09	5:40	1,461,355	"	"	"			105.1	25.2	30.4	-28.5	
7/10/2009	6:15PM	1,499,718	65	47.5	1.1004			105.0	25.1	30.8	-28.0	POSSIBLE MARKED CRACKS
7/13/09	8:30 AM	1,749,680	"	"				105.1	25.2	30.1	-27.8	
7/14	7:50A	1,840,920										
"	9:25	1,845,373										
"	13:40	"										
7/14/09	3:00	1,845,980	65	45	0.9000			105.0	25.1	24.9	-22.7	set point to 65
"	18:15	1,856,536	65	45	0.9000			105.1	25.08	24.65	-22.7	
7/17	12:05	1,993,001	"	"	"			105.1	24.98	24.48	-22.4	
7/20	8:45	2,057,217										
8/11/09	14:30	0	65	43.2	1.2003			105.0	24.8	20.5	-18.0	same as 7/14 as #2 @ structure
8/12/09	8:30	78,950	"	"	"			105.2	24.6	20.2	-17.9	
8/13/09	8:45	184,045	"	"	"			105.2	24.6	20.2	-18.0	
8/14/09	10:15	295,200	"	"	"			105.2	24.5	20.2	-18.0	
8/14/09	19:00	332,290	"	"	"			105.2	24.5	20.1	-18.0	cut cycles = 12,000
8/15/09	11:35	404,437	"	"	"			105.28	24.46	20.22	-18.07	total = 52,000
8/16/09	16:21	600,3	"	"	"			105.25	24.46	20.21	-18.02	COMPIETE RESET
8/17/09	8:45	70,089	"	"	"			105.20	24.53	20.15	-18.09	
9/18/09	9:10	1,745,74	"	"	"			105.0	24.88	20.01	-18.14	
"	9:50	140,085	"	"	"							
"	2:40	201,080	"	"	"							
8/17/09	9:00	280,866	"	"	"			105.35	24.58	20.01	-18.07	FAST SIDE NORMAL STIFF CRACK IS-ONE
8/19/09	9:10	281,561	STOPPED	TEST	THROUGH			105.11	24.60	20.13	-17.86	FLANGE



# Data Log for Fatigue Testing (Bent Plates Project)

## Project # 0 - 5701

Specimen: 303 and Date: 9/29/04

Settings:

Set Point	62.5	P Gain	3.1
Amplitude	40.0	I Gain	2.1
Frequency	1.1	D Gain	7.53
		F Gain	1.62

Shut-off Limits:

Maximum	25	Minimum	20
Displacement (in)		Load (kips)	105
Load (kips)		Error (k)	25

Calculated Values:

Span (k)	42.0	Frequency (Hz)	1.004
Displacement (in)		Maximum	
Load (kips)		Minimum	

Date	Time	Cycles	Set Point (k)	Span (k)	Frequency (Hz)	Displacement (in)		Load (kips)		Controlling Variable Error (k)		Notes
						Maximum	Minimum	Maximum	Minimum	Maximum	Minimum	
9/29/04	15:50	0	62.80	42.0	1.004			100.5	23.51	21.83	-17.01	
9/30/04	13:27	86,260						100.4	23.3	22.0	-19.4	
10/1/04	11:30	174,184						100.4	23.3	22.1	-19.4	
10/1/04	13:36	276,320						100.4	23.3	22.0	-19.3	
10/5/04	12:25	560,982						100.4	23.3	22.0	-19.4	
10/6/04	11:24	652,732						100.3	23.3	22.1	-19.2	
10/6/04	13:26	756,446						100.3	23.3	22.1	-19.4	
10/8/04	07:59	838,950						100.4	23.2	22.2	-19.16	
10/09/04	12:09	942,480						100.17	23.3	22.1	-19.3	
10/9	16:55	961,472						100.05	23.32	22.05	-19.2	ERROR EXTRACT
10/12	10:45	1224,102	"	"	"			100.2	23.3	22.1	-19.3	
10/12	12:30	1231,228						100.2	23.2	22.0	-19.3	MANIPULATED
10/12	14:00	1257,985	"	"	"			100.3	23.3	22.1	-19.3	SAMPLE CRACK OBSERVED
10/13	11:50	1324,484						100.3	23.3	22.1	-19.4	
10/14	9:47	1417,780	"	"	"			100.2	23.2	22.0	-19.2	
10/14	13:30	1436,670						100.4	23.3	22.2	-19.3	
10/15	11:26	1511,140						100.4	23.3	22.2	-19.2	
10/16	13:30	1568,280						100.2	23.2	22.0	-19.2	
10/19	10:36	1893,373	"	"	"			100.7	23.3	22.2	-19.4	
10/19	12:24	1901,607						100.2	23.2	22.1	-19.4	
10/20	9:55	1946,800	"	"	"			100.1	23.2	22.2	-19.3	
10/20	11:28	1992,920						100.3	23.2	22.1	-19.4	
10/21	10:22	2044,280						100.2	23.3	22.1	-19.4	
10/21	13:24	2096,406						100.5	23.3	22.1	-19.3	



# Data Log for Fatigue Testing (Bent Plates Project)

Project # 0 - 5701

Specimen: **2-60A**

and

Date: **7/21/09**

Desired Measurements:

Set Point	68
Amplitude	45.2
Frequency	1.2031

Calculated Values:

Displacement (in)	Maximum	Minimum
Load (Kips)	Maximum	Minimum

Shut-off Limits:

Displacement (in)	Maximum	Minimum
Load (Kips)	Maximum	Minimum
Error (k)	Maximum	Minimum

Settings:

P Gain	4.25
I Gain	3.9
D Gain	6.33
F Gain	.7

Date	Time	Cycles	Set Point (k)	Span (k)	Frequency (Hz)	Displacement (in)		Load (Kips)		Controlling Variable Error (k)		Notes
						Maximum	Minimum	Maximum	Minimum	Maximum	Minimum	
7/21/09	4:00	0	68	45.2	1.2031							
7/22/09	8:25	73,258	"	"	"							
"	10:30	80,500	"	"	"							
"	11:10	"	"	"	"							
7/23	8:15am	172,434	"	"	"							
7/24	7:40am	297,246	"	"	"							
"	7:15	307,200	"	"	"							
7/29	9:00	594,720	"	"	"							
7/28	9:00	697,880	"	"	"							
7/29	9:00	802,224	"	"	"							
7/30	9:00	907,305	"	"	"							
7/31	11:09	1,021,420	"	"	"							
8/3	8:00	1,321,245	"	"	"							
8/4	8:20	1,426,900	"	"	"							
8/5		1,427,119										
8/6												
8/7	15:00	1,427,119	68.19	45.4	1.2031							
8/7	18:40	1,443,789	"	"	"							
8/7	20:00	1,449,512	"	"	"							
8/7	22:30	1,451,654										
			REPAIRED	CRACK	W/	PLATE						
			REPAIRED	CRACK	W/	PLATE						
			REPAIRED	CRACK	W/	PLATE						

Desired: ask → 110k  
 Current Settings: 68k set pt.  
 1.2003 Hz  
 1751, 654

Date	Time	Cycles	Set Point (k)	Span (k)	Frequency (Hz)	Displacement (in)		Load (kips)		Controlling Variable Error (k)		Notes
						Maximum	Minimum	Maximum	Minimum	Maximum	Minimum	
8/20/09	10:40	88521	68	45.3	1.0063			110.1	25.47	20.85	-18.45	RESTART
8/21/09	9:40	100,048	68	45.3	1.1			110.3	25.4	20.7	-18.2	
8/22/09	10:50	417,735	68	45.3	1.1			110.1	25.4	20.6	-18.3	
8/23/09	9:30	516,172	68	45.3	1.1			110.88	25.44	20.51	-18.17	
8/25/09	10:15	519,858	68	45.3	1.1			110.26	25.35	20.35	-18.26	CRACK DO NOT STOP
8/26/09	13:50	639,707	68	45.3	1.1			110.21	25.44	20.78	-19.21	CRACK DO NOT STOP
8/27/09	11:30	733,816	68	45.3	1.1			110.83	25.35	20.70	-18.26	CRACK DO NOT STOP
8/28/09	12:30	842,971	68	45.3	1.1			110.21	25.40	20.70	-18.21	CRACK DO NOT STOP
8/31	10:10	862,177	68	45.3	1.1			110.16	25.44	20.58	-18.29	
9/1/09	8:52	1,149,117	68	45.3	1.1			110.35	25.35	20.68	-18.29	
9/2/09	10:06	1,163,026	68	45.3	1.1			110.45	25.37	20.70	-18.31	
9/10/09	11:20	1,258,463	68	45.3	1.1			110.06	25.37	20.73	-18.24	
9/11/09	3:10	1,258,463	68	45.3	1.1			110.06	25.37	20.73	-18.24	
9/12/09	3:30	1,258,463	68	45.3	1.1			110.16	25.44	20.58	-18.29	
9/13/09	4:35	1,258,463	68	45.3	1.1			110.22	24.84	1.41	1.26	
9/18/09	11:10	7061	68	45.3	1.1			110.1	24.9	14.42	-12.64	NEW SETTINGS SET
9/22/09	5:00	RESET	68	45.3	1.1			110.22	24.84	1.41	1.26	NEW SETTINGS SET
9/23/09	3:20	16,216	68	45.3	1.1			110.22	24.84	1.41	1.26	NEW SETTINGS SET
9/24/09	17:20	17,604	68	45.3	1.1			110.22	24.84	1.41	1.26	NEW SETTINGS SET
9/25/09	11:30	63,736	68	45.3	1.1			110.22	24.84	1.41	1.26	NEW SETTINGS SET
9/26/09	12:00	63,272	68	45.3	1.1			110.22	24.84	1.41	1.26	NEW SETTINGS SET
9/27/09	13:05	69,564	68	45.3	1.1			110.22	24.84	1.41	1.26	NEW SETTINGS SET
9/28/09	13:30	162,340	68	45.3	1.1			110.22	24.84	1.41	1.26	NEW SETTINGS SET
9/29/09	2:10	242,512	68	45.3	1.1			110.22	24.84	1.41	1.26	NEW SETTINGS SET

# Data Log for Fatigue Testing (Bent Plates Project)

## Project # 0 - 5701

Specimen: 60B and 1103109 Date: 11/03/09

Desired Measurements: 40.24 P Gain 2.64  
61.3 I Gain 8.1  
4306 Hz Frequency 3.55  
162 F Gain

Calculated Values: 138 Maximum 32.5 Minimum 20  
35 Displacement (in) Load (kips) Error (K) 20  
35 Displacement (in) Load (kips) Error (K) 20

Shut-off Limits: 138 Maximum 32.5 Minimum 20  
35 Displacement (in) Load (kips) Error (K) 20  
35 Displacement (in) Load (kips) Error (K) 20

Settings: 138 Maximum 32.5 Minimum 20  
35 Displacement (in) Load (kips) Error (K) 20  
35 Displacement (in) Load (kips) Error (K) 20

Date	Time	Cycles	Set Point (k)	Span (k)	Frequency (Hz)	Displacement (in)		Load (kips)		Controlling Variable Error (K)		Notes
						Maximum	Minimum	Maximum	Minimum	Maximum	Minimum	
11/03/09	15:20	~0~	80.74	61.3	8606			134.3	23.3	32.5	-25.8	Setup sheet, stop at 7.00
"	15:53	1764						134.2	23.3	32.3	-25.8	Stop at 7.00 pm
11/04/09	11:25	64354						134.4	23.2	32.2	-25.6	oil: 2.5 + 3.15 22 → 27.5 pm
11/05/09	11:26	141,289						134.3	23.2	32.2	-25.7	
11/06/09	4:52	255,586						134.5	23.3	32.2	-26.0	
11/07/09	~	385,447						134.5	23.3	32.2	-26.0	
11/08/09	5:04	389,410	79.48	56.5	4999 Hz			134.4	23.2	16.6	-13.5	RF Start, new machine
11/11/09	12:27	424,588						134.3	23.2	16.6	-13.5	
11/12/09	14:12	424,588	79.75	56.8	7711			134.3	23.3	26.5	-22.2	NEW SETTINGS
11/20/09	11:44	485,101						134.3	23.4	26.8	-22.0	
11/21/09	13:21	492,664						134.4	23.3	26.8	-22.0	Crack found on NW leg
11/21/09	16:34	501,593						134.3	23.3	26.8	-22.0	CRACK
11/18/09	14:04	501,970	79.40	56.5	7911			134.1	23.1	26.2	-21.2	Error: error 30 low 15
"	14:50	509,200						133.8	23.0	26.0	-21.5	
11/10/09	11:20	561,480						133.8	23.1	26.0	-21.3	
11/20/09	13:16	633,920						133.8	23.1	25.8	-21.4	
11/23/09	12:25	653,478						133.9	23.0	25.8	-21.4	
"	12:00	659,817						133.9	23.0	25.8	-21.4	Stopped for other test performance
"	15:27	687,413						134.0	23.2	25.6	-21.3	Min DC: Low: 20
11/24/09	11:27	695,461						134.0	23.1	25.9	-21.4	
11/25/09	12:44	967,090						133.9	23.2	25.9	-21.4	SHUTDOWN FOR THANKSGIVING
11/25/09	15:15	971,846						132.9	23.2	25.4	-21.4	
11/20/09	15:20	971,846						134.3	23.3	26.0	-22.7	



## **A.2 Strain-Gauge Reading**

Strain gauges placed on the girder were used to determine the stress-range the girder was being cycled at. These readings were checked at the beginning of any run, and then on a day-to-day basis afterwards. A sample of the output and analysis are provided here.

NE-Top	NW-Top	NE-Bot	NW-Bot	SE-Top	SW-Top	SE-Bot	SW-Bot	10V
-2.35E-04	-2.37E-04	2.62E-04	1.96E-04	-2.42E-04	-2.47E-04	2.77E-04	2.08E-04	1.74E-03
-2.27E-04	-2.30E-04	2.54E-04	1.90E-04	-2.34E-04	-2.40E-04	2.69E-04	2.01E-04	1.13E-03
-2.21E-04	-2.25E-04	2.47E-04	1.84E-04	-2.26E-04	-2.34E-04	2.61E-04	1.95E-04	1.43E-03
-2.14E-04	-2.17E-04	2.39E-04	1.77E-04	-2.20E-04	-2.28E-04	2.53E-04	1.89E-04	1.13E-03
-2.08E-04	-2.12E-04	2.33E-04	1.71E-04	-2.13E-04	-2.22E-04	2.46E-04	1.83E-04	1.13E-03
-2.02E-04	-2.06E-04	2.28E-04	1.66E-04	-2.08E-04	-2.16E-04	2.40E-04	1.78E-04	1.43E-03
-1.96E-04	-2.01E-04	2.22E-04	1.61E-04	-2.02E-04	-2.11E-04	2.34E-04	1.73E-04	1.74E-03
-1.92E-04	-1.96E-04	2.16E-04	1.58E-04	-1.97E-04	-2.07E-04	2.28E-04	1.69E-04	1.74E-03
-1.87E-04	-1.92E-04	2.12E-04	1.53E-04	-1.93E-04	-2.03E-04	2.23E-04	1.65E-04	1.13E-03
-1.83E-04	-1.89E-04	2.08E-04	1.50E-04	-1.89E-04	-2.00E-04	2.19E-04	1.61E-04	1.43E-03
-1.80E-04	-1.85E-04	2.04E-04	1.48E-04	-1.87E-04	-1.97E-04	2.15E-04	1.59E-04	1.13E-03
-1.78E-04	-1.83E-04	2.01E-04	1.44E-04	-1.83E-04	-1.94E-04	2.12E-04	1.56E-04	1.13E-03
-1.74E-04	-1.80E-04	1.99E-04	1.42E-04	-1.81E-04	-1.92E-04	2.09E-04	1.54E-04	1.13E-03
-1.73E-04	-1.79E-04	1.97E-04	1.41E-04	-1.79E-04	-1.90E-04	2.07E-04	1.52E-04	1.43E-03
-1.72E-04	-1.77E-04	1.95E-04	1.39E-04	-1.78E-04	-1.89E-04	2.05E-04	1.51E-04	1.43E-03
-1.70E-04	-1.76E-04	1.94E-04	1.39E-04	-1.77E-04	-1.88E-04	2.05E-04	1.50E-04	1.43E-03
-1.70E-04	-1.76E-04	1.94E-04	1.39E-04	-1.76E-04	-1.88E-04	2.03E-04	1.50E-04	1.43E-03
-1.70E-04	-1.76E-04	1.94E-04	1.39E-04	-1.77E-04	-1.88E-04	2.05E-04	1.50E-04	1.43E-03
-1.71E-04	-1.77E-04	1.95E-04	1.39E-04	-1.78E-04	-1.89E-04	2.05E-04	1.51E-04	1.74E-03
-1.74E-04	-1.79E-04	1.97E-04	1.40E-04	-1.79E-04	-1.90E-04	2.07E-04	1.53E-04	1.43E-03
-1.75E-04	-1.81E-04	1.98E-04	1.42E-04	-1.81E-04	-1.92E-04	2.08E-04	1.54E-04	1.13E-03
-1.78E-04	-1.83E-04	2.01E-04	1.45E-04	-1.83E-04	-1.95E-04	2.12E-04	1.56E-04	1.43E-03
-1.81E-04	-1.86E-04	2.05E-04	1.48E-04	-1.88E-04	-1.98E-04	2.16E-04	1.59E-04	8.24E-04
-1.85E-04	-1.91E-04	2.10E-04	1.52E-04	-1.92E-04	-2.01E-04	2.20E-04	1.64E-04	8.24E-04
-1.90E-04	-1.94E-04	2.14E-04	1.56E-04	-1.96E-04	-2.06E-04	2.26E-04	1.68E-04	1.74E-03
-1.96E-04	-1.99E-04	2.20E-04	1.61E-04	-2.01E-04	-2.11E-04	2.31E-04	1.73E-04	1.43E-03
-2.01E-04	-2.05E-04	2.26E-04	1.66E-04	-2.07E-04	-2.17E-04	2.38E-04	1.78E-04	1.13E-03
-2.08E-04	-2.11E-04	2.33E-04	1.72E-04	-2.14E-04	-2.23E-04	2.46E-04	1.84E-04	1.13E-03
-2.15E-04	-2.18E-04	2.39E-04	1.78E-04	-2.21E-04	-2.29E-04	2.53E-04	1.90E-04	1.43E-03
-2.22E-04	-2.24E-04	2.47E-04	1.85E-04	-2.28E-04	-2.35E-04	2.61E-04	1.97E-04	1.43E-03
-2.30E-04	-2.32E-04	2.55E-04	1.93E-04	-2.37E-04	-2.42E-04	2.70E-04	2.04E-04	1.43E-03
-2.39E-04	-2.39E-04	2.63E-04	2.00E-04	-2.45E-04	-2.50E-04	2.79E-04	2.12E-04	1.43E-03
-2.47E-04	-2.48E-04	2.72E-04	2.08E-04	-2.54E-04	-2.58E-04	2.89E-04	2.20E-04	1.74E-03
-2.56E-04	-2.56E-04	2.82E-04	2.16E-04	-2.63E-04	-2.67E-04	2.99E-04	2.28E-04	1.74E-03
-2.67E-04	-2.66E-04	2.92E-04	2.24E-04	-2.74E-04	-2.76E-04	3.10E-04	2.36E-04	2.04E-03
-2.77E-04	-2.74E-04	3.01E-04	2.34E-04	-2.84E-04	-2.85E-04	3.21E-04	2.46E-04	1.43E-03
-2.87E-04	-2.85E-04	3.12E-04	2.43E-04	-2.94E-04	-2.94E-04	3.33E-04	2.55E-04	1.43E-03
-2.98E-04	-2.95E-04	3.23E-04	2.53E-04	-3.06E-04	-3.04E-04	3.45E-04	2.65E-04	1.13E-03



Data continues...

	NE-Top	NW-Top	NE-Bot	NW-Bot	SE-Top	SW-Top	SE-Bot	SW-Bot	Average
MAX STRAIN	-1.70E-04	-1.75E-04	7.39E-04	6.37E-04	-1.75E-04	-1.87E-04	8.00E-04	6.50E-04	
MIN STRAIN	-7.10E-04	-6.89E-04	1.94E-04	1.38E-04	-7.26E-04	-6.87E-04	2.03E-04	1.49E-04	
DIFFERENCE	5.40E-04	5.14E-04	5.45E-04	4.99E-04	5.51E-04	5.00E-04	5.97E-04	5.01E-04	5.31E-04
STRESS (ksi)	1.57E+01	1.49E+01	1.58E+01	1.45E+01	1.60E+01	1.45E+01	1.73E+01	1.45E+01	15.40
TOTAL STRESS (ksi)	-2.06E+01	-2.00E+01	2.14E+01	1.85E+01	-2.11E+01	-1.99E+01	2.32E+01	1.89E+01	
POSITIVE STRESS (ksi)	2.06E+01	2.00E+01	2.14E+01	1.85E+01	2.11E+01	1.99E+01	2.32E+01	1.89E+01	20.44

A stress range of 15.4ksi is calculated.

## B FINITE ELEMENT TESTING FOR FLEXURAL FATIGUE

These are the results for the finite element models used in the flexural fatigue study. The DNV stresses are shown for all three hot-spots on the half-pipe stiffener, and all three different stresses at the 45° location are included. For the plate stiffener the DNV stresses are provided for the middle and edge of the weld toe.

### B.1 Plate-Stiffener

These are the plate-stiffener results only, DNV stresses provided for the middle and edge of the weld length.

bG	tF	tW	bS	tS	aS	aW	lg	Me	DNV Stress Path Mid	DNV Stress Path Edg
12.3	0.8	0.5	5.5	0.4	0	0.3125	2412.33	263.361	1.04667	1.01409
12.3	0.8	0.5	5.5	0.4	2	0.3125	2412.33	263.361	1.06239	1.02051
12.3	0.8	0.5	5.5	0.4	4	0.3125	2412.33	263.361	1.04549	1.0352
12.3	0.8	0.5	5.5	0.4	6	0.3125	2412.33	263.361	1.06425	1.04613
12.3	0.8	0.5	5.5	0.4	8	0.3125	2412.33	263.361	1.04583	1.05005
12.3	0.8	0.5	5.5	0.4	10	0.3125	2412.33	263.361	1.05557	1.05091
12.3	0.8	0.5	5.5	0.4	12	0.3125	2412.33	263.361	1.06481	1.05513
12.3	0.8	0.5	5.5	0.4	14	0.3125	2412.33	263.361	1.05309	1.06442
12.3	0.8	0.5	5.5	0.4	16	0.3125	2412.33	263.361	1.06744	1.07104
12.3	0.8	0.5	5.5	0.4	18	0.3125	2412.33	263.361	1.05351	1.08794
12.3	0.8	0.5	5.5	0.4	20	0.3125	2412.33	263.361	1.06968	1.09948
12.3	0.8	0.5	5.5	0.4	22	0.3125	2412.33	263.361	1.05912	1.10234
12.3	0.8	0.5	5.5	0.4	24	0.3125	2412.33	263.361	1.06805	1.10547
12.3	0.8	0.5	5.5	0.4	26	0.3125	2412.33	263.361	1.05623	1.11409
12.3	0.8	0.5	5.5	0.4	28	0.3125	2412.33	263.361	1.06601	1.13551
12.3	0.8	0.5	5.5	0.4	30	0.3125	2412.33	263.361	1.06034	1.14218
12.3	0.8	0.5	5.5	0.4	32	0.3125	2412.33	263.361	1.06112	1.14363
12.3	0.8	0.5	5.5	0.4	34	0.3125	2412.33	263.361	1.05302	1.16348
12.3	0.8	0.5	5.5	0.4	36	0.3125	2412.33	263.361	1.05525	1.17721
12.3	0.8	0.5	5.5	0.4	38	0.3125	2412.33	263.361	1.06972	1.17578
12.3	0.8	0.5	5.5	0.4	40	0.3125	2412.33	263.361	1.05208	1.19929
12.3	0.8	0.5	5.5	0.4	42	0.3125	2412.33	263.361	1.04453	1.20606
12.3	0.8	0.5	5.5	0.4	44	0.3125	2412.33	263.361	1.0438	1.2077

12.3	0.8	0.5	5.5	0.4	46	0.3125	2412.33	263.361	1.02014	1.23619
12.3	0.8	0.5	5.5	0.4	48	0.3125	2412.33	263.361	1.05198	1.23402
12.3	0.8	0.5	5.5	0.4	50	0.3125	2412.33	263.361	0.995252	1.25751
12.3	0.8	0.5	5.5	0.4	52	0.3125	2412.33	263.361	1.04652	1.25659
12.3	0.8	0.5	5.5	0.4	54	0.3125	2412.33	263.361	1.03803	1.28407
12.3	0.8	0.5	5.5	0.4	56	0.3125	2412.33	263.361	1.02452	1.27778
12.3	0.8	0.5	5.5	0.4	58	0.3125	2412.33	263.361	1.01444	1.30011
12.3	0.8	0.5	5.5	0.4	60	0.3125	2412.33	263.361	0.979264	1.31175
12.3	0.8	0.5	5.5	0.4	62	0.3125	2412.33	263.361	1.02157	1.31697
12.3	0.8	0.5	5.5	0.4	64	0.3125	2412.33	263.361	0.976085	1.3345
12.3	0.8	0.5	5.5	0.4	66	0.3125	2412.33	263.361	0.995951	1.34026
12.3	0.8	0.5	5.5	0.4	68	0.3125	2412.33	263.361	0.986651	1.34045
12.3	0.8	0.5	5.5	0.4	70	0.3125	2412.33	263.361	0.926768	1.35036

## B.2 Half-Pipe Stiffener

These are all the results completed for the half-pip stiffener for the flexural fatigue study. “DNV Stress Path 45 1” represents the DNV principle stress taken at a path that extends at a 45° angle from the web. “DNV Stress Path 90 Z” is the principle stress taken at the end of the half-pipe next the flange’s edge. “DNV Stress Path 0 Z” is the principle stress taken at the half-pipe weld next to the web. “DNV Stress Path Comp” is the stress in the direction perpendicular to the weld at the 45° point. “DNV Stress Path 45 1+” is the principle stress taken along a path that parallel’s the direction of the principle stress, this is the stress that was used for the analysis provided in this report.

<b>bG</b>	<b>tF</b>	<b>tW</b>	<b>bG</b>	<b>tF</b>	<b>tW</b>	<b>bS</b>	<b>tS</b>	<b>aS</b>	<b>aW</b>	<b>DNV Stress Path 45 1</b>	<b>DNV Stress Path 90 Z</b>	<b>DNV Stress Path 0 Z</b>	<b>DNV Stress Path 45 1+</b>	<b>DNV Stress Path Comp</b>
15	0.938	0.8	15	0.938	0.8	6	0.5	30	0.3125	1.06321	0.900343	1.01983	1.07915	0.511081
15	1.25	0.8	15	1.25	0.8	6	0.5	30	0.3125	1.04515	0.907573	0.988847	1.05616	0.505474
15	0.75	0.8	15	0.75	0.8	6	0.5	30	0.3125	1.0856	0.890402	1.0549	1.09894	0.519056
15	0.938	0.8	15	0.938	0.8	5	0.5	30	0.3125	1.06655	1.01861	1.0336	1.0862	0.517429
15	1.25	0.8	15	1.25	0.8	5	0.5	30	0.3125	1.04944	1.0004	1.0218	1.06124	0.512025
15	0.75	0.8	15	0.75	0.8	5	0.5	30	0.3125	1.0889	0.941354	1.04323	1.10782	0.524832
15	0.938	0.8	15	0.938	0.8	4	0.5	30	0.3125	1.08003	0.877521	1.02333	1.09908	0.538369
15	1.25	0.8	15	1.25	0.8	4	0.5	30	0.3125	1.05639	0.915957	1.01059	1.07566	0.529447
15	0.75	0.8	15	0.75	0.8	4	0.5	30	0.3125	1.10173	0.900568	1.03175	1.12179	0.550304
15	0.938	0.8	15	0.938	0.8	6	0.375	30	0.3125	1.04605	0.934171	1.03896	1.05877	0.501688
15	1.25	0.8	15	1.25	0.8	6	0.375	30	0.3125	1.0324	0.934395	1.00838	1.04056	0.498156
15	0.75	0.8	15	0.75	0.8	6	0.375	30	0.3125	1.06602	0.937133	1.06851	1.07663	0.508473
15	0.938	0.8	15	0.938	0.8	5	0.375	30	0.3125	1.04809	1.07345	1.05332	1.06379	0.504623
15	1.25	0.8	15	1.25	0.8	5	0.375	30	0.3125	1.03636	1.03024	1.03619	1.04461	0.502568
15	0.75	0.8	15	0.75	0.8	5	0.375	30	0.3125	1.06709	0.995823	1.06399	1.08256	0.509836
15	0.938	0.8	15	0.938	0.8	4	0.375	30	0.3125	1.06147	0.908247	1.03634	1.07571	0.520705
15	1.25	0.8	15	1.25	0.8	4	0.375	30	0.3125	1.04415	0.942317	1.02245	1.05873	0.516763
15	0.75	0.8	15	0.75	0.8	4	0.375	30	0.3125	1.07843	0.952663	1.04601	1.09383	0.528488
15	0.938	0.8	15	0.938	0.8	6	0.313	30	0.3125	1.03876	0.948734	1.04799	1.05012	0.498496
15	1.25	0.8	15	1.25	0.8	6	0.313	30	0.3125	1.02735	0.945152	1.01832	1.03443	0.495715
15	0.75	0.8	15	0.75	0.8	6	0.313	30	0.3125	1.05715	0.957234	1.07446	1.06655	0.504653
15	0.938	0.8	15	0.938	0.8	5	0.313	30	0.3125	1.04005	1.09613	1.063	1.05403	0.500079
15	1.25	0.8	15	1.25	0.8	5	0.313	30	0.3125	1.03087	1.04164	1.0433	1.03763	0.499233

15	0.75	0.8	15	0.75	0.8	5	0.313	30	0.3125	1.05718	1.0188	1.07392	1.07109	0.504329
15	0.938	0.8	15	0.938	0.8	4	0.313	30	0.3125	1.05263	0.923482	1.04333	1.06475	0.51336
15	1.25	0.8	15	1.25	0.8	4	0.313	30	0.3125	1.03844	0.955652	1.02919	1.05083	0.511498
15	0.75	0.8	15	0.75	0.8	4	0.313	30	0.3125	1.0671	0.978204	1.0535	1.08033	0.519209
15	0.938	0.8	15	0.938	0.8	6	0.313	30	0.25	1.03334	1.05407	1.05214	1.04039	0.49349
15	1.25	0.8	15	1.25	0.8	6	0.313	30	0.25	1.02092	1.02148	1.01694	1.02721	0.493339
15	0.75	0.8	15	0.75	0.8	6	0.313	30	0.25	1.04579	0.999586	1.07196	1.05568	0.496768
15	0.938	0.8	15	0.938	0.8	5	0.313	30	0.25	1.03469	1.01924	1.05388	1.04614	0.495555
15	1.25	0.8	15	1.25	0.8	5	0.313	30	0.25	1.02651	1.06955	1.03945	1.03396	0.495531
15	0.75	0.8	15	0.75	0.8	5	0.313	30	0.25	1.04783	1.14225	1.06722	1.06241	0.494565
15	0.938	0.8	15	0.938	0.8	4	0.313	30	0.25	1.04694	0.973922	1.04154	1.05838	0.508292
15	1.25	0.8	15	1.25	0.8	4	0.313	30	0.25	1.0354	1.00651	1.02462	1.04392	0.507153
15	0.75	0.8	15	0.75	0.8	4	0.313	30	0.25	1.05586	1.09246	1.04969	1.06781	0.510198
15	0.938	0.8	15	0.938	0.8	6	0.313	30	0.375	1.0492	0.965394	1.05209	1.06174	0.505078
15	1.25	0.8	15	1.25	0.8	6	0.313	30	0.375	1.0315	0.907686	1.01544	1.04199	0.499813
15	0.75	0.8	15	0.75	0.8	6	0.313	30	0.375	1.06404	0.998786	1.06901	1.07326	0.510279
15	0.938	0.8	15	0.938	0.8	5	0.313	30	0.375	1.04901	0.998471	1.06922	1.06133	0.506286
15	1.25	0.8	15	1.25	0.8	5	0.313	30	0.375	1.03583	0.976575	1.04976	1.04325	0.502604
15	0.75	0.8	15	0.75	0.8	5	0.313	30	0.375	1.06363	0.965877	1.07825	1.08012	0.511832
15	0.938	0.8	15	0.938	0.8	4	0.313	30	0.375	1.05992	0.949976	1.04751	1.07812	0.521821
15	1.25	0.8	15	1.25	0.8	4	0.313	30	0.375	1.04293	0.910758	1.02726	1.05311	0.514991
15	0.75	0.8	15	0.75	0.8	4	0.313	30	0.375	1.07705	0.92276	1.05214	1.09327	0.526943
15	0.938	0.8	15	0.938	0.8	6	0.313	30	0.3125	1.04333	0.945768	1.02466	1.05558	0.50078
15	1.25	0.8	15	1.25	0.8	6	0.313	30	0.3125	1.03381	0.950739	1.02201	1.04168	0.499545
15	0.75	0.8	15	0.75	0.8	6	0.313	30	0.3125	1.0616	0.950539	1.03743	1.07185	0.506044
15	0.938	0.8	15	0.938	0.8	5	0.313	30	0.3125	1.04671	1.07976	1.04845	1.06198	0.50311

15	1.25	0.8	15	1.25	0.8	5	0.313	30	0.3125	1.03905	1.03684	1.03757	1.04679	0.502824
15	0.75	0.8	15	0.75	0.8	5	0.313	30	0.3125	1.06378	1.00651	1.05992	1.07892	0.506721
15	0.938	0.8	15	0.938	0.8	4	0.313	30	0.3125	1.05932	0.920824	1.03	1.07253	0.516006
15	1.25	0.8	15	1.25	0.8	4	0.313	30	0.3125	1.04682	0.957393	1.03364	1.06002	0.513928
15	0.75	0.8	15	0.75	0.8	4	0.313	30	0.3125	1.07411	0.96819	1.04237	1.08852	0.521955
15	0.938	0.8	15	0.938	0.8	6	0.313	30	0.25	1.03794	1.04444	1.0282	1.04601	0.496124
15	1.25	0.8	15	1.25	0.8	6	0.313	30	0.25	1.0275	1.0234	1.02032	1.03471	0.497593
15	0.75	0.8	15	0.75	0.8	6	0.313	30	0.25	1.05059	0.990943	1.03713	1.06132	0.498747
15	0.938	0.8	15	0.938	0.8	5	0.313	30	0.25	1.04112	1.01196	1.04272	1.05398	0.498693
15	1.25	0.8	15	1.25	0.8	5	0.313	30	0.25	1.03469	1.06707	1.03849	1.04314	0.499258
15	0.75	0.8	15	0.75	0.8	5	0.313	30	0.25	1.05494	1.12249	1.05332	1.07078	0.497734
15	0.938	0.8	15	0.938	0.8	4	0.5	30	0.25	1.0817	0.91978	1.01393	1.10204	0.536556
15	1.25	0.8	15	1.25	0.8	4	0.5	30	0.25	1.06301	0.972339	1.01527	1.07887	0.528551
15	0.75	0.8	15	0.75	0.8	4	0.5	30	0.25	1.09947	0.986235	1.02307	1.1204	0.545516
15	0.938	0.8	15	0.938	0.8	5	0.5	30	0.25	1.06915	0.946157	1.02214	1.0886	0.51634
15	1.25	0.8	15	1.25	0.8	5	0.5	30	0.25	1.05512	1.02366	1.02095	1.06959	0.512276
15	0.75	0.8	15	0.75	0.8	5	0.5	30	0.25	1.08959	1.02055	1.03094	1.11111	0.518805
15	0.938	0.8	15	0.938	0.8	6	0.375	30	0.25	1.04652	1.02445	1.02014	1.05631	0.499774
15	1.25	0.8	15	1.25	0.8	6	0.375	30	0.25	1.03349	1.01056	1.01278	1.04223	0.500192
15	0.75	0.8	15	0.75	0.8	6	0.375	30	0.25	1.06111	0.969068	1.02946	1.07327	0.50304
15	0.938	0.8	15	0.938	0.8	5	0.375	30	0.25	1.05011	0.99082	1.03559	1.06507	0.503643
15	1.25	0.8	15	1.25	0.8	5	0.375	30	0.25	1.04109	1.05391	1.03244	1.05145	0.502845
15	0.75	0.8	15	0.75	0.8	5	0.375	30	0.25	1.06627	1.08891	1.0457	1.08395	0.503686
15	0.938	0.8	15	0.938	0.8	4	0.375	30	0.25	1.06293	0.952471	1.02303	1.07798	0.518797
15	1.25	0.8	15	1.25	0.8	4	0.375	30	0.25	1.05	0.996232	1.02416	1.0614	0.515287
15	0.75	0.8	15	0.75	0.8	4	0.375	30	0.25	1.07535	1.04554	1.03337	1.09116	0.523109

15	0.938	0.8	15	0.938	0.8	4	0.313	30	0.25	1.05345	0.969766	1.02871	1.06595	0.510991
15	1.25	0.8	15	1.25	0.8	4	0.313	30	0.25	1.04362	1.00865	1.02969	1.05289	0.509558
15	0.75	0.8	15	0.75	0.8	4	0.313	30	0.25	1.06304	1.07796	1.03948	1.07631	0.51325
15	0.938	0.8	15	0.938	0.8	6	0.5	30	0.25	1.06509	0.980293	1.00516	1.07855	0.509478
15	1.25	0.8	15	1.25	0.8	6	0.5	30	0.25	1.04719	0.980045	0.998737	1.05942	0.50738
15	0.75	0.8	15	0.75	0.8	6	0.5	30	0.25	1.08303	0.923404	1.01508	1.09814	0.514123
15	0.938	0.8	15	0.938	0.8	6	0.5	30	0.375	1.07762	0.904264	1.00289	1.09529	0.519122
15	1.25	0.8	15	1.25	0.8	6	0.5	30	0.375	1.05702	0.87262	0.998476	1.07196	0.513329
15	0.75	0.8	15	0.75	0.8	6	0.5	30	0.375	1.09587	0.914826	1.01487	1.10956	0.525397
15	0.938	0.8	15	0.938	0.8	5	0.5	30	0.375	1.08054	0.926367	1.02639	1.09868	0.525313
15	1.25	0.8	15	1.25	0.8	5	0.5	30	0.375	1.0633	0.936329	1.02	1.07648	0.518842
15	0.75	0.8	15	0.75	0.8	5	0.5	30	0.375	1.09947	0.894405	1.03618	1.12207	0.53335
15	0.938	0.8	15	0.938	0.8	4	0.5	30	0.375	1.09282	0.893849	1.01378	1.11895	0.548599
15	1.25	0.8	15	1.25	0.8	4	0.5	30	0.375	1.07044	0.875082	1.01761	1.08772	0.535809
15	0.75	0.8	15	0.75	0.8	4	0.5	30	0.375	1.11678	0.850255	1.02148	1.14027	0.559554
15	0.938	0.8	15	0.938	0.8	6	0.375	30	0.375	1.06125	0.943562	1.01924	1.07606	0.510387
15	1.25	0.8	15	1.25	0.8	6	0.375	30	0.375	1.04386	0.900955	1.01321	1.05613	0.50618
15	0.75	0.8	15	0.75	0.8	6	0.375	30	0.375	1.07728	0.966919	1.03054	1.08844	0.515321
15	0.938	0.8	15	0.938	0.8	5	0.375	30	0.375	1.06343	0.970603	1.03927	1.07834	0.513541
15	1.25	0.8	15	1.25	0.8	5	0.375	30	0.375	1.05015	0.963968	1.031	1.05997	0.509726
15	0.75	0.8	15	0.75	0.8	5	0.375	30	0.375	1.07953	0.938474	1.05057	1.09878	0.519432
15	0.938	0.8	15	0.938	0.8	4	0.375	30	0.375	1.07504	0.928681	1.02603	1.09655	0.531455
15	1.25	0.8	15	1.25	0.8	4	0.375	30	0.375	1.05762	0.901168	1.0273	1.07059	0.522899
15	0.75	0.8	15	0.75	0.8	4	0.375	30	0.375	1.09481	0.894605	1.03336	1.11412	0.538541
15	0.938	0.8	15	0.938	0.8	6	0.313	30	0.375	1.0536	0.960279	1.02734	1.06711	0.506909
15	1.25	0.8	15	1.25	0.8	6	0.313	30	0.375	1.03804	0.914274	1.02059	1.04921	0.503421

15	0.75	0.8	15	0.75	0.8	6	0.313	30	0.375	1.06826	0.988694	1.03823	1.07823	0.511251
15	0.938	0.8	15	0.938	0.8	5	0.313	30	0.375	1.05549	0.988563	1.04544	1.06891	0.508899
15	1.25	0.8	15	1.25	0.8	5	0.313	30	0.375	1.0442	0.975289	1.03651	1.05257	0.50616
15	0.75	0.8	15	0.75	0.8	5	0.313	30	0.375	1.06996	0.957892	1.05742	1.08763	0.513846
15	0.938	0.8	15	0.938	0.8	4	0.313	30	0.375	1.06641	0.944928	1.03298	1.08576	0.524052
15	1.25	0.8	15	1.25	0.8	4	0.313	30	0.375	1.05148	0.913711	1.03299	1.06247	0.517372
15	0.75	0.8	15	0.75	0.8	4	0.313	30	0.375	1.08389	0.916212	1.03996	1.10124	0.529359
15	0.938	0.8	15	0.938	0.8	6	0.5	30	0.3125	1.0692	0.895177	1.00079	1.08618	0.513552
15	1.25	0.8	15	1.25	0.8	6	0.5	30	0.3125	1.0534	0.910324	0.999848	1.06541	0.509642
15	0.75	0.8	15	0.75	0.8	6	0.5	30	0.3125	1.09095	0.881936	1.01315	1.10521	0.520387
15	0.938	0.8	15	0.938	0.8	5	0.5	30	0.3125	1.07382	1.00151	1.0285	1.09482	0.520304
15	1.25	0.8	15	1.25	0.8	5	0.5	30	0.3125	1.05885	0.995422	1.02083	1.07182	0.515901
15	0.75	0.8	15	0.75	0.8	5	0.5	30	0.3125	1.09536	0.928643	1.03798	1.1155	0.526551
15	0.938	0.8	15	0.938	0.8	4	0.5	30	0.3125	1.0872	0.87395	1.01294	1.10742	0.541262
15	1.25	0.8	15	1.25	0.8	4	0.5	30	0.3125	1.06594	0.917701	1.01838	1.08624	0.532582
15	0.75	0.8	15	0.75	0.8	4	0.5	30	0.3125	1.10839	0.890166	1.02452	1.12962	0.552756
15	0.938	0.8	15	0.938	0.8	6	0.375	30	0.3125	1.05148	0.92974	1.01652	1.06521	0.504283
15	1.25	0.8	15	1.25	0.8	6	0.375	30	0.3125	1.03981	0.938357	1.01439	1.0489	0.502302
15	0.75	0.8	15	0.75	0.8	6	0.375	30	0.3125	1.07111	0.929044	1.02924	1.08265	0.510087
15	0.938	0.8	15	0.938	0.8	5	0.375	30	0.3125	1.05533	1.05588	1.04176	1.07241	0.507905
15	1.25	0.8	15	1.25	0.8	5	0.375	30	0.3125	1.04525	1.02489	1.0319	1.05462	0.506484
15	0.75	0.8	15	0.75	0.8	5	0.375	30	0.3125	1.074	0.982493	1.05271	1.09076	0.512322
15	0.938	0.8	15	0.938	0.8	4	0.375	30	0.3125	1.06855	0.90514	1.02363	1.08395	0.523626
15	1.25	0.8	15	1.25	0.8	4	0.375	30	0.3125	1.0531	0.944193	1.02784	1.06859	0.519581
15	0.75	0.8	15	0.75	0.8	4	0.375	30	0.3125	1.08555	0.942162	1.03588	1.10217	0.531334
15	0.938	0.8	15	0.938	0.8	6	0.5	30	0.3125	1.06403	0.896209	1.0171	1.08032	0.512441



15	1.25	0.8	15	1.25	0.8	6	0.5	30	0.3125	1.04833	0.907381	0.989894	1.0597	0.508018
15	0.75	0.8	15	0.75	0.8	6	0.5	30	0.3125	1.08873	0.888577	1.04485	1.10236	0.521222
15	0.938	0.8	15	0.938	0.8	5	0.5	30	0.3125	1.06709	1.01254	1.03015	1.08711	0.518652
15	1.25	0.8	15	1.25	0.8	5	0.5	30	0.3125	1.05235	0.999061	1.01964	1.06448	0.514223
15	0.75	0.8	15	0.75	0.8	5	0.5	30	0.3125	1.09181	0.939025	1.05214	1.11106	0.526882
15	0.938	0.8	15	0.938	0.8	4	0.5	30	0.3125	1.07986	0.874603	1.02242	1.09918	0.539144
15	1.25	0.8	15	1.25	0.8	4	0.5	30	0.3125	1.05883	0.916488	1.01168	1.07836	0.531163
15	0.75	0.8	15	0.75	0.8	4	0.5	30	0.3125	1.10417	0.899075	1.03083	1.1245	0.552111
15	0.938	0.8	15	0.938	0.8	6	0.375	30	0.3125	1.0469	0.930045	1.03566	1.05999	0.503139
15	1.25	0.8	15	1.25	0.8	6	0.375	30	0.3125	1.03545	0.934417	1.00862	1.04395	0.500683
15	0.75	0.8	15	0.75	0.8	6	0.375	30	0.3125	1.06928	0.935351	1.05978	1.0802	0.510776
15	0.938	0.8	15	0.938	0.8	5	0.375	30	0.3125	1.04865	1.06751	1.04927	1.06473	0.505904
15	1.25	0.8	15	1.25	0.8	5	0.375	30	0.3125	1.03911	1.02897	1.03389	1.04767	0.504693
15	0.75	0.8	15	0.75	0.8	5	0.375	30	0.3125	1.07015	0.993534	1.07136	1.08596	0.512012
15	0.938	0.8	15	0.938	0.8	4	0.375	30	0.3125	1.06127	0.905524	1.035	1.07577	0.521429
15	1.25	0.8	15	1.25	0.8	4	0.375	30	0.3125	1.04642	0.943002	1.0232	1.06123	0.518323
15	0.75	0.8	15	0.75	0.8	4	0.375	30	0.3125	1.08097	0.951364	1.04501	1.09664	0.530289
15	0.938	0.8	15	0.938	0.8	6	0.313	30	0.3125	1.03949	0.944859	1.04445	1.05119	0.499902
15	1.25	0.8	15	1.25	0.8	6	0.313	30	0.3125	1.03022	0.94551	1.01816	1.0376	0.498164
15	0.75	0.8	15	0.75	0.8	6	0.313	30	0.3125	1.06037	0.95574	1.06657	1.07006	0.506943
15	0.938	0.8	15	0.938	0.8	5	0.313	30	0.3125	1.04051	1.09053	1.05871	1.05485	0.5013
15	1.25	0.8	15	1.25	0.8	5	0.313	30	0.3125	1.03346	1.0405	1.041	1.0405	0.501258
15	0.75	0.8	15	0.75	0.8	5	0.313	30	0.3125	1.06022	1.01679	1.08039	1.07445	0.506485
15	0.938	0.8	15	0.938	0.8	4	0.313	30	0.3125	1.05235	0.920905	1.0418	1.06472	0.514005
15	1.25	0.8	15	1.25	0.8	4	0.313	30	0.3125	1.04057	0.956381	1.02982	1.05317	0.512939
15	0.75	0.8	15	0.75	0.8	4	0.313	30	0.3125	1.06964	0.977135	1.05255	1.08313	0.520957

15	0.938	0.8	15	0.938	0.8	6	0.5	30	0.25	1.06014	0.986626	1.02166	1.07285	0.508353
15	1.25	0.8	15	1.25	0.8	6	0.5	30	0.25	1.04217	0.979761	0.990844	1.05366	0.505517
15	0.75	0.8	15	0.75	0.8	6	0.5	30	0.25	1.08052	0.931462	1.0454	1.09504	0.514561
15	0.938	0.8	15	0.938	0.8	5	0.5	30	0.25	1.06283	0.949572	1.02111	1.08124	0.51489
15	1.25	0.8	15	1.25	0.8	5	0.5	30	0.25	1.04868	1.02505	1.01654	1.06229	0.510569
15	0.75	0.8	15	0.75	0.8	5	0.5	30	0.25	1.08564	1.03618	1.03525	1.10629	0.518612
15	0.938	0.8	15	0.938	0.8	4	0.5	30	0.25	1.07456	0.921831	1.02111	1.09404	0.534499
15	1.25	0.8	15	1.25	0.8	4	0.5	30	0.25	1.05625	0.970878	1.0086	1.07133	0.527508
15	0.75	0.8	15	0.75	0.8	4	0.5	30	0.25	1.09513	0.99846	1.03058	1.1151	0.544695
15	0.938	0.8	15	0.938	0.8	6	0.375	30	0.25	1.042	1.03018	1.03957	1.05105	0.498445
15	1.25	0.8	15	1.25	0.8	6	0.375	30	0.25	1.02916	1.00946	1.00865	1.03719	0.498335
15	0.75	0.8	15	0.75	0.8	6	0.375	30	0.25	1.05892	0.976848	1.05855	1.07048	0.503244
15	0.938	0.8	15	0.938	0.8	5	0.375	30	0.25	1.04368	0.99479	1.04046	1.05754	0.50164
15	1.25	0.8	15	1.25	0.8	5	0.375	30	0.25	1.03498	1.05602	1.03109	1.04451	0.500978
15	0.75	0.8	15	0.75	0.8	5	0.375	30	0.25	1.06192	1.10577	1.0551	1.07866	0.502736
15	0.938	0.8	15	0.938	0.8	4	0.375	30	0.25	1.05585	0.954022	1.03317	1.07007	0.516616
15	1.25	0.8	15	1.25	0.8	4	0.375	30	0.25	1.04368	0.994663	1.01966	1.0544	0.514394
15	0.75	0.8	15	0.75	0.8	4	0.375	30	0.25	1.07062	1.0582	1.04376	1.08542	0.521846
15	0.938	0.8	15	0.938	0.8	6	0.313	30	0.25	1.03405	1.04881	1.04834	1.04148	0.494979
15	1.25	0.8	15	1.25	0.8	6	0.313	30	0.25	1.02391	1.02107	1.01789	1.03052	0.495979
15	0.75	0.8	15	0.75	0.8	6	0.313	30	0.25	1.049	0.997596	1.06478	1.05918	0.499151
15	0.938	0.8	15	0.938	0.8	5	0.313	30	0.25	1.03501	1.01548	1.05042	1.04683	0.496732
15	1.25	0.8	15	1.25	0.8	5	0.313	30	0.25	1.02907	1.06904	1.0385	1.03679	0.497572
15	0.75	0.8	15	0.75	0.8	5	0.313	30	0.25	1.05084	1.13878	1.06499	1.06575	0.496791
15	0.938	0.8	15	0.938	0.8	4	0.313	30	0.25	1.04659	0.971111	1.03993	1.05831	0.508904
15	1.25	0.8	15	1.25	0.8	4	0.313	30	0.25	1.03769	1.0074	1.02608	1.04634	0.508897

15	0.75	0.8	15	0.75	0.8	4	0.313	30	0.25	1.05835	1.09061	1.05104	1.07062	0.511956
15	0.938	0.8	15	0.938	0.8	6	0.5	30	0.375	1.07257	0.907401	1.02023	1.08946	0.518331
15	1.25	0.8	15	1.25	0.8	6	0.5	30	0.375	1.05161	0.869164	0.987783	1.06594	0.511674
15	0.75	0.8	15	0.75	0.8	6	0.5	30	0.375	1.09376	0.924855	1.03449	1.1069	0.526486
15	0.938	0.8	15	0.938	0.8	5	0.5	30	0.375	1.07385	0.932781	1.03715	1.09113	0.523827
15	1.25	0.8	15	1.25	0.8	5	0.5	30	0.375	1.05636	0.937961	1.02726	1.06867	0.516895
15	0.75	0.8	15	0.75	0.8	5	0.5	30	0.375	1.09605	0.901468	1.05637	1.11778	0.533821
15	0.938	0.8	15	0.938	0.8	4	0.5	30	0.375	1.08553	0.896479	1.02554	1.11063	0.546687
15	1.25	0.8	15	1.25	0.8	4	0.5	30	0.375	1.06301	0.873233	1.01025	1.0795	0.534241
15	0.75	0.8	15	0.75	0.8	4	0.5	30	0.375	1.11259	0.856452	1.02803	1.13522	0.559044
15	0.938	0.8	15	0.938	0.8	6	0.375	30	0.375	1.05684	0.945802	1.03938	1.07093	0.509615
15	1.25	0.8	15	1.25	0.8	6	0.375	30	0.375	1.03936	0.896298	1.00653	1.05112	0.504684
15	0.75	0.8	15	0.75	0.8	6	0.375	30	0.375	1.07562	0.976202	1.05121	1.08624	0.516341
15	0.938	0.8	15	0.938	0.8	5	0.375	30	0.375	1.05689	0.977113	1.05542	1.07093	0.511827
15	1.25	0.8	15	1.25	0.8	5	0.375	30	0.375	1.04376	0.96555	1.04101	1.05278	0.507865
15	0.75	0.8	15	0.75	0.8	5	0.375	30	0.375	1.0759	0.946018	1.07509	1.09423	0.519392
15	0.938	0.8	15	0.938	0.8	4	0.375	30	0.375	1.06788	0.931233	1.03953	1.0884	0.529539
15	1.25	0.8	15	1.25	0.8	4	0.375	30	0.375	1.05071	0.899284	1.02173	1.06297	0.521584
15	0.75	0.8	15	0.75	0.8	4	0.375	30	0.375	1.0903	0.901075	1.04266	1.10869	0.537684
15	0.938	0.8	15	0.938	0.8	6	0.313	30	0.375	1.04991	0.961117	1.04813	1.0628	0.506385
15	1.25	0.8	15	1.25	0.8	6	0.313	30	0.375	1.03442	0.908263	1.01579	1.0452	0.502223
15	0.75	0.8	15	0.75	0.8	6	0.313	30	0.375	1.06721	0.996391	1.05869	1.07671	0.512502
15	0.938	0.8	15	0.938	0.8	5	0.313	30	0.375	1.04945	0.99405	1.06398	1.06209	0.507415
15	1.25	0.8	15	1.25	0.8	5	0.313	30	0.375	1.03849	0.976098	1.04765	1.04618	0.504633
15	0.75	0.8	15	0.75	0.8	5	0.313	30	0.375	1.06666	0.964718	1.08364	1.08347	0.513952
15	0.938	0.8	15	0.938	0.8	4	0.313	30	0.375	1.05962	0.947107	1.04681	1.07807	0.522387

15	1.25	0.8	15	1.25	0.8	4	0.313	30	0.375	1.04509	0.911741	1.02815	1.05545	0.516411
15	0.75	0.8	15	0.75	0.8	4	0.313	30	0.375	1.07955	0.922396	1.05026	1.09601	0.528619
15	0.938	0.8	15	0.938	0.8	6	0.5	30	0.3125	1.06047	0.90084	1.01878	1.07614	0.508929
15	1.25	0.8	15	1.25	0.8	6	0.5	30	0.3125	1.04248	0.908076	1.01696	1.05319	0.503329
15	0.938	0.8	15	0.938	0.8	6	0.5	30	0.3125	1.0559	0.903979	1.02866	1.071	0.504917
15	1.25	0.8	15	1.25	0.8	6	0.5	30	0.3125	1.03991	0.911698	1.01751	1.05003	0.500134
15	0.75	0.8	15	0.75	0.8	6	0.5	30	0.3125	1.08104	0.897876	1.04675	1.09367	0.514499
15	0.938	0.8	15	0.938	0.8	5	0.5	30	0.3125	1.05999	1.02696	0.999965	1.07883	0.5116
15	1.25	0.8	15	1.25	0.8	5	0.5	30	0.3125	1.04508	1.0067	0.996919	1.05606	0.507366
15	0.75	0.8	15	0.75	0.8	5	0.5	30	0.3125	1.085	0.950011	1.01269	1.10325	0.520322
15	0.938	0.8	15	0.938	0.8	4	0.5	30	0.3125	1.07445	0.877616	1.01896	1.09277	0.534024
15	1.25	0.8	15	1.25	0.8	4	0.5	30	0.3125	1.0531	0.917358	1.03232	1.07168	0.526257
15	0.75	0.8	15	0.75	0.8	4	0.5	30	0.3125	1.09866	0.905958	0.999224	1.11803	0.546994
15	0.938	0.8	15	0.938	0.8	6	0.375	30	0.3125	1.03854	0.93708	1.04929	1.05044	0.495384
15	1.25	0.8	15	1.25	0.8	6	0.375	30	0.3125	1.02738	0.937772	1.03834	1.0347	0.492872
15	0.75	0.8	15	0.75	0.8	6	0.375	30	0.3125	1.06084	0.944105	1.06796	1.07073	0.503529
15	0.938	0.8	15	0.938	0.8	5	0.375	30	0.3125	1.04137	1.08104	1.02265	1.0563	0.498831
15	1.25	0.8	15	1.25	0.8	5	0.375	30	0.3125	1.03224	1.0355	1.01907	1.03976	0.49812
15	0.75	0.8	15	0.75	0.8	5	0.375	30	0.3125	1.06257	1.0038	1.03469	1.07735	0.505075
15	0.938	0.8	15	0.938	0.8	4	0.375	30	0.3125	1.05584	0.907428	1.03412	1.06941	0.516505
15	1.25	0.8	15	1.25	0.8	4	0.375	30	0.3125	1.04115	0.942989	1.045	1.05516	0.513841
15	0.75	0.8	15	0.75	0.8	4	0.375	30	0.3125	1.07488	0.957322	1.01817	1.0896	0.525067
15	0.938	0.8	15	0.938	0.8	6	0.313	30	0.3125	1.03135	0.950825	1.05899	1.04195	0.492267
15	1.25	0.8	15	1.25	0.8	6	0.313	30	0.3125	1.0226	0.947804	1.04862	1.02891	0.490569
15	0.75	0.8	15	0.75	0.8	6	0.313	30	0.3125	1.05183	0.963431	1.07766	1.06053	0.499655
15	0.938	0.8	15	0.938	0.8	5	0.313	30	0.3125	1.03345	1.10276	1.03416	1.04671	0.494466

15	1.25	0.8	15	1.25	0.8	5	0.313	30	0.3125	1.02701	1.04609	1.03031	1.03312	0.495001
15	0.75	0.8	15	0.75	0.8	5	0.313	30	0.3125	1.05253	1.02585	1.04565	1.06576	0.499614
15	0.938	0.8	15	0.938	0.8	4	0.313	30	0.3125	1.04706	0.922088	1.0425	1.05857	0.509316
15	1.25	0.8	15	1.25	0.8	4	0.313	30	0.3125	1.03565	0.955975	1.05203	1.04756	0.508774
15	0.75	0.8	15	0.75	0.8	4	0.313	30	0.3125	1.06339	0.982218	1.02844	1.07598	0.515818
15	0.938	0.8	15	0.938	0.8	6	0.5	30	0.25	1.05247	0.999275	1.02194	1.06392	0.500976
15	1.25	0.8	15	1.25	0.8	6	0.5	30	0.25	1.03407	0.986044	1.01089	1.04427	0.497632
15	0.75	0.8	15	0.75	0.8	6	0.5	30	0.25	1.07283	0.942322	1.03162	1.08644	0.507701
15	0.938	0.8	15	0.938	0.8	5	0.5	30	0.25	1.05623	0.957566	0.998354	1.07342	0.508064
15	1.25	0.8	15	1.25	0.8	5	0.5	30	0.25	1.04156	1.03069	1.00404	1.05398	0.503684
15	0.75	0.8	15	0.75	0.8	5	0.5	30	0.25	1.07874	1.05191	1.01945	1.09842	0.511829
15	0.938	0.8	15	0.938	0.8	4	0.5	30	0.25	1.06926	0.926572	1.00569	1.08763	0.529293
15	1.25	0.8	15	1.25	0.8	4	0.5	30	0.25	1.05048	0.971881	1.02075	1.06463	0.522341
15	0.75	0.8	15	0.75	0.8	4	0.5	30	0.25	1.08937	1.00819	1.00493	1.10823	0.539187
15	0.938	0.8	15	0.938	0.8	6	0.375	30	0.25	1.03403	1.04178	1.04367	1.04182	0.490731
15	1.25	0.8	15	1.25	0.8	6	0.375	30	0.25	1.0214	1.0146	1.03133	1.02822	0.490497
15	0.75	0.8	15	0.75	0.8	6	0.375	30	0.25	1.05044	0.986992	1.05361	1.06103	0.495781
15	0.938	0.8	15	0.938	0.8	5	0.375	30	0.25	1.03689	1.00171	1.02026	1.04957	0.494751
15	1.25	0.8	15	1.25	0.8	5	0.375	30	0.25	1.02828	1.06047	1.0253	1.03676	0.494375
15	0.75	0.8	15	0.75	0.8	5	0.375	30	0.25	1.05423	1.12067	1.03857	1.06995	0.495531
15	0.938	0.8	15	0.938	0.8	4	0.375	30	0.25	1.05049	0.957344	1.02127	1.06368	0.51158
15	1.25	0.8	15	1.25	0.8	4	0.375	30	0.25	1.03835	0.994552	1.03313	1.04831	0.50963
15	0.75	0.8	15	0.75	0.8	4	0.375	30	0.25	1.0642	1.06694	1.02263	1.0779	0.516171
15	0.938	0.8	15	0.938	0.8	6	0.313	30	0.25	1.02619	1.05914	1.05441	1.03243	0.487283
15	1.25	0.8	15	1.25	0.8	6	0.313	30	0.25	1.01655	1.0251	1.04156	1.02204	0.488326
15	0.75	0.8	15	0.75	0.8	6	0.313	30	0.25	1.04039	1.00663	1.0642	1.04962	0.491593

15	0.938	0.8	15	0.938	0.8	5	0.313	30	0.25	1.02835	1.02138	1.03184	1.03904	0.489987
15	1.25	0.8	15	1.25	0.8	5	0.313	30	0.25	1.02276	1.07269	1.0362	1.02954	0.491253
15	0.75	0.8	15	0.75	0.8	5	0.313	30	0.25	1.04299	1.15242	1.04845	1.05691	0.489596
15	0.938	0.8	15	0.938	0.8	4	0.313	30	0.25	1.04133	0.973581	1.03014	1.05211	0.504071
15	1.25	0.8	15	1.25	0.8	4	0.313	30	0.25	1.03269	1.00686	1.04006	1.0407	0.504433
15	0.75	0.8	15	0.75	0.8	4	0.313	30	0.25	1.05176	1.09846	1.03251	1.06297	0.506342
15	0.938	0.8	15	0.938	0.8	6	0.5	30	0.375	1.06445	0.916934	1.04104	1.08009	0.511024
15	1.25	0.8	15	1.25	0.8	6	0.5	30	0.375	1.0427	0.873242	1.01993	1.05581	0.503695
15	0.75	0.8	15	0.75	0.8	6	0.5	30	0.375	1.08608	0.937478	1.0523	1.09827	0.519861
15	0.938	0.8	15	0.938	0.8	5	0.5	30	0.375	1.06673	0.943255	0.995534	1.08295	0.516944
15	1.25	0.8	15	1.25	0.8	5	0.5	30	0.375	1.04863	0.944123	1.00289	1.05978	0.50985
15	0.75	0.8	15	0.75	0.8	5	0.5	30	0.375	1.08926	0.909613	1.00339	1.11	0.527337
15	0.938	0.8	15	0.938	0.8	4	0.5	30	0.375	1.08025	0.900324	1.04013	1.10432	0.541863
15	1.25	0.8	15	1.25	0.8	4	0.5	30	0.375	1.05707	0.873217	1.03342	1.07267	0.529322
15	0.75	0.8	15	0.75	0.8	4	0.5	30	0.375	1.10725	0.860862	1.01184	1.129	0.554228
15	0.938	0.8	15	0.938	0.8	6	0.375	30	0.375	1.04853	0.954587	1.06096	1.06138	0.50213
15	1.25	0.8	15	1.25	0.8	6	0.375	30	0.375	1.03093	0.899456	1.03984	1.04156	0.496894
15	0.75	0.8	15	0.75	0.8	6	0.375	30	0.375	1.06726	0.988149	1.07199	1.07691	0.509275
15	0.938	0.8	15	0.938	0.8	5	0.375	30	0.375	1.04965	0.986671	1.01897	1.06266	0.504982
15	1.25	0.8	15	1.25	0.8	5	0.375	30	0.375	1.03655	0.970722	1.02475	1.04452	0.501218
15	0.75	0.8	15	0.75	0.8	5	0.375	30	0.375	1.06839	0.953514	1.02728	1.08571	0.512595
15	0.938	0.8	15	0.938	0.8	4	0.375	30	0.375	1.06265	0.934102	1.05483	1.08221	0.524952
15	1.25	0.8	15	1.25	0.8	4	0.375	30	0.375	1.04531	0.898547	1.04597	1.05683	0.517154
15	0.75	0.8	15	0.75	0.8	4	0.375	30	0.375	1.08443	0.904616	1.03012	1.10195	0.532799
15	0.938	0.8	15	0.938	0.8	6	0.313	30	0.375	1.04181	0.968682	1.06992	1.05355	0.499029
15	1.25	0.8	15	1.25	0.8	6	0.313	30	0.375	1.02654	0.910348	1.04943	1.03632	0.494715

15	0.75	0.8	15	0.75	0.8	6	0.313	30	0.375	1.05877	1.00693	1.08062	1.06734	0.505442
15	0.938	0.8	15	0.938	0.8	5	0.313	30	0.375	1.04244	1.00232	1.03044	1.05412	0.500837
15	1.25	0.8	15	1.25	0.8	5	0.313	30	0.375	1.0318	0.98027	1.03552	1.03857	0.498384
15	0.75	0.8	15	0.75	0.8	5	0.313	30	0.375	1.05908	0.971123	1.0389	1.07491	0.507274
15	0.938	0.8	15	0.938	0.8	4	0.313	30	0.375	1.05454	0.94926	1.06259	1.07213	0.518047
15	1.25	0.8	15	1.25	0.8	4	0.313	30	0.375	1.0401	0.910616	1.05277	1.04983	0.512339
15	0.75	0.8	15	0.75	0.8	4	0.313	30	0.375	1.07354	0.925158	1.03984	1.08917	0.523834
15	0.938	0.8	15	0.938	0.8	6	0.5	30	0.25	1.05945	0.992295	1.02459	1.07178	0.507007
15	1.25	0.8	15	1.25	0.8	6	0.5	30	0.25	1.0389	0.980596	0.988748	1.05004	0.502813
15	0.75	0.8	15	0.75	0.8	6	0.5	30	0.25	1.07744	0.933755	1.05373	1.09169	0.512361
15	0.938	0.8	15	0.938	0.8	5	0.5	30	0.25	1.06249	0.953619	1.02362	1.08052	0.513783
15	1.25	0.8	15	1.25	0.8	5	0.5	30	0.25	1.04584	1.02566	1.01684	1.0591	0.508388
15	0.75	0.8	15	0.75	0.8	5	0.5	30	0.25	1.0828	1.03991	1.03604	1.10314	0.51655
15	0.938	0.8	15	0.938	0.8	4	0.5	30	0.25	1.0748	0.925248	1.02188	1.09396	0.533755
15	1.25	0.8	15	1.25	0.8	4	0.5	30	0.25	1.05366	0.970258	1.0065	1.06853	0.525501
15	0.75	0.8	15	0.75	0.8	4	0.5	30	0.25	1.09274	1.00078	1.02899	1.11237	0.542889
15	0.938	0.8	15	0.938	0.8	6	0.375	30	0.25	1.04121	1.03576	1.04312	1.04986	0.496949
15	1.25	0.8	15	1.25	0.8	6	0.375	30	0.25	1.02601	1.01015	1.00732	1.0337	0.49563
15	0.75	0.8	15	0.75	0.8	6	0.375	30	0.25	1.05567	0.979113	1.06627	1.06694	0.500867
15	0.938	0.8	15	0.938	0.8	5	0.375	30	0.25	1.0433	0.998745	1.04363	1.05678	0.500442
15	1.25	0.8	15	1.25	0.8	5	0.375	30	0.25	1.03228	1.05659	1.03185	1.0415	0.498855
15	0.75	0.8	15	0.75	0.8	5	0.375	30	0.25	1.05891	1.10949	1.05681	1.07532	0.500515
15	0.938	0.8	15	0.938	0.8	4	0.375	30	0.25	1.05613	0.95706	1.03451	1.07004	0.515931
15	1.25	0.8	15	1.25	0.8	4	0.375	30	0.25	1.04127	0.993816	1.01801	1.05181	0.512539
15	0.75	0.8	15	0.75	0.8	4	0.375	30	0.25	1.06812	1.06029	1.04236	1.08259	0.520038
15	0.938	0.8	15	0.938	0.8	6	0.5	30	0.375	1.07173	0.912087	1.0236	1.08825	0.517031

15	1.25	0.8	15	1.25	0.8	6	0.5	30	0.375	1.04827	0.869255	0.986181	1.06224	0.509093
15	0.75	0.8	15	0.75	0.8	6	0.5	30	0.375	1.09062	0.927778	1.04719	1.10347	0.524326
15	0.938	0.8	15	0.938	0.8	5	0.5	30	0.375	1.07329	0.937618	1.0416	1.09024	0.522655
15	1.25	0.8	15	1.25	0.8	5	0.5	30	0.375	1.0533	0.938799	1.02886	1.06527	0.514623
15	0.75	0.8	15	0.75	0.8	5	0.5	30	0.375	1.0931	0.902928	1.04845	1.11451	0.531757
15	0.938	0.8	15	0.938	0.8	4	0.5	30	0.375	1.0857	0.899705	1.02582	1.11053	0.54598
15	1.25	0.8	15	1.25	0.8	4	0.5	30	0.375	1.0605	0.872456	1.00892	1.07675	0.532521
15	0.938	0.8	15	0.938	0.8	6	0.375	30	0.375	1.05334	0.951346	1.05343	1.06677	0.506179
15	1.25	0.8	15	1.25	0.8	6	0.375	30	0.375	1.03352	0.896854	1.03514	1.04465	0.499996
15	0.75	0.8	15	0.75	0.8	6	0.375	30	0.375	1.06986	0.981128	1.08007	1.07995	0.51218
15	0.938	0.8	15	0.938	0.8	5	0.375	30	0.375	1.05393	0.983715	1.0292	1.06742	0.508684
15	1.25	0.8	15	1.25	0.8	5	0.375	30	0.375	1.03848	0.967067	1.02138	1.0469	0.50379
15	0.75	0.8	15	0.75	0.8	5	0.375	30	0.375	1.07062	0.948965	1.04189	1.08839	0.515392
15	0.938	0.8	15	0.938	0.8	4	0.375	30	0.375	1.06594	0.934061	1.05714	1.08591	0.527643
15	1.25	0.8	15	1.25	0.8	4	0.375	30	0.375	1.04622	0.897928	1.04207	1.058	0.518634
15	0.75	0.8	15	0.75	0.8	4	0.375	30	0.375	1.08574	0.90208	1.04202	1.10359	0.534714
15	0.938	0.8	15	0.938	0.8	6	0.313	30	0.375	1.04659	0.966131	1.06301	1.05887	0.50303
15	1.25	0.8	15	1.25	0.8	6	0.313	30	0.375	1.02888	0.908364	1.04417	1.0391	0.497666
15	0.75	0.8	15	0.75	0.8	6	0.313	30	0.375	1.0615	1.00067	1.08782	1.07049	0.508368
15	0.938	0.8	15	0.938	0.8	5	0.313	30	0.375	1.0467	1.00002	1.03988	1.05883	0.504449
15	1.25	0.8	15	1.25	0.8	5	0.313	30	0.375	1.03352	0.977003	1.03178	1.04069	0.500765
15	0.75	0.8	15	0.75	0.8	5	0.313	30	0.375	1.06145	0.967105	1.05197	1.07772	0.51006
15	0.938	0.8	15	0.938	0.8	4	0.313	30	0.375	1.05782	0.949652	1.06498	1.07577	0.52063
15	1.25	0.8	15	1.25	0.8	4	0.313	30	0.375	1.04084	0.910172	1.0489	1.05079	0.51363
15	0.75	0.8	15	0.75	0.8	4	0.313	30	0.375	1.07499	0.923044	1.05115	1.09093	0.525718
15	0.75	0.8	15	0.75	0.8	6	0.5	30	0.3125	1.08323	0.891894	1.05286	1.09633	0.517256



15	0.938	0.8	15	0.938	0.8	5	0.5	30	0.3125	1.06413	1.02161	1.01042	1.08353	0.515392
15	1.25	0.8	15	1.25	0.8	5	0.5	30	0.3125	1.04709	1.00149	0.994773	1.0586	0.510118
15	0.75	0.8	15	0.75	0.8	5	0.5	30	0.3125	1.08683	0.943632	1.02356	1.10554	0.523023
15	0.938	0.8	15	0.938	0.8	4	0.5	30	0.3125	1.07772	0.877156	1.02945	1.09645	0.536941
15	1.25	0.8	15	1.25	0.8	4	0.5	30	0.3125	1.05414	0.915878	1.02882	1.07305	0.527985
15	0.75	0.8	15	0.75	0.8	4	0.5	30	0.3125	1.0997	0.90171	1.00698	1.11944	0.549001
15	0.938	0.8	15	0.938	0.8	6	0.375	30	0.3125	1.0433	0.934571	1.04076	1.05576	0.499498
15	1.25	0.8	15	1.25	0.8	6	0.375	30	0.3125	1.02981	0.934819	1.03637	1.03768	0.496001
15	0.75	0.8	15	0.75	0.8	6	0.375	30	0.3125	1.06354	0.938596	1.07272	1.0739	0.506559
15	0.938	0.8	15	0.938	0.8	5	0.375	30	0.3125	1.04566	1.07649	1.03237	1.06112	0.50262
15	1.25	0.8	15	1.25	0.8	5	0.375	30	0.3125	1.03409	1.0307	1.01614	1.04208	0.500702
15	0.75	0.8	15	0.75	0.8	5	0.375	30	0.3125	1.06488	0.997922	1.04463	1.08012	0.507962
15	0.938	0.8	15	0.938	0.8	4	0.375	30	0.3125	1.0592	0.907684	1.04436	1.07315	0.519319
15	1.25	0.8	15	1.25	0.8	4	0.375	30	0.3125	1.04204	0.941836	1.04144	1.05633	0.515355
15	0.75	0.8	15	0.75	0.8	4	0.375	30	0.3125	1.07631	0.953663	1.02459	1.0914	0.527142
15	0.938	0.8	15	0.938	0.8	6	0.313	30	0.3125	1.03608	0.948932	1.05137	1.04719	0.496336
15	1.25	0.8	15	1.25	0.8	6	0.313	30	0.3125	1.02484	0.945432	1.04593	1.03163	0.493578
15	0.75	0.8	15	0.75	0.8	6	0.313	30	0.3125	1.05466	0.958523	1.08169	1.06381	0.502725
15	0.938	0.8	15	0.938	0.8	5	0.313	30	0.3125	1.03771	1.09896	1.04318	1.05148	0.498165
15	1.25	0.8	15	1.25	0.8	5	0.313	30	0.3125	1.02868	1.0416	1.02701	1.0352	0.497417
15	0.75	0.8	15	0.75	0.8	5	0.313	30	0.3125	1.05497	1.02059	1.05467	1.06866	0.502496
15	0.938	0.8	15	0.938	0.8	4	0.313	30	0.3125	1.05042	0.922759	1.05257	1.06227	0.512026
15	1.25	0.8	15	1.25	0.8	4	0.313	30	0.3125	1.0364	0.954929	1.04851	1.04855	0.510123
15	0.75	0.8	15	0.75	0.8	4	0.313	30	0.3125	1.06497	0.979029	1.03413	1.07791	0.517869
15	0.75	0.8	15	0.75	0.8	4	0.5	30	0.375	1.11017	0.857178	1.0301	1.13254	0.557299
15	0.938	0.8	15	0.938	0.8	6	0.375	30	0.375	1.05601	0.95041	1.04317	1.06971	0.508255

15	1.25	0.8	15	1.25	0.8	6	0.375	30	0.375	1.03622	0.8961	1.00575	1.04764	0.502171
15	0.75	0.8	15	0.75	0.8	6	0.375	30	0.375	1.07239	0.979011	1.06245	1.08272	0.514084
15	0.938	0.8	15	0.938	0.8	5	0.375	30	0.375	1.05634	0.981848	1.06043	1.07004	0.510625
15	1.25	0.8	15	1.25	0.8	5	0.375	30	0.375	1.04091	0.966256	1.04297	1.04961	0.505708
15	0.75	0.8	15	0.75	0.8	5	0.375	30	0.375	1.07283	0.947436	1.06878	1.09083	0.517231
15	0.938	0.8	15	0.938	0.8	4	0.375	30	0.375	1.0681	0.934273	1.0401	1.08835	0.528891
15	1.25	0.8	15	1.25	0.8	4	0.375	30	0.375	1.04839	0.898376	1.02073	1.06044	0.520034
15	0.75	0.8	15	0.75	0.8	4	0.375	30	0.375	1.08779	0.901637	1.04467	1.10593	0.535948
15	0.938	0.8	15	0.938	0.8	6	0.5	30	0.25	1.05682	0.994128	1.01514	1.06885	0.50491
15	1.25	0.8	15	1.25	0.8	6	0.5	30	0.25	1.03919	0.984393	1.01261	1.04998	0.502083
15	0.75	0.8	15	0.75	0.8	6	0.5	30	0.25	1.07508	0.935599	1.02897	1.08911	0.510547
15	0.938	0.8	15	0.938	0.8	5	0.5	30	0.25	1.06022	0.954656	1.01025	1.078	0.511807
15	1.25	0.8	15	1.25	0.8	5	0.5	30	0.25	1.04357	1.02618	1.00142	1.05654	0.506485
15	0.75	0.8	15	0.75	0.8	5	0.5	30	0.25	1.08067	1.04318	1.02687	1.10081	0.514669
15	0.938	0.8	15	0.938	0.8	4	0.5	30	0.25	1.07249	0.925331	1.01405	1.09133	0.532256
15	1.25	0.8	15	1.25	0.8	4	0.5	30	0.25	1.0544	0.973226	1.02682	1.06889	0.52543
15	0.75	0.8	15	0.75	0.8	4	0.5	30	0.25	1.09055	1.00255	1.00113	1.10985	0.541393
15	0.938	0.8	15	0.938	0.8	6	0.375	30	0.25	1.03856	1.0376	1.03783	1.04692	0.494791
15	1.25	0.8	15	1.25	0.8	6	0.375	30	0.25	1.02638	1.01375	1.03191	1.03374	0.494877
15	0.75	0.8	15	0.75	0.8	6	0.375	30	0.25	1.05319	0.980895	1.05077	1.06422	0.49892
15	0.938	0.8	15	0.938	0.8	5	0.375	30	0.25	1.041	0.999679	1.03121	1.05424	0.498478
15	1.25	0.8	15	1.25	0.8	5	0.375	30	0.25	1.03011	1.05646	1.02203	1.03907	0.497002
15	0.75	0.8	15	0.75	0.8	5	0.375	30	0.25	1.05662	1.11257	1.04565	1.07281	0.498553
15	0.938	0.8	15	0.938	0.8	4	0.375	30	0.25	1.05385	0.956974	1.029	1.06747	0.514465
15	1.25	0.8	15	1.25	0.8	4	0.375	30	0.25	1.04215	0.996356	1.03904	1.05239	0.512515
15	0.75	0.8	15	0.75	0.8	4	0.375	30	0.25	1.06583	1.06192	1.01773	1.07997	0.518489

15	0.938	0.8	15	0.938	0.8	6	0.313	30	0.25	1.03073	1.05576	1.04919	1.0375	0.49134
15	1.25	0.8	15	1.25	0.8	6	0.313	30	0.25	1.02137	1.0248	1.04155	1.02736	0.492603
15	0.75	0.8	15	0.75	0.8	6	0.313	30	0.25	1.04329	1.00118	1.06135	1.05295	0.494793
15	0.938	0.8	15	0.938	0.8	5	0.313	30	0.25	1.03245	1.02001	1.04191	1.04366	0.493645
15	1.25	0.8	15	1.25	0.8	5	0.313	30	0.25	1.02442	1.06894	1.03262	1.03163	0.493727
15	0.75	0.8	15	0.75	0.8	5	0.313	30	0.25	1.04553	1.14503	1.05492	1.0599	0.492622
15	0.938	0.8	15	0.938	0.8	4	0.313	30	0.25	1.04471	0.973711	1.0375	1.05588	0.506868
15	1.25	0.8	15	1.25	0.8	4	0.313	30	0.25	1.03639	1.00881	1.04601	1.04463	0.507168
15	0.75	0.8	15	0.75	0.8	4	0.313	30	0.25	1.05355	1.09392	1.02692	1.0652	0.508649
15	0.938	0.8	15	0.938	0.8	6	0.5	30	0.375	1.06906	0.913061	1.03263	1.08529	0.514983
15	1.25	0.8	15	1.25	0.8	6	0.5	30	0.375	1.04547	0.869985	1.01635	1.05914	0.506908
15	0.75	0.8	15	0.75	0.8	6	0.5	30	0.375	1.0882	0.929936	1.06197	1.10082	0.522526
15	0.938	0.8	15	0.938	0.8	5	0.5	30	0.375	1.07086	0.939633	1.00668	1.08758	0.520654
15	1.25	0.8	15	1.25	0.8	5	0.5	30	0.375	1.05075	0.940042	1.0003	1.06241	0.512622
15	0.75	0.8	15	0.75	0.8	5	0.5	30	0.375	1.09101	0.904636	1.02032	1.11219	0.52995
15	0.938	0.8	15	0.938	0.8	4	0.5	30	0.375	1.08349	0.899585	1.04222	1.10799	0.544677
15	1.25	0.8	15	1.25	0.8	4	0.5	30	0.375	1.05819	0.872249	1.02959	1.0741	0.531051
15	0.75	0.8	15	0.75	0.8	4	0.5	30	0.375	1.1082	0.85777	1.02477	1.13026	0.55609
15	0.938	0.8	15	0.938	0.8	5	0.25	30	0.375	1.04285	1.00717	1.07679	1.05404	0.503225
15	0.938	0.8	15	0.938	0.8	5	0.625	30	0.375	1.09081	0.891822	1.02394	1.11119	0.537332
15	0.938	0.8	15	0.938	0.8	5	0.438	30	0.375	1.06458	0.960679	1.05105	1.07984	0.516171
15	0.938	0.8	15	0.938	0.8	5	0.563	30	0.375	1.08212	0.914358	1.03248	1.10079	0.529789
15	0.938	0.8	15	0.938	0.8	5	0.688	30	0.375	1.0992	0.870417	1.01614	1.12128	0.545113
15	0.938	0.8	15	0.938	0.8	5	0.75	30	0.375	1.10724	0.850249	1.00916	1.13097	0.55301
15	0.938	0.8	15	0.938	0.8	5	0.813	30	0.375	1.11489	0.831298	1.003	1.14023	0.560938
15	0.938	0.8	15	0.938	0.8	5	0.875	30	0.375	1.12216	0.813451	0.997652	1.14906	0.568829

15	0.938	0.8	15	0.938	0.8	5	0.938	30	0.375	1.12904	0.796598	0.993092	1.15745	0.576629
15	0.938	0.8	15	0.938	0.8	5	1	30	0.375	1.13554	0.784902	0.989248	1.16536	0.584496
15	0.5	0.8	15	0.5	0.8	5	0.313	30	0.375	1.10761	0.924701	1.09322	1.12451	0.528482
15	0.625	0.8	15	0.625	0.8	5	0.313	30	0.375	1.08428	0.936387	1.09627	1.0991	0.517023
15	1.5	0.8	15	1.5	0.8	5	0.313	30	0.375	1.0302	0.965792	1.03704	1.04127	0.504475
15	1.75	0.8	15	1.75	0.8	5	0.313	30	0.375	1.02512	0.968733	1.03538	1.03491	0.505458
15	2	0.8	15	2	0.8	5	0.313	30	0.375	1.02348	0.955153	1.03807	1.03301	0.505862
15	0.938	0.8	15	0.938	0.8	1	0.5	30	0.375	1.0438	0.916715	1.0366	1.08682	0.565734
15	0.938	0.8	15	0.938	0.8	2	0.5	30	0.375	1.07481	0.854307	1.04	1.11031	0.572782
15	0.938	0.8	15	0.938	0.8	2	0.5	30	0.375	1.08404	0.846871	1.03687	1.11598	0.570238
15	0.938	0.8	15	0.938	0.8	3	0.5	30	0.375	1.08828	0.823689	1.05593	1.11385	0.563581
15	0.938	0.8	15	0.938	0.8	3	0.5	30	0.375	1.08831	0.851685	1.0308	1.11037	0.554256
15	0.938	0.8	15	0.938	0.8	4	0.5	30	0.375	1.08076	0.983733	1.02242	1.10064	0.53607
15	0.938	0.8	15	0.938	0.8	5	0.5	30	0.375	1.07836	0.948783	1.00376	1.09515	0.529251
15	0.938	0.8	15	0.938	0.8	6	0.5	30	0.375	1.07092	0.914692	1.01401	1.08785	0.520133
15	0.938	0.8	15	0.938	0.8	1	0.375	30	0.3125	1.04215	0.90779	1.03336	1.074	0.550258
15	0.938	0.8	15	0.938	0.8	1	0.375	30	0.3125	1.05208	0.88103	1.02643	1.08407	0.553597
15	0.938	0.8	15	0.938	0.8	1	0.375	30	0.3125	1.05753	0.871316	1.03399	1.08702	0.552694
15	0.938	0.8	15	0.938	0.8	2	0.375	30	0.3125	1.0623	0.902788	1.0449	1.08989	0.550903
15	0.938	0.8	15	0.938	0.8	2	0.375	30	0.3125	1.06431	0.910202	1.04342	1.09363	0.55012
15	0.938	0.8	15	0.938	0.8	2	0.375	30	0.3125	1.0645	0.944401	1.03494	1.08945	0.546538
15	0.938	0.8	15	0.938	0.8	2	0.375	30	0.3125	1.0683	0.919483	1.03282	1.09161	0.544199
15	0.938	0.8	15	0.938	0.8	2	0.375	30	0.3125	1.06404	0.886066	1.04081	1.08866	0.540708
15	0.938	0.8	15	0.938	0.8	3	0.375	30	0.3125	1.06553	0.874776	1.04775	1.08366	0.537299
15	0.938	0.8	15	0.938	0.8	3	0.375	30	0.3125	1.06559	0.890688	1.04481	1.0887	0.534465
15	0.938	0.8	15	0.938	0.8	3	0.375	30	0.3125	1.06328	0.914139	1.04202	1.08224	0.529818

15	0.938	0.8	15	0.938	0.8	3	0.375	30	0.3125	1.0646	0.957294	1.01462	1.08077	0.526838
15	0.938	0.8	15	0.938	0.8	3	0.375	30	0.3125	1.06024	0.986123	1.02851	1.07804	0.523055
15	0.5	0.8	15	0.5	0.8	5	0.375	30	0.375	1.12609	0.914612	1.03573	1.14039	0.540088
15	0.6	0.8	15	0.6	0.8	5	0.375	30	0.375	1.10015	0.919002	1.02049	1.12191	0.532722
15	0.7	0.8	15	0.7	0.8	5	0.375	30	0.375	1.08753	0.960238	1.00852	1.10814	0.525339
15	0.8	0.8	15	0.8	0.8	5	0.375	30	0.375	1.07696	0.931579	1.00946	1.08927	0.520349
15	0.9	0.8	15	0.9	0.8	5	0.375	30	0.375	1.06403	0.986655	1.03198	1.07621	0.516236
15	1	0.8	15	1	0.8	5	0.375	30	0.375	1.05594	0.969488	1.02673	1.06772	0.515083
15	1.1	0.8	15	1.1	0.8	5	0.375	30	0.375	1.05383	0.941219	1.03735	1.06494	0.512188
15	1.2	0.8	15	1.2	0.8	5	0.375	30	0.375	1.04717	0.946122	1.03997	1.05945	0.511855
15	1.3	0.8	15	1.3	0.8	5	0.375	30	0.375	1.04622	1.04678	1.04098	1.05569	0.510946
15	1.4	0.8	15	1.4	0.8	5	0.375	30	0.375	1.04186	0.945602	1.03561	1.05375	0.512346
15	1.5	0.8	15	1.5	0.8	5	0.375	30	0.375	1.03699	1.06682	1.03784	1.049	0.512804
15	1.6	0.8	15	1.6	0.8	5	0.375	30	0.375	1.03652	0.949614	1.03328	1.04883	0.510961
15	1.7	0.8	15	1.7	0.8	5	0.375	30	0.375	1.03393	0.888923	1.03499	1.04651	0.511714
15	1.8	0.8	15	1.8	0.8	5	0.375	30	0.375	1.03489	1.01719	1.03558	1.04751	0.511548
15	1.9	0.8	15	1.9	0.8	5	0.375	30	0.375	1.03195	0.954567	1.0346	1.04259	0.511461
15	2	0.8	15	2	0.8	5	0.375	30	0.375	1.02985	0.976789	1.0355	1.04027	0.511242
15	2.1	0.8	15	2.1	0.8	5	0.375	30	0.375	1.02734	0.895971	1.03821	1.03891	0.510172
15	2.2	0.8	15	2.2	0.8	5	0.375	30	0.375	1.02505	0.974263	1.03657	1.03843	0.512439
15	2.3	0.8	15	2.3	0.8	5	0.375	30	0.375	1.02465	0.981825	1.03372	1.03622	0.51019
15	2.4	0.8	15	2.4	0.8	5	0.375	30	0.375	1.02525	0.980265	1.04235	1.03385	0.509407
15	2.5	0.8	15	2.5	0.8	5	0.375	30	0.375	1.02423	0.987687	1.03869	1.03382	0.510319
15	2.6	0.8	15	2.6	0.8	5	0.375	30	0.375	1.02315	0.908753	1.03056	1.0332	0.509083
15	2.7	0.8	15	2.7	0.8	5	0.375	30	0.375	1.02157	0.913566	1.03935	1.03119	0.508583
15	2.8	0.8	15	2.8	0.8	5	0.375	30	0.375	1.02127	0.916738	1.03178	1.0314	0.509169

15	2.9	0.8	15	2.9	0.8	5	0.375	30	0.375	1.0212	0.96461	1.03594	1.03147	0.50972
15	0.938	0.8	15	0.938	0.8	5	0.375	30	0.1	1.03673	0.995951	1.03635	1.04363	0.49257
15	0.938	0.8	15	0.938	0.8	5	0.375	30	0.12857	1.03791	0.989504	1.03267	1.04668	0.494977
15	0.938	0.8	15	0.938	0.8	5	0.375	30	0.15714	1.03975	0.944842	1.02776	1.04991	0.49706
15	0.938	0.8	15	0.938	0.8	5	0.375	30	0.18571	1.04185	0.90852	1.02167	1.05378	0.499046
15	0.938	0.8	15	0.938	0.8	5	0.375	30	0.21429	1.04711	0.895922	1.01922	1.0574	0.501169
15	0.938	0.8	15	0.938	0.8	5	0.375	30	0.24286	1.04915	0.910032	1.01415	1.06198	0.503624
15	0.938	0.8	15	0.938	0.8	5	0.375	30	0.27143	1.05039	0.950611	1.01136	1.06418	0.505145
15	0.938	0.8	15	0.938	0.8	5	0.375	30	0.3	1.05319	0.996766	1.00888	1.06321	0.507679
15	0.938	0.8	15	0.938	0.8	5	0.375	30	0.32857	1.05607	1.08318	1.0206	1.07028	0.510437
15	0.938	0.8	15	0.938	0.8	5	0.375	30	0.35714	1.05969	1.00813	1.02465	1.0735	0.514875
15	0.938	0.8	15	0.938	0.8	5	0.375	30	0.38571	1.06214	0.973006	1.02865	1.07562	0.517413
15	0.938	0.8	15	0.938	0.8	5	0.375	30	0.41429	1.06509	0.938831	1.03486	1.07773	0.519846
15	0.938	0.8	15	0.938	0.8	5	0.375	30	0.44286	1.06723	0.917121	1.05419	1.08226	0.523497
15	0.938	0.8	15	0.938	0.8	5	0.375	30	0.47143	1.07134	0.907352	1.06219	1.08444	0.525367
15	0.938	0.8	15	0.938	0.8	5	0.375	30	0.5	1.07538	0.918606	1.06538	1.08749	0.527728
15	0.938	0.8	15	0.938	0.8	5	0.375	30	0.52857	1.07914	0.929885	1.06782	1.09239	0.530543
15	0.938	0.8	15	0.938	0.8	5	0.375	30	0.55714	1.08082	0.914212	1.06125	1.09347	0.532672
15	0.938	0.8	15	0.938	0.8	5	0.375	30	0.58571	1.08448	0.915681	1.06412	1.09749	0.535638
15	0.938	0.8	15	0.938	0.8	5	0.375	30	0.61429	1.08763	0.887578	1.06792	1.10247	0.538742
15	0.938	0.8	15	0.938	0.8	5	0.375	30	0.64286	1.09012	0.868842	1.07062	1.10793	0.542043
15	0.938	0.8	15	0.938	0.8	5	0.375	30	0.67143	1.09208	0.850409	1.08133	1.10873	0.545285
15	0.938	0.8	15	0.938	0.8	5	0.375	30	0.7	1.09401	0.844251	1.08325	1.11362	0.548802
15	0.938	0.8	15	0.938	0.8	5	0.375	30	0.72857	1.09567	0.836064	1.08298	1.11865	0.552278
15	0.938	0.8	15	0.938	0.8	5	0.375	30	0.75714	1.0972	0.83801	1.0825	1.12397	0.555992
15	0.938	0.8	15	0.938	0.8	5	0.375	30	0.78571	1.10037	0.859665	1.0867	1.12463	0.557469

15	0.938	0.8	15	0.938	0.8	1	0.375	30	0.375	1.04395	0.944176	1.02773	1.08163	0.557289
15	0.938	0.8	15	0.938	0.8	1	0.375	30	0.375	1.05675	0.880591	1.02713	1.09072	0.558939
15	0.938	0.8	15	0.938	0.8	1	0.375	30	0.375	1.06258	0.840837	1.0403	1.095	0.558609
15	0.938	0.8	15	0.938	0.8	2	0.375	30	0.375	1.06599	0.832728	1.04595	1.0986	0.558724
15	0.938	0.8	15	0.938	0.8	2	0.375	30	0.375	1.06946	0.850517	1.04556	1.10013	0.555155
15	0.938	0.8	15	0.938	0.8	2	0.375	30	0.375	1.07185	0.882466	1.04366	1.09799	0.552705
15	0.938	0.8	15	0.938	0.8	2	0.375	30	0.375	1.0733	0.910408	1.02586	1.09861	0.551099
15	0.938	0.8	15	0.938	0.8	2	0.375	30	0.375	1.07292	0.919601	1.04971	1.09524	0.546722
15	0.938	0.8	15	0.938	0.8	3	0.375	30	0.375	1.07143	0.913779	1.05861	1.09334	0.545104
15	0.938	0.8	15	0.938	0.8	3	0.375	30	0.375	1.07358	0.900119	1.06107	1.09626	0.540926
15	0.938	0.8	15	0.938	0.8	3	0.375	30	0.375	1.0716	0.889083	1.04507	1.0888	0.536165
15	0.938	0.8	15	0.938	0.8	3	0.375	30	0.375	1.06978	0.905886	1.0151	1.08519	0.533994
15	0.938	0.8	15	0.938	0.8	3	0.375	30	0.375	1.06817	0.917445	1.03043	1.08983	0.530277
15	0.938	0.8	15	0.938	0.8	4	0.375	30	0.375	1.06734	0.946706	1.04268	1.0815	0.527556
15	0.938	0.8	15	0.938	0.8	4	0.375	30	0.375	1.06729	0.974727	1.04317	1.0855	0.524075
15	0.938	0.8	15	0.938	0.8	4	0.375	30	0.375	1.06307	1.0238	1.04189	1.0789	0.520567
15	0.938	0.8	15	0.938	0.8	4	0.375	30	0.375	1.06232	0.971109	1.02921	1.07422	0.518098
15	0.938	0.8	15	0.938	0.8	4	0.375	30	0.375	1.06229	0.942856	0.999394	1.07641	0.516499
15	0.938	0.8	15	0.938	0.8	5	0.375	30	0.375	1.0602	0.940059	1.05645	1.07088	0.513718
15	0.938	0.8	15	0.938	0.8	5	0.375	30	0.375	1.05906	0.963101	1.0626	1.06921	0.512049
15	0.938	0.8	15	0.938	0.8	5	0.375	30	0.375	1.05671	1.0181	1.03146	1.0669	0.509215
15	0.938	0.8	15	0.938	0.8	5	0.375	30	0.375	1.05803	1.01551	1.02078	1.06945	0.508487
15	0.938	0.8	15	0.938	0.8	6	0.375	30	0.375	1.0553	1.02085	1.03347	1.06653	0.507421
15	0.938	0.8	15	0.938	0.8	6	0.375	30	0.375	1.05405	0.971129	1.0468	1.06363	0.507741

## C FINITE ELEMENT TESTING FOR DISTORTIONAL FATIGUE

These are the data for the distortional finite element analysis. The DNV stresses are provided for the relevant hot-spots (always the location of the maximum stress in the model).

### C.1 Plate-Stiffener Finite Element Analysis

<b>bG</b>	<b>tF</b>	<b>tW</b>	<b>bS</b>	<b>tS</b>	<b>aS</b>	<b>aW</b>	<b>dC</b>	<b>hC</b>	<b>bC</b>	<b>tC</b>	<b>aCW</b>	<b>DNV Stres</b>
12.30	0.80	0.50	4.00	0.40	40.00	0.31	3.00	1.00	3.00	0.31	0.19	49.81
12.30	0.80	0.50	4.00	0.40	20.00	0.31	3.00	1.00	3.00	0.31	0.19	20.92
12.30	0.80	0.50	4.00	0.40	25.00	0.31	3.00	1.00	3.00	0.31	0.19	27.06
12.30	0.80	0.50	4.00	0.40	30.00	0.31	3.00	1.00	3.00	0.31	0.19	34.02
12.30	0.80	0.50	4.00	0.40	35.00	0.31	3.00	1.00	3.00	0.31	0.19	41.65
12.30	0.80	0.50	4.00	0.40	45.00	0.31	3.00	1.00	3.00	0.31	0.19	58.42
12.30	0.80	0.50	4.00	0.40	50.00	0.31	3.00	1.00	3.00	0.31	0.19	67.39
12.30	0.80	0.50	4.00	0.40	55.00	0.31	3.00	1.00	3.00	0.31	0.19	76.64
12.30	0.80	0.50	4.00	0.40	60.00	0.31	3.00	1.00	3.00	0.31	0.19	85.53
12.30	0.80	0.50	4.00	0.40	65.00	0.31	3.00	1.00	3.00	0.31	0.19	94.49
12.30	0.80	0.50	4.00	0.40	70.00	0.31	3.00	1.00	3.00	0.31	0.19	103.64
12.30	0.80	0.50	4.00	0.40	20.00	0.31	3.00	2.00	4.00	0.31	0.19	58.49
12.30	0.80	0.50	4.00	0.40	25.00	0.31	3.00	2.00	4.00	0.31	0.19	74.68
12.30	0.80	0.50	4.00	0.40	30.00	0.31	3.00	2.00	4.00	0.31	0.19	91.46
12.30	0.80	0.50	4.00	0.40	35.00	0.31	3.00	2.00	4.00	0.31	0.19	108.71
12.30	0.80	0.50	4.00	0.40	40.00	0.31	3.00	2.00	4.00	0.31	0.19	126.31
12.30	0.80	0.50	4.00	0.40	45.00	0.31	3.00	2.00	4.00	0.31	0.19	144.09
12.30	0.80	0.50	4.00	0.40	50.00	0.31	3.00	2.00	4.00	0.31	0.19	161.90
12.30	0.80	0.50	4.00	0.40	55.00	0.31	3.00	2.00	4.00	0.31	0.19	179.59
12.30	0.80	0.50	4.00	0.40	60.00	0.31	3.00	2.00	4.00	0.31	0.19	196.96
12.30	0.80	0.50	4.00	0.40	65.00	0.31	3.00	2.00	4.00	0.31	0.19	213.94
12.30	0.80	0.50	4.00	0.40	70.00	0.31	3.00	2.00	4.00	0.31	0.19	230.34
12.30	0.80	0.50	4.00	0.40	40.00	0.31	3.00	2.00	4.00	0.31	0.13	151.08
12.30	0.80	0.50	4.00	0.40	40.00	0.31	3.00	2.00	4.00	0.31	0.16	144.66
12.30	0.80	0.50	4.00	0.40	40.00	0.31	3.00	2.00	4.00	0.31	0.22	115.26
12.30	0.80	0.50	4.00	0.40	40.00	0.31	3.00	2.00	4.00	0.31	0.25	115.73



12.30	0.80	0.50	4.00	0.40	40.00	0.31	3.00	2.00	4.00	0.31	0.28	119.21
12.30	0.80	0.50	4.00	0.40	40.00	0.31	3.00	2.00	4.00	0.31	0.31	115.71
12.30	0.80	0.50	4.00	0.40	40.00	0.31	3.00	2.00	4.00	0.31	0.34	102.40
12.30	0.80	0.50	4.00	0.40	40.00	0.31	3.00	2.00	4.00	0.31	0.38	93.74
12.30	0.80	0.50	4.00	0.40	40.00	0.31	3.00	2.00	4.00	0.31	0.41	93.38
12.30	0.80	0.50	4.00	0.40	40.00	0.31	3.00	2.00	4.00	0.31	0.44	96.91
12.30	0.80	0.50	4.00	0.40	40.00	0.31	3.00	2.00	4.00	0.31	0.47	96.50
12.30	0.80	0.50	4.00	0.40	40.00	0.31	3.00	2.00	4.00	0.31	0.50	87.14
12.30	0.80	0.50	4.00	0.40	40.00	0.31	3.00	2.00	4.00	0.31	0.53	78.14
12.30	0.80	0.50	4.00	0.40	40.00	0.31	3.00	2.00	4.00	0.31	0.56	75.69
12.30	0.80	0.50	4.00	0.40	40.00	0.31	3.00	2.00	4.00	0.31	0.59	77.34
12.30	0.80	0.50	4.00	0.40	40.00	0.31	3.00	2.00	4.00	0.31	0.63	77.86
12.30	0.80	0.50	4.00	0.40	40.00	0.31	3.00	2.00	4.00	0.31	0.66	70.21
12.30	0.80	0.50	4.00	0.40	40.00	0.31	3.00	2.00	4.00	0.31	0.69	61.40
12.30	0.80	0.50	4.00	0.40	40.00	0.31	3.00	2.00	4.00	0.31	0.72	58.10
12.30	0.80	0.50	4.00	0.40	40.00	0.31	3.00	2.00	4.00	0.31	0.75	58.54
12.30	0.80	0.50	4.00	0.40	40.00	0.31	3.00	2.00	4.00	0.31	0.78	57.63
12.30	0.80	0.50	4.00	0.40	40.00	0.31	3.00	2.00	4.00	0.31	0.81	51.80
12.30	0.80	0.50	4.00	0.40	40.00	0.31	3.00	2.00	4.00	0.31	0.84	43.35
12.30	0.80	0.50	4.00	0.40	40.00	0.31	3.00	2.00	4.00	0.31	0.88	40.06
12.30	0.80	0.50	4.00	0.40	40.00	0.31	3.00	2.00	4.00	0.31	0.91	40.54
12.30	0.80	0.50	4.00	0.40	40.00	0.31	3.00	2.00	4.00	0.31	0.94	40.30
12.30	0.80	0.50	4.00	0.40	40.00	0.31	3.00	2.00	4.00	0.31	0.97	37.28
12.30	0.80	0.50	4.00	0.40	40.00	0.31	3.00	2.00	4.00	0.31	1.00	29.36
12.30	0.80	0.50	4.00	0.13	40.00	0.31	3.00	2.00	4.00	0.31	0.19	2064.72
12.30	0.80	0.50	4.00	0.16	40.00	0.31	3.00	2.00	4.00	0.31	0.19	1279.01
12.30	0.80	0.50	4.00	0.19	40.00	0.31	3.00	2.00	4.00	0.31	0.19	895.50
12.30	0.80	0.50	4.00	0.22	40.00	0.31	3.00	2.00	4.00	0.31	0.19	623.31
12.30	0.80	0.50	4.00	0.25	40.00	0.31	3.00	2.00	4.00	0.31	0.19	452.30
12.30	0.80	0.50	4.00	0.28	40.00	0.31	3.00	2.00	4.00	0.31	0.19	337.67
12.30	0.80	0.50	4.00	0.31	40.00	0.31	3.00	2.00	4.00	0.31	0.19	257.94
12.30	0.80	0.50	4.00	0.34	40.00	0.31	3.00	2.00	4.00	0.31	0.19	199.86
12.30	0.80	0.50	4.00	0.38	40.00	0.31	3.00	2.00	4.00	0.31	0.19	154.78
12.30	0.80	0.50	4.00	0.41	40.00	0.31	3.00	2.00	4.00	0.31	0.19	119.37
12.30	0.80	0.50	4.00	0.44	40.00	0.31	3.00	2.00	4.00	0.31	0.19	94.96
12.30	0.80	0.50	4.00	0.47	40.00	0.31	3.00	2.00	4.00	0.31	0.19	81.31
12.30	0.80	0.50	4.00	0.50	40.00	0.31	3.00	2.00	4.00	0.31	0.19	68.22
12.30	0.80	0.50	4.00	0.53	40.00	0.31	3.00	2.00	4.00	0.31	0.19	59.19

12.30	0.80	0.50	4.00	0.56	40.00	0.31	3.00	2.00	4.00	0.31	0.19	51.67
12.30	0.80	0.50	4.00	0.59	40.00	0.31	3.00	2.00	4.00	0.31	0.19	45.30
12.30	0.80	0.50	4.00	0.63	40.00	0.31	3.00	2.00	4.00	0.31	0.19	40.17
12.30	0.80	0.50	4.00	0.66	40.00	0.31	3.00	2.00	4.00	0.31	0.19	34.89
12.30	0.80	0.50	4.00	0.69	40.00	0.31	3.00	2.00	4.00	0.31	0.19	31.91
12.30	0.80	0.50	4.00	0.72	40.00	0.31	3.00	2.00	4.00	0.31	0.19	28.13
12.30	0.80	0.50	4.00	0.75	40.00	0.31	3.00	2.00	4.00	0.31	0.19	24.69
12.30	0.80	0.50	4.00	0.78	40.00	0.31	3.00	2.00	4.00	0.31	0.19	22.13
12.30	0.80	0.50	4.00	0.81	40.00	0.31	3.00	2.00	4.00	0.31	0.19	20.13
12.30	0.80	0.50	4.00	0.84	40.00	0.31	3.00	2.00	4.00	0.31	0.19	18.27
12.30	0.80	0.50	4.00	0.88	40.00	0.31	3.00	2.00	4.00	0.31	0.19	16.64
12.30	0.80	0.50	4.00	0.91	40.00	0.31	3.00	2.00	4.00	0.31	0.19	15.19
12.30	0.80	0.50	4.00	0.94	40.00	0.31	3.00	2.00	4.00	0.31	0.19	13.90
12.30	0.80	0.50	4.00	0.97	40.00	0.31	3.00	2.00	4.00	0.31	0.19	12.77
12.30	0.80	0.50	4.00	1.00	40.00	0.31	3.00	2.00	4.00	0.31	0.19	11.70
12.30	0.80	0.50	4.00	0.40	40.00	0.31	3.00	2.00	4.00	0.13	0.19	105.59
12.30	0.80	0.50	4.00	0.40	40.00	0.31	3.00	2.00	4.00	0.16	0.19	115.63
12.30	0.80	0.50	4.00	0.40	40.00	0.31	3.00	2.00	4.00	0.19	0.19	121.36
12.30	0.80	0.50	4.00	0.40	40.00	0.31	3.00	2.00	4.00	0.22	0.19	124.40
12.30	0.80	0.50	4.00	0.40	40.00	0.31	3.00	2.00	4.00	0.25	0.19	125.73
12.30	0.80	0.50	4.00	0.40	40.00	0.31	3.00	2.00	4.00	0.28	0.19	126.20
12.30	0.80	0.50	4.00	0.40	40.00	0.31	3.00	2.00	4.00	0.34	0.19	126.40
12.30	0.80	0.50	4.00	0.40	40.00	0.31	3.00	2.00	4.00	0.38	0.19	126.17
12.30	0.80	0.50	4.00	0.40	40.00	0.31	3.00	2.00	4.00	0.41	0.19	125.92
12.30	0.80	0.50	4.00	0.40	40.00	0.31	3.00	2.00	4.00	0.44	0.19	125.69
12.30	0.80	0.50	4.00	0.40	40.00	0.31	3.00	2.00	4.00	0.47	0.19	125.49
12.30	0.80	0.50	4.00	0.40	40.00	0.31	3.00	2.00	4.00	0.50	0.19	125.35
12.30	0.80	0.50	4.00	0.40	40.00	0.31	3.00	2.00	4.00	0.53	0.19	125.16
12.30	0.80	0.50	4.00	0.40	40.00	0.31	3.00	2.00	4.00	0.56	0.19	124.98
12.30	0.80	0.50	4.00	0.40	40.00	0.31	3.00	2.00	4.00	0.59	0.19	124.83
12.30	0.80	0.50	4.00	0.40	40.00	0.31	3.00	2.00	4.00	0.63	0.19	124.69
12.30	0.80	0.50	4.00	0.40	40.00	0.31	3.00	2.00	4.00	0.66	0.19	124.58
12.30	0.80	0.50	4.00	0.40	40.00	0.31	3.00	2.00	4.00	0.69	0.19	124.45
12.30	0.80	0.50	4.00	0.40	40.00	0.31	3.00	2.00	4.00	0.72	0.19	124.34
12.30	0.80	0.50	4.00	0.40	40.00	0.31	3.00	2.00	4.00	0.75	0.19	124.23
12.30	0.80	0.50	4.00	0.40	40.00	0.31	3.00	2.00	4.00	0.78	0.19	124.13
12.30	0.80	0.50	4.00	0.40	40.00	0.31	3.00	2.00	4.00	0.81	0.19	124.04
12.30	0.80	0.50	4.00	0.40	40.00	0.31	3.00	2.00	4.00	0.84	0.19	123.95

12.30	0.80	0.50	4.00	0.40	40.00	0.31	3.00	2.00	4.00	0.88	0.19	123.86
12.30	0.80	0.50	4.00	0.40	40.00	0.31	3.00	2.00	4.00	0.91	0.19	123.79
12.30	0.80	0.50	4.00	0.40	40.00	0.31	3.00	2.00	4.00	0.94	0.19	123.71
12.30	0.80	0.50	4.00	0.40	40.00	0.31	3.00	2.00	4.00	0.97	0.19	123.64
12.30	0.80	0.50	4.00	0.40	40.00	0.31	3.00	2.00	4.00	1.00	0.19	123.57
12.30	0.80	0.50	4.00	0.40	1.00	0.31	3.00	2.00	4.00	0.31	0.19	4.31
12.30	0.80	0.50	4.00	0.40	15.00	0.31	3.00	2.00	4.00	0.31	0.19	35.56
12.30	0.80	0.50	4.00	0.20	5.00	0.31	3.00	1.00	4.00	0.10	0.06	82.02
12.30	0.80	0.50	4.00	0.20	5.00	0.31	3.00	1.00	4.00	0.10	0.13	28.74
12.30	0.80	0.50	4.00	0.20	5.00	0.31	3.00	1.00	4.00	0.10	0.19	9.59
12.30	0.80	0.50	4.00	0.20	5.00	0.31	3.00	1.00	4.00	0.10	0.25	5.00
12.30	0.80	0.50	4.00	0.20	5.00	0.31	3.00	1.00	4.00	0.20	0.06	71.03
12.30	0.80	0.50	4.00	0.20	5.00	0.31	3.00	1.00	4.00	0.20	0.13	42.14
12.30	0.80	0.50	4.00	0.20	5.00	0.31	3.00	1.00	4.00	0.20	0.19	25.20
12.30	0.80	0.50	4.00	0.20	5.00	0.31	3.00	1.00	4.00	0.20	0.25	8.12
12.30	0.80	0.50	4.00	0.20	5.00	0.31	3.00	1.00	4.00	0.30	0.06	64.43
12.30	0.80	0.50	4.00	0.20	5.00	0.31	3.00	1.00	4.00	0.30	0.13	42.78
12.30	0.80	0.50	4.00	0.20	5.00	0.31	3.00	1.00	4.00	0.30	0.19	30.10
12.30	0.80	0.50	4.00	0.20	5.00	0.31	3.00	1.00	4.00	0.30	0.25	12.31
12.30	0.80	0.50	4.00	0.20	5.00	0.31	3.00	1.00	4.00	0.40	0.06	58.90
12.30	0.80	0.50	4.00	0.20	5.00	0.31	3.00	1.00	4.00	0.40	0.13	41.13
12.30	0.80	0.50	4.00	0.20	5.00	0.31	3.00	1.00	4.00	0.40	0.19	30.71
12.30	0.80	0.50	4.00	0.20	5.00	0.31	3.00	1.00	4.00	0.40	0.25	14.31
12.30	0.80	0.50	4.00	0.20	5.00	0.31	3.00	1.00	4.00	0.50	0.06	54.78
12.30	0.80	0.50	4.00	0.20	5.00	0.31	3.00	1.00	4.00	0.50	0.13	39.27
12.30	0.80	0.50	4.00	0.20	5.00	0.31	3.00	1.00	4.00	0.50	0.19	30.04
12.30	0.80	0.50	4.00	0.20	5.00	0.31	3.00	1.00	4.00	0.50	0.25	14.80
12.30	0.80	0.50	4.00	0.20	5.00	0.31	3.00	1.00	4.00	0.60	0.06	52.01
12.30	0.80	0.50	4.00	0.20	5.00	0.31	3.00	1.00	4.00	0.60	0.13	37.63
12.30	0.80	0.50	4.00	0.20	5.00	0.31	3.00	1.00	4.00	0.60	0.19	29.03
12.30	0.80	0.50	4.00	0.20	5.00	0.31	3.00	1.00	4.00	0.60	0.25	14.65
12.30	0.80	0.50	4.00	0.20	5.00	0.31	3.00	1.00	4.00	0.70	0.06	49.76
12.30	0.80	0.50	4.00	0.20	5.00	0.31	3.00	1.00	4.00	0.70	0.13	36.39
12.30	0.80	0.50	4.00	0.20	5.00	0.31	3.00	1.00	4.00	0.70	0.19	28.25
12.30	0.80	0.50	4.00	0.20	5.00	0.31	3.00	1.00	4.00	0.70	0.25	14.39
12.30	0.80	0.50	4.00	0.30	5.00	0.31	3.00	1.00	4.00	0.10	0.06	30.97
12.30	0.80	0.50	4.00	0.30	5.00	0.31	3.00	1.00	4.00	0.10	0.13	10.75
12.30	0.80	0.50	4.00	0.30	5.00	0.31	3.00	1.00	4.00	0.10	0.19	4.26

12.30	0.80	0.50	4.00	0.30	5.00	0.31	3.00	1.00	4.00	0.10	0.25	2.62
12.30	0.80	0.50	4.00	0.30	5.00	0.31	3.00	1.00	4.00	0.20	0.06	26.20
12.30	0.80	0.50	4.00	0.30	5.00	0.31	3.00	1.00	4.00	0.20	0.13	16.83
12.30	0.80	0.50	4.00	0.30	5.00	0.31	3.00	1.00	4.00	0.20	0.19	7.22
12.30	0.80	0.50	4.00	0.30	5.00	0.31	3.00	1.00	4.00	0.20	0.25	2.92
12.30	0.80	0.50	4.00	0.30	5.00	0.31	3.00	1.00	4.00	0.30	0.06	22.58
12.30	0.80	0.50	4.00	0.30	5.00	0.31	3.00	1.00	4.00	0.30	0.13	16.02
12.30	0.80	0.50	4.00	0.30	5.00	0.31	3.00	1.00	4.00	0.30	0.19	8.84
12.30	0.80	0.50	4.00	0.30	5.00	0.31	3.00	1.00	4.00	0.30	0.25	4.65
12.30	0.80	0.50	4.00	0.30	5.00	0.31	3.00	1.00	4.00	0.40	0.06	20.05
12.30	0.80	0.50	4.00	0.30	5.00	0.31	3.00	1.00	4.00	0.40	0.13	14.78
12.30	0.80	0.50	4.00	0.30	5.00	0.31	3.00	1.00	4.00	0.40	0.19	8.94
12.30	0.80	0.50	4.00	0.30	5.00	0.31	3.00	1.00	4.00	0.40	0.25	5.38
12.30	0.80	0.50	4.00	0.30	5.00	0.31	3.00	1.00	4.00	0.50	0.06	18.36
12.30	0.80	0.50	4.00	0.30	5.00	0.31	3.00	1.00	4.00	0.50	0.13	13.73
12.30	0.80	0.50	4.00	0.30	5.00	0.31	3.00	1.00	4.00	0.50	0.19	8.60
12.30	0.80	0.50	4.00	0.30	5.00	0.31	3.00	1.00	4.00	0.50	0.25	5.44
12.30	0.80	0.50	4.00	0.30	5.00	0.31	3.00	1.00	4.00	0.60	0.06	17.31
12.30	0.80	0.50	4.00	0.30	5.00	0.31	3.00	1.00	4.00	0.60	0.13	12.89
12.30	0.80	0.50	4.00	0.30	5.00	0.31	3.00	1.00	4.00	0.60	0.19	8.11
12.30	0.80	0.50	4.00	0.30	5.00	0.31	3.00	1.00	4.00	0.60	0.25	5.22
12.30	0.80	0.50	4.00	0.30	5.00	0.31	3.00	1.00	4.00	0.70	0.06	16.44
12.30	0.80	0.50	4.00	0.30	5.00	0.31	3.00	1.00	4.00	0.70	0.13	12.24
12.30	0.80	0.50	4.00	0.30	5.00	0.31	3.00	1.00	4.00	0.70	0.19	7.73
12.30	0.80	0.50	4.00	0.30	5.00	0.31	3.00	1.00	4.00	0.70	0.25	4.99
12.30	0.80	0.50	4.00	0.40	5.00	0.31	3.00	1.00	4.00	0.10	0.06	27.67
12.30	0.80	0.50	4.00	0.40	5.00	0.31	3.00	1.00	4.00	0.10	0.13	8.93
12.30	0.80	0.50	4.00	0.40	5.00	0.31	3.00	1.00	4.00	0.10	0.19	4.70
12.30	0.80	0.50	4.00	0.40	5.00	0.31	3.00	1.00	4.00	0.10	0.25	2.35
12.30	0.80	0.50	4.00	0.40	5.00	0.31	3.00	1.00	4.00	0.20	0.06	21.98
12.30	0.80	0.50	4.00	0.40	5.00	0.31	3.00	1.00	4.00	0.20	0.13	11.84
12.30	0.80	0.50	4.00	0.40	5.00	0.31	3.00	1.00	4.00	0.20	0.19	7.67
12.30	0.80	0.50	4.00	0.40	5.00	0.31	3.00	1.00	4.00	0.20	0.25	3.92
12.30	0.80	0.50	4.00	0.40	5.00	0.31	3.00	1.00	4.00	0.30	0.06	18.10
12.30	0.80	0.50	4.00	0.40	5.00	0.31	3.00	1.00	4.00	0.30	0.13	10.62
12.30	0.80	0.50	4.00	0.40	5.00	0.31	3.00	1.00	4.00	0.30	0.19	8.00
12.30	0.80	0.50	4.00	0.40	5.00	0.31	3.00	1.00	4.00	0.30	0.25	4.86
12.30	0.80	0.50	4.00	0.40	5.00	0.31	3.00	1.00	4.00	0.40	0.06	15.63

12.30	0.80	0.50	4.00	0.40	5.00	0.31	3.00	1.00	4.00	0.40	0.13	9.35
12.30	0.80	0.50	4.00	0.40	5.00	0.31	3.00	1.00	4.00	0.40	0.19	7.53
12.30	0.80	0.50	4.00	0.40	5.00	0.31	3.00	1.00	4.00	0.40	0.25	4.98
12.30	0.80	0.50	4.00	0.40	5.00	0.31	3.00	1.00	4.00	0.50	0.06	14.05
12.30	0.80	0.50	4.00	0.40	5.00	0.31	3.00	1.00	4.00	0.50	0.13	8.45
12.30	0.80	0.50	4.00	0.40	5.00	0.31	3.00	1.00	4.00	0.50	0.19	6.99
12.30	0.80	0.50	4.00	0.40	5.00	0.31	3.00	1.00	4.00	0.50	0.25	4.81
12.30	0.80	0.50	4.00	0.40	5.00	0.31	3.00	1.00	4.00	0.60	0.06	13.07
12.30	0.80	0.50	4.00	0.40	5.00	0.31	3.00	1.00	4.00	0.60	0.13	7.82
12.30	0.80	0.50	4.00	0.40	5.00	0.31	3.00	1.00	4.00	0.60	0.19	6.50
12.30	0.80	0.50	4.00	0.40	5.00	0.31	3.00	1.00	4.00	0.60	0.25	4.57
12.30	0.80	0.50	4.00	0.40	5.00	0.31	3.00	1.00	4.00	0.70	0.06	12.28
12.30	0.80	0.50	4.00	0.40	5.00	0.31	3.00	1.00	4.00	0.70	0.13	7.35
12.30	0.80	0.50	4.00	0.40	5.00	0.31	3.00	1.00	4.00	0.70	0.19	6.15
12.30	0.80	0.50	4.00	0.40	5.00	0.31	3.00	1.00	4.00	0.70	0.25	4.36
12.30	0.80	0.50	4.00	0.50	5.00	0.31	3.00	1.00	4.00	0.10	0.06	15.44
12.30	0.80	0.50	4.00	0.50	5.00	0.31	3.00	1.00	4.00	0.10	0.13	7.25
12.30	0.80	0.50	4.00	0.50	5.00	0.31	3.00	1.00	4.00	0.10	0.19	4.23
12.30	0.80	0.50	4.00	0.50	5.00	0.31	3.00	1.00	4.00	0.10	0.25	3.99
12.30	0.80	0.50	4.00	0.50	5.00	0.31	3.00	1.00	4.00	0.20	0.06	11.83
12.30	0.80	0.50	4.00	0.50	5.00	0.31	3.00	1.00	4.00	0.20	0.13	8.56
12.30	0.80	0.50	4.00	0.50	5.00	0.31	3.00	1.00	4.00	0.20	0.19	5.89
12.30	0.80	0.50	4.00	0.50	5.00	0.31	3.00	1.00	4.00	0.20	0.25	5.03
12.30	0.80	0.50	4.00	0.50	5.00	0.31	3.00	1.00	4.00	0.30	0.06	9.40
12.30	0.80	0.50	4.00	0.50	5.00	0.31	3.00	1.00	4.00	0.30	0.13	7.42
12.30	0.80	0.50	4.00	0.50	5.00	0.31	3.00	1.00	4.00	0.30	0.19	5.80
12.30	0.80	0.50	4.00	0.50	5.00	0.31	3.00	1.00	4.00	0.30	0.25	5.38
12.30	0.80	0.50	4.00	0.50	5.00	0.31	3.00	1.00	4.00	0.40	0.06	7.93
12.30	0.80	0.50	4.00	0.50	5.00	0.31	3.00	1.00	4.00	0.40	0.13	6.45
12.30	0.80	0.50	4.00	0.50	5.00	0.31	3.00	1.00	4.00	0.40	0.19	5.29
12.30	0.80	0.50	4.00	0.50	5.00	0.31	3.00	1.00	4.00	0.40	0.25	5.26
12.30	0.80	0.50	4.00	0.50	5.00	0.31	3.00	1.00	4.00	0.50	0.06	7.03
12.30	0.80	0.50	4.00	0.50	5.00	0.31	3.00	1.00	4.00	0.50	0.13	5.80
12.30	0.80	0.50	4.00	0.50	5.00	0.31	3.00	1.00	4.00	0.50	0.19	4.83
12.30	0.80	0.50	4.00	0.50	5.00	0.31	3.00	1.00	4.00	0.50	0.25	5.03
12.30	0.80	0.50	4.00	0.50	5.00	0.31	3.00	1.00	4.00	0.60	0.06	6.49
12.30	0.80	0.50	4.00	0.50	5.00	0.31	3.00	1.00	4.00	0.60	0.13	5.36
12.30	0.80	0.50	4.00	0.50	5.00	0.31	3.00	1.00	4.00	0.60	0.19	4.46

12.30	0.80	0.50	4.00	0.50	5.00	0.31	3.00	1.00	4.00	0.60	0.25	4.80
12.30	0.80	0.50	4.00	0.50	5.00	0.31	3.00	1.00	4.00	0.70	0.06	6.08
12.30	0.80	0.50	4.00	0.50	5.00	0.31	3.00	1.00	4.00	0.70	0.13	5.05
12.30	0.80	0.50	4.00	0.50	5.00	0.31	3.00	1.00	4.00	0.70	0.19	4.19
12.30	0.80	0.50	4.00	0.50	5.00	0.31	3.00	1.00	4.00	0.70	0.25	4.62
12.30	0.80	0.50	4.00	0.60	5.00	0.31	3.00	1.00	4.00	0.10	0.06	9.38
12.30	0.80	0.50	4.00	0.60	5.00	0.31	3.00	1.00	4.00	0.10	0.13	6.19
12.30	0.80	0.50	4.00	0.60	5.00	0.31	3.00	1.00	4.00	0.10	0.19	4.49
12.30	0.80	0.50	4.00	0.60	5.00	0.31	3.00	1.00	4.00	0.10	0.25	3.73
12.30	0.80	0.50	4.00	0.60	5.00	0.31	3.00	1.00	4.00	0.20	0.06	6.78
12.30	0.80	0.50	4.00	0.60	5.00	0.31	3.00	1.00	4.00	0.20	0.13	7.04
12.30	0.80	0.50	4.00	0.60	5.00	0.31	3.00	1.00	4.00	0.20	0.19	5.41
12.30	0.80	0.50	4.00	0.60	5.00	0.31	3.00	1.00	4.00	0.20	0.25	4.46
12.30	0.80	0.50	4.00	0.60	5.00	0.31	3.00	1.00	4.00	0.30	0.06	5.00
12.30	0.80	0.50	4.00	0.60	5.00	0.31	3.00	1.00	4.00	0.30	0.13	6.13
12.30	0.80	0.50	4.00	0.60	5.00	0.31	3.00	1.00	4.00	0.30	0.19	5.22
12.30	0.80	0.50	4.00	0.60	5.00	0.31	3.00	1.00	4.00	0.30	0.25	4.64
12.30	0.80	0.50	4.00	0.60	5.00	0.31	3.00	1.00	4.00	0.40	0.06	3.96
12.30	0.80	0.50	4.00	0.60	5.00	0.31	3.00	1.00	4.00	0.40	0.13	5.39
12.30	0.80	0.50	4.00	0.60	5.00	0.31	3.00	1.00	4.00	0.40	0.19	4.81
12.30	0.80	0.50	4.00	0.60	5.00	0.31	3.00	1.00	4.00	0.40	0.25	4.48
12.30	0.80	0.50	4.00	0.60	5.00	0.31	3.00	1.00	4.00	0.50	0.06	3.33
12.30	0.80	0.50	4.00	0.60	5.00	0.31	3.00	1.00	4.00	0.50	0.13	4.90
12.30	0.80	0.50	4.00	0.60	5.00	0.31	3.00	1.00	4.00	0.50	0.19	4.47
12.30	0.80	0.50	4.00	0.60	5.00	0.31	3.00	1.00	4.00	0.50	0.25	4.27
12.30	0.80	0.50	4.00	0.60	5.00	0.31	3.00	1.00	4.00	0.60	0.06	2.96
12.30	0.80	0.50	4.00	0.60	5.00	0.31	3.00	1.00	4.00	0.60	0.13	4.57
12.30	0.80	0.50	4.00	0.60	5.00	0.31	3.00	1.00	4.00	0.60	0.19	4.21
12.30	0.80	0.50	4.00	0.60	5.00	0.31	3.00	1.00	4.00	0.60	0.25	4.08
12.30	0.80	0.50	4.00	0.60	5.00	0.31	3.00	1.00	4.00	0.70	0.06	2.70
12.30	0.80	0.50	4.00	0.60	5.00	0.31	3.00	1.00	4.00	0.70	0.13	4.34
12.30	0.80	0.50	4.00	0.60	5.00	0.31	3.00	1.00	4.00	0.70	0.19	4.02
12.30	0.80	0.50	4.00	0.60	5.00	0.31	3.00	1.00	4.00	0.70	0.25	3.93
12.30	0.80	0.50	4.00	0.70	5.00	0.31	3.00	1.00	4.00	0.10	0.06	7.88
12.30	0.80	0.50	4.00	0.70	5.00	0.31	3.00	1.00	4.00	0.10	0.13	4.60
12.30	0.80	0.50	4.00	0.70	5.00	0.31	3.00	1.00	4.00	0.10	0.19	3.88
12.30	0.80	0.50	4.00	0.70	5.00	0.31	3.00	1.00	4.00	0.10	0.25	3.25
12.30	0.80	0.50	4.00	0.70	5.00	0.31	3.00	1.00	4.00	0.20	0.06	6.03

12.30	0.80	0.50	4.00	0.70	5.00	0.31	3.00	1.00	4.00	0.20	0.13	5.01
12.30	0.80	0.50	4.00	0.70	5.00	0.31	3.00	1.00	4.00	0.20	0.19	4.43
12.30	0.80	0.50	4.00	0.70	5.00	0.31	3.00	1.00	4.00	0.20	0.25	3.66
12.30	0.80	0.50	4.00	0.70	5.00	0.31	3.00	1.00	4.00	0.30	0.06	4.77
12.30	0.80	0.50	4.00	0.70	5.00	0.31	3.00	1.00	4.00	0.30	0.13	4.33
12.30	0.80	0.50	4.00	0.70	5.00	0.31	3.00	1.00	4.00	0.30	0.19	4.20
12.30	0.80	0.50	4.00	0.70	5.00	0.31	3.00	1.00	4.00	0.30	0.25	3.69
12.30	0.80	0.50	4.00	0.70	5.00	0.31	3.00	1.00	4.00	0.40	0.06	4.06
12.30	0.80	0.50	4.00	0.70	5.00	0.31	3.00	1.00	4.00	0.40	0.13	3.81
12.30	0.80	0.50	4.00	0.70	5.00	0.31	3.00	1.00	4.00	0.40	0.19	3.86
12.30	0.80	0.50	4.00	0.70	5.00	0.31	3.00	1.00	4.00	0.40	0.25	3.53
12.30	0.80	0.50	4.00	0.70	5.00	0.31	3.00	1.00	4.00	0.50	0.06	3.64
12.30	0.80	0.50	4.00	0.70	5.00	0.31	3.00	1.00	4.00	0.50	0.13	3.47
12.30	0.80	0.50	4.00	0.70	5.00	0.31	3.00	1.00	4.00	0.50	0.19	3.59
12.30	0.80	0.50	4.00	0.70	5.00	0.31	3.00	1.00	4.00	0.50	0.25	3.35
12.30	0.80	0.50	4.00	0.70	5.00	0.31	3.00	1.00	4.00	0.60	0.06	3.40
12.30	0.80	0.50	4.00	0.70	5.00	0.31	3.00	1.00	4.00	0.60	0.13	3.26
12.30	0.80	0.50	4.00	0.70	5.00	0.31	3.00	1.00	4.00	0.60	0.19	3.39
12.30	0.80	0.50	4.00	0.70	5.00	0.31	3.00	1.00	4.00	0.60	0.25	3.21
12.30	0.80	0.50	4.00	0.70	5.00	0.31	3.00	1.00	4.00	0.70	0.06	3.22
12.30	0.80	0.50	4.00	0.70	5.00	0.31	3.00	1.00	4.00	0.70	0.13	3.10
12.30	0.80	0.50	4.00	0.70	5.00	0.31	3.00	1.00	4.00	0.70	0.19	3.24
12.30	0.80	0.50	4.00	0.70	5.00	0.31	3.00	1.00	4.00	0.70	0.25	3.09
12.30	0.80	0.50	4.00	0.80	5.00	0.31	3.00	1.00	4.00	0.10	0.06	5.47
12.30	0.80	0.50	4.00	0.80	5.00	0.31	3.00	1.00	4.00	0.10	0.13	3.55
12.30	0.80	0.50	4.00	0.80	5.00	0.31	3.00	1.00	4.00	0.10	0.19	2.70
12.30	0.80	0.50	4.00	0.80	5.00	0.31	3.00	1.00	4.00	0.10	0.25	1.79
12.30	0.80	0.50	4.00	0.80	5.00	0.31	3.00	1.00	4.00	0.20	0.06	4.13
12.30	0.80	0.50	4.00	0.80	5.00	0.31	3.00	1.00	4.00	0.20	0.13	3.79
12.30	0.80	0.50	4.00	0.80	5.00	0.31	3.00	1.00	4.00	0.20	0.19	3.05
12.30	0.80	0.50	4.00	0.80	5.00	0.31	3.00	1.00	4.00	0.20	0.25	2.09
12.30	0.80	0.50	4.00	0.80	5.00	0.31	3.00	1.00	4.00	0.30	0.06	3.24
12.30	0.80	0.50	4.00	0.80	5.00	0.31	3.00	1.00	4.00	0.30	0.13	3.24
12.30	0.80	0.50	4.00	0.80	5.00	0.31	3.00	1.00	4.00	0.30	0.19	2.84
12.30	0.80	0.50	4.00	0.80	5.00	0.31	3.00	1.00	4.00	0.30	0.25	2.10
12.30	0.80	0.50	4.00	0.80	5.00	0.31	3.00	1.00	4.00	0.40	0.06	2.75
12.30	0.80	0.50	4.00	0.80	5.00	0.31	3.00	1.00	4.00	0.40	0.13	2.82
12.30	0.80	0.50	4.00	0.80	5.00	0.31	3.00	1.00	4.00	0.40	0.19	2.56

12.30	0.80	0.50	4.00	0.80	5.00	0.31	3.00	1.00	4.00	0.40	0.25	1.96
12.30	0.80	0.50	4.00	0.80	5.00	0.31	3.00	1.00	4.00	0.50	0.06	2.47
12.30	0.80	0.50	4.00	0.80	5.00	0.31	3.00	1.00	4.00	0.50	0.13	2.56
12.30	0.80	0.50	4.00	0.80	5.00	0.31	3.00	1.00	4.00	0.50	0.19	2.35
12.30	0.80	0.50	4.00	0.80	5.00	0.31	3.00	1.00	4.00	0.50	0.25	1.81
12.30	0.80	0.50	4.00	0.80	5.00	0.31	3.00	1.00	4.00	0.60	0.06	2.30
12.30	0.80	0.50	4.00	0.80	5.00	0.31	3.00	1.00	4.00	0.60	0.13	2.40
12.30	0.80	0.50	4.00	0.80	5.00	0.31	3.00	1.00	4.00	0.60	0.19	2.20
12.30	0.80	0.50	4.00	0.80	5.00	0.31	3.00	1.00	4.00	0.60	0.25	1.69
12.30	0.80	0.50	4.00	0.80	5.00	0.31	3.00	1.00	4.00	0.70	0.06	2.19
12.30	0.80	0.50	4.00	0.80	5.00	0.31	3.00	1.00	4.00	0.70	0.13	2.28
12.30	0.80	0.50	4.00	0.80	5.00	0.31	3.00	1.00	4.00	0.70	0.19	2.09
12.30	0.80	0.50	4.00	0.80	5.00	0.31	3.00	1.00	4.00	0.70	0.25	1.60
12.30	0.80	0.50	4.00	0.20	10.00	0.31	3.00	1.00	4.00	0.10	0.06	122.78
12.30	0.80	0.50	4.00	0.20	10.00	0.31	3.00	1.00	4.00	0.10	0.13	57.15
12.30	0.80	0.50	4.00	0.20	10.00	0.31	3.00	1.00	4.00	0.10	0.19	27.49
12.30	0.80	0.50	4.00	0.20	10.00	0.31	3.00	1.00	4.00	0.10	0.25	12.87
12.30	0.80	0.50	4.00	0.20	10.00	0.31	3.00	1.00	4.00	0.20	0.06	118.64
12.30	0.80	0.50	4.00	0.20	10.00	0.31	3.00	1.00	4.00	0.20	0.13	82.81
12.30	0.80	0.50	4.00	0.20	10.00	0.31	3.00	1.00	4.00	0.20	0.19	58.54
12.30	0.80	0.50	4.00	0.20	10.00	0.31	3.00	1.00	4.00	0.20	0.25	26.47
12.30	0.80	0.50	4.00	0.20	10.00	0.31	3.00	1.00	4.00	0.30	0.06	113.68
12.30	0.80	0.50	4.00	0.20	10.00	0.31	3.00	1.00	4.00	0.30	0.13	87.14
12.30	0.80	0.50	4.00	0.20	10.00	0.31	3.00	1.00	4.00	0.30	0.19	69.44
12.30	0.80	0.50	4.00	0.20	10.00	0.31	3.00	1.00	4.00	0.30	0.25	37.36
12.30	0.80	0.50	4.00	0.20	10.00	0.31	3.00	1.00	4.00	0.40	0.06	107.30
12.30	0.80	0.50	4.00	0.20	10.00	0.31	3.00	1.00	4.00	0.40	0.13	86.12
12.30	0.80	0.50	4.00	0.20	10.00	0.31	3.00	1.00	4.00	0.40	0.19	72.02
12.30	0.80	0.50	4.00	0.20	10.00	0.31	3.00	1.00	4.00	0.40	0.25	42.12
12.30	0.80	0.50	4.00	0.20	10.00	0.31	3.00	1.00	4.00	0.50	0.06	102.04
12.30	0.80	0.50	4.00	0.20	10.00	0.31	3.00	1.00	4.00	0.50	0.13	84.06
12.30	0.80	0.50	4.00	0.20	10.00	0.31	3.00	1.00	4.00	0.50	0.19	71.82
12.30	0.80	0.50	4.00	0.20	10.00	0.31	3.00	1.00	4.00	0.50	0.25	43.66
12.30	0.80	0.50	4.00	0.20	10.00	0.31	3.00	1.00	4.00	0.60	0.06	98.42
12.30	0.80	0.50	4.00	0.20	10.00	0.31	3.00	1.00	4.00	0.60	0.13	82.07
12.30	0.80	0.50	4.00	0.20	10.00	0.31	3.00	1.00	4.00	0.60	0.19	70.82
12.30	0.80	0.50	4.00	0.20	10.00	0.31	3.00	1.00	4.00	0.60	0.25	43.86
12.30	0.80	0.50	4.00	0.20	10.00	0.31	3.00	1.00	4.00	0.70	0.06	95.43



12.30	0.80	0.50	4.00	0.20	10.00	0.31	3.00	1.00	4.00	0.70	0.13	80.52
12.30	0.80	0.50	4.00	0.20	10.00	0.31	3.00	1.00	4.00	0.70	0.19	69.94
12.30	0.80	0.50	4.00	0.20	10.00	0.31	3.00	1.00	4.00	0.70	0.25	43.71
12.30	0.80	0.50	4.00	0.30	10.00	0.31	3.00	1.00	4.00	0.10	0.06	42.49
12.30	0.80	0.50	4.00	0.30	10.00	0.31	3.00	1.00	4.00	0.10	0.13	8.41
12.30	0.80	0.50	4.00	0.30	10.00	0.31	3.00	1.00	4.00	0.10	0.19	6.44
12.30	0.80	0.50	4.00	0.30	10.00	0.31	3.00	1.00	4.00	0.10	0.25	3.56
12.30	0.80	0.50	4.00	0.30	10.00	0.31	3.00	1.00	4.00	0.20	0.06	38.62
12.30	0.80	0.50	4.00	0.30	10.00	0.31	3.00	1.00	4.00	0.20	0.13	23.62
12.30	0.80	0.50	4.00	0.30	10.00	0.31	3.00	1.00	4.00	0.20	0.19	7.75
12.30	0.80	0.50	4.00	0.30	10.00	0.31	3.00	1.00	4.00	0.20	0.25	2.88
12.30	0.80	0.50	4.00	0.30	10.00	0.31	3.00	1.00	4.00	0.30	0.06	35.29
12.30	0.80	0.50	4.00	0.30	10.00	0.31	3.00	1.00	4.00	0.30	0.13	25.30
12.30	0.80	0.50	4.00	0.30	10.00	0.31	3.00	1.00	4.00	0.30	0.19	12.92
12.30	0.80	0.50	4.00	0.30	10.00	0.31	3.00	1.00	4.00	0.30	0.25	5.42
12.30	0.80	0.50	4.00	0.30	10.00	0.31	3.00	1.00	4.00	0.40	0.06	33.22
12.30	0.80	0.50	4.00	0.30	10.00	0.31	3.00	1.00	4.00	0.40	0.13	25.25
12.30	0.80	0.50	4.00	0.30	10.00	0.31	3.00	1.00	4.00	0.40	0.19	14.90
12.30	0.80	0.50	4.00	0.30	10.00	0.31	3.00	1.00	4.00	0.40	0.25	7.64
12.30	0.80	0.50	4.00	0.30	10.00	0.31	3.00	1.00	4.00	0.50	0.06	31.89
12.30	0.80	0.50	4.00	0.30	10.00	0.31	3.00	1.00	4.00	0.50	0.13	24.82
12.30	0.80	0.50	4.00	0.30	10.00	0.31	3.00	1.00	4.00	0.50	0.19	15.53
12.30	0.80	0.50	4.00	0.30	10.00	0.31	3.00	1.00	4.00	0.50	0.25	8.65
12.30	0.80	0.50	4.00	0.30	10.00	0.31	3.00	1.00	4.00	0.60	0.06	31.12
12.30	0.80	0.50	4.00	0.30	10.00	0.31	3.00	1.00	4.00	0.60	0.13	24.29
12.30	0.80	0.50	4.00	0.30	10.00	0.31	3.00	1.00	4.00	0.60	0.19	15.54
12.30	0.80	0.50	4.00	0.30	10.00	0.31	3.00	1.00	4.00	0.60	0.25	8.97
12.30	0.80	0.50	4.00	0.30	10.00	0.31	3.00	1.00	4.00	0.70	0.06	30.32
12.30	0.80	0.50	4.00	0.30	10.00	0.31	3.00	1.00	4.00	0.70	0.13	23.77
12.30	0.80	0.50	4.00	0.30	10.00	0.31	3.00	1.00	4.00	0.70	0.19	15.44
12.30	0.80	0.50	4.00	0.30	10.00	0.31	3.00	1.00	4.00	0.70	0.25	9.07
12.30	0.80	0.50	4.00	0.40	10.00	0.31	3.00	1.00	4.00	0.10	0.06	37.23
12.30	0.80	0.50	4.00	0.40	10.00	0.31	3.00	1.00	4.00	0.10	0.13	5.98
12.30	0.80	0.50	4.00	0.40	10.00	0.31	3.00	1.00	4.00	0.10	0.19	1.39
12.30	0.80	0.50	4.00	0.40	10.00	0.31	3.00	1.00	4.00	0.20	0.06	29.92
12.30	0.80	0.50	4.00	0.40	10.00	0.31	3.00	1.00	4.00	0.20	0.13	12.73
12.30	0.80	0.50	4.00	0.40	10.00	0.31	3.00	1.00	4.00	0.20	0.19	5.45
12.30	0.80	0.50	4.00	0.40	10.00	0.31	3.00	1.00	4.00	0.20	0.25	1.06

12.30	0.80	0.50	4.00	0.40	10.00	0.31	3.00	1.00	4.00	0.30	0.06	24.64
12.30	0.80	0.50	4.00	0.40	10.00	0.31	3.00	1.00	4.00	0.30	0.13	12.13
12.30	0.80	0.50	4.00	0.40	10.00	0.31	3.00	1.00	4.00	0.30	0.19	7.40
12.30	0.80	0.50	4.00	0.40	10.00	0.31	3.00	1.00	4.00	0.30	0.25	2.13
12.30	0.80	0.50	4.00	0.40	10.00	0.31	3.00	1.00	4.00	0.40	0.06	21.61
12.30	0.80	0.50	4.00	0.40	10.00	0.31	3.00	1.00	4.00	0.40	0.13	11.21
12.30	0.80	0.50	4.00	0.40	10.00	0.31	3.00	1.00	4.00	0.40	0.19	7.65
12.30	0.80	0.50	4.00	0.40	10.00	0.31	3.00	1.00	4.00	0.40	0.25	2.84
12.30	0.80	0.50	4.00	0.40	10.00	0.31	3.00	1.00	4.00	0.50	0.06	19.88
12.30	0.80	0.50	4.00	0.40	10.00	0.31	3.00	1.00	4.00	0.50	0.13	10.58
12.30	0.80	0.50	4.00	0.40	10.00	0.31	3.00	1.00	4.00	0.50	0.19	7.51
12.30	0.80	0.50	4.00	0.40	10.00	0.31	3.00	1.00	4.00	0.50	0.25	3.11
12.30	0.80	0.50	4.00	0.40	10.00	0.31	3.00	1.00	4.00	0.60	0.06	18.97
12.30	0.80	0.50	4.00	0.40	10.00	0.31	3.00	1.00	4.00	0.60	0.13	10.14
12.30	0.80	0.50	4.00	0.40	10.00	0.31	3.00	1.00	4.00	0.60	0.19	7.25
12.30	0.80	0.50	4.00	0.40	10.00	0.31	3.00	1.00	4.00	0.60	0.25	3.18
12.30	0.80	0.50	4.00	0.40	10.00	0.31	3.00	1.00	4.00	0.70	0.06	18.19
12.30	0.80	0.50	4.00	0.40	10.00	0.31	3.00	1.00	4.00	0.70	0.13	9.79
12.30	0.80	0.50	4.00	0.40	10.00	0.31	3.00	1.00	4.00	0.70	0.19	7.05
12.30	0.80	0.50	4.00	0.40	10.00	0.31	3.00	1.00	4.00	0.70	0.25	3.19
12.30	0.80	0.50	4.00	0.50	10.00	0.31	3.00	1.00	4.00	0.10	0.06	18.19
12.30	0.80	0.50	4.00	0.50	10.00	0.31	3.00	1.00	4.00	0.10	0.13	4.63
12.30	0.80	0.50	4.00	0.50	10.00	0.31	3.00	1.00	4.00	0.10	0.25	1.12
12.30	0.80	0.50	4.00	0.50	10.00	0.31	3.00	1.00	4.00	0.20	0.06	13.97
12.30	0.80	0.50	4.00	0.50	10.00	0.31	3.00	1.00	4.00	0.20	0.13	7.70
12.30	0.80	0.50	4.00	0.50	10.00	0.31	3.00	1.00	4.00	0.20	0.19	3.35
12.30	0.80	0.50	4.00	0.50	10.00	0.31	3.00	1.00	4.00	0.20	0.25	1.25
12.30	0.80	0.50	4.00	0.50	10.00	0.31	3.00	1.00	4.00	0.30	0.06	10.70
12.30	0.80	0.50	4.00	0.50	10.00	0.31	3.00	1.00	4.00	0.30	0.13	6.67
12.30	0.80	0.50	4.00	0.50	10.00	0.31	3.00	1.00	4.00	0.30	0.19	3.89
12.30	0.80	0.50	4.00	0.50	10.00	0.31	3.00	1.00	4.00	0.30	0.25	1.89
12.30	0.80	0.50	4.00	0.50	10.00	0.31	3.00	1.00	4.00	0.40	0.06	8.85
12.30	0.80	0.50	4.00	0.50	10.00	0.31	3.00	1.00	4.00	0.40	0.13	5.67
12.30	0.80	0.50	4.00	0.50	10.00	0.31	3.00	1.00	4.00	0.40	0.19	3.59
12.30	0.80	0.50	4.00	0.50	10.00	0.31	3.00	1.00	4.00	0.40	0.25	2.05
12.30	0.80	0.50	4.00	0.50	10.00	0.31	3.00	1.00	4.00	0.50	0.06	7.83
12.30	0.80	0.50	4.00	0.50	10.00	0.31	3.00	1.00	4.00	0.50	0.13	5.03
12.30	0.80	0.50	4.00	0.50	10.00	0.31	3.00	1.00	4.00	0.50	0.19	3.22

12.30	0.80	0.50	4.00	0.50	10.00	0.31	3.00	1.00	4.00	0.50	0.25	1.94
12.30	0.80	0.50	4.00	0.50	10.00	0.31	3.00	1.00	4.00	0.60	0.06	7.30
12.30	0.80	0.50	4.00	0.50	10.00	0.31	3.00	1.00	4.00	0.60	0.13	4.63
12.30	0.80	0.50	4.00	0.50	10.00	0.31	3.00	1.00	4.00	0.60	0.19	2.89
12.30	0.80	0.50	4.00	0.50	10.00	0.31	3.00	1.00	4.00	0.60	0.25	1.77
12.30	0.80	0.50	4.00	0.50	10.00	0.31	3.00	1.00	4.00	0.70	0.06	6.89
12.30	0.80	0.50	4.00	0.50	10.00	0.31	3.00	1.00	4.00	0.70	0.13	4.33
12.30	0.80	0.50	4.00	0.50	10.00	0.31	3.00	1.00	4.00	0.70	0.19	2.65
12.30	0.80	0.50	4.00	0.50	10.00	0.31	3.00	1.00	4.00	0.70	0.25	1.62
12.30	0.80	0.50	4.00	0.60	10.00	0.31	3.00	1.00	4.00	0.10	0.06	9.70
12.30	0.80	0.50	4.00	0.60	10.00	0.31	3.00	1.00	4.00	0.10	0.13	4.41
12.30	0.80	0.50	4.00	0.60	10.00	0.31	3.00	1.00	4.00	0.10	0.19	2.04
12.30	0.80	0.50	4.00	0.60	10.00	0.31	3.00	1.00	4.00	0.10	0.25	1.36
12.30	0.80	0.50	4.00	0.60	10.00	0.31	3.00	1.00	4.00	0.20	0.06	6.96
12.30	0.80	0.50	4.00	0.60	10.00	0.31	3.00	1.00	4.00	0.20	0.13	6.38
12.30	0.80	0.50	4.00	0.60	10.00	0.31	3.00	1.00	4.00	0.20	0.19	3.45
12.30	0.80	0.50	4.00	0.30	15.00	0.31	3.00	1.00	4.00	0.30	0.13	37.47
12.30	0.80	0.50	4.00	0.30	15.00	0.31	3.00	1.00	4.00	0.30	0.19	20.91
12.30	0.80	0.50	4.00	0.30	15.00	0.31	3.00	1.00	4.00	0.30	0.25	10.92
12.30	0.80	0.50	4.00	0.30	15.00	0.31	3.00	1.00	4.00	0.50	0.13	39.05
12.30	0.80	0.50	4.00	0.30	15.00	0.31	3.00	1.00	4.00	0.50	0.19	26.15
12.30	0.80	0.50	4.00	0.30	15.00	0.31	3.00	1.00	4.00	0.50	0.25	16.25
12.30	0.80	0.50	4.00	0.30	15.00	0.31	3.00	1.00	4.00	0.70	0.13	38.49
12.30	0.80	0.50	4.00	0.30	15.00	0.31	3.00	1.00	4.00	0.70	0.19	26.84
12.30	0.80	0.50	4.00	0.30	15.00	0.31	3.00	1.00	4.00	0.70	0.25	17.41
12.30	0.80	0.50	4.00	0.50	15.00	0.31	3.00	1.00	4.00	0.30	0.13	6.66
12.30	0.80	0.50	4.00	0.50	15.00	0.31	3.00	1.00	4.00	0.30	0.19	3.23
12.30	0.80	0.50	4.00	0.50	15.00	0.31	3.00	1.00	4.00	0.30	0.25	2.28
12.30	0.80	0.50	4.00	0.50	15.00	0.31	3.00	1.00	4.00	0.50	0.13	5.54
12.30	0.80	0.50	4.00	0.50	15.00	0.31	3.00	1.00	4.00	0.50	0.19	3.46
12.30	0.80	0.50	4.00	0.50	15.00	0.31	3.00	1.00	4.00	0.50	0.25	2.79
12.30	0.80	0.50	4.00	0.50	15.00	0.31	3.00	1.00	4.00	0.70	0.13	5.21
12.30	0.80	0.50	4.00	0.50	15.00	0.31	3.00	1.00	4.00	0.70	0.19	3.43
12.30	0.80	0.50	4.00	0.50	15.00	0.31	3.00	1.00	4.00	0.70	0.25	3.03
12.30	0.80	0.50	4.00	0.70	15.00	0.31	3.00	1.00	4.00	0.30	0.13	2.68
12.30	0.80	0.50	4.00	0.70	15.00	0.31	3.00	1.00	4.00	0.30	0.19	1.54
12.30	0.80	0.50	4.00	0.70	15.00	0.31	3.00	1.00	4.00	0.50	0.13	1.55
12.30	0.80	0.50	4.00	0.70	15.00	0.31	3.00	1.00	4.00	0.70	0.13	1.18

12.30	0.80	0.50	4.00	0.30	25.00	0.31	3.00	1.00	4.00	0.30	0.13	66.72
12.30	0.80	0.50	4.00	0.30	25.00	0.31	3.00	1.00	4.00	0.30	0.19	40.91
12.30	0.80	0.50	4.00	0.30	25.00	0.31	3.00	1.00	4.00	0.30	0.25	24.26
12.30	0.80	0.50	4.00	0.30	25.00	0.31	3.00	1.00	4.00	0.50	0.13	72.33
12.30	0.80	0.50	4.00	0.30	25.00	0.31	3.00	1.00	4.00	0.50	0.19	51.37
12.30	0.80	0.50	4.00	0.30	25.00	0.31	3.00	1.00	4.00	0.50	0.25	34.25
12.30	0.80	0.50	4.00	0.30	25.00	0.31	3.00	1.00	4.00	0.70	0.13	72.66
12.30	0.80	0.50	4.00	0.30	25.00	0.31	3.00	1.00	4.00	0.70	0.19	53.49
12.30	0.80	0.50	4.00	0.30	25.00	0.31	3.00	1.00	4.00	0.70	0.25	36.89
12.30	0.80	0.50	4.00	0.50	25.00	0.31	3.00	1.00	4.00	0.30	0.13	9.47
12.30	0.80	0.50	4.00	0.50	25.00	0.31	3.00	1.00	4.00	0.30	0.19	6.07
12.30	0.80	0.50	4.00	0.50	25.00	0.31	3.00	1.00	4.00	0.30	0.25	5.29
12.30	0.80	0.50	4.00	0.50	25.00	0.31	3.00	1.00	4.00	0.50	0.13	9.69
12.30	0.80	0.50	4.00	0.50	25.00	0.31	3.00	1.00	4.00	0.50	0.19	7.34
12.30	0.80	0.50	4.00	0.50	25.00	0.31	3.00	1.00	4.00	0.50	0.25	6.38
12.30	0.80	0.50	4.00	0.50	25.00	0.31	3.00	1.00	4.00	0.70	0.13	10.00
12.30	0.80	0.50	4.00	0.50	25.00	0.31	3.00	1.00	4.00	0.70	0.19	7.90
12.30	0.80	0.50	4.00	0.50	25.00	0.31	3.00	1.00	4.00	0.70	0.25	7.02
12.30	0.80	0.50	4.00	0.70	25.00	0.31	3.00	1.00	4.00	0.30	0.13	2.73
12.30	0.80	0.50	4.00	0.70	25.00	0.31	3.00	1.00	4.00	0.30	0.19	2.13
12.30	0.80	0.50	4.00	0.70	25.00	0.31	3.00	1.00	4.00	0.30	0.25	1.68
12.30	0.80	0.50	4.00	0.70	25.00	0.31	3.00	1.00	4.00	0.50	0.13	2.24
12.30	0.80	0.50	4.00	0.70	25.00	0.31	3.00	1.00	4.00	0.50	0.19	2.19
12.30	0.80	0.50	4.00	0.70	25.00	0.31	3.00	1.00	4.00	0.50	0.25	1.75
12.30	0.80	0.50	4.00	0.70	25.00	0.31	3.00	1.00	4.00	0.70	0.13	2.22
12.30	0.80	0.50	4.00	0.70	25.00	0.31	3.00	1.00	4.00	0.70	0.19	2.26
12.30	0.80	0.50	4.00	0.70	25.00	0.31	3.00	1.00	4.00	0.70	0.25	1.86
12.30	0.80	0.50	4.00	0.30	35.00	0.31	3.00	1.00	4.00	0.30	0.13	101.46
12.30	0.80	0.50	4.00	0.30	35.00	0.31	3.00	1.00	4.00	0.30	0.19	64.92
12.30	0.80	0.50	4.00	0.30	35.00	0.31	3.00	1.00	4.00	0.30	0.25	40.32
12.30	0.80	0.50	4.00	0.30	35.00	0.31	3.00	1.00	4.00	0.50	0.13	110.44
12.30	0.80	0.50	4.00	0.30	35.00	0.31	3.00	1.00	4.00	0.50	0.19	80.41
12.30	0.80	0.50	4.00	0.30	35.00	0.31	3.00	1.00	4.00	0.50	0.25	55.10
12.30	0.80	0.50	4.00	0.30	35.00	0.31	3.00	1.00	4.00	0.70	0.13	111.49
12.30	0.80	0.50	4.00	0.30	35.00	0.31	3.00	1.00	4.00	0.70	0.19	83.90
12.30	0.80	0.50	4.00	0.30	35.00	0.31	3.00	1.00	4.00	0.70	0.25	59.21
12.30	0.80	0.50	4.00	0.50	35.00	0.31	3.00	1.00	4.00	0.30	0.13	14.45
12.30	0.80	0.50	4.00	0.50	35.00	0.31	3.00	1.00	4.00	0.30	0.19	10.34

12.30	0.80	0.50	4.00	0.50	35.00	0.31	3.00	1.00	4.00	0.30	0.25	8.85
12.30	0.80	0.50	4.00	0.50	35.00	0.31	3.00	1.00	4.00	0.50	0.13	15.38
12.30	0.80	0.50	4.00	0.50	35.00	0.31	3.00	1.00	4.00	0.50	0.19	12.32
12.30	0.80	0.50	4.00	0.50	35.00	0.31	3.00	1.00	4.00	0.50	0.25	10.53
12.30	0.80	0.50	4.00	0.50	35.00	0.31	3.00	1.00	4.00	0.70	0.13	16.13
12.30	0.80	0.50	4.00	0.50	35.00	0.31	3.00	1.00	4.00	0.70	0.19	13.33
12.30	0.80	0.50	4.00	0.50	35.00	0.31	3.00	1.00	4.00	0.70	0.25	11.57
12.30	0.80	0.50	4.00	0.70	35.00	0.31	3.00	1.00	4.00	0.30	0.13	3.89
12.30	0.80	0.50	4.00	0.70	35.00	0.31	3.00	1.00	4.00	0.30	0.19	3.43
12.30	0.80	0.50	4.00	0.70	35.00	0.31	3.00	1.00	4.00	0.30	0.25	2.83
12.30	0.80	0.50	4.00	0.70	35.00	0.31	3.00	1.00	4.00	0.50	0.13	3.46
12.30	0.80	0.50	4.00	0.70	35.00	0.31	3.00	1.00	4.00	0.50	0.19	3.55
12.30	0.80	0.50	4.00	0.70	35.00	0.31	3.00	1.00	4.00	0.50	0.25	2.97
12.30	0.80	0.50	4.00	0.70	35.00	0.31	3.00	1.00	4.00	0.70	0.13	3.51
12.30	0.80	0.50	4.00	0.70	35.00	0.31	3.00	1.00	4.00	0.70	0.19	3.68
12.30	0.80	0.50	4.00	0.70	35.00	0.31	3.00	1.00	4.00	0.70	0.25	3.16
12.30	0.80	0.50	4.00	0.30	45.00	0.31	3.00	1.00	4.00	0.30	0.13	140.78
12.30	0.80	0.50	4.00	0.30	45.00	0.31	3.00	1.00	4.00	0.30	0.19	92.16
12.30	0.80	0.50	4.00	0.30	45.00	0.31	3.00	1.00	4.00	0.30	0.25	58.64
12.30	0.80	0.50	4.00	0.30	45.00	0.31	3.00	1.00	4.00	0.50	0.13	152.20
12.30	0.80	0.50	4.00	0.30	45.00	0.31	3.00	1.00	4.00	0.50	0.19	112.38
12.30	0.80	0.50	4.00	0.30	45.00	0.31	3.00	1.00	4.00	0.50	0.25	78.18
12.30	0.80	0.50	4.00	0.30	45.00	0.31	3.00	1.00	4.00	0.70	0.13	153.72
12.30	0.80	0.50	4.00	0.30	45.00	0.31	3.00	1.00	4.00	0.70	0.19	117.09
12.30	0.80	0.50	4.00	0.30	45.00	0.31	3.00	1.00	4.00	0.70	0.25	83.71
12.30	0.80	0.50	4.00	0.50	45.00	0.31	3.00	1.00	4.00	0.30	0.13	20.69
12.30	0.80	0.50	4.00	0.50	45.00	0.31	3.00	1.00	4.00	0.30	0.19	15.42
12.30	0.80	0.50	4.00	0.50	45.00	0.31	3.00	1.00	4.00	0.30	0.25	12.67
12.30	0.80	0.50	4.00	0.50	45.00	0.31	3.00	1.00	4.00	0.50	0.13	21.96
12.30	0.80	0.50	4.00	0.50	45.00	0.31	3.00	1.00	4.00	0.50	0.19	18.01
12.30	0.80	0.50	4.00	0.50	45.00	0.31	3.00	1.00	4.00	0.50	0.25	14.94
12.30	0.80	0.50	4.00	0.50	45.00	0.31	3.00	1.00	4.00	0.70	0.13	23.07
12.30	0.80	0.50	4.00	0.50	45.00	0.31	3.00	1.00	4.00	0.70	0.19	19.43
12.30	0.80	0.50	4.00	0.50	45.00	0.31	3.00	1.00	4.00	0.70	0.25	16.35
12.30	0.80	0.50	4.00	0.70	45.00	0.31	3.00	1.00	4.00	0.30	0.13	5.23
12.30	0.80	0.50	4.00	0.70	45.00	0.31	3.00	1.00	4.00	0.30	0.19	4.84
12.30	0.80	0.50	4.00	0.70	45.00	0.31	3.00	1.00	4.00	0.30	0.25	4.11
12.30	0.80	0.50	4.00	0.70	45.00	0.31	3.00	1.00	4.00	0.50	0.13	4.64

12.30	0.80	0.50	4.00	0.70	45.00	0.31	3.00	1.00	4.00	0.50	0.19	4.96
12.30	0.80	0.50	4.00	0.70	45.00	0.31	3.00	1.00	4.00	0.50	0.25	4.30
12.30	0.80	0.50	4.00	0.70	45.00	0.31	3.00	1.00	4.00	0.70	0.13	4.71
12.30	0.80	0.50	4.00	0.70	45.00	0.31	3.00	1.00	4.00	0.70	0.19	5.15
12.30	0.80	0.50	4.00	0.70	45.00	0.31	3.00	1.00	4.00	0.70	0.25	4.57
12.30	0.80	0.50	4.00	0.30	55.00	0.31	3.00	1.00	4.00	0.30	0.13	183.22
12.30	0.80	0.50	4.00	0.30	55.00	0.31	3.00	1.00	4.00	0.30	0.19	121.65
12.30	0.80	0.50	4.00	0.30	55.00	0.31	3.00	1.00	4.00	0.30	0.25	78.61
12.30	0.80	0.50	4.00	0.30	55.00	0.31	3.00	1.00	4.00	0.50	0.13	196.35
12.30	0.80	0.50	4.00	0.30	55.00	0.31	3.00	1.00	4.00	0.50	0.19	146.30
12.30	0.80	0.50	4.00	0.30	55.00	0.31	3.00	1.00	4.00	0.50	0.25	102.83
12.30	0.80	0.50	4.00	0.30	55.00	0.31	3.00	1.00	4.00	0.70	0.13	198.05
12.30	0.80	0.50	4.00	0.30	55.00	0.31	3.00	1.00	4.00	0.70	0.19	152.06
12.30	0.80	0.50	4.00	0.30	55.00	0.31	3.00	1.00	4.00	0.70	0.25	109.65
12.30	0.80	0.50	4.00	0.50	55.00	0.31	3.00	1.00	4.00	0.30	0.13	27.78
12.30	0.80	0.50	4.00	0.50	55.00	0.31	3.00	1.00	4.00	0.30	0.19	21.09
12.30	0.80	0.50	4.00	0.50	55.00	0.31	3.00	1.00	4.00	0.30	0.25	16.33
12.30	0.80	0.50	4.00	0.50	55.00	0.31	3.00	1.00	4.00	0.50	0.13	29.19
12.30	0.80	0.50	4.00	0.50	55.00	0.31	3.00	1.00	4.00	0.50	0.19	24.23
12.30	0.80	0.50	4.00	0.50	55.00	0.31	3.00	1.00	4.00	0.50	0.25	19.14
12.30	0.80	0.50	4.00	0.50	55.00	0.31	3.00	1.00	4.00	0.70	0.13	30.58
12.30	0.80	0.50	4.00	0.50	55.00	0.31	3.00	1.00	4.00	0.70	0.19	26.01
12.30	0.80	0.50	4.00	0.50	55.00	0.31	3.00	1.00	4.00	0.70	0.25	20.95
12.30	0.80	0.50	4.00	0.70	55.00	0.31	3.00	1.00	4.00	0.30	0.13	6.73
12.30	0.80	0.50	4.00	0.70	55.00	0.31	3.00	1.00	4.00	0.30	0.19	6.36
12.30	0.80	0.50	4.00	0.70	55.00	0.31	3.00	1.00	4.00	0.30	0.25	5.46
12.30	0.80	0.50	4.00	0.70	55.00	0.31	3.00	1.00	4.00	0.50	0.13	5.90
12.30	0.80	0.50	4.00	0.70	55.00	0.31	3.00	1.00	4.00	0.50	0.19	6.46
12.30	0.80	0.50	4.00	0.70	55.00	0.31	3.00	1.00	4.00	0.50	0.25	5.71
12.30	0.80	0.50	4.00	0.70	55.00	0.31	3.00	1.00	4.00	0.70	0.13	5.98
12.30	0.80	0.50	4.00	0.70	55.00	0.31	3.00	1.00	4.00	0.70	0.19	6.70
12.30	0.80	0.50	4.00	0.70	55.00	0.31	3.00	1.00	4.00	0.70	0.25	6.04
12.30	0.80	0.50	4.00	0.30	5.00	0.31	3.00	2.00	4.00	0.30	0.13	26.21
12.30	0.80	0.50	4.00	0.30	5.00	0.31	3.00	2.00	4.00	0.30	0.19	22.67
12.30	0.80	0.50	4.00	0.30	5.00	0.31	3.00	2.00	4.00	0.30	0.25	16.36
12.30	0.80	0.50	4.00	0.30	5.00	0.31	3.00	2.00	4.00	0.50	0.13	24.04
12.30	0.80	0.50	4.00	0.30	5.00	0.31	3.00	2.00	4.00	0.50	0.19	22.31
12.30	0.80	0.50	4.00	0.30	5.00	0.31	3.00	2.00	4.00	0.50	0.25	17.23

12.30	0.80	0.50	4.00	0.30	5.00	0.31	3.00	2.00	4.00	0.70	0.13	22.67
12.30	0.80	0.50	4.00	0.30	5.00	0.31	3.00	2.00	4.00	0.70	0.19	21.34
12.30	0.80	0.50	4.00	0.30	5.00	0.31	3.00	2.00	4.00	0.70	0.25	16.92
12.30	0.80	0.50	4.00	0.50	5.00	0.31	3.00	2.00	4.00	0.30	0.13	7.75
12.30	0.80	0.50	4.00	0.50	5.00	0.31	3.00	2.00	4.00	0.30	0.19	6.60
12.30	0.80	0.50	4.00	0.50	5.00	0.31	3.00	2.00	4.00	0.30	0.25	5.86
12.30	0.80	0.50	4.00	0.50	5.00	0.31	3.00	2.00	4.00	0.50	0.13	6.31
12.30	0.80	0.50	4.00	0.50	5.00	0.31	3.00	2.00	4.00	0.50	0.19	5.71
12.30	0.80	0.50	4.00	0.50	5.00	0.31	3.00	2.00	4.00	0.50	0.25	5.51
12.30	0.80	0.50	4.00	0.50	5.00	0.31	3.00	2.00	4.00	0.70	0.13	5.63
12.30	0.80	0.50	4.00	0.50	5.00	0.31	3.00	2.00	4.00	0.70	0.19	5.16
12.30	0.80	0.50	4.00	0.50	5.00	0.31	3.00	2.00	4.00	0.70	0.25	5.07
12.30	0.80	0.50	4.00	0.70	5.00	0.31	3.00	2.00	4.00	0.30	0.13	3.69
12.30	0.80	0.50	4.00	0.70	5.00	0.31	3.00	2.00	4.00	0.30	0.19	3.72
12.30	0.80	0.50	4.00	0.70	5.00	0.31	3.00	2.00	4.00	0.30	0.25	3.44
12.30	0.80	0.50	4.00	0.70	5.00	0.31	3.00	2.00	4.00	0.50	0.13	2.78
12.30	0.80	0.50	4.00	0.70	5.00	0.31	3.00	2.00	4.00	0.50	0.19	3.07
12.30	0.80	0.50	4.00	0.70	5.00	0.31	3.00	2.00	4.00	0.50	0.25	3.08
12.30	0.80	0.50	4.00	0.70	5.00	0.31	3.00	2.00	4.00	0.70	0.13	2.39
12.30	0.80	0.50	4.00	0.70	5.00	0.31	3.00	2.00	4.00	0.70	0.19	2.70
12.30	0.80	0.50	4.00	0.70	5.00	0.31	3.00	2.00	4.00	0.70	0.25	2.78
12.30	0.80	0.50	4.00	0.30	15.00	0.31	3.00	2.00	4.00	0.30	0.13	91.71
12.30	0.80	0.50	4.00	0.30	15.00	0.31	3.00	2.00	4.00	0.30	0.19	84.34
12.30	0.80	0.50	4.00	0.30	15.00	0.31	3.00	2.00	4.00	0.30	0.25	67.10
12.30	0.80	0.50	4.00	0.30	15.00	0.31	3.00	2.00	4.00	0.50	0.13	89.62
12.30	0.80	0.50	4.00	0.30	15.00	0.31	3.00	2.00	4.00	0.50	0.19	85.89
12.30	0.80	0.50	4.00	0.30	15.00	0.31	3.00	2.00	4.00	0.50	0.25	71.35
12.30	0.80	0.50	4.00	0.30	15.00	0.31	3.00	2.00	4.00	0.70	0.13	87.77
12.30	0.80	0.50	4.00	0.30	15.00	0.31	3.00	2.00	4.00	0.70	0.19	84.87
12.30	0.80	0.50	4.00	0.30	15.00	0.31	3.00	2.00	4.00	0.70	0.25	71.70
12.30	0.80	0.50	4.00	0.50	15.00	0.31	3.00	2.00	4.00	0.30	0.13	22.82
12.30	0.80	0.50	4.00	0.50	15.00	0.31	3.00	2.00	4.00	0.30	0.19	18.52
12.30	0.80	0.50	4.00	0.50	15.00	0.31	3.00	2.00	4.00	0.30	0.25	16.61
12.30	0.80	0.50	4.00	0.50	15.00	0.31	3.00	2.00	4.00	0.50	0.13	21.24
12.30	0.80	0.50	4.00	0.50	15.00	0.31	3.00	2.00	4.00	0.50	0.19	18.23
12.30	0.80	0.50	4.00	0.50	15.00	0.31	3.00	2.00	4.00	0.50	0.25	17.46
12.30	0.80	0.50	4.00	0.50	15.00	0.31	3.00	2.00	4.00	0.70	0.13	20.66
12.30	0.80	0.50	4.00	0.50	15.00	0.31	3.00	2.00	4.00	0.70	0.19	17.99

12.30	0.80	0.50	4.00	0.50	15.00	0.31	3.00	2.00	4.00	0.70	0.25	17.43
12.30	0.80	0.50	4.00	0.70	15.00	0.31	3.00	2.00	4.00	0.30	0.13	8.74
12.30	0.80	0.50	4.00	0.70	15.00	0.31	3.00	2.00	4.00	0.30	0.19	8.17
12.30	0.80	0.50	4.00	0.70	15.00	0.31	3.00	2.00	4.00	0.30	0.25	6.45
12.30	0.80	0.50	4.00	0.70	15.00	0.31	3.00	2.00	4.00	0.50	0.13	7.35
12.30	0.80	0.50	4.00	0.70	15.00	0.31	3.00	2.00	4.00	0.50	0.19	7.41
12.30	0.80	0.50	4.00	0.70	15.00	0.31	3.00	2.00	4.00	0.50	0.25	6.38
12.30	0.80	0.50	4.00	0.70	15.00	0.31	3.00	2.00	4.00	0.70	0.13	6.85
12.30	0.80	0.50	4.00	0.70	15.00	0.31	3.00	2.00	4.00	0.70	0.19	6.98
12.30	0.80	0.50	4.00	0.70	15.00	0.31	3.00	2.00	4.00	0.70	0.25	6.12
12.30	0.80	0.50	4.00	0.30	25.00	0.31	3.00	2.00	4.00	0.30	0.13	165.01
12.30	0.80	0.50	4.00	0.30	25.00	0.31	3.00	2.00	4.00	0.30	0.19	153.97
12.30	0.80	0.50	4.00	0.30	25.00	0.31	3.00	2.00	4.00	0.30	0.25	124.08
12.30	0.80	0.50	4.00	0.30	25.00	0.31	3.00	2.00	4.00	0.50	0.13	163.14
12.30	0.80	0.50	4.00	0.30	25.00	0.31	3.00	2.00	4.00	0.50	0.19	157.44
12.30	0.80	0.50	4.00	0.30	25.00	0.31	3.00	2.00	4.00	0.50	0.25	132.01
12.30	0.80	0.50	4.00	0.30	25.00	0.31	3.00	2.00	4.00	0.70	0.13	160.71
12.30	0.80	0.50	4.00	0.30	25.00	0.31	3.00	2.00	4.00	0.70	0.19	156.30
12.30	0.80	0.50	4.00	0.30	25.00	0.31	3.00	2.00	4.00	0.70	0.25	133.04
12.30	0.80	0.50	4.00	0.50	25.00	0.31	3.00	2.00	4.00	0.30	0.13	40.02
12.30	0.80	0.50	4.00	0.50	25.00	0.31	3.00	2.00	4.00	0.30	0.19	32.88
12.30	0.80	0.50	4.00	0.50	25.00	0.31	3.00	2.00	4.00	0.30	0.25	30.47
12.30	0.80	0.50	4.00	0.50	25.00	0.31	3.00	2.00	4.00	0.50	0.13	38.68
12.30	0.80	0.50	4.00	0.50	25.00	0.31	3.00	2.00	4.00	0.50	0.19	33.44
12.30	0.80	0.50	4.00	0.50	25.00	0.31	3.00	2.00	4.00	0.50	0.25	32.64
12.30	0.80	0.50	4.00	0.50	25.00	0.31	3.00	2.00	4.00	0.70	0.13	38.29
12.30	0.80	0.50	4.00	0.50	25.00	0.31	3.00	2.00	4.00	0.70	0.19	33.59
12.30	0.80	0.50	4.00	0.50	25.00	0.31	3.00	2.00	4.00	0.70	0.25	33.10
12.30	0.80	0.50	4.00	0.70	25.00	0.31	3.00	2.00	4.00	0.30	0.13	14.65
12.30	0.80	0.50	4.00	0.70	25.00	0.31	3.00	2.00	4.00	0.30	0.19	13.95
12.30	0.80	0.50	4.00	0.70	25.00	0.31	3.00	2.00	4.00	0.30	0.25	11.38
12.30	0.80	0.50	4.00	0.70	25.00	0.31	3.00	2.00	4.00	0.50	0.13	13.14
12.30	0.80	0.50	4.00	0.70	25.00	0.31	3.00	2.00	4.00	0.50	0.19	13.42
12.30	0.80	0.50	4.00	0.70	25.00	0.31	3.00	2.00	4.00	0.50	0.25	11.84
12.30	0.80	0.50	4.00	0.70	25.00	0.31	3.00	2.00	4.00	0.70	0.13	12.68
12.30	0.80	0.50	4.00	0.70	25.00	0.31	3.00	2.00	4.00	0.70	0.19	13.09
12.30	0.80	0.50	4.00	0.70	25.00	0.31	3.00	2.00	4.00	0.70	0.25	11.78
12.30	0.80	0.50	4.00	0.30	35.00	0.31	3.00	2.00	4.00	0.30	0.13	243.87



12.30	0.80	0.50	4.00	0.30	35.00	0.31	3.00	2.00	4.00	0.30	0.19	228.58
12.30	0.80	0.50	4.00	0.30	35.00	0.31	3.00	2.00	4.00	0.30	0.25	184.92
12.30	0.80	0.50	4.00	0.30	35.00	0.31	3.00	2.00	4.00	0.50	0.13	241.49
12.30	0.80	0.50	4.00	0.30	35.00	0.31	3.00	2.00	4.00	0.50	0.19	233.56
12.30	0.80	0.50	4.00	0.30	35.00	0.31	3.00	2.00	4.00	0.50	0.25	196.39
12.30	0.80	0.50	4.00	0.30	35.00	0.31	3.00	2.00	4.00	0.70	0.13	238.33
12.30	0.80	0.50	4.00	0.30	35.00	0.31	3.00	2.00	4.00	0.70	0.19	232.16
12.30	0.80	0.50	4.00	0.30	35.00	0.31	3.00	2.00	4.00	0.70	0.25	198.07
12.30	0.80	0.50	4.00	0.50	35.00	0.31	3.00	2.00	4.00	0.30	0.13	59.06
12.30	0.80	0.50	4.00	0.50	35.00	0.31	3.00	2.00	4.00	0.30	0.19	48.85
12.30	0.80	0.50	4.00	0.50	35.00	0.31	3.00	2.00	4.00	0.30	0.25	45.83
12.30	0.80	0.50	4.00	0.50	35.00	0.31	3.00	2.00	4.00	0.50	0.13	57.60
12.30	0.80	0.50	4.00	0.50	35.00	0.31	3.00	2.00	4.00	0.50	0.19	50.00
12.30	0.80	0.50	4.00	0.50	35.00	0.31	3.00	2.00	4.00	0.50	0.25	49.15
12.30	0.80	0.50	4.00	0.50	35.00	0.31	3.00	2.00	4.00	0.70	0.13	57.33
12.30	0.80	0.50	4.00	0.50	35.00	0.31	3.00	2.00	4.00	0.70	0.19	50.48
12.30	0.80	0.50	4.00	0.50	35.00	0.31	3.00	2.00	4.00	0.70	0.25	50.05
12.30	0.80	0.50	4.00	0.70	35.00	0.31	3.00	2.00	4.00	0.30	0.13	21.48
12.30	0.80	0.50	4.00	0.70	35.00	0.31	3.00	2.00	4.00	0.30	0.19	20.66
12.30	0.80	0.50	4.00	0.70	35.00	0.31	3.00	2.00	4.00	0.30	0.25	17.23
12.30	0.80	0.50	4.00	0.70	35.00	0.31	3.00	2.00	4.00	0.50	0.13	19.65
12.30	0.80	0.50	4.00	0.70	35.00	0.31	3.00	2.00	4.00	0.50	0.19	20.18
12.30	0.80	0.50	4.00	0.70	35.00	0.31	3.00	2.00	4.00	0.50	0.25	18.06
12.30	0.80	0.50	4.00	0.70	35.00	0.31	3.00	2.00	4.00	0.70	0.13	19.19
12.30	0.80	0.50	4.00	0.70	35.00	0.31	3.00	2.00	4.00	0.70	0.19	19.91
12.30	0.80	0.50	4.00	0.70	35.00	0.31	3.00	2.00	4.00	0.70	0.25	18.16
12.30	0.80	0.50	4.00	0.30	45.00	0.31	3.00	2.00	4.00	0.30	0.13	326.36
12.30	0.80	0.50	4.00	0.30	45.00	0.31	3.00	2.00	4.00	0.30	0.19	306.14
12.30	0.80	0.50	4.00	0.30	45.00	0.31	3.00	2.00	4.00	0.30	0.25	247.90
12.30	0.80	0.50	4.00	0.30	45.00	0.31	3.00	2.00	4.00	0.50	0.13	322.40
12.30	0.80	0.50	4.00	0.30	45.00	0.31	3.00	2.00	4.00	0.50	0.19	311.96
12.30	0.80	0.50	4.00	0.30	45.00	0.31	3.00	2.00	4.00	0.50	0.25	262.58
12.30	0.80	0.50	4.00	0.30	45.00	0.31	3.00	2.00	4.00	0.70	0.13	318.25
12.30	0.80	0.50	4.00	0.30	45.00	0.31	3.00	2.00	4.00	0.70	0.19	310.11
12.30	0.80	0.50	4.00	0.30	45.00	0.31	3.00	2.00	4.00	0.70	0.25	264.80
12.30	0.80	0.50	4.00	0.50	45.00	0.31	3.00	2.00	4.00	0.30	0.13	79.52
12.30	0.80	0.50	4.00	0.50	45.00	0.31	3.00	2.00	4.00	0.30	0.19	65.95
12.30	0.80	0.50	4.00	0.50	45.00	0.31	3.00	2.00	4.00	0.30	0.25	62.16

12.30	0.80	0.50	4.00	0.50	45.00	0.31	3.00	2.00	4.00	0.50	0.13	77.43
12.30	0.80	0.50	4.00	0.50	45.00	0.31	3.00	2.00	4.00	0.50	0.19	67.36
12.30	0.80	0.50	4.00	0.50	45.00	0.31	3.00	2.00	4.00	0.50	0.25	66.41
12.30	0.80	0.50	4.00	0.50	45.00	0.31	3.00	2.00	4.00	0.70	0.13	77.15
12.30	0.80	0.50	4.00	0.50	45.00	0.31	3.00	2.00	4.00	0.70	0.19	68.07
12.30	0.80	0.50	4.00	0.50	45.00	0.31	3.00	2.00	4.00	0.70	0.25	67.65
12.30	0.80	0.50	4.00	0.70	45.00	0.31	3.00	2.00	4.00	0.30	0.13	29.08
12.30	0.80	0.50	4.00	0.70	45.00	0.31	3.00	2.00	4.00	0.30	0.19	28.05
12.30	0.80	0.50	4.00	0.70	45.00	0.31	3.00	2.00	4.00	0.30	0.25	23.63
12.30	0.80	0.50	4.00	0.70	45.00	0.31	3.00	2.00	4.00	0.50	0.13	26.64
12.30	0.80	0.50	4.00	0.70	45.00	0.31	3.00	2.00	4.00	0.50	0.19	27.40
12.30	0.80	0.50	4.00	0.70	45.00	0.31	3.00	2.00	4.00	0.50	0.25	24.70
12.30	0.80	0.50	4.00	0.70	45.00	0.31	3.00	2.00	4.00	0.70	0.13	26.09
12.30	0.80	0.50	4.00	0.70	45.00	0.31	3.00	2.00	4.00	0.70	0.19	27.11
12.30	0.80	0.50	4.00	0.70	45.00	0.31	3.00	2.00	4.00	0.70	0.25	24.90
12.30	0.80	0.50	4.00	0.30	55.00	0.31	3.00	2.00	4.00	0.30	0.13	409.80
12.30	0.80	0.50	4.00	0.30	55.00	0.31	3.00	2.00	4.00	0.30	0.19	384.15
12.30	0.80	0.50	4.00	0.30	55.00	0.31	3.00	2.00	4.00	0.30	0.25	311.02
12.30	0.80	0.50	4.00	0.30	55.00	0.31	3.00	2.00	4.00	0.50	0.13	403.47
12.30	0.80	0.50	4.00	0.30	55.00	0.31	3.00	2.00	4.00	0.50	0.19	390.29
12.30	0.80	0.50	4.00	0.30	55.00	0.31	3.00	2.00	4.00	0.50	0.25	328.58
12.30	0.80	0.50	4.00	0.30	55.00	0.31	3.00	2.00	4.00	0.70	0.13	398.07
12.30	0.80	0.50	4.00	0.30	55.00	0.31	3.00	2.00	4.00	0.70	0.19	387.79
12.30	0.80	0.50	4.00	0.30	55.00	0.31	3.00	2.00	4.00	0.70	0.25	331.19
12.30	0.80	0.50	4.00	0.50	55.00	0.31	3.00	2.00	4.00	0.30	0.13	100.66
12.30	0.80	0.50	4.00	0.50	55.00	0.31	3.00	2.00	4.00	0.30	0.19	83.56
12.30	0.80	0.50	4.00	0.50	55.00	0.31	3.00	2.00	4.00	0.30	0.25	78.85
12.30	0.80	0.50	4.00	0.50	55.00	0.31	3.00	2.00	4.00	0.50	0.13	97.59
12.30	0.80	0.50	4.00	0.50	55.00	0.31	3.00	2.00	4.00	0.50	0.19	84.99
12.30	0.80	0.50	4.00	0.50	55.00	0.31	3.00	2.00	4.00	0.50	0.25	83.88
12.30	0.80	0.50	4.00	0.50	55.00	0.31	3.00	2.00	4.00	0.70	0.13	97.16
12.30	0.80	0.50	4.00	0.50	55.00	0.31	3.00	2.00	4.00	0.70	0.19	85.82
12.30	0.80	0.50	4.00	0.50	55.00	0.31	3.00	2.00	4.00	0.70	0.25	85.38
12.30	0.80	0.50	4.00	0.70	55.00	0.31	3.00	2.00	4.00	0.30	0.13	37.13
12.30	0.80	0.50	4.00	0.70	55.00	0.31	3.00	2.00	4.00	0.30	0.19	35.80
12.30	0.80	0.50	4.00	0.70	55.00	0.31	3.00	2.00	4.00	0.30	0.25	30.28
12.30	0.80	0.50	4.00	0.70	55.00	0.31	3.00	2.00	4.00	0.50	0.13	33.89
12.30	0.80	0.50	4.00	0.70	55.00	0.31	3.00	2.00	4.00	0.50	0.19	34.85

12.30	0.80	0.50	4.00	0.70	55.00	0.31	3.00	2.00	4.00	0.50	0.25	31.53
12.30	0.80	0.50	4.00	0.70	55.00	0.31	3.00	2.00	4.00	0.70	0.13	33.19
12.30	0.80	0.50	4.00	0.70	55.00	0.31	3.00	2.00	4.00	0.70	0.19	34.48
12.30	0.80	0.50	4.00	0.70	55.00	0.31	3.00	2.00	4.00	0.70	0.25	31.77
12.30	0.80	0.50	4.00	0.30	5.00	0.31	3.00	3.00	4.00	0.30	0.13	25.22
12.30	0.80	0.50	4.00	0.30	5.00	0.31	3.00	3.00	4.00	0.30	0.19	24.79
12.30	0.80	0.50	4.00	0.30	5.00	0.31	3.00	3.00	4.00	0.30	0.25	20.21
12.30	0.80	0.50	4.00	0.30	5.00	0.31	3.00	3.00	4.00	0.50	0.13	23.02
12.30	0.80	0.50	4.00	0.30	5.00	0.31	3.00	3.00	4.00	0.50	0.19	24.28
12.30	0.80	0.50	4.00	0.30	5.00	0.31	3.00	3.00	4.00	0.50	0.25	20.96
12.30	0.80	0.50	4.00	0.30	5.00	0.31	3.00	3.00	4.00	0.70	0.13	21.81
12.30	0.80	0.50	4.00	0.30	5.00	0.31	3.00	3.00	4.00	0.70	0.19	23.30
12.30	0.80	0.50	4.00	0.30	5.00	0.31	3.00	3.00	4.00	0.70	0.25	20.48
12.30	0.80	0.50	4.00	0.50	5.00	0.31	3.00	3.00	4.00	0.30	0.13	7.19
12.30	0.80	0.50	4.00	0.50	5.00	0.31	3.00	3.00	4.00	0.30	0.19	6.76
12.30	0.80	0.50	4.00	0.50	5.00	0.31	3.00	3.00	4.00	0.30	0.25	5.98
12.30	0.80	0.50	4.00	0.50	5.00	0.31	3.00	3.00	4.00	0.50	0.13	5.96
12.30	0.80	0.50	4.00	0.50	5.00	0.31	3.00	3.00	4.00	0.50	0.19	5.94
12.30	0.80	0.50	4.00	0.50	5.00	0.31	3.00	3.00	4.00	0.50	0.25	5.61
12.30	0.80	0.50	4.00	0.50	5.00	0.31	3.00	3.00	4.00	0.70	0.13	5.39
12.30	0.80	0.50	4.00	0.50	5.00	0.31	3.00	3.00	4.00	0.70	0.19	5.40
12.30	0.80	0.50	4.00	0.50	5.00	0.31	3.00	3.00	4.00	0.70	0.25	5.19
12.30	0.80	0.50	4.00	0.70	5.00	0.31	3.00	3.00	4.00	0.30	0.13	3.29
12.30	0.80	0.50	4.00	0.70	5.00	0.31	3.00	3.00	4.00	0.30	0.19	3.45
12.30	0.80	0.50	4.00	0.70	5.00	0.31	3.00	3.00	4.00	0.30	0.25	3.06
12.30	0.80	0.50	4.00	0.70	5.00	0.31	3.00	3.00	4.00	0.50	0.13	2.38
12.30	0.80	0.50	4.00	0.70	5.00	0.31	3.00	3.00	4.00	0.50	0.19	2.77
12.30	0.80	0.50	4.00	0.70	5.00	0.31	3.00	3.00	4.00	0.50	0.25	2.71
12.30	0.80	0.50	4.00	0.70	5.00	0.31	3.00	3.00	4.00	0.70	0.13	1.99
12.30	0.80	0.50	4.00	0.70	5.00	0.31	3.00	3.00	4.00	0.70	0.19	2.40
12.30	0.80	0.50	4.00	0.70	5.00	0.31	3.00	3.00	4.00	0.70	0.25	2.42
12.30	0.80	0.50	4.00	0.30	15.00	0.31	3.00	3.00	4.00	0.30	0.13	89.54
12.30	0.80	0.50	4.00	0.30	15.00	0.31	3.00	3.00	4.00	0.30	0.19	96.80
12.30	0.80	0.50	4.00	0.30	15.00	0.31	3.00	3.00	4.00	0.30	0.25	84.63
12.30	0.80	0.50	4.00	0.30	15.00	0.31	3.00	3.00	4.00	0.50	0.13	86.58
12.30	0.80	0.50	4.00	0.30	15.00	0.31	3.00	3.00	4.00	0.50	0.19	96.78
12.30	0.80	0.50	4.00	0.30	15.00	0.31	3.00	3.00	4.00	0.50	0.25	87.20
12.30	0.80	0.50	4.00	0.30	15.00	0.31	3.00	3.00	4.00	0.70	0.13	84.86

12.30	0.80	0.50	4.00	0.30	15.00	0.31	3.00	3.00	4.00	0.70	0.19	95.42
12.30	0.80	0.50	4.00	0.30	15.00	0.31	3.00	3.00	4.00	0.70	0.25	86.77
12.30	0.80	0.50	4.00	0.50	15.00	0.31	3.00	3.00	4.00	0.30	0.13	25.09
12.30	0.80	0.50	4.00	0.50	15.00	0.31	3.00	3.00	4.00	0.30	0.19	23.72
12.30	0.80	0.50	4.00	0.50	15.00	0.31	3.00	3.00	4.00	0.30	0.25	21.85
12.30	0.80	0.50	4.00	0.50	15.00	0.31	3.00	3.00	4.00	0.50	0.13	23.73
12.30	0.80	0.50	4.00	0.50	15.00	0.31	3.00	3.00	4.00	0.50	0.19	23.20
12.30	0.80	0.50	4.00	0.50	15.00	0.31	3.00	3.00	4.00	0.50	0.25	22.23
12.30	0.80	0.50	4.00	0.50	15.00	0.31	3.00	3.00	4.00	0.70	0.13	23.24
12.30	0.80	0.50	4.00	0.50	15.00	0.31	3.00	3.00	4.00	0.70	0.19	22.85
12.30	0.80	0.50	4.00	0.50	15.00	0.31	3.00	3.00	4.00	0.70	0.25	22.08
12.30	0.80	0.50	4.00	0.70	15.00	0.31	3.00	3.00	4.00	0.30	0.13	11.67
12.30	0.80	0.50	4.00	0.70	15.00	0.31	3.00	3.00	4.00	0.30	0.19	11.01
12.30	0.80	0.50	4.00	0.70	15.00	0.31	3.00	3.00	4.00	0.30	0.25	9.51
12.30	0.80	0.50	4.00	0.70	15.00	0.31	3.00	3.00	4.00	0.50	0.13	10.35
12.30	0.80	0.50	4.00	0.70	15.00	0.31	3.00	3.00	4.00	0.50	0.19	10.18
12.30	0.80	0.50	4.00	0.70	15.00	0.31	3.00	3.00	4.00	0.50	0.25	9.41
12.30	0.80	0.50	4.00	0.70	15.00	0.31	3.00	3.00	4.00	0.70	0.13	9.86
12.30	0.80	0.50	4.00	0.70	15.00	0.31	3.00	3.00	4.00	0.70	0.19	9.73
12.30	0.80	0.50	4.00	0.70	15.00	0.31	3.00	3.00	4.00	0.70	0.25	9.15
12.30	0.80	0.50	4.00	0.30	25.00	0.31	3.00	3.00	4.00	0.30	0.13	160.55
12.30	0.80	0.50	4.00	0.30	25.00	0.31	3.00	3.00	4.00	0.30	0.19	176.36
12.30	0.80	0.50	4.00	0.30	25.00	0.31	3.00	3.00	4.00	0.30	0.25	155.61
12.30	0.80	0.50	4.00	0.30	25.00	0.31	3.00	3.00	4.00	0.50	0.13	156.84
12.30	0.80	0.50	4.00	0.30	25.00	0.31	3.00	3.00	4.00	0.50	0.19	176.85
12.30	0.80	0.50	4.00	0.30	25.00	0.31	3.00	3.00	4.00	0.50	0.25	160.17
12.30	0.80	0.50	4.00	0.30	25.00	0.31	3.00	3.00	4.00	0.70	0.13	154.51
12.30	0.80	0.50	4.00	0.30	25.00	0.31	3.00	3.00	4.00	0.70	0.19	175.01
12.30	0.80	0.50	4.00	0.30	25.00	0.31	3.00	3.00	4.00	0.70	0.25	159.74
12.30	0.80	0.50	4.00	0.50	25.00	0.31	3.00	3.00	4.00	0.30	0.13	45.16
12.30	0.80	0.50	4.00	0.50	25.00	0.31	3.00	3.00	4.00	0.30	0.19	43.01
12.30	0.80	0.50	4.00	0.50	25.00	0.31	3.00	3.00	4.00	0.30	0.25	40.23
12.30	0.80	0.50	4.00	0.50	25.00	0.31	3.00	3.00	4.00	0.50	0.13	43.93
12.30	0.80	0.50	4.00	0.50	25.00	0.31	3.00	3.00	4.00	0.50	0.19	42.96
12.30	0.80	0.50	4.00	0.50	25.00	0.31	3.00	3.00	4.00	0.50	0.25	41.49
12.30	0.80	0.50	4.00	0.50	25.00	0.31	3.00	3.00	4.00	0.70	0.13	43.54
12.30	0.80	0.50	4.00	0.50	25.00	0.31	3.00	3.00	4.00	0.70	0.19	42.80
12.30	0.80	0.50	4.00	0.50	25.00	0.31	3.00	3.00	4.00	0.70	0.25	41.64

12.30	0.80	0.50	4.00	0.70	25.00	0.31	3.00	3.00	4.00	0.30	0.13	20.98
12.30	0.80	0.50	4.00	0.70	25.00	0.31	3.00	3.00	4.00	0.30	0.19	19.86
12.30	0.80	0.50	4.00	0.70	25.00	0.31	3.00	3.00	4.00	0.30	0.25	17.63
12.30	0.80	0.50	4.00	0.70	25.00	0.31	3.00	3.00	4.00	0.50	0.13	19.46
12.30	0.80	0.50	4.00	0.70	25.00	0.31	3.00	3.00	4.00	0.50	0.19	19.10
12.30	0.80	0.50	4.00	0.70	25.00	0.31	3.00	3.00	4.00	0.50	0.25	17.95
12.30	0.80	0.50	4.00	0.70	25.00	0.31	3.00	3.00	4.00	0.70	0.13	18.96
12.30	0.80	0.50	4.00	0.70	25.00	0.31	3.00	3.00	4.00	0.70	0.19	18.69
12.30	0.80	0.50	4.00	0.70	25.00	0.31	3.00	3.00	4.00	0.70	0.25	17.82
12.30	0.80	0.50	4.00	0.30	35.00	0.31	3.00	3.00	4.00	0.30	0.13	236.30
12.30	0.80	0.50	4.00	0.30	35.00	0.31	3.00	3.00	4.00	0.30	0.19	260.67
12.30	0.80	0.50	4.00	0.30	35.00	0.31	3.00	3.00	4.00	0.30	0.25	230.51
12.30	0.80	0.50	4.00	0.30	35.00	0.31	3.00	3.00	4.00	0.50	0.13	231.14
12.30	0.80	0.50	4.00	0.30	35.00	0.31	3.00	3.00	4.00	0.50	0.19	261.22
12.30	0.80	0.50	4.00	0.30	35.00	0.31	3.00	3.00	4.00	0.50	0.25	236.85
12.30	0.80	0.50	4.00	0.30	35.00	0.31	3.00	3.00	4.00	0.70	0.13	228.04
12.30	0.80	0.50	4.00	0.30	35.00	0.31	3.00	3.00	4.00	0.70	0.19	258.78
12.30	0.80	0.50	4.00	0.30	35.00	0.31	3.00	3.00	4.00	0.70	0.25	236.37
12.30	0.80	0.50	4.00	0.50	35.00	0.31	3.00	3.00	4.00	0.30	0.13	66.76
12.30	0.80	0.50	4.00	0.50	35.00	0.31	3.00	3.00	4.00	0.30	0.19	63.81
12.30	0.80	0.50	4.00	0.50	35.00	0.31	3.00	3.00	4.00	0.30	0.25	59.97
12.30	0.80	0.50	4.00	0.50	35.00	0.31	3.00	3.00	4.00	0.50	0.13	65.40
12.30	0.80	0.50	4.00	0.50	35.00	0.31	3.00	3.00	4.00	0.50	0.19	64.00
12.30	0.80	0.50	4.00	0.50	35.00	0.31	3.00	3.00	4.00	0.50	0.25	61.96
12.30	0.80	0.50	4.00	0.50	35.00	0.31	3.00	3.00	4.00	0.70	0.13	65.08
12.30	0.80	0.50	4.00	0.50	35.00	0.31	3.00	3.00	4.00	0.70	0.19	63.98
12.30	0.80	0.50	4.00	0.50	35.00	0.31	3.00	3.00	4.00	0.70	0.25	62.37
12.30	0.80	0.50	4.00	0.70	35.00	0.31	3.00	3.00	4.00	0.30	0.13	31.15
12.30	0.80	0.50	4.00	0.70	35.00	0.31	3.00	3.00	4.00	0.30	0.19	29.56
12.30	0.80	0.50	4.00	0.70	35.00	0.31	3.00	3.00	4.00	0.30	0.25	26.49
12.30	0.80	0.50	4.00	0.70	35.00	0.31	3.00	3.00	4.00	0.50	0.13	29.21
12.30	0.80	0.50	4.00	0.70	35.00	0.31	3.00	3.00	4.00	0.50	0.19	28.69
12.30	0.80	0.50	4.00	0.70	35.00	0.31	3.00	3.00	4.00	0.50	0.25	27.13
12.30	0.80	0.50	4.00	0.70	35.00	0.31	3.00	3.00	4.00	0.70	0.13	28.66
12.30	0.80	0.50	4.00	0.70	35.00	0.31	3.00	3.00	4.00	0.70	0.19	28.27
12.30	0.80	0.50	4.00	0.70	35.00	0.31	3.00	3.00	4.00	0.70	0.25	27.09
12.30	0.80	0.50	4.00	0.30	45.00	0.31	3.00	3.00	4.00	0.30	0.13	314.90
12.30	0.80	0.50	4.00	0.30	45.00	0.31	3.00	3.00	4.00	0.30	0.19	347.47

12.30	0.80	0.50	4.00	0.30	45.00	0.31	3.00	3.00	4.00	0.30	0.25	307.21
12.30	0.80	0.50	4.00	0.30	45.00	0.31	3.00	3.00	4.00	0.50	0.13	307.33
12.30	0.80	0.50	4.00	0.30	45.00	0.31	3.00	3.00	4.00	0.50	0.19	347.42
12.30	0.80	0.50	4.00	0.30	45.00	0.31	3.00	3.00	4.00	0.50	0.25	314.97
12.30	0.80	0.50	4.00	0.30	45.00	0.31	3.00	3.00	4.00	0.70	0.13	303.24
12.30	0.80	0.50	4.00	0.30	45.00	0.31	3.00	3.00	4.00	0.70	0.19	344.18
12.30	0.80	0.50	4.00	0.30	45.00	0.31	3.00	3.00	4.00	0.70	0.25	314.30
12.30	0.80	0.50	4.00	0.50	45.00	0.31	3.00	3.00	4.00	0.30	0.13	89.45
12.30	0.80	0.50	4.00	0.50	45.00	0.31	3.00	3.00	4.00	0.30	0.19	85.58
12.30	0.80	0.50	4.00	0.50	45.00	0.31	3.00	3.00	4.00	0.30	0.25	80.48
12.30	0.80	0.50	4.00	0.50	45.00	0.31	3.00	3.00	4.00	0.50	0.13	87.54
12.30	0.80	0.50	4.00	0.50	45.00	0.31	3.00	3.00	4.00	0.50	0.19	85.67
12.30	0.80	0.50	4.00	0.50	45.00	0.31	3.00	3.00	4.00	0.50	0.25	82.99
12.30	0.80	0.50	4.00	0.50	45.00	0.31	3.00	3.00	4.00	0.70	0.13	87.17
12.30	0.80	0.50	4.00	0.50	45.00	0.31	3.00	3.00	4.00	0.70	0.19	85.71
12.30	0.80	0.50	4.00	0.50	45.00	0.31	3.00	3.00	4.00	0.70	0.25	83.57
12.30	0.80	0.50	4.00	0.70	45.00	0.31	3.00	3.00	4.00	0.30	0.13	41.95
12.30	0.80	0.50	4.00	0.70	45.00	0.31	3.00	3.00	4.00	0.30	0.19	39.84
12.30	0.80	0.50	4.00	0.70	45.00	0.31	3.00	3.00	4.00	0.30	0.25	35.81
12.30	0.80	0.50	4.00	0.70	45.00	0.31	3.00	3.00	4.00	0.50	0.13	39.34
12.30	0.80	0.50	4.00	0.70	45.00	0.31	3.00	3.00	4.00	0.50	0.19	38.64
12.30	0.80	0.50	4.00	0.70	45.00	0.31	3.00	3.00	4.00	0.50	0.25	36.63
12.30	0.80	0.50	4.00	0.70	45.00	0.31	3.00	3.00	4.00	0.70	0.13	38.66
12.30	0.80	0.50	4.00	0.70	45.00	0.31	3.00	3.00	4.00	0.70	0.19	38.14
12.30	0.80	0.50	4.00	0.70	45.00	0.31	3.00	3.00	4.00	0.70	0.25	36.63
12.30	0.80	0.50	4.00	0.30	55.00	0.31	3.00	3.00	4.00	0.30	0.13	393.83
12.30	0.80	0.50	4.00	0.30	55.00	0.31	3.00	3.00	4.00	0.30	0.19	434.01
12.30	0.80	0.50	4.00	0.30	55.00	0.31	3.00	3.00	4.00	0.30	0.25	383.30
12.30	0.80	0.50	4.00	0.30	55.00	0.31	3.00	3.00	4.00	0.50	0.13	383.15
12.30	0.80	0.50	4.00	0.30	55.00	0.31	3.00	3.00	4.00	0.50	0.19	432.85
12.30	0.80	0.50	4.00	0.30	55.00	0.31	3.00	3.00	4.00	0.50	0.25	392.18
12.30	0.80	0.50	4.00	0.30	55.00	0.31	3.00	3.00	4.00	0.70	0.13	377.83
12.30	0.80	0.50	4.00	0.30	55.00	0.31	3.00	3.00	4.00	0.70	0.19	428.61
12.30	0.80	0.50	4.00	0.30	55.00	0.31	3.00	3.00	4.00	0.70	0.25	391.17
12.30	0.80	0.50	4.00	0.50	55.00	0.31	3.00	3.00	4.00	0.30	0.13	112.43
12.30	0.80	0.50	4.00	0.50	55.00	0.31	3.00	3.00	4.00	0.30	0.19	107.56
12.30	0.80	0.50	4.00	0.50	55.00	0.31	3.00	3.00	4.00	0.30	0.25	101.08
12.30	0.80	0.50	4.00	0.50	55.00	0.31	3.00	3.00	4.00	0.50	0.13	109.68

12.30	0.80	0.50	4.00	0.50	55.00	0.31	3.00	3.00	4.00	0.50	0.19	107.34
12.30	0.80	0.50	4.00	0.50	55.00	0.31	3.00	3.00	4.00	0.50	0.25	103.95
12.30	0.80	0.50	4.00	0.50	55.00	0.31	3.00	3.00	4.00	0.70	0.13	109.17
12.30	0.80	0.50	4.00	0.50	55.00	0.31	3.00	3.00	4.00	0.70	0.19	107.31
12.30	0.80	0.50	4.00	0.50	55.00	0.31	3.00	3.00	4.00	0.70	0.25	104.61
12.30	0.80	0.50	4.00	0.70	55.00	0.31	3.00	3.00	4.00	0.30	0.13	53.00
12.30	0.80	0.50	4.00	0.70	55.00	0.31	3.00	3.00	4.00	0.30	0.19	50.31
12.30	0.80	0.50	4.00	0.70	55.00	0.31	3.00	3.00	4.00	0.30	0.25	45.23
12.30	0.80	0.50	4.00	0.70	55.00	0.31	3.00	3.00	4.00	0.50	0.13	49.53
12.30	0.80	0.50	4.00	0.70	55.00	0.31	3.00	3.00	4.00	0.50	0.19	48.65
12.30	0.80	0.50	4.00	0.70	55.00	0.31	3.00	3.00	4.00	0.50	0.25	46.14
12.30	0.80	0.50	4.00	0.70	55.00	0.31	3.00	3.00	4.00	0.70	0.13	48.65
12.30	0.80	0.50	4.00	0.70	55.00	0.31	3.00	3.00	4.00	0.70	0.19	48.00
12.30	0.80	0.50	4.00	0.70	55.00	0.31	3.00	3.00	4.00	0.70	0.25	46.13
12.30	0.80	0.50	4.00	0.30	5.00	0.31	3.00	4.00	4.00	0.30	0.13	31.24
12.30	0.80	0.50	4.00	0.30	5.00	0.31	3.00	4.00	4.00	0.30	0.19	20.15
12.30	0.80	0.50	4.00	0.30	5.00	0.31	3.00	4.00	4.00	0.30	0.25	20.13
12.30	0.80	0.50	4.00	0.30	5.00	0.31	3.00	4.00	4.00	0.50	0.13	27.09
12.30	0.80	0.50	4.00	0.30	5.00	0.31	3.00	4.00	4.00	0.50	0.19	19.75
12.30	0.80	0.50	4.00	0.30	5.00	0.31	3.00	4.00	4.00	0.50	0.25	20.88
12.30	0.80	0.50	4.00	0.30	5.00	0.31	3.00	4.00	4.00	0.70	0.13	24.94
12.30	0.80	0.50	4.00	0.30	5.00	0.31	3.00	4.00	4.00	0.70	0.19	19.03
12.30	0.80	0.50	4.00	0.30	5.00	0.31	3.00	4.00	4.00	0.70	0.25	20.31
12.30	0.80	0.50	4.00	0.50	5.00	0.31	3.00	4.00	4.00	0.30	0.13	5.98
12.30	0.80	0.50	4.00	0.50	5.00	0.31	3.00	4.00	4.00	0.30	0.19	5.98
12.30	0.80	0.50	4.00	0.50	5.00	0.31	3.00	4.00	4.00	0.30	0.25	4.97
12.30	0.80	0.50	4.00	0.50	5.00	0.31	3.00	4.00	4.00	0.50	0.13	4.86
12.30	0.80	0.50	4.00	0.50	5.00	0.31	3.00	4.00	4.00	0.50	0.19	5.15
12.30	0.80	0.50	4.00	0.50	5.00	0.31	3.00	4.00	4.00	0.50	0.25	4.63
12.30	0.80	0.50	4.00	0.50	5.00	0.31	3.00	4.00	4.00	0.70	0.13	4.32
12.30	0.80	0.50	4.00	0.50	5.00	0.31	3.00	4.00	4.00	0.70	0.19	4.60
12.30	0.80	0.50	4.00	0.50	5.00	0.31	3.00	4.00	4.00	0.70	0.25	4.22
12.30	0.80	0.50	4.00	0.70	5.00	0.31	3.00	4.00	4.00	0.30	0.13	2.51
12.30	0.80	0.50	4.00	0.70	5.00	0.31	3.00	4.00	4.00	0.30	0.19	2.62
12.30	0.80	0.50	4.00	0.70	5.00	0.31	3.00	4.00	4.00	0.30	0.25	2.53
12.30	0.80	0.50	4.00	0.70	5.00	0.31	3.00	4.00	4.00	0.50	0.13	1.68
12.30	0.80	0.50	4.00	0.70	5.00	0.31	3.00	4.00	4.00	0.50	0.19	2.02
12.30	0.80	0.50	4.00	0.70	5.00	0.31	3.00	4.00	4.00	0.50	0.25	2.19

12.30	0.80	0.50	4.00	0.70	5.00	0.31	3.00	4.00	4.00	0.70	0.13	1.34
12.30	0.80	0.50	4.00	0.70	5.00	0.31	3.00	4.00	4.00	0.70	0.19	1.70
12.30	0.80	0.50	4.00	0.70	5.00	0.31	3.00	4.00	4.00	0.70	0.25	1.92
12.30	0.80	0.50	4.00	0.30	15.00	0.31	3.00	4.00	4.00	0.30	0.13	106.23
12.30	0.80	0.50	4.00	0.30	15.00	0.31	3.00	4.00	4.00	0.30	0.19	84.16
12.30	0.80	0.50	4.00	0.30	15.00	0.31	3.00	4.00	4.00	0.30	0.25	89.80
12.30	0.80	0.50	4.00	0.30	15.00	0.31	3.00	4.00	4.00	0.50	0.13	98.15
12.30	0.80	0.50	4.00	0.30	15.00	0.31	3.00	4.00	4.00	0.50	0.19	84.40
12.30	0.80	0.50	4.00	0.30	15.00	0.31	3.00	4.00	4.00	0.50	0.25	91.87
12.30	0.80	0.50	4.00	0.30	15.00	0.31	3.00	4.00	4.00	0.70	0.13	94.32
12.30	0.80	0.50	4.00	0.30	15.00	0.31	3.00	4.00	4.00	0.70	0.19	83.53
12.30	0.80	0.50	4.00	0.30	15.00	0.31	3.00	4.00	4.00	0.70	0.25	91.14
12.30	0.80	0.50	4.00	0.50	15.00	0.31	3.00	4.00	4.00	0.30	0.13	23.52
12.30	0.80	0.50	4.00	0.50	15.00	0.31	3.00	4.00	4.00	0.30	0.19	24.24
12.30	0.80	0.50	4.00	0.50	15.00	0.31	3.00	4.00	4.00	0.30	0.25	21.45
12.30	0.80	0.50	4.00	0.50	15.00	0.31	3.00	4.00	4.00	0.50	0.13	22.49
12.30	0.80	0.50	4.00	0.50	15.00	0.31	3.00	4.00	4.00	0.50	0.19	23.71
12.30	0.80	0.50	4.00	0.50	15.00	0.31	3.00	4.00	4.00	0.50	0.25	21.73
12.30	0.80	0.50	4.00	0.50	15.00	0.31	3.00	4.00	4.00	0.70	0.13	22.13
12.30	0.80	0.50	4.00	0.50	15.00	0.31	3.00	4.00	4.00	0.70	0.19	23.28
12.30	0.80	0.50	4.00	0.50	15.00	0.31	3.00	4.00	4.00	0.70	0.25	21.56
12.30	0.80	0.50	4.00	0.70	15.00	0.31	3.00	4.00	4.00	0.30	0.13	11.55
12.30	0.80	0.50	4.00	0.70	15.00	0.31	3.00	4.00	4.00	0.30	0.19	10.89
12.30	0.80	0.50	4.00	0.70	15.00	0.31	3.00	4.00	4.00	0.30	0.25	9.95
12.30	0.80	0.50	4.00	0.70	15.00	0.31	3.00	4.00	4.00	0.50	0.13	10.27
12.30	0.80	0.50	4.00	0.70	15.00	0.31	3.00	4.00	4.00	0.50	0.19	10.08
12.30	0.80	0.50	4.00	0.70	15.00	0.31	3.00	4.00	4.00	0.50	0.25	9.74
12.30	0.80	0.50	4.00	0.70	15.00	0.31	3.00	4.00	4.00	0.70	0.13	9.80
12.30	0.80	0.50	4.00	0.70	15.00	0.31	3.00	4.00	4.00	0.70	0.19	9.66
12.30	0.80	0.50	4.00	0.70	15.00	0.31	3.00	4.00	4.00	0.70	0.25	9.44
12.30	0.80	0.50	4.00	0.30	25.00	0.31	3.00	4.00	4.00	0.30	0.13	189.71
12.30	0.80	0.50	4.00	0.30	25.00	0.31	3.00	4.00	4.00	0.30	0.19	154.40
12.30	0.80	0.50	4.00	0.30	25.00	0.31	3.00	4.00	4.00	0.30	0.25	166.39
12.30	0.80	0.50	4.00	0.30	25.00	0.31	3.00	4.00	4.00	0.50	0.13	177.14
12.30	0.80	0.50	4.00	0.30	25.00	0.31	3.00	4.00	4.00	0.50	0.19	155.41
12.30	0.80	0.50	4.00	0.30	25.00	0.31	3.00	4.00	4.00	0.50	0.25	169.92
12.30	0.80	0.50	4.00	0.30	25.00	0.31	3.00	4.00	4.00	0.70	0.13	171.34
12.30	0.80	0.50	4.00	0.30	25.00	0.31	3.00	4.00	4.00	0.70	0.19	154.36



12.30	0.80	0.50	4.00	0.30	25.00	0.31	3.00	4.00	4.00	0.70	0.25	168.96
12.30	0.80	0.50	4.00	0.50	25.00	0.31	3.00	4.00	4.00	0.30	0.13	43.31
12.30	0.80	0.50	4.00	0.50	25.00	0.31	3.00	4.00	4.00	0.30	0.19	44.99
12.30	0.80	0.50	4.00	0.50	25.00	0.31	3.00	4.00	4.00	0.30	0.25	40.33
12.30	0.80	0.50	4.00	0.50	25.00	0.31	3.00	4.00	4.00	0.50	0.13	42.56
12.30	0.80	0.50	4.00	0.50	25.00	0.31	3.00	4.00	4.00	0.50	0.19	44.88
12.30	0.80	0.50	4.00	0.50	25.00	0.31	3.00	4.00	4.00	0.50	0.25	41.40
12.30	0.80	0.50	4.00	0.50	25.00	0.31	3.00	4.00	4.00	0.70	0.13	42.38
12.30	0.80	0.50	4.00	0.50	25.00	0.31	3.00	4.00	4.00	0.70	0.19	44.57
12.30	0.80	0.50	4.00	0.50	25.00	0.31	3.00	4.00	4.00	0.70	0.25	41.49
12.30	0.80	0.50	4.00	0.70	25.00	0.31	3.00	4.00	4.00	0.30	0.13	21.50
12.30	0.80	0.50	4.00	0.70	25.00	0.31	3.00	4.00	4.00	0.30	0.19	20.41
12.30	0.80	0.50	4.00	0.70	25.00	0.31	3.00	4.00	4.00	0.30	0.25	19.07
12.30	0.80	0.50	4.00	0.70	25.00	0.31	3.00	4.00	4.00	0.50	0.13	20.04
12.30	0.80	0.50	4.00	0.70	25.00	0.31	3.00	4.00	4.00	0.50	0.19	19.66
12.30	0.80	0.50	4.00	0.70	25.00	0.31	3.00	4.00	4.00	0.50	0.25	19.20
12.30	0.80	0.50	4.00	0.70	25.00	0.31	3.00	4.00	4.00	0.70	0.13	19.54
12.30	0.80	0.50	4.00	0.70	25.00	0.31	3.00	4.00	4.00	0.70	0.19	19.27
12.30	0.80	0.50	4.00	0.70	25.00	0.31	3.00	4.00	4.00	0.70	0.25	18.99
12.30	0.80	0.50	4.00	0.30	35.00	0.31	3.00	4.00	4.00	0.30	0.13	279.28
12.30	0.80	0.50	4.00	0.30	35.00	0.31	3.00	4.00	4.00	0.30	0.19	228.75
12.30	0.80	0.50	4.00	0.30	35.00	0.31	3.00	4.00	4.00	0.30	0.25	247.11
12.30	0.80	0.50	4.00	0.30	35.00	0.31	3.00	4.00	4.00	0.50	0.13	260.88
12.30	0.80	0.50	4.00	0.30	35.00	0.31	3.00	4.00	4.00	0.50	0.19	230.18
12.30	0.80	0.50	4.00	0.30	35.00	0.31	3.00	4.00	4.00	0.50	0.25	251.87
12.30	0.80	0.50	4.00	0.30	35.00	0.31	3.00	4.00	4.00	0.70	0.13	252.78
12.30	0.80	0.50	4.00	0.30	35.00	0.31	3.00	4.00	4.00	0.70	0.19	228.85
12.30	0.80	0.50	4.00	0.30	35.00	0.31	3.00	4.00	4.00	0.70	0.25	250.62
12.30	0.80	0.50	4.00	0.50	35.00	0.31	3.00	4.00	4.00	0.30	0.13	64.56
12.30	0.80	0.50	4.00	0.50	35.00	0.31	3.00	4.00	4.00	0.30	0.19	67.26
12.30	0.80	0.50	4.00	0.50	35.00	0.31	3.00	4.00	4.00	0.30	0.25	60.53
12.30	0.80	0.50	4.00	0.50	35.00	0.31	3.00	4.00	4.00	0.50	0.13	63.88
12.30	0.80	0.50	4.00	0.50	35.00	0.31	3.00	4.00	4.00	0.50	0.19	67.34
12.30	0.80	0.50	4.00	0.50	35.00	0.31	3.00	4.00	4.00	0.50	0.25	62.24
12.30	0.80	0.50	4.00	0.50	35.00	0.31	3.00	4.00	4.00	0.70	0.13	63.83
12.30	0.80	0.50	4.00	0.50	35.00	0.31	3.00	4.00	4.00	0.70	0.19	67.10
12.30	0.80	0.50	4.00	0.50	35.00	0.31	3.00	4.00	4.00	0.70	0.25	62.55
12.30	0.80	0.50	4.00	0.70	35.00	0.31	3.00	4.00	4.00	0.30	0.13	32.28

12.30	0.80	0.50	4.00	0.70	35.00	0.31	3.00	4.00	4.00	0.30	0.19	30.75
12.30	0.80	0.50	4.00	0.70	35.00	0.31	3.00	4.00	4.00	0.30	0.25	28.94
12.30	0.80	0.50	4.00	0.70	35.00	0.31	3.00	4.00	4.00	0.50	0.13	30.44
12.30	0.80	0.50	4.00	0.70	35.00	0.31	3.00	4.00	4.00	0.50	0.19	29.90
12.30	0.80	0.50	4.00	0.70	35.00	0.31	3.00	4.00	4.00	0.50	0.25	29.29
12.30	0.80	0.50	4.00	0.70	35.00	0.31	3.00	4.00	4.00	0.70	0.13	29.88
12.30	0.80	0.50	4.00	0.70	35.00	0.31	3.00	4.00	4.00	0.70	0.19	29.49
12.30	0.80	0.50	4.00	0.70	35.00	0.31	3.00	4.00	4.00	0.70	0.25	29.14
12.30	0.80	0.50	4.00	0.30	45.00	0.31	3.00	4.00	4.00	0.30	0.13	372.75
12.30	0.80	0.50	4.00	0.30	45.00	0.31	3.00	4.00	4.00	0.30	0.19	305.19
12.30	0.80	0.50	4.00	0.30	45.00	0.31	3.00	4.00	4.00	0.30	0.25	329.69
12.30	0.80	0.50	4.00	0.30	45.00	0.31	3.00	4.00	4.00	0.50	0.13	346.94
12.30	0.80	0.50	4.00	0.30	45.00	0.31	3.00	4.00	4.00	0.50	0.19	306.51
12.30	0.80	0.50	4.00	0.30	45.00	0.31	3.00	4.00	4.00	0.50	0.25	335.30
12.30	0.80	0.50	4.00	0.30	45.00	0.31	3.00	4.00	4.00	0.70	0.13	336.18
12.30	0.80	0.50	4.00	0.30	45.00	0.31	3.00	4.00	4.00	0.70	0.19	304.75
12.30	0.80	0.50	4.00	0.30	45.00	0.31	3.00	4.00	4.00	0.70	0.25	333.61
12.30	0.80	0.50	4.00	0.50	45.00	0.31	3.00	4.00	4.00	0.30	0.13	86.78
12.30	0.80	0.50	4.00	0.50	45.00	0.31	3.00	4.00	4.00	0.30	0.19	90.48
12.30	0.80	0.50	4.00	0.50	45.00	0.31	3.00	4.00	4.00	0.30	0.25	81.46
12.30	0.80	0.50	4.00	0.50	45.00	0.31	3.00	4.00	4.00	0.50	0.13	85.82
12.30	0.80	0.50	4.00	0.50	45.00	0.31	3.00	4.00	4.00	0.50	0.19	90.44
12.30	0.80	0.50	4.00	0.50	45.00	0.31	3.00	4.00	4.00	0.50	0.25	83.61
12.30	0.80	0.50	4.00	0.50	45.00	0.31	3.00	4.00	4.00	0.70	0.13	85.82
12.30	0.80	0.50	4.00	0.50	45.00	0.31	3.00	4.00	4.00	0.70	0.19	90.17
12.30	0.80	0.50	4.00	0.50	45.00	0.31	3.00	4.00	4.00	0.70	0.25	84.06
12.30	0.80	0.50	4.00	0.70	45.00	0.31	3.00	4.00	4.00	0.30	0.13	43.68
12.30	0.80	0.50	4.00	0.70	45.00	0.31	3.00	4.00	4.00	0.30	0.19	41.64
12.30	0.80	0.50	4.00	0.70	45.00	0.31	3.00	4.00	4.00	0.30	0.25	39.27
12.30	0.80	0.50	4.00	0.70	45.00	0.31	3.00	4.00	4.00	0.50	0.13	41.20
12.30	0.80	0.50	4.00	0.70	45.00	0.31	3.00	4.00	4.00	0.50	0.19	40.47
12.30	0.80	0.50	4.00	0.70	45.00	0.31	3.00	4.00	4.00	0.50	0.25	39.70
12.30	0.80	0.50	4.00	0.70	45.00	0.31	3.00	4.00	4.00	0.70	0.13	40.50
12.30	0.80	0.50	4.00	0.70	45.00	0.31	3.00	4.00	4.00	0.70	0.19	39.98
12.30	0.80	0.50	4.00	0.70	45.00	0.31	3.00	4.00	4.00	0.70	0.25	39.54
12.30	0.80	0.50	4.00	0.30	55.00	0.31	3.00	4.00	4.00	0.30	0.13	467.11
12.30	0.80	0.50	4.00	0.30	55.00	0.31	3.00	4.00	4.00	0.30	0.19	381.31
12.30	0.80	0.50	4.00	0.30	55.00	0.31	3.00	4.00	4.00	0.30	0.25	411.54

12.30	0.80	0.50	4.00	0.30	55.00	0.31	3.00	4.00	4.00	0.50	0.13	432.79
12.30	0.80	0.50	4.00	0.30	55.00	0.31	3.00	4.00	4.00	0.50	0.19	382.12
12.30	0.80	0.50	4.00	0.30	55.00	0.31	3.00	4.00	4.00	0.50	0.25	417.71
12.30	0.80	0.50	4.00	0.30	55.00	0.31	3.00	4.00	4.00	0.70	0.13	419.01
12.30	0.80	0.50	4.00	0.30	55.00	0.31	3.00	4.00	4.00	0.70	0.19	379.78
12.30	0.80	0.50	4.00	0.30	55.00	0.31	3.00	4.00	4.00	0.70	0.25	415.44
12.30	0.80	0.50	4.00	0.50	55.00	0.31	3.00	4.00	4.00	0.30	0.13	109.20
12.30	0.80	0.50	4.00	0.50	55.00	0.31	3.00	4.00	4.00	0.30	0.19	113.86
12.30	0.80	0.50	4.00	0.50	55.00	0.31	3.00	4.00	4.00	0.30	0.25	102.43
12.30	0.80	0.50	4.00	0.50	55.00	0.31	3.00	4.00	4.00	0.50	0.13	107.73
12.30	0.80	0.50	4.00	0.50	55.00	0.31	3.00	4.00	4.00	0.50	0.19	113.48
12.30	0.80	0.50	4.00	0.50	55.00	0.31	3.00	4.00	4.00	0.50	0.25	104.86
12.30	0.80	0.50	4.00	0.50	55.00	0.31	3.00	4.00	4.00	0.70	0.13	107.69
12.30	0.80	0.50	4.00	0.50	55.00	0.31	3.00	4.00	4.00	0.70	0.19	113.08
12.30	0.80	0.50	4.00	0.50	55.00	0.31	3.00	4.00	4.00	0.70	0.25	105.38
12.30	0.80	0.50	4.00	0.70	55.00	0.31	3.00	4.00	4.00	0.30	0.13	55.29
12.30	0.80	0.50	4.00	0.70	55.00	0.31	3.00	4.00	4.00	0.30	0.19	52.68
12.30	0.80	0.50	4.00	0.70	55.00	0.31	3.00	4.00	4.00	0.30	0.25	49.67
12.30	0.80	0.50	4.00	0.70	55.00	0.31	3.00	4.00	4.00	0.50	0.13	51.99
12.30	0.80	0.50	4.00	0.70	55.00	0.31	3.00	4.00	4.00	0.50	0.19	51.06
12.30	0.80	0.50	4.00	0.70	55.00	0.31	3.00	4.00	4.00	0.50	0.25	50.09
12.30	0.80	0.50	4.00	0.70	55.00	0.31	3.00	4.00	4.00	0.70	0.13	51.08
12.30	0.80	0.50	4.00	0.70	55.00	0.31	3.00	4.00	4.00	0.70	0.19	50.42
12.30	0.80	0.50	4.00	0.70	55.00	0.31	3.00	4.00	4.00	0.70	0.25	49.88

## C.2 Half-Pipe Stiffener with Intermediate Connection Plate

bG	tF	tW	bS	tS	aS	bFP	tFP	dC	hC	bC	tC	aCW	DNV Stress
12.3	0.8	0.5	4	0.3	20	4	0.3125	3	1	4	0.3125	0.1875	49.77
12.3	0.8	0.5	4	0.3	20	4	0.3125	3	1	4	0.3125	0.1875	47.17
12.3	0.8	0.5	4	0.3	20	4	0.3125	3	1	4	0.3125	0.1875	45.98
12.3	0.8	0.5	4	0.3	20	4	0.3125	3	1	4	0.3125	0.1875	44.36
12.3	0.8	0.5	4	0.3	20	4	0.3125	3	1	4	0.3125	0.1875	36.73
12.3	0.8	0.5	4	0.3	20	4	0.3125	3	1	4	0.3125	0.1875	30.61
12.3	0.8	0.5	4	0.3	20	4	0.3125	3	1	4	0.3125	0.1875	9.82
12.3	0.8	0.5	4	0.3	20	4	0.3125	3	1	4	0.3125	0.1875	4.99
12.3	0.8	0.5	4	0.5	20	4	0.3125	3	1	4	0.3125	0.1875	13.76
12.3	0.8	0.5	4	0.5	20	4	0.3125	3	1	4	0.3125	0.1875	13.26
12.3	0.8	0.5	4	0.5	20	4	0.3125	3	1	4	0.3125	0.1875	12.46
12.3	0.8	0.5	4	0.5	20	4	0.3125	3	1	4	0.3125	0.1875	11.47
12.3	0.8	0.5	4	0.5	20	4	0.3125	3	1	4	0.3125	0.1875	9.71
12.3	0.8	0.5	4	0.5	20	4	0.3125	3	1	4	0.3125	0.1875	7.35
12.3	0.8	0.5	4	0.5	20	4	0.3125	3	1	4	0.3125	0.1875	2.21
12.3	0.8	0.5	4	0.5	20	4	0.3125	3	1	4	0.3125	0.1875	1.22
12.3	0.8	0.5	4	0.7	20	4	0.3125	3	1	4	0.3125	0.1875	6.90
12.3	0.8	0.5	4	0.7	20	4	0.3125	3	1	4	0.3125	0.1875	6.62
12.3	0.8	0.5	4	0.7	20	4	0.3125	3	1	4	0.3125	0.1875	6.19
12.3	0.8	0.5	4	0.7	20	4	0.3125	3	1	4	0.3125	0.1875	5.67
12.3	0.8	0.5	4	0.7	20	4	0.3125	3	1	4	0.3125	0.1875	4.84
12.3	0.8	0.5	4	0.7	20	4	0.3125	3	1	4	0.3125	0.1875	3.76
12.3	0.8	0.5	4	0.7	20	4	0.3125	3	1	4	0.3125	0.1875	1.57
12.3	0.8	0.5	4	0.3	40	4	0.3125	3	1	4	0.3125	0.1875	47.70
12.3	0.8	0.5	4	0.3	40	4	0.3125	3	1	4	0.3125	0.1875	44.62
12.3	0.8	0.5	4	0.3	40	4	0.3125	3	1	4	0.3125	0.1875	43.62
12.3	0.8	0.5	4	0.3	40	4	0.3125	3	1	4	0.3125	0.1875	40.50
12.3	0.8	0.5	4	0.3	40	4	0.3125	3	1	4	0.3125	0.1875	33.67
12.3	0.8	0.5	4	0.3	40	4	0.3125	3	1	4	0.3125	0.1875	25.94
12.3	0.8	0.5	4	0.3	40	4	0.3125	3	1	4	0.3125	0.1875	4.57
12.3	0.8	0.5	4	0.5	40	4	0.3125	3	1	4	0.3125	0.1875	15.48

12.3	0.8	0.5	4	0.5	40	4	0.3125	3	1	4	0.3125	0.1875	14.57
12.3	0.8	0.5	4	0.5	40	4	0.3125	3	1	4	0.3125	0.1875	13.71
12.3	0.8	0.5	4	0.5	40	4	0.3125	3	1	4	0.3125	0.1875	12.34
12.3	0.8	0.5	4	0.5	40	4	0.3125	3	1	4	0.3125	0.1875	10.17
12.3	0.8	0.5	4	0.5	40	4	0.3125	3	1	4	0.3125	0.1875	7.34
12.3	0.8	0.5	4	0.7	40	4	0.3125	3	1	4	0.3125	0.1875	7.67
12.3	0.8	0.5	4	0.7	40	4	0.3125	3	1	4	0.3125	0.1875	7.25
12.3	0.8	0.5	4	0.7	40	4	0.3125	3	1	4	0.3125	0.1875	6.67
12.3	0.8	0.5	4	0.7	40	4	0.3125	3	1	4	0.3125	0.1875	5.95
12.3	0.8	0.5	4	0.7	40	4	0.3125	3	1	4	0.3125	0.1875	4.90
12.3	0.8	0.5	4	0.7	40	4	0.3125	3	1	4	0.3125	0.1875	3.53
12.3	0.8	0.5	4	0.3	20	4	0.3125	3	2	4	0.3125	0.1875	32.59
12.3	0.8	0.5	4	0.3	20	4	0.3125	3	2	4	0.3125	0.1875	31.00
12.3	0.8	0.5	4	0.3	20	4	0.3125	3	2	4	0.3125	0.1875	30.49
12.3	0.8	0.5	4	0.3	20	4	0.3125	3	2	4	0.3125	0.1875	28.95
12.3	0.8	0.5	4	0.3	20	4	0.3125	3	2	4	0.3125	0.1875	23.93
12.3	0.8	0.5	4	0.3	20	4	0.3125	3	2	4	0.3125	0.1875	18.90
12.3	0.8	0.5	4	0.3	20	4	0.3125	3	2	4	0.3125	0.1875	2.76
12.3	0.8	0.5	4	0.3	20	4	0.3125	3	2	4	0.3125	0.1875	1.71
12.3	0.8	0.5	4	0.5	20	4	0.3125	3	2	4	0.3125	0.1875	9.32
12.3	0.8	0.5	4	0.5	20	4	0.3125	3	2	4	0.3125	0.1875	8.96
12.3	0.8	0.5	4	0.5	20	4	0.3125	3	2	4	0.3125	0.1875	8.30
12.3	0.8	0.5	4	0.5	20	4	0.3125	3	2	4	0.3125	0.1875	7.55
12.3	0.8	0.5	4	0.5	20	4	0.3125	3	2	4	0.3125	0.1875	6.19
12.3	0.8	0.5	4	0.5	20	4	0.3125	3	2	4	0.3125	0.1875	4.44
12.3	0.8	0.5	4	0.7	20	4	0.3125	3	2	4	0.3125	0.1875	4.62
12.3	0.8	0.5	4	0.7	20	4	0.3125	3	2	4	0.3125	0.1875	4.39
12.3	0.8	0.5	4	0.7	20	4	0.3125	3	2	4	0.3125	0.1875	4.04
12.3	0.8	0.5	4	0.7	20	4	0.3125	3	2	4	0.3125	0.1875	3.63
12.3	0.8	0.5	4	0.7	20	4	0.3125	3	2	4	0.3125	0.1875	2.99
12.3	0.8	0.5	4	0.7	20	4	0.3125	3	2	4	0.3125	0.1875	2.18
12.3	0.8	0.5	4	0.3	40	4	0.3125	3	2	4	0.3125	0.1875	32.65
12.3	0.8	0.5	4	0.3	40	4	0.3125	3	2	4	0.3125	0.1875	30.57
12.3	0.8	0.5	4	0.3	40	4	0.3125	3	2	4	0.3125	0.1875	29.78
12.3	0.8	0.5	4	0.3	40	4	0.3125	3	2	4	0.3125	0.1875	27.13
12.3	0.8	0.5	4	0.3	40	4	0.3125	3	2	4	0.3125	0.1875	22.05
12.3	0.8	0.5	4	0.3	40	4	0.3125	3	2	4	0.3125	0.1875	15.64
12.3	0.8	0.5	4	0.5	40	4	0.3125	3	2	4	0.3125	0.1875	10.44

12.3	0.8	0.5	4	0.5	40	4	0.3125	3	2	4	0.3125	0.1875	9.71
12.3	0.8	0.5	4	0.5	40	4	0.3125	3	2	4	0.3125	0.1875	8.94
12.3	0.8	0.5	4	0.5	40	4	0.3125	3	2	4	0.3125	0.1875	7.79
12.3	0.8	0.5	4	0.5	40	4	0.3125	3	2	4	0.3125	0.1875	6.08
12.3	0.8	0.5	4	0.5	40	4	0.3125	3	2	4	0.3125	0.1875	3.73
12.3	0.8	0.5	4	0.7	40	4	0.3125	3	2	4	0.3125	0.1875	5.12
12.3	0.8	0.5	4	0.7	40	4	0.3125	3	2	4	0.3125	0.1875	4.75
12.3	0.8	0.5	4	0.7	40	4	0.3125	3	2	4	0.3125	0.1875	4.25
12.3	0.8	0.5	4	0.7	40	4	0.3125	3	2	4	0.3125	0.1875	3.64
12.3	0.8	0.5	4	0.7	40	4	0.3125	3	2	4	0.3125	0.1875	2.80
12.3	0.8	0.5	4	0.7	40	4	0.3125	3	2	4	0.3125	0.1875	1.66
12.3	0.8	0.5	4	0.3	20	4	0.3125	3	3	4	0.3125	0.1875	16.75
12.3	0.8	0.5	4	0.3	20	4	0.3125	3	3	4	0.3125	0.1875	16.17
12.3	0.8	0.5	4	0.3	20	4	0.3125	3	3	4	0.3125	0.1875	16.15
12.3	0.8	0.5	4	0.3	20	4	0.3125	3	3	4	0.3125	0.1875	14.76
12.3	0.8	0.5	4	0.3	20	4	0.3125	3	3	4	0.3125	0.1875	12.01
12.3	0.8	0.5	4	0.3	20	4	0.3125	3	3	4	0.3125	0.1875	8.04
12.3	0.8	0.5	4	0.5	20	4	0.3125	3	3	4	0.3125	0.1875	5.26
12.3	0.8	0.5	4	0.5	20	4	0.3125	3	3	4	0.3125	0.1875	5.02
12.3	0.8	0.5	4	0.5	20	4	0.3125	3	3	4	0.3125	0.1875	4.53
12.3	0.8	0.5	4	0.5	20	4	0.3125	3	3	4	0.3125	0.1875	3.99
12.3	0.8	0.5	4	0.5	20	4	0.3125	3	3	4	0.3125	0.1875	2.99
12.3	0.8	0.5	4	0.5	20	4	0.3125	3	3	4	0.3125	0.1875	1.78
12.3	0.8	0.5	4	0.7	20	4	0.3125	3	3	4	0.3125	0.1875	2.61
12.3	0.8	0.5	4	0.7	20	4	0.3125	3	3	4	0.3125	0.1875	2.43
12.3	0.8	0.5	4	0.7	20	4	0.3125	3	3	4	0.3125	0.1875	2.16
12.3	0.8	0.5	4	0.7	20	4	0.3125	3	3	4	0.3125	0.1875	1.85
12.3	0.8	0.5	4	0.7	20	4	0.3125	3	3	4	0.3125	0.1875	1.40
12.3	0.8	0.5	4	0.3	40	4	0.3125	3	3	4	0.3125	0.1875	18.46
12.3	0.8	0.5	4	0.3	40	4	0.3125	3	3	4	0.3125	0.1875	17.35
12.3	0.8	0.5	4	0.3	40	4	0.3125	3	3	4	0.3125	0.1875	16.72
12.3	0.8	0.5	4	0.3	40	4	0.3125	3	3	4	0.3125	0.1875	14.56
12.3	0.8	0.5	4	0.3	40	4	0.3125	3	3	4	0.3125	0.1875	11.07
12.3	0.8	0.5	4	0.3	40	4	0.3125	3	3	4	0.3125	0.1875	5.12
12.3	0.8	0.5	4	0.5	40	4	0.3125	3	3	4	0.3125	0.1875	5.82
12.3	0.8	0.5	4	0.5	40	4	0.3125	3	3	4	0.3125	0.1875	5.28
12.3	0.8	0.5	4	0.5	40	4	0.3125	3	3	4	0.3125	0.1875	4.60
12.3	0.8	0.5	4	0.5	40	4	0.3125	3	3	4	0.3125	0.1875	3.67

12.3	0.8	0.5	4	0.5	40	4	0.3125	3	3	4	0.3125	0.1875	2.38
12.3	0.8	0.5	4	0.7	40	4	0.3125	3	3	4	0.3125	0.1875	2.87
12.3	0.8	0.5	4	0.7	40	4	0.3125	3	3	4	0.3125	0.1875	2.56
12.3	0.8	0.5	4	0.7	40	4	0.3125	3	3	4	0.3125	0.1875	2.15
12.3	0.8	0.5	4	0.7	40	4	0.3125	3	3	4	0.3125	0.1875	1.65
12.3	0.8	0.5	4	0.7	40	4	0.3125	3	3	4	0.3125	0.1875	1.00
12.3	0.8	0.5	4	0.3	20	4	0.3125	3	4	4	0.3125	0.1875	2.96
12.3	0.8	0.5	4	0.3	20	4	0.3125	3	4	4	0.3125	0.1875	3.47
12.3	0.8	0.5	4	0.3	20	4	0.3125	3	4	4	0.3125	0.1875	3.63
12.3	0.8	0.5	4	0.3	20	4	0.3125	3	4	4	0.3125	0.1875	2.73
12.3	0.8	0.5	4	0.3	20	4	0.3125	3	4	4	0.3125	0.1875	1.57
12.3	0.8	0.5	4	0.5	20	4	0.3125	3	4	4	0.3125	0.1875	1.64
12.3	0.8	0.5	4	0.5	20	4	0.3125	3	4	4	0.3125	0.1875	1.55
12.3	0.8	0.5	4	0.5	20	4	0.3125	3	4	4	0.3125	0.1875	1.21
12.3	0.8	0.5	4	0.3	40	4	0.3125	3	4	4	0.3125	0.1875	5.53
12.3	0.8	0.5	4	0.3	40	4	0.3125	3	4	4	0.3125	0.1875	5.41
12.3	0.8	0.5	4	0.3	40	4	0.3125	3	4	4	0.3125	0.1875	4.92
12.3	0.8	0.5	4	0.3	40	4	0.3125	3	4	4	0.3125	0.1875	3.35
12.3	0.8	0.5	4	0.5	40	4	0.3125	3	4	4	0.3125	0.1875	1.72
12.3	0.8	0.5	4	0.5	40	4	0.3125	3	4	4	0.3125	0.1875	1.39
12.3	0.8	0.5	4	0.3	40	4	0.3125	3	4	4	0.3125	0.0625	2.97
12.3	0.8	0.5	4	0.3	40	4	0.3125	3	4	4	0.3125	0.0625	3.63
12.3	0.8	0.5	4	0.3	40	4	0.3125	3	4	4	0.3125	0.0625	3.90
12.3	0.8	0.5	4	0.3	40	4	0.3125	3	4	4	0.3125	0.0625	2.60
12.3	0.8	0.5	4	0.3	40	4	0.3125	3	4	4	0.3125	0.0625	1.19
12.3	0.8	0.5	4	0.5	40	4	0.3125	3	4	4	0.3125	0.0625	1.57
12.3	0.8	0.5	4	0.5	40	4	0.3125	3	4	4	0.3125	0.0625	1.25
12.3	0.8	0.5	4	0.3	40	4	0.3125	3	4	4	0.3125	0.125	4.44
12.3	0.8	0.5	4	0.3	40	4	0.3125	3	4	4	0.3125	0.125	4.55
12.3	0.8	0.5	4	0.3	40	4	0.3125	3	4	4	0.3125	0.125	4.40
12.3	0.8	0.5	4	0.3	40	4	0.3125	3	4	4	0.3125	0.125	3.03
12.3	0.8	0.5	4	0.3	40	4	0.3125	3	4	4	0.3125	0.125	1.01
12.3	0.8	0.5	4	0.5	40	4	0.3125	3	4	4	0.3125	0.125	1.62
12.3	0.8	0.5	4	0.5	40	4	0.3125	3	4	4	0.3125	0.125	1.30
12.3	0.8	0.5	4	0.3	40	4	0.3125	3	0.5	4	0.3125	0.0625	53.82
12.3	0.8	0.5	4	0.3	40	4	0.3125	3	0.5	4	0.3125	0.0625	49.63
12.3	0.8	0.5	4	0.3	40	4	0.3125	3	0.5	4	0.3125	0.0625	19.98
12.3	0.8	0.5	4	0.3	40	4	0.3125	3	0.5	4	0.3125	0.0625	11.21

12.3	0.8	0.5	4	0.4	40	4	0.3125	3	0.5	4	0.3125	0.0625	25.68
12.3	0.8	0.5	4	0.4	40	4	0.3125	3	0.5	4	0.3125	0.0625	22.12
12.3	0.8	0.5	4	0.4	40	4	0.3125	3	0.5	4	0.3125	0.0625	7.50
12.3	0.8	0.5	4	0.4	40	4	0.3125	3	0.5	4	0.3125	0.0625	4.97
12.3	0.8	0.5	4	0.5	40	4	0.3125	3	0.5	4	0.3125	0.0625	12.50
12.3	0.8	0.5	4	0.5	40	4	0.3125	3	0.5	4	0.3125	0.0625	9.24
12.3	0.8	0.5	4	0.5	40	4	0.3125	3	0.5	4	0.3125	0.0625	2.12
12.3	0.8	0.5	4	0.5	40	4	0.3125	3	0.5	4	0.3125	0.0625	1.02
12.3	0.8	0.5	4	0.6	40	4	0.3125	3	0.5	4	0.3125	0.0625	8.64
12.3	0.8	0.5	4	0.6	40	4	0.3125	3	0.5	4	0.3125	0.0625	6.43
12.3	0.8	0.5	4	0.6	40	4	0.3125	3	0.5	4	0.3125	0.0625	1.68
12.3	0.8	0.5	4	0.7	40	4	0.3125	3	0.5	4	0.3125	0.0625	6.44
12.3	0.8	0.5	4	0.7	40	4	0.3125	3	0.5	4	0.3125	0.0625	4.92
12.3	0.8	0.5	4	0.7	40	4	0.3125	3	0.5	4	0.3125	0.0625	1.58
12.3	0.8	0.5	4	0.3	40	4	0.3125	3	0.5	4	0.3125	0.125	44.01
12.3	0.8	0.5	4	0.3	40	4	0.3125	3	0.5	4	0.3125	0.125	38.49
12.3	0.8	0.5	4	0.3	40	4	0.3125	3	0.5	4	0.3125	0.125	13.79
12.3	0.8	0.5	4	0.3	40	4	0.3125	3	0.5	4	0.3125	0.125	8.19
12.3	0.8	0.5	4	0.4	40	4	0.3125	3	0.5	4	0.3125	0.125	19.80
12.3	0.8	0.5	4	0.4	40	4	0.3125	3	0.5	4	0.3125	0.125	14.58
12.3	0.8	0.5	4	0.4	40	4	0.3125	3	0.5	4	0.3125	0.125	2.93
12.3	0.8	0.5	4	0.4	40	4	0.3125	3	0.5	4	0.3125	0.125	1.79
12.3	0.8	0.5	4	0.5	40	4	0.3125	3	0.5	4	0.3125	0.125	12.40
12.3	0.8	0.5	4	0.5	40	4	0.3125	3	0.5	4	0.3125	0.125	9.16
12.3	0.8	0.5	4	0.5	40	4	0.3125	3	0.5	4	0.3125	0.125	1.85
12.3	0.8	0.5	4	0.6	40	4	0.3125	3	0.5	4	0.3125	0.125	8.54
12.3	0.8	0.5	4	0.6	40	4	0.3125	3	0.5	4	0.3125	0.125	6.38
12.3	0.8	0.5	4	0.6	40	4	0.3125	3	0.5	4	0.3125	0.125	1.45
12.3	0.8	0.5	4	0.7	40	4	0.3125	3	0.5	4	0.3125	0.125	6.17
12.3	0.8	0.5	4	0.7	40	4	0.3125	3	0.5	4	0.3125	0.125	4.66
12.3	0.8	0.5	4	0.7	40	4	0.3125	3	0.5	4	0.3125	0.125	1.20
12.3	0.8	0.5	4	0.3	40	4	0.3125	3	0.5	4	0.3125	0.1875	39.54
12.3	0.8	0.5	4	0.3	40	4	0.3125	3	0.5	4	0.3125	0.1875	31.13
12.3	0.8	0.5	4	0.3	40	4	0.3125	3	0.5	4	0.3125	0.1875	7.98
12.3	0.8	0.5	4	0.3	40	4	0.3125	3	0.5	4	0.3125	0.1875	1.79
12.3	0.8	0.5	4	0.4	40	4	0.3125	3	0.5	4	0.3125	0.1875	20.68
12.3	0.8	0.5	4	0.4	40	4	0.3125	3	0.5	4	0.3125	0.1875	15.86
12.3	0.8	0.5	4	0.4	40	4	0.3125	3	0.5	4	0.3125	0.1875	3.20



12.3	0.8	0.5	4	0.5	40	4	0.3125	3	0.5	4	0.3125	0.1875	12.28
12.3	0.8	0.5	4	0.5	40	4	0.3125	3	0.5	4	0.3125	0.1875	9.15
12.3	0.8	0.5	4	0.5	40	4	0.3125	3	0.5	4	0.3125	0.1875	1.51
12.3	0.8	0.5	4	0.6	40	4	0.3125	3	0.5	4	0.3125	0.1875	8.06
12.3	0.8	0.5	4	0.6	40	4	0.3125	3	0.5	4	0.3125	0.1875	5.90
12.3	0.8	0.5	4	0.6	40	4	0.3125	3	0.5	4	0.3125	0.1875	1.06
12.3	0.8	0.5	4	0.7	40	4	0.3125	3	0.5	4	0.3125	0.1875	6.01
12.3	0.8	0.5	4	0.7	40	4	0.3125	3	0.5	4	0.3125	0.1875	4.52
12.3	0.8	0.5	4	0.7	40	4	0.3125	3	0.5	4	0.3125	0.1875	1.18
12.3	0.8	0.5	4	0.3	40	4	0.3125	3	0.5	4	0.3125	0.25	39.99
12.3	0.8	0.5	4	0.3	40	4	0.3125	3	0.5	4	0.3125	0.25	33.61
12.3	0.8	0.5	4	0.3	40	4	0.3125	3	0.5	4	0.3125	0.25	10.29
12.3	0.8	0.5	4	0.3	40	4	0.3125	3	0.5	4	0.3125	0.25	3.10
12.3	0.8	0.5	4	0.4	40	4	0.3125	3	0.5	4	0.3125	0.25	19.29
12.3	0.8	0.5	4	0.4	40	4	0.3125	3	0.5	4	0.3125	0.25	14.70
12.3	0.8	0.5	4	0.4	40	4	0.3125	3	0.5	4	0.3125	0.25	2.88
12.3	0.8	0.5	4	0.5	40	4	0.3125	3	0.5	4	0.3125	0.25	11.32
12.3	0.8	0.5	4	0.5	40	4	0.3125	3	0.5	4	0.3125	0.25	8.14
12.3	0.8	0.5	4	0.5	40	4	0.3125	3	0.5	4	0.3125	0.25	1.05
12.3	0.8	0.5	4	0.6	40	4	0.3125	3	0.5	4	0.3125	0.25	7.94
12.3	0.8	0.5	4	0.6	40	4	0.3125	3	0.5	4	0.3125	0.25	5.83
12.3	0.8	0.5	4	0.6	40	4	0.3125	3	0.5	4	0.3125	0.25	1.09
12.3	0.8	0.5	4	0.7	40	4	0.3125	3	0.5	4	0.3125	0.25	5.82
12.3	0.8	0.5	4	0.7	40	4	0.3125	3	0.5	4	0.3125	0.25	4.36
12.3	0.8	0.5	4	0.7	40	4	0.3125	3	0.5	4	0.3125	0.25	1.10

### C.3 Half-Pipe Stiffener without Intermediate Connection Plate

bG	tF	tW	bS	tS	aS	aW	dC	hC	bC	tC	aCW	DNV Stress
12.3	0.8	0.5	4	0.3	15	0.3125	3	0.5	4	0.1	0.0625	45.33
12.3	0.8	0.5	4	0.3	15	0.3125	3	0.5	4	0.3	0.0625	66.66
12.3	0.8	0.5	4	0.3	15	0.3125	3	0.5	4	0.5	0.0625	85.14
12.3	0.8	0.5	4	0.3	15	0.3125	3	0.5	4	0.7	0.0625	58.02
12.3	0.8	0.5	4	0.4	15	0.3125	3	0.5	4	0.1	0.0625	25.31
12.3	0.8	0.5	4	0.4	15	0.3125	3	0.5	4	0.3	0.0625	32.80
12.3	0.8	0.5	4	0.4	15	0.3125	3	0.5	4	0.5	0.0625	41.22

12.3	0.8	0.5	4	0.4	15	0.3125	3	0.5	4	0.7	0.0625	56.69
12.3	0.8	0.5	4	0.5	15	0.3125	3	0.5	4	0.1	0.0625	16.21
12.3	0.8	0.5	4	0.5	15	0.3125	3	0.5	4	0.3	0.0625	17.11
12.3	0.8	0.5	4	0.5	15	0.3125	3	0.5	4	0.5	0.0625	20.96
12.3	0.8	0.5	4	0.5	15	0.3125	3	0.5	4	0.7	0.0625	52.09
12.3	0.8	0.5	4	0.6	15	0.3125	3	0.5	4	0.1	0.0625	11.30
12.3	0.8	0.5	4	0.6	15	0.3125	3	0.5	4	0.3	0.0625	12.01
12.3	0.8	0.5	4	0.6	15	0.3125	3	0.5	4	0.5	0.0625	14.59
12.3	0.8	0.5	4	0.6	15	0.3125	3	0.5	4	0.7	0.0625	30.39
12.3	0.8	0.5	4	0.7	15	0.3125	3	0.5	4	0.1	0.0625	8.35
12.3	0.8	0.5	4	0.7	15	0.3125	3	0.5	4	0.3	0.0625	8.90
12.3	0.8	0.5	4	0.7	15	0.3125	3	0.5	4	0.5	0.0625	10.24
12.3	0.8	0.5	4	0.7	15	0.3125	3	0.5	4	0.7	0.0625	17.42
12.3	0.8	0.5	4	0.3	15	0.3125	3	0.5	4	0.1	0.125	42.96
12.3	0.8	0.5	4	0.3	15	0.3125	3	0.5	4	0.3	0.125	56.36
12.3	0.8	0.5	4	0.3	15	0.3125	3	0.5	4	0.5	0.125	72.28
12.3	0.8	0.5	4	0.3	15	0.3125	3	0.5	4	0.7	0.125	97.50
12.3	0.8	0.5	4	0.4	15	0.3125	3	0.5	4	0.1	0.125	23.59
12.3	0.8	0.5	4	0.4	15	0.3125	3	0.5	4	0.3	0.125	26.60
12.3	0.8	0.5	4	0.4	15	0.3125	3	0.5	4	0.5	0.125	42.05
12.3	0.8	0.5	4	0.4	15	0.3125	3	0.5	4	0.7	0.125	78.10
12.3	0.8	0.5	4	0.5	15	0.3125	3	0.5	4	0.1	0.125	15.35
12.3	0.8	0.5	4	0.5	15	0.3125	3	0.5	4	0.3	0.125	16.86
12.3	0.8	0.5	4	0.5	15	0.3125	3	0.5	4	0.5	0.125	24.17
12.3	0.8	0.5	4	0.5	15	0.3125	3	0.5	4	0.7	0.125	42.63
12.3	0.8	0.5	4	0.6	15	0.3125	3	0.5	4	0.1	0.125	10.78
12.3	0.8	0.5	4	0.6	15	0.3125	3	0.5	4	0.3	0.125	11.70
12.3	0.8	0.5	4	0.6	15	0.3125	3	0.5	4	0.5	0.125	14.73
12.3	0.8	0.5	4	0.6	15	0.3125	3	0.5	4	0.7	0.125	22.33
12.3	0.8	0.5	4	0.7	15	0.3125	3	0.5	4	0.1	0.125	8.00
12.3	0.8	0.5	4	0.7	15	0.3125	3	0.5	4	0.3	0.125	8.51
12.3	0.8	0.5	4	0.7	15	0.3125	3	0.5	4	0.5	0.125	9.28
12.3	0.8	0.5	4	0.7	15	0.3125	3	0.5	4	0.7	0.125	12.00
12.3	0.8	0.5	4	0.3	15	0.3125	3	0.5	4	0.1	0.1875	39.58
12.3	0.8	0.5	4	0.3	15	0.3125	3	0.5	4	0.3	0.1875	53.18
12.3	0.8	0.5	4	0.3	15	0.3125	3	0.5	4	0.5	0.1875	82.49
12.3	0.8	0.5	4	0.3	15	0.3125	3	0.5	4	0.7	0.1875	95.13
12.3	0.8	0.5	4	0.4	15	0.3125	3	0.5	4	0.1	0.1875	22.53

12.3	0.8	0.5	4	0.4	15	0.3125	3	0.5	4	0.3	0.1875	28.08
12.3	0.8	0.5	4	0.4	15	0.3125	3	0.5	4	0.5	0.1875	41.62
12.3	0.8	0.5	4	0.4	15	0.3125	3	0.5	4	0.7	0.1875	56.67
12.3	0.8	0.5	4	0.5	15	0.3125	3	0.5	4	0.1	0.1875	14.62
12.3	0.8	0.5	4	0.5	15	0.3125	3	0.5	4	0.3	0.1875	16.66
12.3	0.8	0.5	4	0.5	15	0.3125	3	0.5	4	0.5	0.1875	21.58
12.3	0.8	0.5	4	0.5	15	0.3125	3	0.5	4	0.7	0.1875	32.89
12.3	0.8	0.5	4	0.6	15	0.3125	3	0.5	4	0.1	0.1875	10.29
12.3	0.8	0.5	4	0.6	15	0.3125	3	0.5	4	0.3	0.1875	11.07
12.3	0.8	0.5	4	0.6	15	0.3125	3	0.5	4	0.5	0.1875	12.89
12.3	0.8	0.5	4	0.6	15	0.3125	3	0.5	4	0.7	0.1875	20.58
12.3	0.8	0.5	4	0.7	15	0.3125	3	0.5	4	0.1	0.1875	7.69
12.3	0.8	0.5	4	0.7	15	0.3125	3	0.5	4	0.3	0.1875	8.25
12.3	0.8	0.5	4	0.7	15	0.3125	3	0.5	4	0.5	0.1875	9.36
12.3	0.8	0.5	4	0.7	15	0.3125	3	0.5	4	0.7	0.1875	13.45
12.3	0.8	0.5	4	0.3	15	0.3125	3	0.5	4	0.1	0.25	38.34
12.3	0.8	0.5	4	0.3	15	0.3125	3	0.5	4	0.3	0.25	54.33
12.3	0.8	0.5	4	0.3	15	0.3125	3	0.5	4	0.5	0.25	68.10
12.3	0.8	0.5	4	0.3	15	0.3125	3	0.5	4	0.7	0.25	85.47
12.3	0.8	0.5	4	0.4	15	0.3125	3	0.5	4	0.1	0.25	21.31
12.3	0.8	0.5	4	0.4	15	0.3125	3	0.5	4	0.3	0.25	25.91
12.3	0.8	0.5	4	0.4	15	0.3125	3	0.5	4	0.5	0.25	35.14
12.3	0.8	0.5	4	0.4	15	0.3125	3	0.5	4	0.7	0.25	58.23
12.3	0.8	0.5	4	0.5	15	0.3125	3	0.5	4	0.1	0.25	13.85
12.3	0.8	0.5	4	0.5	15	0.3125	3	0.5	4	0.3	0.25	15.43
12.3	0.8	0.5	4	0.5	15	0.3125	3	0.5	4	0.5	0.25	20.64
12.3	0.8	0.5	4	0.5	15	0.3125	3	0.5	4	0.7	0.25	34.75
12.3	0.8	0.5	4	0.6	15	0.3125	3	0.5	4	0.1	0.25	9.84
12.3	0.8	0.5	4	0.6	15	0.3125	3	0.5	4	0.3	0.25	10.84
12.3	0.8	0.5	4	0.6	15	0.3125	3	0.5	4	0.5	0.25	13.52
12.3	0.8	0.5	4	0.6	15	0.3125	3	0.5	4	0.7	0.25	20.19
12.3	0.8	0.5	4	0.7	15	0.3125	3	0.5	4	0.1	0.25	7.37
12.3	0.8	0.5	4	0.7	15	0.3125	3	0.5	4	0.3	0.25	7.97
12.3	0.8	0.5	4	0.7	15	0.3125	3	0.5	4	0.5	0.25	9.14
12.3	0.8	0.5	4	0.7	15	0.3125	3	0.5	4	0.7	0.25	12.01
12.3	0.8	0.5	4	0.3	15	0.3125	3	1.5	4	0.1	0.0625	47.58
12.3	0.8	0.5	4	0.3	15	0.3125	3	1.5	4	0.3	0.0625	65.56
12.3	0.8	0.5	4	0.3	15	0.3125	3	1.5	4	0.5	0.0625	77.42

12.3	0.8	0.5	4	0.3	15	0.3125	3	1.5	4	0.7	0.0625	50.66
12.3	0.8	0.5	4	0.4	15	0.3125	3	1.5	4	0.1	0.0625	26.57
12.3	0.8	0.5	4	0.4	15	0.3125	3	1.5	4	0.3	0.0625	33.10
12.3	0.8	0.5	4	0.4	15	0.3125	3	1.5	4	0.5	0.0625	39.60
12.3	0.8	0.5	4	0.4	15	0.3125	3	1.5	4	0.7	0.0625	50.17
12.3	0.8	0.5	4	0.5	15	0.3125	3	1.5	4	0.1	0.0625	16.97
12.3	0.8	0.5	4	0.5	15	0.3125	3	1.5	4	0.3	0.0625	17.95
12.3	0.8	0.5	4	0.5	15	0.3125	3	1.5	4	0.5	0.0625	21.50
12.3	0.8	0.5	4	0.5	15	0.3125	3	1.5	4	0.7	0.0625	46.25
12.3	0.8	0.5	4	0.6	15	0.3125	3	1.5	4	0.1	0.0625	11.81
12.3	0.8	0.5	4	0.6	15	0.3125	3	1.5	4	0.3	0.0625	12.55
12.3	0.8	0.5	4	0.6	15	0.3125	3	1.5	4	0.5	0.0625	14.94
12.3	0.8	0.5	4	0.6	15	0.3125	3	1.5	4	0.7	0.0625	27.72
12.3	0.8	0.5	4	0.7	15	0.3125	3	1.5	4	0.1	0.0625	8.71
12.3	0.8	0.5	4	0.7	15	0.3125	3	1.5	4	0.3	0.0625	9.26
12.3	0.8	0.5	4	0.7	15	0.3125	3	1.5	4	0.5	0.0625	10.54
12.3	0.8	0.5	4	0.7	15	0.3125	3	1.5	4	0.7	0.0625	16.52
12.3	0.8	0.5	4	0.3	15	0.3125	3	1.5	4	0.1	0.125	45.04
12.3	0.8	0.5	4	0.3	15	0.3125	3	1.5	4	0.3	0.125	56.42
12.3	0.8	0.5	4	0.3	15	0.3125	3	1.5	4	0.5	0.125	68.32
12.3	0.8	0.5	4	0.3	15	0.3125	3	1.5	4	0.7	0.125	82.98
12.3	0.8	0.5	4	0.4	15	0.3125	3	1.5	4	0.1	0.125	24.80
12.3	0.8	0.5	4	0.4	15	0.3125	3	1.5	4	0.3	0.125	27.96
12.3	0.8	0.5	4	0.4	15	0.3125	3	1.5	4	0.5	0.125	40.80
12.3	0.8	0.5	4	0.4	15	0.3125	3	1.5	4	0.7	0.125	66.37
12.3	0.8	0.5	4	0.5	15	0.3125	3	1.5	4	0.1	0.125	16.11
12.3	0.8	0.5	4	0.5	15	0.3125	3	1.5	4	0.3	0.125	17.67
12.3	0.8	0.5	4	0.5	15	0.3125	3	1.5	4	0.5	0.125	23.87
12.3	0.8	0.5	4	0.5	15	0.3125	3	1.5	4	0.7	0.125	37.47
12.3	0.8	0.5	4	0.6	15	0.3125	3	1.5	4	0.1	0.125	11.29
12.3	0.8	0.5	4	0.6	15	0.3125	3	1.5	4	0.3	0.125	12.20
12.3	0.8	0.5	4	0.6	15	0.3125	3	1.5	4	0.5	0.125	14.90
12.3	0.8	0.5	4	0.6	15	0.3125	3	1.5	4	0.7	0.125	20.97
12.3	0.8	0.5	4	0.7	15	0.3125	3	1.5	4	0.1	0.125	8.35
12.3	0.8	0.5	4	0.7	15	0.3125	3	1.5	4	0.3	0.125	8.83
12.3	0.8	0.5	4	0.7	15	0.3125	3	1.5	4	0.5	0.125	9.66
12.3	0.8	0.5	4	0.7	15	0.3125	3	1.5	4	0.7	0.125	12.19
12.3	0.8	0.5	4	0.3	15	0.3125	3	1.5	4	0.1	0.1875	41.83

12.3	0.8	0.5	4	0.3	15	0.3125	3	1.5	4	0.3	0.1875	54.17
12.3	0.8	0.5	4	0.3	15	0.3125	3	1.5	4	0.5	0.1875	75.98
12.3	0.8	0.5	4	0.3	15	0.3125	3	1.5	4	0.7	0.1875	79.29
12.3	0.8	0.5	4	0.4	15	0.3125	3	1.5	4	0.1	0.1875	23.76
12.3	0.8	0.5	4	0.4	15	0.3125	3	1.5	4	0.3	0.1875	28.87
12.3	0.8	0.5	4	0.4	15	0.3125	3	1.5	4	0.5	0.1875	39.40
12.3	0.8	0.5	4	0.4	15	0.3125	3	1.5	4	0.7	0.1875	49.26
12.3	0.8	0.5	4	0.5	15	0.3125	3	1.5	4	0.1	0.1875	15.36
12.3	0.8	0.5	4	0.5	15	0.3125	3	1.5	4	0.3	0.1875	17.30
12.3	0.8	0.5	4	0.5	15	0.3125	3	1.5	4	0.5	0.1875	21.54
12.3	0.8	0.5	4	0.5	15	0.3125	3	1.5	4	0.7	0.1875	30.22
12.3	0.8	0.5	4	0.6	15	0.3125	3	1.5	4	0.1	0.1875	10.77
12.3	0.8	0.5	4	0.6	15	0.3125	3	1.5	4	0.3	0.1875	11.56
12.3	0.8	0.5	4	0.6	15	0.3125	3	1.5	4	0.5	0.1875	13.42
12.3	0.8	0.5	4	0.6	15	0.3125	3	1.5	4	0.7	0.1875	19.72
12.3	0.8	0.5	4	0.7	15	0.3125	3	1.5	4	0.1	0.1875	8.03
12.3	0.8	0.5	4	0.7	15	0.3125	3	1.5	4	0.3	0.1875	8.59
12.3	0.8	0.5	4	0.7	15	0.3125	3	1.5	4	0.5	0.1875	9.72
12.3	0.8	0.5	4	0.7	15	0.3125	3	1.5	4	0.7	0.1875	13.18
12.3	0.8	0.5	4	0.3	15	0.3125	3	1.5	4	0.1	0.25	40.37
12.3	0.8	0.5	4	0.3	15	0.3125	3	1.5	4	0.3	0.25	54.25
12.3	0.8	0.5	4	0.3	15	0.3125	3	1.5	4	0.5	0.25	63.59
12.3	0.8	0.5	4	0.3	15	0.3125	3	1.5	4	0.7	0.25	73.26
12.3	0.8	0.5	4	0.4	15	0.3125	3	1.5	4	0.1	0.25	22.40
12.3	0.8	0.5	4	0.4	15	0.3125	3	1.5	4	0.3	0.25	26.75
12.3	0.8	0.5	4	0.4	15	0.3125	3	1.5	4	0.5	0.25	34.68
12.3	0.8	0.5	4	0.4	15	0.3125	3	1.5	4	0.7	0.25	51.74
12.3	0.8	0.5	4	0.5	15	0.3125	3	1.5	4	0.1	0.25	14.53
12.3	0.8	0.5	4	0.5	15	0.3125	3	1.5	4	0.3	0.25	16.16
12.3	0.8	0.5	4	0.5	15	0.3125	3	1.5	4	0.5	0.25	20.90
12.3	0.8	0.5	4	0.5	15	0.3125	3	1.5	4	0.7	0.25	31.75
12.3	0.8	0.5	4	0.6	15	0.3125	3	1.5	4	0.1	0.25	10.31
12.3	0.8	0.5	4	0.6	15	0.3125	3	1.5	4	0.3	0.25	11.32
12.3	0.8	0.5	4	0.6	15	0.3125	3	1.5	4	0.5	0.25	13.80
12.3	0.8	0.5	4	0.6	15	0.3125	3	1.5	4	0.7	0.25	19.18
12.3	0.8	0.5	4	0.7	15	0.3125	3	1.5	4	0.1	0.25	7.71
12.3	0.8	0.5	4	0.7	15	0.3125	3	1.5	4	0.3	0.25	8.30
12.3	0.8	0.5	4	0.7	15	0.3125	3	1.5	4	0.5	0.25	9.43

12.3	0.8	0.5	4	0.7	15	0.3125	3	1.5	4	0.7	0.25	11.95
12.3	0.8	0.5	4	0.3	35	0.3125	3	0.5	4	0.1	0.0625	42.35
12.3	0.8	0.5	4	0.3	35	0.3125	3	0.5	4	0.3	0.0625	53.78
12.3	0.8	0.5	4	0.3	35	0.3125	3	0.5	4	0.5	0.0625	90.79
12.3	0.8	0.5	4	0.3	35	0.3125	3	0.5	4	0.7	0.0625	65.04
12.3	0.8	0.5	4	0.4	35	0.3125	3	0.5	4	0.1	0.0625	24.74
12.3	0.8	0.5	4	0.4	35	0.3125	3	0.5	4	0.3	0.0625	29.59
12.3	0.8	0.5	4	0.4	35	0.3125	3	0.5	4	0.5	0.0625	48.38
12.3	0.8	0.5	4	0.4	35	0.3125	3	0.5	4	0.7	0.0625	46.27
12.3	0.8	0.5	4	0.5	35	0.3125	3	0.5	4	0.1	0.0625	16.64
12.3	0.8	0.5	4	0.5	35	0.3125	3	0.5	4	0.3	0.0625	18.45
12.3	0.8	0.5	4	0.5	35	0.3125	3	0.5	4	0.5	0.0625	25.14
12.3	0.8	0.5	4	0.5	35	0.3125	3	0.5	4	0.7	0.0625	36.82
12.3	0.8	0.5	4	0.6	35	0.3125	3	0.5	4	0.1	0.0625	12.10
12.3	0.8	0.5	4	0.6	35	0.3125	3	0.5	4	0.3	0.0625	12.72
12.3	0.8	0.5	4	0.6	35	0.3125	3	0.5	4	0.5	0.0625	14.86
12.3	0.8	0.5	4	0.6	35	0.3125	3	0.5	4	0.7	0.0625	29.02
12.3	0.8	0.5	4	0.7	35	0.3125	3	0.5	4	0.1	0.0625	9.24
12.3	0.8	0.5	4	0.7	35	0.3125	3	0.5	4	0.3	0.0625	9.78
12.3	0.8	0.5	4	0.7	35	0.3125	3	0.5	4	0.5	0.0625	11.14
12.3	0.8	0.5	4	0.7	35	0.3125	3	0.5	4	0.7	0.0625	18.84
12.3	0.8	0.5	4	0.3	35	0.3125	3	0.5	4	0.1	0.125	39.98
12.3	0.8	0.5	4	0.3	35	0.3125	3	0.5	4	0.3	0.125	55.04
12.3	0.8	0.5	4	0.3	35	0.3125	3	0.5	4	0.5	0.125	68.44
12.3	0.8	0.5	4	0.3	35	0.3125	3	0.5	4	0.7	0.125	66.82
12.3	0.8	0.5	4	0.4	35	0.3125	3	0.5	4	0.1	0.125	23.35
12.3	0.8	0.5	4	0.4	35	0.3125	3	0.5	4	0.3	0.125	27.53
12.3	0.8	0.5	4	0.4	35	0.3125	3	0.5	4	0.5	0.125	36.15
12.3	0.8	0.5	4	0.4	35	0.3125	3	0.5	4	0.7	0.125	62.31
12.3	0.8	0.5	4	0.5	35	0.3125	3	0.5	4	0.1	0.125	15.83
12.3	0.8	0.5	4	0.5	35	0.3125	3	0.5	4	0.3	0.125	17.10
12.3	0.8	0.5	4	0.5	35	0.3125	3	0.5	4	0.5	0.125	22.18
12.3	0.8	0.5	4	0.5	35	0.3125	3	0.5	4	0.7	0.125	44.08
12.3	0.8	0.5	4	0.6	35	0.3125	3	0.5	4	0.1	0.125	11.61
12.3	0.8	0.5	4	0.6	35	0.3125	3	0.5	4	0.3	0.125	12.52
12.3	0.8	0.5	4	0.6	35	0.3125	3	0.5	4	0.5	0.125	15.36
12.3	0.8	0.5	4	0.6	35	0.3125	3	0.5	4	0.7	0.125	26.19
12.3	0.8	0.5	4	0.7	35	0.3125	3	0.5	4	0.1	0.125	8.93

12.3	0.8	0.5	4	0.7	35	0.3125	3	0.5	4	0.3	0.125	9.54
12.3	0.8	0.5	4	0.7	35	0.3125	3	0.5	4	0.5	0.125	10.82
12.3	0.8	0.5	4	0.7	35	0.3125	3	0.5	4	0.7	0.125	15.12
12.3	0.8	0.5	4	0.3	35	0.3125	3	0.5	4	0.1	0.1875	37.01
12.3	0.8	0.5	4	0.3	35	0.3125	3	0.5	4	0.3	0.1875	44.95
12.3	0.8	0.5	4	0.3	35	0.3125	3	0.5	4	0.5	0.1875	70.82
12.3	0.8	0.5	4	0.3	35	0.3125	3	0.5	4	0.7	0.1875	92.82
12.3	0.8	0.5	4	0.4	35	0.3125	3	0.5	4	0.1	0.1875	22.03
12.3	0.8	0.5	4	0.4	35	0.3125	3	0.5	4	0.3	0.1875	25.38
12.3	0.8	0.5	4	0.4	35	0.3125	3	0.5	4	0.5	0.1875	39.80
12.3	0.8	0.5	4	0.4	35	0.3125	3	0.5	4	0.7	0.1875	58.74
12.3	0.8	0.5	4	0.5	35	0.3125	3	0.5	4	0.1	0.1875	15.15
12.3	0.8	0.5	4	0.5	35	0.3125	3	0.5	4	0.3	0.1875	16.82
12.3	0.8	0.5	4	0.5	35	0.3125	3	0.5	4	0.5	0.1875	23.45
12.3	0.8	0.5	4	0.5	35	0.3125	3	0.5	4	0.7	0.1875	34.56
12.3	0.8	0.5	4	0.6	35	0.3125	3	0.5	4	0.1	0.1875	11.17
12.3	0.8	0.5	4	0.6	35	0.3125	3	0.5	4	0.3	0.1875	12.05
12.3	0.8	0.5	4	0.6	35	0.3125	3	0.5	4	0.5	0.1875	14.37
12.3	0.8	0.5	4	0.6	35	0.3125	3	0.5	4	0.7	0.1875	20.57
12.3	0.8	0.5	4	0.7	35	0.3125	3	0.5	4	0.1	0.1875	8.65
12.3	0.8	0.5	4	0.7	35	0.3125	3	0.5	4	0.3	0.1875	9.21
12.3	0.8	0.5	4	0.7	35	0.3125	3	0.5	4	0.5	0.1875	10.25
12.3	0.8	0.5	4	0.7	35	0.3125	3	0.5	4	0.7	0.1875	13.96
12.3	0.8	0.5	4	0.3	35	0.3125	3	0.5	4	0.1	0.25	35.38
12.3	0.8	0.5	4	0.3	35	0.3125	3	0.5	4	0.3	0.25	49.29
12.3	0.8	0.5	4	0.3	35	0.3125	3	0.5	4	0.5	0.25	67.13
12.3	0.8	0.5	4	0.3	35	0.3125	3	0.5	4	0.7	0.25	73.26
12.3	0.8	0.5	4	0.4	35	0.3125	3	0.5	4	0.1	0.25	21.13
12.3	0.8	0.5	4	0.4	35	0.3125	3	0.5	4	0.3	0.25	26.60
12.3	0.8	0.5	4	0.4	35	0.3125	3	0.5	4	0.5	0.25	34.77
12.3	0.8	0.5	4	0.4	35	0.3125	3	0.5	4	0.7	0.25	50.03
12.3	0.8	0.5	4	0.5	35	0.3125	3	0.5	4	0.1	0.25	14.44
12.3	0.8	0.5	4	0.5	35	0.3125	3	0.5	4	0.3	0.25	15.85
12.3	0.8	0.5	4	0.5	35	0.3125	3	0.5	4	0.5	0.25	18.96
12.3	0.8	0.5	4	0.5	35	0.3125	3	0.5	4	0.7	0.25	33.86
12.3	0.8	0.5	4	0.6	35	0.3125	3	0.5	4	0.1	0.25	10.77
12.3	0.8	0.5	4	0.6	35	0.3125	3	0.5	4	0.3	0.25	11.68
12.3	0.8	0.5	4	0.6	35	0.3125	3	0.5	4	0.5	0.25	13.73

12.3	0.8	0.5	4	0.6	35	0.3125	3	0.5	4	0.7	0.25	21.86
12.3	0.8	0.5	4	0.7	35	0.3125	3	0.5	4	0.1	0.25	8.40
12.3	0.8	0.5	4	0.7	35	0.3125	3	0.5	4	0.3	0.25	9.04
12.3	0.8	0.5	4	0.7	35	0.3125	3	0.5	4	0.5	0.25	10.19
12.3	0.8	0.5	4	0.7	35	0.3125	3	0.5	4	0.7	0.25	14.26
12.3	0.8	0.5	4	0.3	35	0.3125	3	1.5	4	0.1	0.0625	44.90
12.3	0.8	0.5	4	0.3	35	0.3125	3	1.5	4	0.3	0.0625	55.16
12.3	0.8	0.5	4	0.3	35	0.3125	3	1.5	4	0.5	0.0625	82.15
12.3	0.8	0.5	4	0.3	35	0.3125	3	1.5	4	0.7	0.0625	52.51
12.3	0.8	0.5	4	0.4	35	0.3125	3	1.5	4	0.1	0.0625	26.65
12.3	0.8	0.5	4	0.4	35	0.3125	3	1.5	4	0.3	0.0625	31.16
12.3	0.8	0.5	4	0.4	35	0.3125	3	1.5	4	0.5	0.0625	45.69
12.3	0.8	0.5	4	0.4	35	0.3125	3	1.5	4	0.7	0.0625	40.89
12.3	0.8	0.5	4	0.5	35	0.3125	3	1.5	4	0.1	0.0625	18.08
12.3	0.8	0.5	4	0.5	35	0.3125	3	1.5	4	0.3	0.0625	19.82
12.3	0.8	0.5	4	0.5	35	0.3125	3	1.5	4	0.5	0.0625	25.48
12.3	0.8	0.5	4	0.5	35	0.3125	3	1.5	4	0.7	0.0625	34.58
12.3	0.8	0.5	4	0.6	35	0.3125	3	1.5	4	0.1	0.0625	13.19
12.3	0.8	0.5	4	0.6	35	0.3125	3	1.5	4	0.3	0.0625	13.82
12.3	0.8	0.5	4	0.6	35	0.3125	3	1.5	4	0.5	0.0625	15.97
12.3	0.8	0.5	4	0.6	35	0.3125	3	1.5	4	0.7	0.0625	27.88
12.3	0.8	0.5	4	0.7	35	0.3125	3	1.5	4	0.1	0.0625	10.09
12.3	0.8	0.5	4	0.7	35	0.3125	3	1.5	4	0.3	0.0625	10.63
12.3	0.8	0.5	4	0.7	35	0.3125	3	1.5	4	0.5	0.0625	12.00
12.3	0.8	0.5	4	0.7	35	0.3125	3	1.5	4	0.7	0.0625	18.56
12.3	0.8	0.5	4	0.3	35	0.3125	3	1.5	4	0.1	0.125	42.46
12.3	0.8	0.5	4	0.3	35	0.3125	3	1.5	4	0.3	0.125	55.12
12.3	0.8	0.5	4	0.3	35	0.3125	3	1.5	4	0.5	0.125	63.40
12.3	0.8	0.5	4	0.3	35	0.3125	3	1.5	4	0.7	0.125	57.78
12.3	0.8	0.5	4	0.4	35	0.3125	3	1.5	4	0.1	0.125	25.17
12.3	0.8	0.5	4	0.4	35	0.3125	3	1.5	4	0.3	0.125	29.18
12.3	0.8	0.5	4	0.4	35	0.3125	3	1.5	4	0.5	0.125	36.50
12.3	0.8	0.5	4	0.4	35	0.3125	3	1.5	4	0.7	0.125	55.18
12.3	0.8	0.5	4	0.5	35	0.3125	3	1.5	4	0.1	0.125	17.22
12.3	0.8	0.5	4	0.5	35	0.3125	3	1.5	4	0.3	0.125	18.66
12.3	0.8	0.5	4	0.5	35	0.3125	3	1.5	4	0.5	0.125	23.38
12.3	0.8	0.5	4	0.5	35	0.3125	3	1.5	4	0.7	0.125	39.98
12.3	0.8	0.5	4	0.6	35	0.3125	3	1.5	4	0.1	0.125	12.70



12.3	0.8	0.5	4	0.6	35	0.3125	3	1.5	4	0.3	0.125	13.68
12.3	0.8	0.5	4	0.6	35	0.3125	3	1.5	4	0.5	0.125	16.36
12.3	0.8	0.5	4	0.6	35	0.3125	3	1.5	4	0.7	0.125	24.91
12.3	0.8	0.5	4	0.7	35	0.3125	3	1.5	4	0.1	0.125	9.79
12.3	0.8	0.5	4	0.7	35	0.3125	3	1.5	4	0.3	0.125	10.41
12.3	0.8	0.5	4	0.7	35	0.3125	3	1.5	4	0.5	0.125	11.66
12.3	0.8	0.5	4	0.7	35	0.3125	3	1.5	4	0.7	0.125	15.35
12.3	0.8	0.5	4	0.3	35	0.3125	3	1.5	4	0.1	0.1875	39.50
12.3	0.8	0.5	4	0.3	35	0.3125	3	1.5	4	0.3	0.1875	47.02
12.3	0.8	0.5	4	0.3	35	0.3125	3	1.5	4	0.5	0.1875	67.16
12.3	0.8	0.5	4	0.3	35	0.3125	3	1.5	4	0.7	0.1875	77.59
12.3	0.8	0.5	4	0.4	35	0.3125	3	1.5	4	0.1	0.1875	23.93
12.3	0.8	0.5	4	0.4	35	0.3125	3	1.5	4	0.3	0.1875	27.32
12.3	0.8	0.5	4	0.4	35	0.3125	3	1.5	4	0.5	0.1875	39.13
12.3	0.8	0.5	4	0.4	35	0.3125	3	1.5	4	0.7	0.1875	51.25
12.3	0.8	0.5	4	0.5	35	0.3125	3	1.5	4	0.1	0.1875	16.60
12.3	0.8	0.5	4	0.5	35	0.3125	3	1.5	4	0.3	0.1875	18.30
12.3	0.8	0.5	4	0.5	35	0.3125	3	1.5	4	0.5	0.1875	23.99
12.3	0.8	0.5	4	0.5	35	0.3125	3	1.5	4	0.7	0.1875	32.10
12.3	0.8	0.5	4	0.6	35	0.3125	3	1.5	4	0.1	0.1875	12.28
12.3	0.8	0.5	4	0.6	35	0.3125	3	1.5	4	0.3	0.1875	13.15
12.3	0.8	0.5	4	0.6	35	0.3125	3	1.5	4	0.5	0.1875	15.42
12.3	0.8	0.5	4	0.6	35	0.3125	3	1.5	4	0.7	0.1875	20.74
12.3	0.8	0.5	4	0.7	35	0.3125	3	1.5	4	0.1	0.1875	9.51
12.3	0.8	0.5	4	0.7	35	0.3125	3	1.5	4	0.3	0.1875	10.06
12.3	0.8	0.5	4	0.7	35	0.3125	3	1.5	4	0.5	0.1875	11.19
12.3	0.8	0.5	4	0.7	35	0.3125	3	1.5	4	0.7	0.1875	14.56
12.3	0.8	0.5	4	0.3	35	0.3125	3	1.5	4	0.1	0.25	37.86
12.3	0.8	0.5	4	0.3	35	0.3125	3	1.5	4	0.3	0.25	50.30
12.3	0.8	0.5	4	0.3	35	0.3125	3	1.5	4	0.5	0.25	62.71
12.3	0.8	0.5	4	0.3	35	0.3125	3	1.5	4	0.7	0.25	61.90
12.3	0.8	0.5	4	0.4	35	0.3125	3	1.5	4	0.1	0.25	23.00
12.3	0.8	0.5	4	0.4	35	0.3125	3	1.5	4	0.3	0.25	28.12
12.3	0.8	0.5	4	0.4	35	0.3125	3	1.5	4	0.5	0.25	34.61
12.3	0.8	0.5	4	0.4	35	0.3125	3	1.5	4	0.7	0.25	45.43
12.3	0.8	0.5	4	0.5	35	0.3125	3	1.5	4	0.1	0.25	15.84
12.3	0.8	0.5	4	0.5	35	0.3125	3	1.5	4	0.3	0.25	17.31
12.3	0.8	0.5	4	0.5	35	0.3125	3	1.5	4	0.5	0.25	20.39

12.3	0.8	0.5	4	0.5	35	0.3125	3	1.5	4	0.7	0.25	32.86
12.3	0.8	0.5	4	0.6	35	0.3125	3	1.5	4	0.1	0.25	11.87
12.3	0.8	0.5	4	0.6	35	0.3125	3	1.5	4	0.3	0.25	12.82
12.3	0.8	0.5	4	0.6	35	0.3125	3	1.5	4	0.5	0.25	14.88
12.3	0.8	0.5	4	0.6	35	0.3125	3	1.5	4	0.7	0.25	21.87
12.3	0.8	0.5	4	0.7	35	0.3125	3	1.5	4	0.1	0.25	9.26
12.3	0.8	0.5	4	0.7	35	0.3125	3	1.5	4	0.3	0.25	9.92
12.3	0.8	0.5	4	0.7	35	0.3125	3	1.5	4	0.5	0.25	11.09
12.3	0.8	0.5	4	0.7	35	0.3125	3	1.5	4	0.7	0.25	14.70
12.3	0.8	0.5	4	0.3	55	0.3125	3	0.5	4	0.1	0.0625	46.14
12.3	0.8	0.5	4	0.3	55	0.3125	3	0.5	4	0.3	0.0625	55.39
12.3	0.8	0.5	4	0.3	55	0.3125	3	0.5	4	0.5	0.0625	99.07
12.3	0.8	0.5	4	0.3	55	0.3125	3	0.5	4	0.7	0.0625	109.13
12.3	0.8	0.5	4	0.4	55	0.3125	3	0.5	4	0.1	0.0625	28.33
12.3	0.8	0.5	4	0.4	55	0.3125	3	0.5	4	0.3	0.0625	32.54
12.3	0.8	0.5	4	0.4	55	0.3125	3	0.5	4	0.5	0.0625	61.13
12.3	0.8	0.5	4	0.4	55	0.3125	3	0.5	4	0.7	0.0625	73.77
12.3	0.8	0.5	4	0.5	55	0.3125	3	0.5	4	0.1	0.0625	19.62
12.3	0.8	0.5	4	0.5	55	0.3125	3	0.5	4	0.3	0.0625	21.79
12.3	0.8	0.5	4	0.5	55	0.3125	3	0.5	4	0.5	0.0625	35.00
12.3	0.8	0.5	4	0.5	55	0.3125	3	0.5	4	0.7	0.0625	41.34
12.3	0.8	0.5	4	0.6	55	0.3125	3	0.5	4	0.1	0.0625	14.39
12.3	0.8	0.5	4	0.6	55	0.3125	3	0.5	4	0.3	0.0625	15.53
12.3	0.8	0.5	4	0.6	55	0.3125	3	0.5	4	0.5	0.0625	19.19
12.3	0.8	0.5	4	0.6	55	0.3125	3	0.5	4	0.7	0.0625	25.61
12.3	0.8	0.5	4	0.7	55	0.3125	3	0.5	4	0.1	0.0625	10.98
12.3	0.8	0.5	4	0.7	55	0.3125	3	0.5	4	0.3	0.0625	11.67
12.3	0.8	0.5	4	0.7	55	0.3125	3	0.5	4	0.5	0.0625	12.78
12.3	0.8	0.5	4	0.7	55	0.3125	3	0.5	4	0.7	0.0625	18.00
12.3	0.8	0.5	4	0.3	55	0.3125	3	0.5	4	0.1	0.125	43.41
12.3	0.8	0.5	4	0.3	55	0.3125	3	0.5	4	0.3	0.125	58.88
12.3	0.8	0.5	4	0.3	55	0.3125	3	0.5	4	0.5	0.125	90.07
12.3	0.8	0.5	4	0.3	55	0.3125	3	0.5	4	0.7	0.125	77.70
12.3	0.8	0.5	4	0.4	55	0.3125	3	0.5	4	0.1	0.125	27.24
12.3	0.8	0.5	4	0.4	55	0.3125	3	0.5	4	0.3	0.125	33.63
12.3	0.8	0.5	4	0.4	55	0.3125	3	0.5	4	0.5	0.125	48.24
12.3	0.8	0.5	4	0.4	55	0.3125	3	0.5	4	0.7	0.125	58.45
12.3	0.8	0.5	4	0.5	55	0.3125	3	0.5	4	0.1	0.125	18.94

12.3	0.8	0.5	4	0.5	55	0.3125	3	0.5	4	0.3	0.125	20.63
12.3	0.8	0.5	4	0.5	55	0.3125	3	0.5	4	0.5	0.125	24.57
12.3	0.8	0.5	4	0.5	55	0.3125	3	0.5	4	0.7	0.125	46.36
12.3	0.8	0.5	4	0.6	55	0.3125	3	0.5	4	0.1	0.125	13.97
12.3	0.8	0.5	4	0.6	55	0.3125	3	0.5	4	0.3	0.125	14.99
12.3	0.8	0.5	4	0.6	55	0.3125	3	0.5	4	0.5	0.125	17.48
12.3	0.8	0.5	4	0.6	55	0.3125	3	0.5	4	0.7	0.125	30.11
12.3	0.8	0.5	4	0.7	55	0.3125	3	0.5	4	0.1	0.125	10.71
12.3	0.8	0.5	4	0.7	55	0.3125	3	0.5	4	0.3	0.125	11.42
12.3	0.8	0.5	4	0.7	55	0.3125	3	0.5	4	0.5	0.125	12.82
12.3	0.8	0.5	4	0.7	55	0.3125	3	0.5	4	0.7	0.125	18.95
12.3	0.8	0.5	4	0.3	55	0.3125	3	0.5	4	0.1	0.1875	42.19
12.3	0.8	0.5	4	0.3	55	0.3125	3	0.5	4	0.3	0.1875	55.20
12.3	0.8	0.5	4	0.3	55	0.3125	3	0.5	4	0.5	0.1875	72.60
12.3	0.8	0.5	4	0.3	55	0.3125	3	0.5	4	0.7	0.1875	90.93
12.3	0.8	0.5	4	0.4	55	0.3125	3	0.5	4	0.1	0.1875	25.82
12.3	0.8	0.5	4	0.4	55	0.3125	3	0.5	4	0.3	0.1875	29.46
12.3	0.8	0.5	4	0.4	55	0.3125	3	0.5	4	0.5	0.1875	44.68
12.3	0.8	0.5	4	0.4	55	0.3125	3	0.5	4	0.7	0.1875	76.34
12.3	0.8	0.5	4	0.5	55	0.3125	3	0.5	4	0.1	0.1875	18.29
12.3	0.8	0.5	4	0.5	55	0.3125	3	0.5	4	0.3	0.1875	20.29
12.3	0.8	0.5	4	0.5	55	0.3125	3	0.5	4	0.5	0.1875	28.14
12.3	0.8	0.5	4	0.5	55	0.3125	3	0.5	4	0.7	0.1875	44.97
12.3	0.8	0.5	4	0.6	55	0.3125	3	0.5	4	0.1	0.1875	13.58
12.3	0.8	0.5	4	0.6	55	0.3125	3	0.5	4	0.3	0.1875	14.80
12.3	0.8	0.5	4	0.6	55	0.3125	3	0.5	4	0.5	0.1875	18.40
12.3	0.8	0.5	4	0.6	55	0.3125	3	0.5	4	0.7	0.1875	25.99
12.3	0.8	0.5	4	0.7	55	0.3125	3	0.5	4	0.1	0.1875	10.43
12.3	0.8	0.5	4	0.7	55	0.3125	3	0.5	4	0.3	0.1875	11.07
12.3	0.8	0.5	4	0.7	55	0.3125	3	0.5	4	0.5	0.1875	12.14
12.3	0.8	0.5	4	0.7	55	0.3125	3	0.5	4	0.7	0.1875	14.90
12.3	0.8	0.5	4	0.3	55	0.3125	3	0.5	4	0.1	0.25	39.02
12.3	0.8	0.5	4	0.3	55	0.3125	3	0.5	4	0.3	0.25	50.98
12.3	0.8	0.5	4	0.3	55	0.3125	3	0.5	4	0.5	0.25	80.88
12.3	0.8	0.5	4	0.3	55	0.3125	3	0.5	4	0.7	0.25	89.38
12.3	0.8	0.5	4	0.4	55	0.3125	3	0.5	4	0.1	0.25	25.15
12.3	0.8	0.5	4	0.4	55	0.3125	3	0.5	4	0.3	0.25	30.72
12.3	0.8	0.5	4	0.4	55	0.3125	3	0.5	4	0.5	0.25	45.81

12.3	0.8	0.5	4	0.4	55	0.3125	3	0.5	4	0.7	0.25	58.49
12.3	0.8	0.5	4	0.5	55	0.3125	3	0.5	4	0.1	0.25	17.78
12.3	0.8	0.5	4	0.5	55	0.3125	3	0.5	4	0.3	0.25	20.17
12.3	0.8	0.5	4	0.5	55	0.3125	3	0.5	4	0.5	0.25	26.31
12.3	0.8	0.5	4	0.5	55	0.3125	3	0.5	4	0.7	0.25	37.55
12.3	0.8	0.5	4	0.6	55	0.3125	3	0.5	4	0.1	0.25	13.19
12.3	0.8	0.5	4	0.6	55	0.3125	3	0.5	4	0.3	0.25	14.12
12.3	0.8	0.5	4	0.6	55	0.3125	3	0.5	4	0.5	0.25	16.34
12.3	0.8	0.5	4	0.6	55	0.3125	3	0.5	4	0.7	0.25	25.04
12.3	0.8	0.5	4	0.7	55	0.3125	3	0.5	4	0.1	0.25	10.19
12.3	0.8	0.5	4	0.7	55	0.3125	3	0.5	4	0.3	0.25	10.85
12.3	0.8	0.5	4	0.7	55	0.3125	3	0.5	4	0.5	0.25	12.19
12.3	0.8	0.5	4	0.7	55	0.3125	3	0.5	4	0.7	0.25	16.88
12.3	0.8	0.5	4	0.3	55	0.3125	3	1.5	4	0.1	0.0625	48.94
12.3	0.8	0.5	4	0.3	55	0.3125	3	1.5	4	0.3	0.0625	57.66
12.3	0.8	0.5	4	0.3	55	0.3125	3	1.5	4	0.5	0.0625	92.50
12.3	0.8	0.5	4	0.3	55	0.3125	3	1.5	4	0.7	0.0625	90.94
12.3	0.8	0.5	4	0.4	55	0.3125	3	1.5	4	0.1	0.0625	30.44
12.3	0.8	0.5	4	0.4	55	0.3125	3	1.5	4	0.3	0.0625	34.65
12.3	0.8	0.5	4	0.4	55	0.3125	3	1.5	4	0.5	0.0625	58.16
12.3	0.8	0.5	4	0.4	55	0.3125	3	1.5	4	0.7	0.0625	63.58
12.3	0.8	0.5	4	0.5	55	0.3125	3	1.5	4	0.1	0.0625	21.24
12.3	0.8	0.5	4	0.5	55	0.3125	3	1.5	4	0.3	0.0625	23.44
12.3	0.8	0.5	4	0.5	55	0.3125	3	1.5	4	0.5	0.0625	34.56
12.3	0.8	0.5	4	0.5	55	0.3125	3	1.5	4	0.7	0.0625	38.41
12.3	0.8	0.5	4	0.6	55	0.3125	3	1.5	4	0.1	0.0625	15.63
12.3	0.8	0.5	4	0.6	55	0.3125	3	1.5	4	0.3	0.0625	16.78
12.3	0.8	0.5	4	0.6	55	0.3125	3	1.5	4	0.5	0.0625	20.16
12.3	0.8	0.5	4	0.6	55	0.3125	3	1.5	4	0.7	0.0625	25.87
12.3	0.8	0.5	4	0.7	55	0.3125	3	1.5	4	0.1	0.0625	11.94
12.3	0.8	0.5	4	0.7	55	0.3125	3	1.5	4	0.3	0.0625	12.63
12.3	0.8	0.5	4	0.7	55	0.3125	3	1.5	4	0.5	0.0625	13.82
12.3	0.8	0.5	4	0.7	55	0.3125	3	1.5	4	0.7	0.0625	18.59
12.3	0.8	0.5	4	0.3	55	0.3125	3	1.5	4	0.1	0.125	46.41
12.3	0.8	0.5	4	0.3	55	0.3125	3	1.5	4	0.3	0.125	60.32
12.3	0.8	0.5	4	0.3	55	0.3125	3	1.5	4	0.5	0.125	82.82
12.3	0.8	0.5	4	0.3	55	0.3125	3	1.5	4	0.7	0.125	66.63
12.3	0.8	0.5	4	0.4	55	0.3125	3	1.5	4	0.1	0.125	29.38

12.3	0.8	0.5	4	0.4	55	0.3125	3	1.5	4	0.3	0.125	35.39
12.3	0.8	0.5	4	0.4	55	0.3125	3	1.5	4	0.5	0.125	46.96
12.3	0.8	0.5	4	0.4	55	0.3125	3	1.5	4	0.7	0.125	53.36
12.3	0.8	0.5	4	0.5	55	0.3125	3	1.5	4	0.1	0.125	20.50
12.3	0.8	0.5	4	0.5	55	0.3125	3	1.5	4	0.3	0.125	22.32
12.3	0.8	0.5	4	0.5	55	0.3125	3	1.5	4	0.5	0.125	26.27
12.3	0.8	0.5	4	0.5	55	0.3125	3	1.5	4	0.7	0.125	43.88
12.3	0.8	0.5	4	0.6	55	0.3125	3	1.5	4	0.1	0.125	15.19
12.3	0.8	0.5	4	0.6	55	0.3125	3	1.5	4	0.3	0.125	16.29
12.3	0.8	0.5	4	0.6	55	0.3125	3	1.5	4	0.5	0.125	18.82
12.3	0.8	0.5	4	0.6	55	0.3125	3	1.5	4	0.7	0.125	29.27
12.3	0.8	0.5	4	0.7	55	0.3125	3	1.5	4	0.1	0.125	11.66
12.3	0.8	0.5	4	0.7	55	0.3125	3	1.5	4	0.3	0.125	12.41
12.3	0.8	0.5	4	0.7	55	0.3125	3	1.5	4	0.5	0.125	13.83
12.3	0.8	0.5	4	0.7	55	0.3125	3	1.5	4	0.7	0.125	19.08
12.3	0.8	0.5	4	0.3	55	0.3125	3	1.5	4	0.1	0.1875	44.89
12.3	0.8	0.5	4	0.3	55	0.3125	3	1.5	4	0.3	0.1875	56.44
12.3	0.8	0.5	4	0.3	55	0.3125	3	1.5	4	0.5	0.1875	69.55
12.3	0.8	0.5	4	0.3	55	0.3125	3	1.5	4	0.7	0.1875	80.33
12.3	0.8	0.5	4	0.4	55	0.3125	3	1.5	4	0.1	0.1875	27.87
12.3	0.8	0.5	4	0.4	55	0.3125	3	1.5	4	0.3	0.1875	31.92
12.3	0.8	0.5	4	0.4	55	0.3125	3	1.5	4	0.5	0.1875	45.15
12.3	0.8	0.5	4	0.4	55	0.3125	3	1.5	4	0.7	0.1875	68.30
12.3	0.8	0.5	4	0.5	55	0.3125	3	1.5	4	0.1	0.1875	19.88
12.3	0.8	0.5	4	0.5	55	0.3125	3	1.5	4	0.3	0.1875	22.09
12.3	0.8	0.5	4	0.5	55	0.3125	3	1.5	4	0.5	0.1875	29.07
12.3	0.8	0.5	4	0.5	55	0.3125	3	1.5	4	0.7	0.1875	41.76
12.3	0.8	0.5	4	0.6	55	0.3125	3	1.5	4	0.1	0.1875	14.82
12.3	0.8	0.5	4	0.6	55	0.3125	3	1.5	4	0.3	0.1875	16.11
12.3	0.8	0.5	4	0.6	55	0.3125	3	1.5	4	0.5	0.1875	19.45
12.3	0.8	0.5	4	0.6	55	0.3125	3	1.5	4	0.7	0.1875	25.63
12.3	0.8	0.5	4	0.7	55	0.3125	3	1.5	4	0.1	0.1875	11.38
12.3	0.8	0.5	4	0.7	55	0.3125	3	1.5	4	0.3	0.1875	12.04
12.3	0.8	0.5	4	0.7	55	0.3125	3	1.5	4	0.5	0.1875	13.19
12.3	0.8	0.5	4	0.7	55	0.3125	3	1.5	4	0.7	0.1875	15.86
12.3	0.8	0.5	4	0.3	55	0.3125	3	1.5	4	0.1	0.25	41.92
12.3	0.8	0.5	4	0.3	55	0.3125	3	1.5	4	0.3	0.25	53.39
12.3	0.8	0.5	4	0.3	55	0.3125	3	1.5	4	0.5	0.25	77.49

12.3	0.8	0.5	4	0.3	55	0.3125	3	1.5	4	0.7	0.25	76.75
12.3	0.8	0.5	4	0.4	55	0.3125	3	1.5	4	0.1	0.25	27.29
12.3	0.8	0.5	4	0.4	55	0.3125	3	1.5	4	0.3	0.25	32.75
12.3	0.8	0.5	4	0.4	55	0.3125	3	1.5	4	0.5	0.25	45.42
12.3	0.8	0.5	4	0.4	55	0.3125	3	1.5	4	0.7	0.25	53.17
12.3	0.8	0.5	4	0.5	55	0.3125	3	1.5	4	0.1	0.25	19.40
12.3	0.8	0.5	4	0.5	55	0.3125	3	1.5	4	0.3	0.25	21.81
12.3	0.8	0.5	4	0.5	55	0.3125	3	1.5	4	0.5	0.25	27.35
12.3	0.8	0.5	4	0.5	55	0.3125	3	1.5	4	0.7	0.25	36.37
12.3	0.8	0.5	4	0.6	55	0.3125	3	1.5	4	0.1	0.25	14.42
12.3	0.8	0.5	4	0.6	55	0.3125	3	1.5	4	0.3	0.25	15.41
12.3	0.8	0.5	4	0.6	55	0.3125	3	1.5	4	0.5	0.25	17.74
12.3	0.8	0.5	4	0.6	55	0.3125	3	1.5	4	0.7	0.25	25.56
12.3	0.8	0.5	4	0.7	55	0.3125	3	1.5	4	0.1	0.25	11.15
12.3	0.8	0.5	4	0.7	55	0.3125	3	1.5	4	0.3	0.25	11.84
12.3	0.8	0.5	4	0.7	55	0.3125	3	1.5	4	0.5	0.25	13.24
12.3	0.8	0.5	4	0.7	55	0.3125	3	1.5	4	0.7	0.25	17.50

## References

- AASHTO (2007) *AASHTO LRFD Bridge Construction Specifications*, American Association of State Highway and Transportation Officials, Washington, DC
- AISC (2005) *AISC Steel Construction Manual*, American Institute of Steel Construction Inc., Chicago
- Anamia, K., Sauseb R., and Abbas, H. H. (2005) "Fatigue of web-flange weld of corrugated web girders: 1. Influence of web corrugation geometry and flange geometry on web-flange weld toe stresses." *International Journal of Fatigue*, Elsevier Ltd., 27(4), 373-381.
- Anamia, K., and Sauseb, R. (2005) "Fatigue of web-flange weld of corrugated web girders: 2. Analytical evaluation of fatigue strength of corrugated web-flange weld." *International Journal of Fatigue*, Elsevier Ltd., 27(4), 383-393.
- ANSYS version 11.0, (2007) (computer software), ANSYS Inc., Canonsburg, PA.
- Battistini, Anthony. "Skewed Cross Frame Connection Stiffness." *Thesis presented to The University of Texas*. Austin, TX, December 2009.
- Berglund, E. M. and Schultz, A. (2006). "Girder Differential Deflection and Distortion-Induced Fatigue in Skewed Steel Bridges." *Journal of Bridge Engineering*, ASCE, 11 (2), p 169-177.
- DNV (2010) *Fatigue Design of Offshore Structures*, Det Norske Veritas, Høvik, Norway.
- Fisher, J. W., Kulak, G. L., and Smith, I. F. C. (1998) *A Fatigue Primer for Structural Engineers*, National Steel Bridge Alliance, Chicago.
- Fricke, W. (2003) "Fatigue analysis of welded joints: state of development." *Marine Structures*, Elsevier Ltd., 16(3), 185-200.
- Ojalvo, M., and Chambers, R.S. (1977) "Effects of Warping Restraints on I-Beam Buckling." *ASCE Journal of the Structural Division*, 103(12), 2351-2360.
- Quadrato, Craig. "Stability of Skewed I-Shaped Girder Bridges Using Bent Plate

- Connections” *Dissertation presented to The University of Texas*. Austin, TX, May 2010.
- Roy, S., Fisher, J. W., and Yen, B. T. (2003) "Fatigue resistance of welded details enhanced by ultrasonic impact treatment (UIT)." *International Journal of Fatigue*, Elsevier Ltd., 25(9-11), 1239-1247.
- Sause, R., Abbas, H. H., Driver, R. G., Anami, K., and Fisher, J. W. (2003). "Fatigue Resistance of Corrugated Web Girders." ATLSS Report No. 03-20, PennDOT, Bethlehem, PA, 2003.
- Sause, R., Abbas, H. H., Driver, R. G., Anami, K., and Fisher, J. W. (2006) "Fatigue Life of Girders with Trapezoidal Corrugated Webs." *Journal of Structural Engineering*, ASCE, 132(7), 1070-1078.
- Sedgewick, R. (1998) *Algorithms in C++ Third Edition Parts 1-4*, Addison-Wesley, Reading, Massachusetts.
- Unsworth, J. F. (2003) "Heavy Axle Load Effects on Fatigue Life of Steel Bridges." *Transportation Research Record*, National Research Council, (1825), 38-47.
- Weisstein, E. W. (2010). "Least Squares Fitting." *Wolfram Mathworld* <<http://mathworld.wolfram.com/LeastSquaresFitting.html>> (March 3, 2010)
- (2010). "FLOPS." *Wikipedia* <<http://en.wikipedia.org/wiki/FLOPS>> (June 29, 2010).
- (2010). "Genetic Algorithm." *Wikipedia* <[http://en.wikipedia.org/wiki/Genetic\\_algorithms](http://en.wikipedia.org/wiki/Genetic_algorithms)> (May 15, 2010).



## VITA

Andrew Wahr was born in Boulder Colorado on the 2<sup>nd</sup> of June, 1985. From a young age he planned on a career as a civil engineer, and prepared for his academic studies accordingly. In 2003 he graduated from Fairview High School in Boulder and traveled to West Lafayette Indiana to attend Purdue University and study Civil Engineering. In 2005 he took two years off from his studies in order to serve as a missionary for his church in Eastern Washington following which he returned to Purdue and completed his bachelor's in civil engineering in December of 2009. After having received his degree, he moved down to Austin Texas in the following month and began a master's education in structural engineering. This thesis represents the culmination of those efforts and the beginning of a new career in structural engineering.

Permanent Address: 2670 Iliff st.

Boulder, Co 80305

This thesis was typed by the author.